Proceedings of the

FLUID AMPLIFICATION SYMPOSIUM

October 1965

VOLUME III

U.S. ARMY MATERIEL COMMAND
HARRY DIAMOND LABORATORIES
WASHINGTON, D.C. 20438

DISCLAIMER NOTICE

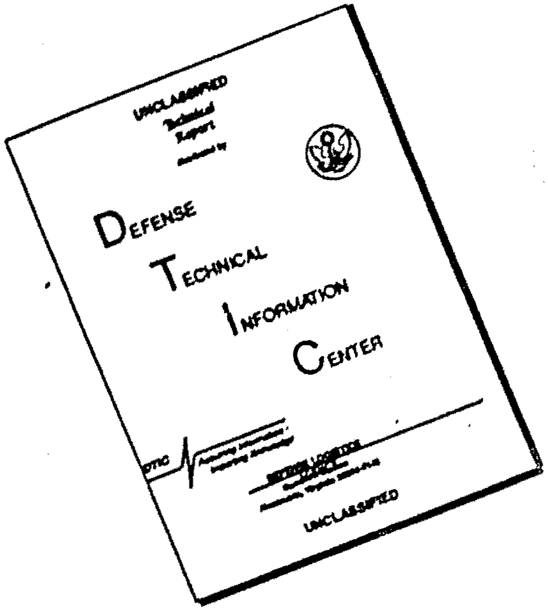

THIS DOCUMENT IS BEST QUALITY AVAILABLE. THE COPY FURNISHED TO DTIC CONTAINED A SIGNIFICANT NUMBER OF PAGES WHICH DO NOT REPRODUCE LEGIBLY.

AVAILABILITY/LIMITATION NOTICES

Proceedings of the

FLUID AMPLIFICATION SYMPOSIUM

Sponsored by the

HARRY DIAMOND LABORATORIES

26, 27, and 28 October 1965

VOLUME III

U.S. ARMY MATERIEL COMMAND
HARRY DIAMOND LABORATORIE
WASHINGTON, D.C. 20438

CONTENTS

CONTENTS (Cont'd)

EXPERIMENTAL STUDY OF A PROPORTIONAL FLUID AMPLIFIER

by
Cyrille Pavlin
Societe BERTIN & Cie, PLAISIR (S.&.O.) FRANCE

ABSTRACT

An amplifier has been designed and tested which applies the principle of the lever to aerodynamic jet deflection. The device yields good performances as a mass flow amplifier and provides facilities for matching impedances between stages. It can operate as a differential pressure sensor.

INTRODUCTION

The fluid amplifier that we studied has a unique control region shape. The leading idea was to avoid momentum control since this causes difficulties as the size of the device decreases. If the control jet velocity is to be similar to that of the power jet, the ratio of the control slot width to the power jet width will be the same as the flow gain ratio, neglecting boundary layers. The effect of the boundary layer is to reduce the velocity, requiring a compensating change in control jet size. Fabrication problems become increasingly difficult if this approach is followed.

Therefore, we tried to find another type of interaction using the pressure effect as a means of bending the power jet. In order that the pressure may rise with a small amount of control flow, the power jet has to be enclosed between two walls downstream of the injection region. These walls are convergent, so that they act like an aerodynamic lever to increase the jet deflection.

DESCRIPTION OF THE DEVICE

The power flow rectangular channel emerges between the control ports, the offset downstream walls of which are progressively converging towards the power jet. They are limited by sharp edges sufficiently close to the power jet as to give only a narrow outlet to the control flow, which must push back the power jet against the opposite edge in order to exit (Fig. 1, 2).*

The other parts of the amplifier are rather standard; after a certain path length in a constant pressure medium, the power jet is diverted between two active channels, adjacent or separated by a bleed line. We generally preferred this last arrangement because the inner splitters of the active channels being located at the maximum slope of velocity profile, the mass flow rate in both channels is small when the flow gain is maximum.

***Figures appear on pages 11 through 15.**

Flow patterns in the injection region are shown with no control flow (Fig. 3) and with control flow (Fig. 4).

POWER JET SHAPE

Without control flow (Fig. 3)

The control ports being closed, the power jet has no deflection and passes at an equal distance from the wall edges of the control capacities. Residual air in the capacities is carried out by viscous effects. If the edges, initially removed are progressively moved towards the jet, air is ejected from the capacities where a vacuum appears at first. But from a certain distance to the jet, vacuum begins to decrease and then gives place to an overpressure. In figure 5 the pressure in the capacities is plotted against e/w

e : distance between the edges
w : the main jet channel width

for a given geometry.

With control flow (Fig. 4)

With a non-zero control flow, pressure rises on both sides of the power jet in the control capacities, no matter from which side the control flow originates. However, a slight unbalanced pressure arises on the fed control side bending the main flow towards the opposite wall in the capacity. The power flow, when impinging the wall, is strongly repelled with a marked angle from its initial direction, because of the convergent shape of the wall.

As a result, unlike most fluid amplifiers the power jet is deflected towards the input control side.

The main purpose of such a design is to give, with a very simple geometry, a substantially better flow gain than that obtained with conventional fluid amplifiers.

MECHANISM OF DEVIATION

The power jet spreads by turbulent mixing in the control capacities with a velocity distribution decaying with the distance from the jet center line.

With no control flow, the mean streamline which grazes the wall edge comes necessarily from an edge of the free power jet issuing inside the control capacities. It obeys KORST's escaping criterion: its total pressure is just equal to the surrounding static pressure outside the control capacities. In other words, the dynamic pressure on that streamline just balances the pressure difference between the capacity and downstream. In the steady state, air entrainment from the capacities reaches equilibrium when the pressure in the capacities agrees with the above condition.

When the power jet is strongly deflected, or when the wall edges are very close to the jet, a narrow local overpressure strip exists on one or both sides of the jet, just at the extremity of the convergent walls. In the first case, the overpressure produces the jet deflection. KORST's escaping criterion is still applicable, but to the maximum value of the overpressure. This explains the pressure rise in one control capacity when the other one is fed.

The importance of the overpressure strip in the deflection mechanism is clearly shown by the poor gain of an amplifier, the control capacities of which are limited by spoilers, as can be seen in Fig. 5. Suppression of the "aerodynamic lever" leads to a large reduction of gain.

EXPERIMENTAL RESULTS

Experimental models

Experimental work was undertaken with two homothetic models in order to test somewhat the scaling effects.

The general features of the amplifier are outlined in Fig. 2. The channel width w is about 0.15 cm (0.06 inch) in the larger model, with an aspect ratio of 6.7. The other model is reduced in a ratio of about 3. Edge distance e is variable.

The receiver position is movable and was adjusted for best operating conditions.

Tests were carried out with low dynamic pressure (3 psi at most).

Performances

General features

The amplifier appears to be sensitive to control flow without threshold until the output flow reaches a maximum in connection with the power jet position just in front of the receiver.

Stability appears rather good unless the flow gain be very high, as observed by other experimenters.

Mass flow gain

Let us call q_{o1} and q_{o2} the mass flows through the active outputs, q_{c1} and q_{c2} the control mass flows. We define mass flow gain as the ratio of the change in output to the change in input control.

$$G = \frac{q_{o1} - q_{o2}}{q_{c1} - q_{c2}}$$

The gain, with e/w optimum, is usually between 10 and 100. A scale reduction tends to improve the performance.

Dynamic response

Until now, we have proceeded only to limited dynamic tests. We did not measure the gain, but only the phase shift between the input and the output on the smaller model. Harmonic control input signals were applied using a pneumatic oscillator. The dynamic measurements of output response to control flow fluctuation were carried out using a two-channel constant temperature hot-wire anemometer arrangement. Simultaneous readings of input control and output stream velocity fluctuations were recorded on a dual-trace oscilloscope. The pictures, Fig. 7, in which are superimposed the input signal and successively the left output, the bleed and the right output, show that for 80 cps harmonic input, the lag between the output and the input is about 3 ms. This lag can be separated in two parts: the transport lag in the receivers and the specific lag of the amplifier (power jet settlement in the capacities).

Amplifier output impedance

To get a high sensitivity, a slight jet deflection must induce a large difference between the mass flow received in the active channels. Therefore the splitters of the receiver should cut the jet stream in a region where the transverse pressure gradient is maximum.

In this zone, the jet dynamic pressure is low and the high transverse velocity gradient is unfavorable to a good jet pressure recovery. As a result, the pressure recovery always remains small compared to the jet dynamic pressure. The device is a mass flow amplifier.

Input impedance

The input impedance is, by definition, the ratio of the change in input pressure to the change in control mass flow.

$$Z_c = \frac{\Delta P_c}{\Delta q_c}$$

This depends on geometric dimensions; therefore, we prefer to characterize the input of an amplifier by the change in input pressure divided by the dynamic pressure of the power jet stream for full deflection. This change is usually small because the power jet entrains the control flow almost equally in both the deflected and the undeflected positions.

Impedance matching a two-stage cascade

An amplifier suitably controlled by a preceding stage must have its control flow uniquely fed by the power flow of the first stage. In

particular, when the power jet of the first stage does not feed one active channel, the mass flow through this channel must be effectively zero.

This can be realized only in two ways:

1) If a difference exists between the ambient pressure in the first stage and the pressure in the control capacities of the second stage, the pneumatic resistance of the junction channel must be as high as possible.

2) If there is no pressure difference, the resistance of the junction channel may be low.

The first solution which gives a high input impedance must be rejected because, as we saw above, the output impedance of such an amplifier is low.

The second one can be realized by two means:

a) If the ambient pressure in the two amplifiers is the same, the gap, (e), between edges of the convergent walls in the second stage must be adjusted so as to make the pressure in the capacity equal to ambient pressure. In general, this is possible because the pressure in the control capacities can be adjusted to a level higher or lower than ambient.

b) If the gap between wall edges is optimized for the maximum gain, the pressure in the control capacities is fixed generally to a value lower than the outside pressure. We can lower the level of the ambient pressure in the first stage by separating this zone from the atmosphere and by suitably loading the bleed.

We could verify that two amplifiers having mass flow gains of 50 and 10 with outputs to atmosphere gave a mass flow gain of 500 when staged (Fig. 6).

Channel decoupling

The 3-channel receiver, with central vent, has an interesting characteristic; when both active channels are fed, a load change of one of them modifies only very slightly the mass flow through the other one. This decoupling may be advantageous in practice.

Differential sensor operation

The jet bending inside the control capacities is always very small, the deflection angle being determined by the overpressure zones existing at the exit of the convergent edges. The result is that the

pressure difference between the jet sides in the amplifier is also small. Then if we join the control capacities to two reservoirs by very low loss pipes, we can detect a slight pressure difference between them. The control flow is blown or sucked according as the mean level pressure in the reservoirs is higher or lower than the pressure in the control capacities without control flow. This device is very sensitive to differential pressure ($\Delta p \approx 1$ mm H_2O) and, in a relatively wide region, insensitive to the mean value of the pressure (± 400 mm H_2O).

The output signal is a mass flow change which can be amplified in a pure fluid regulating system.

In such an application it appears that the power jet behaves like a fluid membrane; the function of which is read by a differential flow.

CONCLUSION

It has been shown that introducing small geometrical differences in a conventional amplifier yields a new type amplifier having quite different operating characteristics. In the new device, momentum balance plays a minor role and mass flow is actually controlled through viscosity effects, so that it is probable that it will operate successfully even in tiny modules. Moreover, the behavior of the device is very sensitive to slight changes in convergent wall shape, so that a large range of operation possibilities including bistable can be contemplated. The rather good dynamic characteristics are felt to be due to the simplicity of its design. For the present it must be considered that the device acts as a mass flow amplifier, providing a gain in the range 10-100, inclusive.

FLOW AMPLIFIER DEVICE

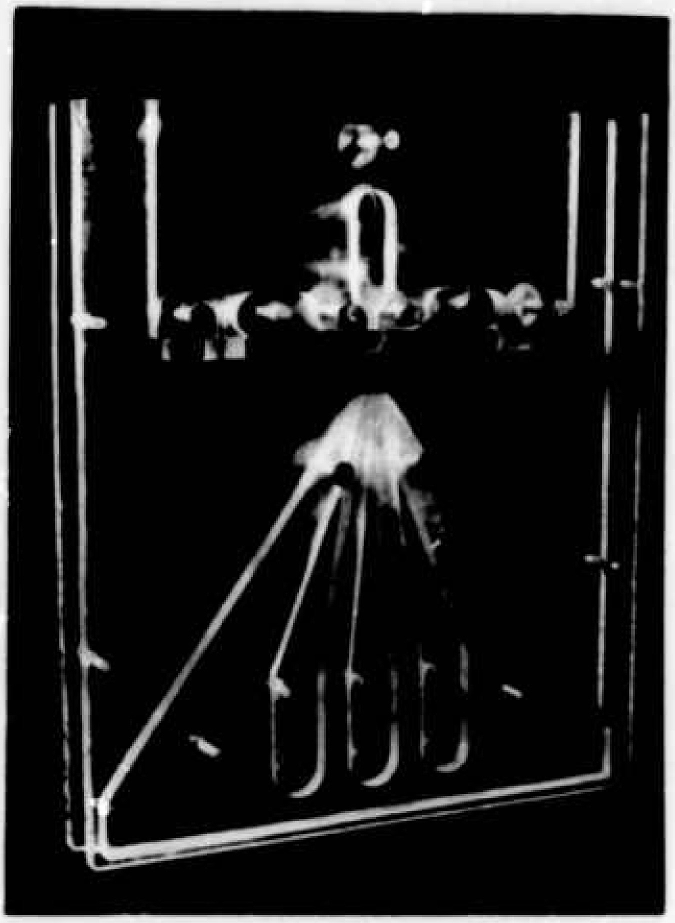

Experimental model

Fig . 1

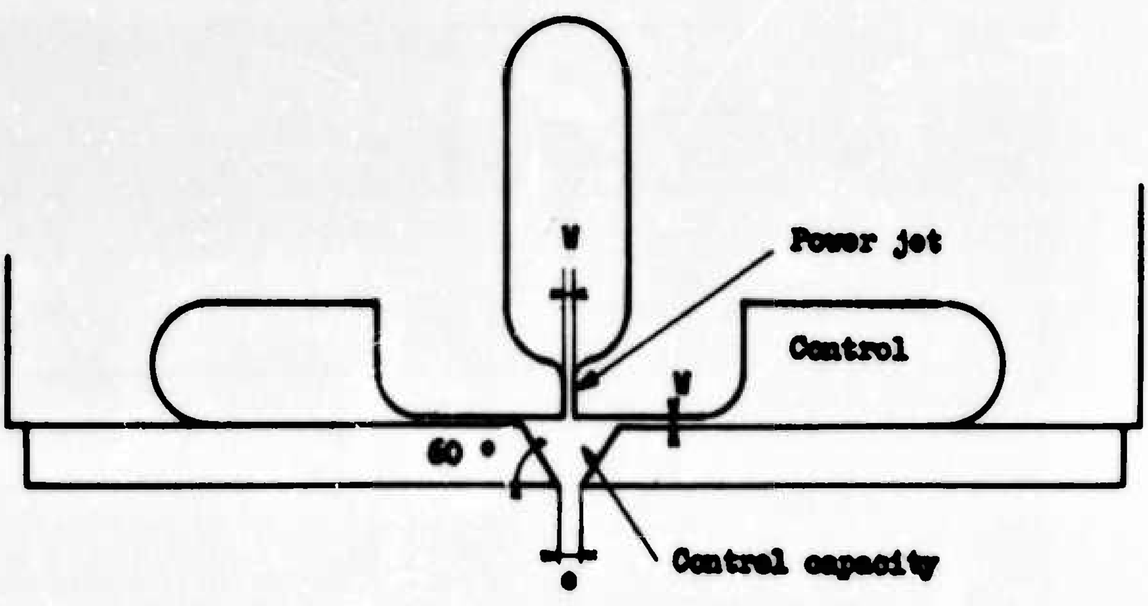

Fig . 2

POWER JET CONFIGURATION

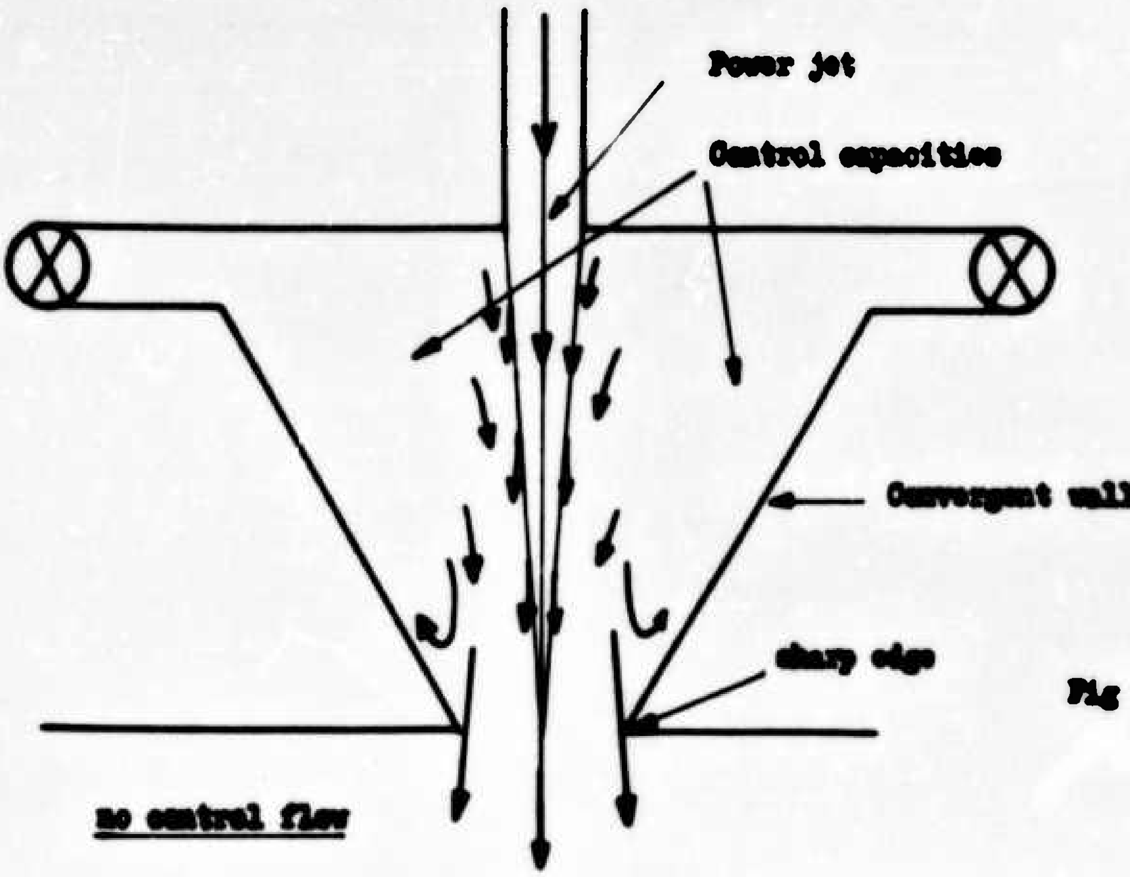

no control flow

Fig . 3

Fig . 4

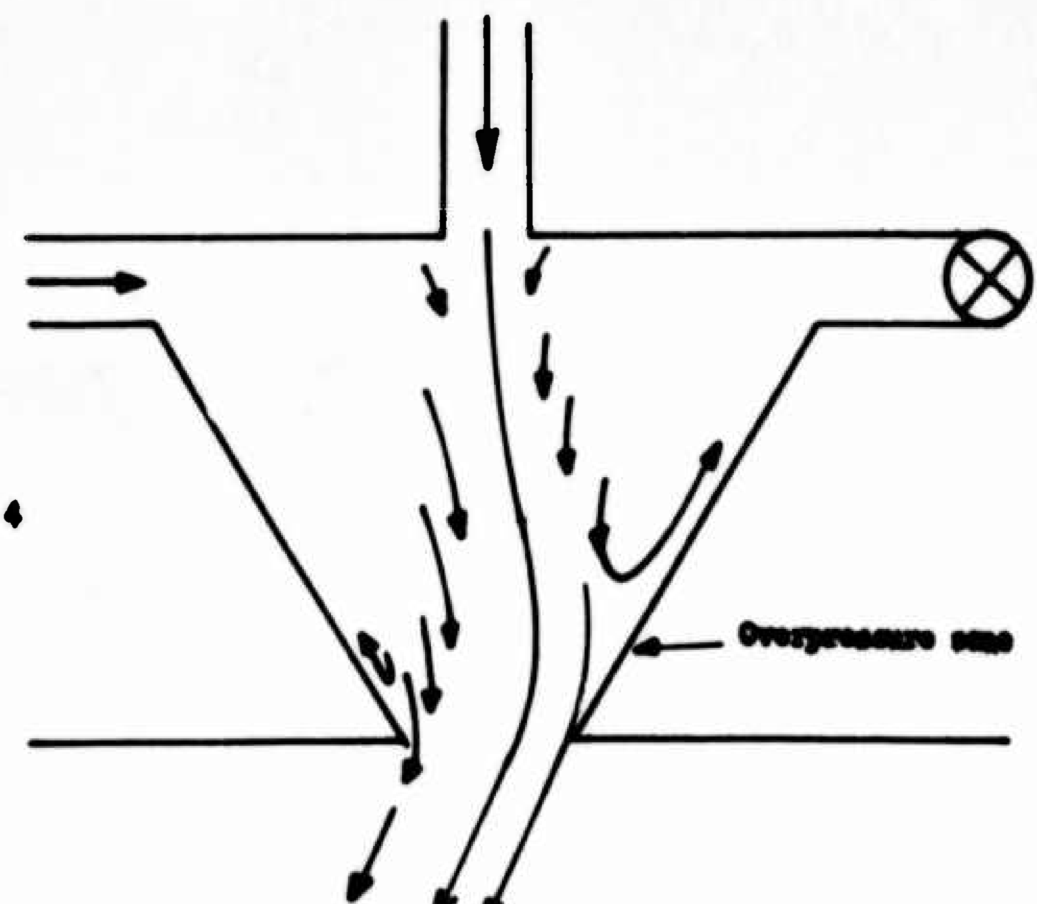

left side control flow

FLOW AMPLIFIER

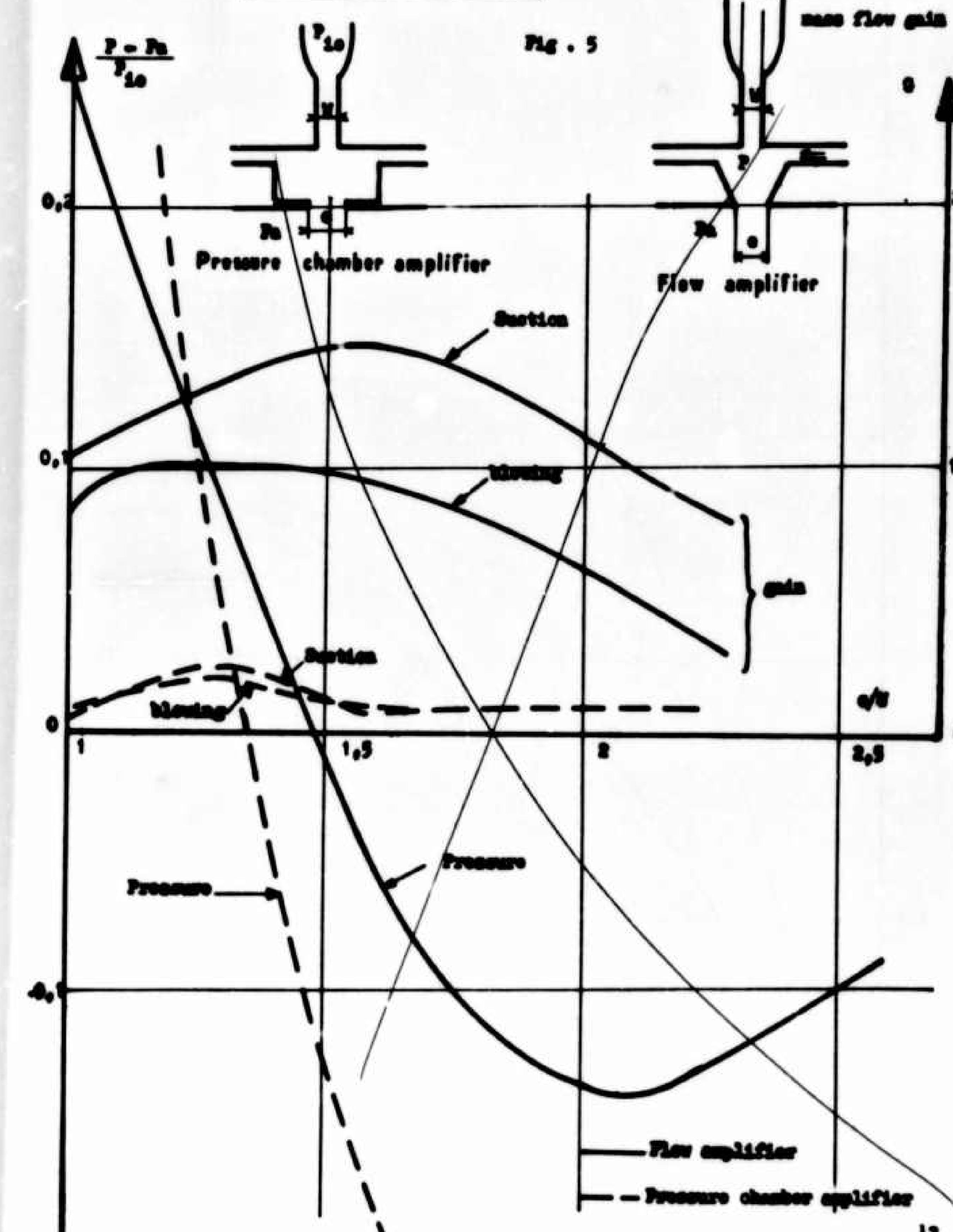

TWO STAGED FLOW AMPLIFIERS

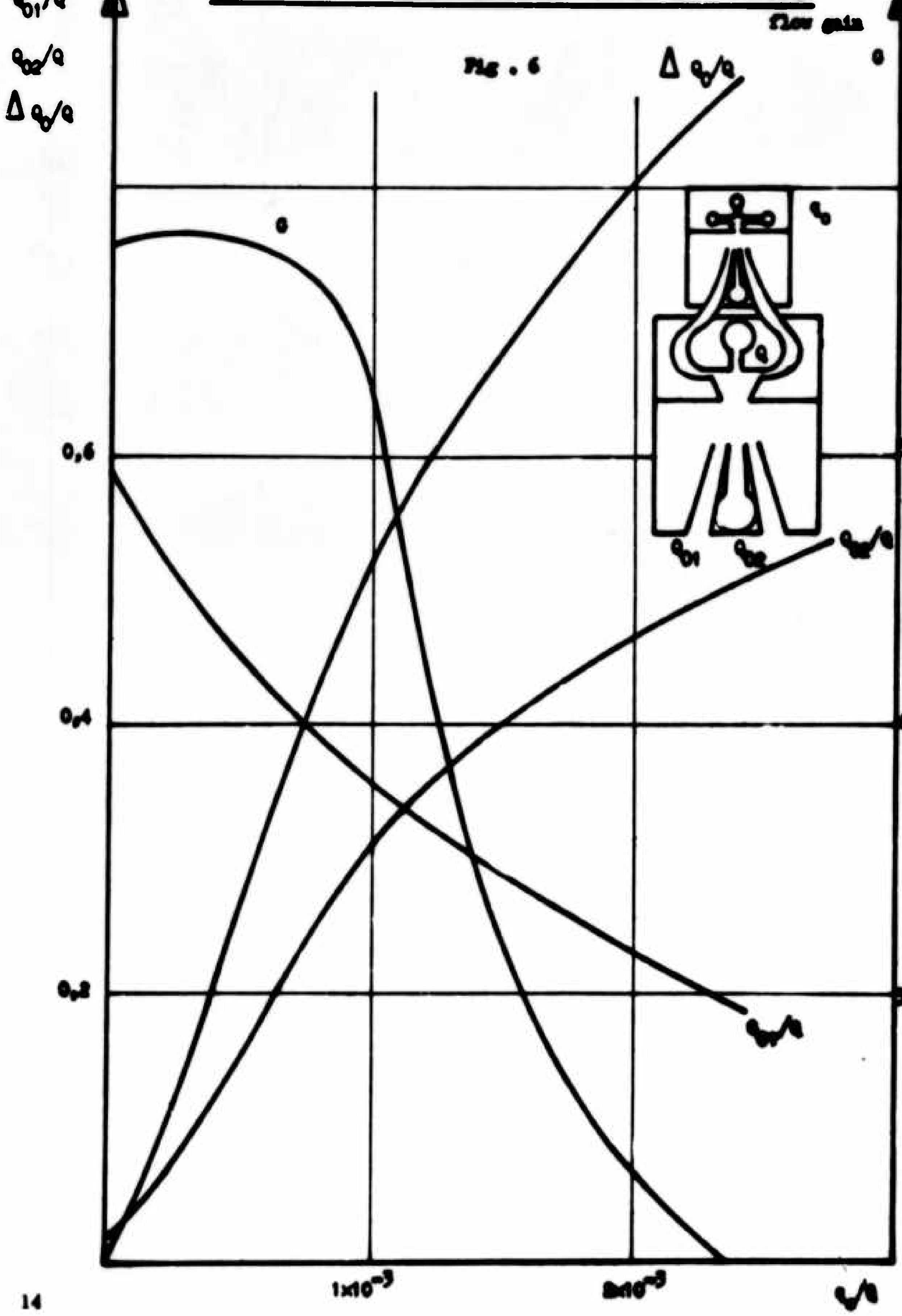

Fig . 6

DYNAMIC RESPONSE

scale : 2mm/cm

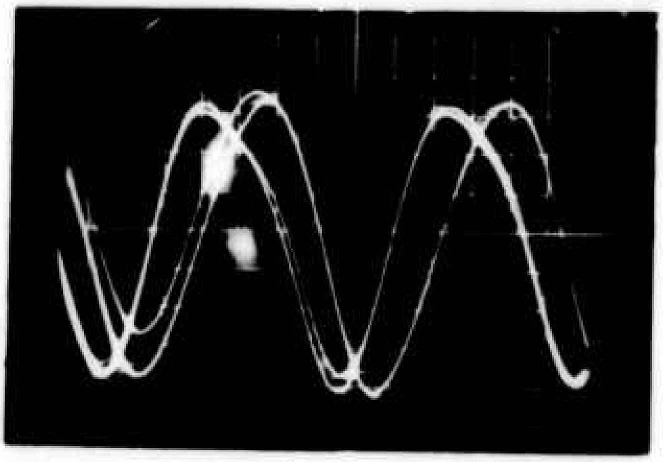

input

adjacent receiver

output

Fig. 7

output

input

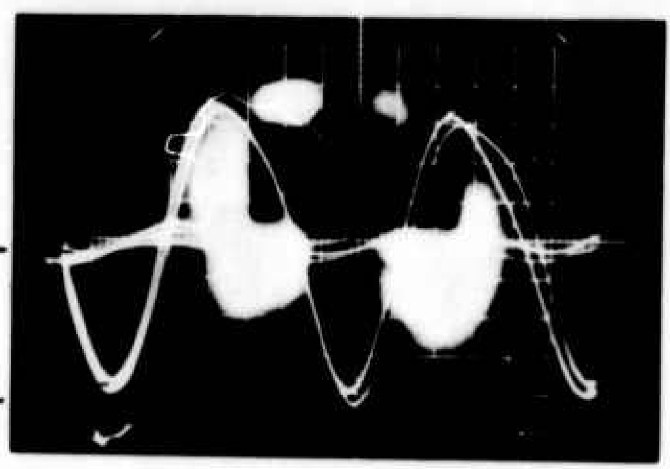

central blood channel

output

Opposite receiver

input

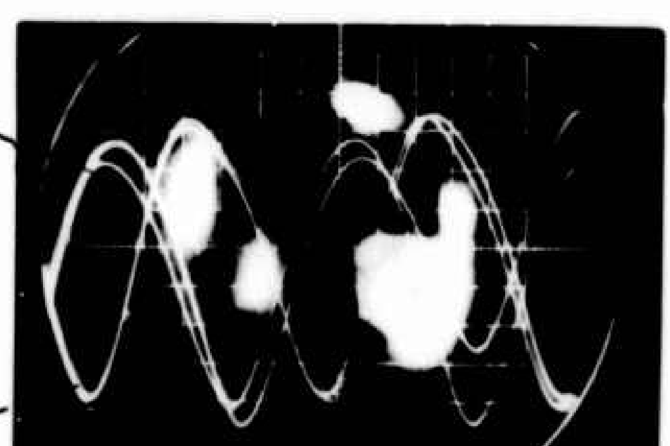

(Reprint of NASA TM X-52120)

BISTABLE FLUID JET AMPLIFIER WITH LOW SENSITIVITY TO RECEIVER REVERSE FLOW

by William S. Griffin
Lewis Research Center
Cleveland, Ohio

TECHNICAL PREPRINT prepared for

Third Fluid Amplification Symposium
sponsored by the U. S. Army Materiel Command
Washington, D. C., October 26-28, 1965

NATIONAL AERONAUTICS AND SPACE ADMINISTRATION

E-3119

BISTABLE FLUID JET AMPLIFIER WITH LOW SENSITIVITY TO RECEIVER REVERSE FLOW

by William S. Griffin

Lewis Research Center
National Aeronautics and Space Administration
Cleveland, Ohio

ABSTRACT

A selected bistable fluid jet amplifier is presented which exhibits low receiver-interaction region coupling and which also has reasonable receiver power recoveries and control signal pressures and flows. The receivers are specifically designed to handle load reverse flow such as might be delivered by a piston. If the control signal pressure is increased approximately 50 percent above that necessary to switch the power jet into an unblocked receiver, the jet may be switched into a receiver pressurized at 40 percent of supply.

INTRODUCTION

In 1959 and 1960, Diamond Ordnance Fuze Laboratories (now HDL) introduced a series of fluid signal processing devices which were called fluid amplifiers or fluid interaction devices. Unlike the more conventional fluid signal processing devices available at that time, fluid interaction devices possessed no moving mechanical parts and relied instead on the interaction of streams of fluid for their operation. Their simplicity, ruggedness, and lack of moving parts made them appear quite reliable and suitable for use in extreme environments. Potential applications included the use of fluid interaction devices as control components in the vicinity of a nuclear rocket engine, on jet engine inlet and engine controls, and in hot gas servosystems. Considerable interest was aroused in their application and a number of companies and government agencies became active in the field.

Unfortunately, the practical development of useful fluid amplifier circuits proved more difficult than had originally been supposed. The fluid amplifiers of that time were often unstable or noisy when their receivers were blocked, and load-amplifier interactions occurred which were not well understood and degraded system performance. A particular load-amplifier interaction effect which proved quite troublesome was the coupling between a fluid jet amplifier and a blocked, highly capacitive load such as a piston or a bellows. In practical servosystems, however, bellows or piston loads are quite common and their destabilizing effects on fluid jet amplifiers tended to hinder the development of fluid amplifier servosystems.

This paper presents a NASA developed, bistable fluid jet amplifier which was specifically designed to handle such loads and the reverse flow which they can deliver into the receivers of the amplifier. The design presented is still in the developmental stage and needs improvement; however, it is capable of driving a capacitive or reverse flowing load at high speed and with much smaller control signals than would be required of more conventional fluid jet amplifiers under similar loading conditions. It is the purpose of this paper to furnish the designer with an amplifier design which, although in need of refinement, will enable him to apply fluid jet amplifiers in systems where load-amplifier interactions have been heretofore troublesome.

DEVELOPMENT OF A FLUID JET AMPLIFIER CAPABLE OF HANDLING RECEIVER REVERSE FLOW

Description of the Problem

Figure 1 shows a fluid jet amplifier of conventional design driving a dead-ended, highly capacitive load such as a piston. In figure 1(a) the amplifier has been driving the load for a sufficiently long time for all transient effects to die out. If, as shown in figure 1(b), the power jet is switched to the right hand receiver, the volume load will start to discharge. The discharge flow forms a reverse flowing jet which impinges on the power jet in the vicinity of the interaction region. Since the reverse flow initially has a stagnation pressure equal to the maximum static pressure that the amplifier can develop when driving a blocked load, its momentum will keep the main power jet of the amplifier firmly attached to the right-hand wall. In addition, the flow delivered by the reverse flowing jet probably upsets the flow geometry of the interaction region in much the same manner as application of a control signal. Thus, to switch the main power jet back into the reverse flowing receiver, shown in figure 1(c), a control signal much larger than normal must be applied.

Figures 2 and 3 show typical control pressures and flows required to switch a fluid jet amplifier of the design shown in figure 1 into a reverse flowing receiver. As can be seen, the required control pressures and flows rise sharply as a function of the reverse flowing supply pressure of the receiver p_r/p_s. Since this particular fluid jet amplifier design could develop a blocked receiver pressure of 55 percent of the amplifier supply pressure, unduly high control signals are required to assure that it will switch into a highly capacitive load. Otherwise, time must be allowed for the load to discharge to an acceptably low pressure before switching. These restrictions of control signal levels and switching speed considerably limit the usefulness of conventionally designed fluid jet amplifiers as power valves for piston or bellows loads.

Design Approaches

Two conflicting requirements had to be fulfilled to develop a fluid jet amplifier which could handle receiver reverse flow. First, the receiver reverse flow had to be diverted away from the interaction region and, preferably, a quiet ambient atmosphere supplied to the interaction region. Second, the receiver had to develop satisfactory pressure and flow recoveries during normal, forward-flowing operation. Both changes in amplifier geometry and the interaction of flow fields could be used to accomplish this task. The former approach was chosen, primarily because of the lack of flow visualization equipment at the time of the amplifier development.

The resultant amplifier design is shown in figure 4. Figure 5 shows an expanded view of the interaction region and inlet portion of the receivers. As can be seen, the receivers in the NASA Model 7 design are pointed away from the interaction region and reverse flow exiting from them will flow out the vents V_3. The entrance to the vent V_3 is widened slightly so that the extra flow entrained by the reverse flowing receiver jet will be captured and diverted away from instead of into the interaction region. A separate vent V_2 is used to provide entrainment flow to the interaction region. The baffle wall between V_2 and V_3 prevents receiver spillover flow or reverse flow from interfering with the entrainment flow. All vents are connected to atmosphere.

The interaction region (fig. 5) differs somewhat from conventional practice. A set of control port restrictions are used to prevent control flow from entering the interaction region. These control port restrictions have zero offset and are machined in the same pass as the main power nozzle. The use of zero offset enables small machining errors to be self-canceling. Another benefit is that the control flow required by the control port during absence of a control signal is reduced.

Figure 6 shows hypothetical flow patterns in the amplifier receivers during operation. In figure 6(a) the amplifier is driving a conventional orifice load. One portion of the flow is delivered to the load while the other part is exhausted through the vent V_3. Because the baffle wall isolates the interaction region from the flow going out through the vent V_3, the receiver may be completely blocked with little or no noise occurring on its output.

Figure 6(b) shows operation of the amplifier when one of its receivers is reverse flowing. Because the receiver is directed away from the interaction region, the load reverse flow is dumped out through the vent V_3. Thus, little interference with the interaction region occurs, and the main power jet may be switched into the reverse flowing receiver by means of a small control signal.

EXPERIMENTAL PERFORMANCE OF NASA MODEL 7 AMPLIFIER

Equipment and Test Procedures

A series of static tests were conducted on the NASA Model 7 amplifier to determine its performance under various loading conditions. Dynamic performance, although important, was not evaluated at this time.

The amplifier (fig. 7) was machined out of an acrylic block by a pantagraph engraving machine. The power throat section was 0.101 centimeter (0.040 in.) wide by 0.152 centimeter (0.060 in.) deep. Wall surface roughness was estimated as being equal or less than 0.0005 centimeter (0.0002 in.) in the vicinity of the power nozzle and interaction region. No particular effort was made to trim the amplifier for symmetrical performance other than exercising suitable care in machining the entire unit. It should be pointed out, however, that the performance of the interaction region is very sensitive to small manufacturing errors, and much difficulty was experienced in trying to machine additional units which yielded the same performance.

Measurements of amplifier triggering pressures and flows as a function of receiver loading were conducted with the test setup shown schematically in figure 8. A servopressure controller was used to maintain either constant positive or negative pressures on one of the two receivers of the amplifier, regardless of the flow through the receiver. Total error in receiver pressure by this method was no greater than 2 percent of the nominal value. The other receiver was optionally loaded with a needle valve or left open to atmosphere. The point of triggering was determined by observing the point at which the trace on the X-Y recorder plot made a sudden break from the previously smooth curve.

Control port cross-flow characteristics were measured with the test setup shown in figure 9. The servopressure controller was again used to maintain atmospheric pressure at the amplifier control port at which the flow was being measured. Thus, a flow resistor with a linear pressure drop-mass flow characteristic could be used to measure control port cross-flow without changing the ambient pressure supplied to the control port.

Receiver characteristics were measured with the setup shown schematically in figure 10. The servopressure controller was again used to maintain the pressure upstream of the linear flow element constant but at a negative pressure equal to the amplifier supply pressure of 6.88×10^3 newtons per meter squared (1.0 psig). Thus, measurements of receiver flow could be made at subambient pressures.

All tests of the Model 7 amplifier were conducted at a supply pressure of 6.88×10^3 newtons per meter squared (1.0 psig) and a temperature of 298° K (75° F).

Sources and Magnitudes of Error

Combined nonlinearity and hysteresis of the pressure transducers and the readout devices were estimated as 1 percent full scale. The nonlinearity of the linear flow elements was also approximately 1 percent of full scale. The transducers, readout device, and the flow element, if applicable, were calibrated as a single unit and in terms of the variable being measured. Estimated calibration accuracy was 1 percent of full scale for pressure measurements and 3 percent of full scale for flow measurements. Reading error, which occurred when switching pressures and flows were read off the X-Y recorder plots, was approximately 0.2 to 0.3 percent of supply pressures and flows to the power nozzle. Total instrumentation and reading error for switching pressures and flows is estimated as being equal or less than 0.4 percent of the amplifier supply pressure and 0.5 percent of its supply flow, respectively. Total instrumentation error for control port cross-flow characteristics is estimated as 0.2 percent of the supply pressure and 0.3 percent of the supply flow, respectively. Total instrumentation and calibration error for the receiver output characteristics is estimated as 2 percent of supply pressure and 4 percent of supply flow.

A set of errors was apparently caused by nonrepeatable variations in the internal flow pattern of the amplifier. The lack of repeatability varied from a minimum for receiver and control port cross-flow characteristics to a maximum when the amplifier was switching into a reverse flowing receiver. In some cases, two distinct triggering pressures were observed. In the other cases, the lack of repeatability is included in the reading error previously discussed.

A variation in performance characteristics was noted from one amplifier to the other. This lack of reproducibility was apparently caused by machining errors and varied from a minimum for receiver pressure flow characteristics to a maximum when control port characteristics were measured. Not enough amplifiers were machined and tested at the time of writing of this report to establish meaningful figures for the observed performance variations; however, preliminary observations indicated that, for carefully machined units, variations in triggering pressures and flow of approximately ±50 percent or more of the nominal values could be expected. The particular errors in machining which caused these performance variations have not been determined. Nozzle and interaction region wall roughness appear to be major contributors. It was found that any given fluid jet amplifier could be trimmed for symmetrical performance by shaving a small amount of material off the portion of the control port restriction which was in contact with the main power stream. By this procedure, amplifiers could be made with performance characteristics approximately equal to the amplifier reported in this paper. No experiments were performed to find the sensitivity of amplifier performance to variations resulting from photoetching type proc

DISCUSSION OF RESULTS

Although some coupling between the receiver and the interaction still exists in the NASA Model 7 amplifier (figs. 11 and 12), it is much smaller than the coupling present in an amplifier of more conventional design. A control pressure of only 9 percent of supply pressure was required to switch the particular amplifier tested into a receiver pressurized at 100 percent of supply pressure. The more conventional unit, on the other hand, is practically inoperable after the reverse flowing receiver pressure is above 40 percent of the supply pressure to the main power nozzle. If the receiver pressure into which the main power jet is flowing is increased, the jet attachment becomes more stable and harder to switch (fig. 13). This behavior exists for receiver pressures up to 100 percent of supply and is not typical of amplifiers of the type shown in figure 1.

Figure 14 shows the effects of a "worst possible case" in which the receiver on which the power jet is attached is blocked and the opposite receiver is reverse flowed. As can be seen, a control pressure of 15 percent of supply pressure is adequate to switch the amplifier into a reverse flowing receiver pressurized at 100 percent of supply. In practical situations, it is quite doubtful if such a combination of receiver flows and pressures could be achieved by a damped, second order load such as a piston.

Unfortunately, although the NASA Model 7 fluid jet amplifier has been made relatively insensitive to the effects of receiver return flow, its switching characteristics are strongly affected by a negatively pressurized receiver. Figure 15 shows that a negative receiver pressure of only 15 to 20 percent of supply pressure is sufficient to cause the jet to switch into that receiver. This triggering sensitivity to negative receiver pressure will become important when the amplifier is used to drive a piston. If the amplifier is driving the piston and the piston velocity builds up to a maximum value, the piston could consume a flow of approximately 110 percent of the flow supplied to the main jet power nozzle (fig. 16). However, if the amplifier is switched to the other side to decelerate the piston, the piston will, for a short period of time, continue to draw the same amount of flow out of the receiver. The experimental receiver performance curves shown in figure 16 indicate that a flow of 100 percent of supply out of a receiver will cause a negative pressure of 40 percent of supply if the main power jet is directed towards the other receiver. This negative receiver pressure is sufficient to cause the main power jet to switch back and again accelerate the piston to maximum velocity.

Fortunately, this reverse switching may be avoided if a steady pressure is maintained on the amplifier control ports. Figure 17 shows the control port pressures and flows required to switch the main power jet away from a negatively pressurized receiver and the minimum pressures and flows to keep the jet from switching back (called reverse switching in the figures). As is shown in figure 17, if the negative receiver pressure is less than 50 percent of supply, the control pressures and flows necessary to switch the jet away from a negatively pressurized receiver are more than enough to keep it away. A negative receiver pressure of 50 percent of supply will

correspond to a flow greater than the amplifier was capable of delivering to the piston load and hence is not likely to be encountered in a non-resonant load. Consequently, if the driver stage used to drive the Model 7 amplifier maintains continuous pressures and flows in the amplifier control ports, the Model 7 amplifier would not be expected to switch because of the negative receiver pressures created by piston deceleration.

Figure 17 also shows the presence of two distinct triggering pressures. The pressure at which the amplifier would switch appeared to be a function of how rapidly the control signal was applied.

A combination of receiver loads not investigated was a negative receiver pressure on the side on which the jet was attached and a positive pressure (hence implying reverse flow) on the side toward which the jet was being switched. However, omission of this combination of loads is not expected to be serious since both are not likely to occur at the same time. If a piston load is being driven by the amplifier, maximum receiver pressure will be developed only when the piston is moving very slowly and hence drawing very little flow. Conversely, maximum flow will be drawn by the piston only when the pressure differential across it is a minimum. Hence the conditions of most difficult switching are probably given by either figures 11 and 12, or figure 17.

The control port cross-flow characteristics of the amplifier are shown in figure 18. As is seen, flow entrainment into the control port is low during the absence of a control signal. Control port cross flow does not start to become significant until a control pressure in excess of 5 percent of supply is applied to the opposite control port. A control port pressure of 10 percent of supply, which is sufficient to cause the amplifier to switch under practically any piston load, causes a control port cross flow of only 4 percent of supply. This value of cross flow is quite low and can probably be handled without difficulty by most passive or active fluid logic elements of conventional design (cf., fig. 1).

CONCLUSIONS

It is concluded that a bistable fluid jet amplifier with reasonable receiver pressure and flow recoveries can be made which exhibits greatly reduced sensitivity to receiver loading effects. The design is particularly good at handling receiver reverse flow, such as might be delivered by a piston and bellows, and should find application for such loads. At the supply pressure tested (1.0 psig), application of continuous control pressures and flows of 15 and 10 percent of supply, respectively, are sufficient to enable the amplifier tested to drive a piston load under most conceivable modes of operation.

The design is not yet optimized, and it is concluded that the performance of the interaction region is sensitive to small manufacturing errors. Any particular amplifier may be trimmed to give symmetrical performance,

after which it will continue to give reproducible results. However, a new interaction region design must be developed which will give the necessary jet deflection angles, have short length, and exhibit reduced performance sensitivity to the manufacturing process. One possibility is the more conventional interaction region shown in figure 1.

The design presented in this paper is basically incompressible and will not work well at supply pressures approaching critical or greater. Work should be done to develop an amplifier with a supersonic nozzle which can operate at more useful supply pressures.

NOMENCLATURE

D_j width of main power nozzle, m (in.)

h height of channels in fluid jet amplifier, m (in.)

$\dot{m}$ mass rate of flow, kg/sec (lb_m/sec)

p pressure, N/m^2 ($lb_f/in.^2$) gage

Subscripts:

c control

r receivers

s supply conditions

v vent

Superscript:

o angle, deg

BIBLIOGRAPHY

Abbey, P. L., et al.: "Fluid Amplifier State of the Art. Vol I - Research and Development - Fluid Amplifiers and Logic," NASA CR-101, October 1964.

Bowles, R. E.: "State of the Art of Pure Fluid Systems," Fluid Jet Control Devices, ASME, 1962, pp. 7-22.

Brown, F. T., ed.: "Fluid Jet Control Devices," ASME, 1962.

Gray, W. A.; and Stern, Hans: "Fluid Amplifiers - Capabilities and Applications," Control Engrg., February 1964.

Kompass, E. J., et al.: "Perspective on Fluid Amplifiers," Control Engrg., September 1964.

Warren, R. W.: "Wall Effect and Binary Devices," Proceedings of the Diamond Ordnance Fuze Laboratories, Washington, D. C., Fluid Amplification Symposium, Vol. 1, Nov. 15, 1962, pp. 11-20.

Warren, R. W.; and Peperone, S. J.: "Fluid Amplification. 1. Basic Principles," Diamond Ordnance Fuze Laboratories Report TR-1039, August 1962.

Warren, R. W.: "Interconnection of Fluid Amplification Elements," Proceedings of the Harry Diamond Laboratories, Washington, D. C., Fluid Amplification Symposium, Vol. 3, May 1964, pp. 53-72.

"Proceedings of the Diamond Ordnance Fuze Laboratories, Washington, D. C., Fluid Amplification Symposium," Vol. 1, Nov. 15, 1962.

"Proceedings of the Harry Diamond Laboratories, Washington, D. C., Fluid Amplification Symposium," Vol. 3, May 1964.

E-3119

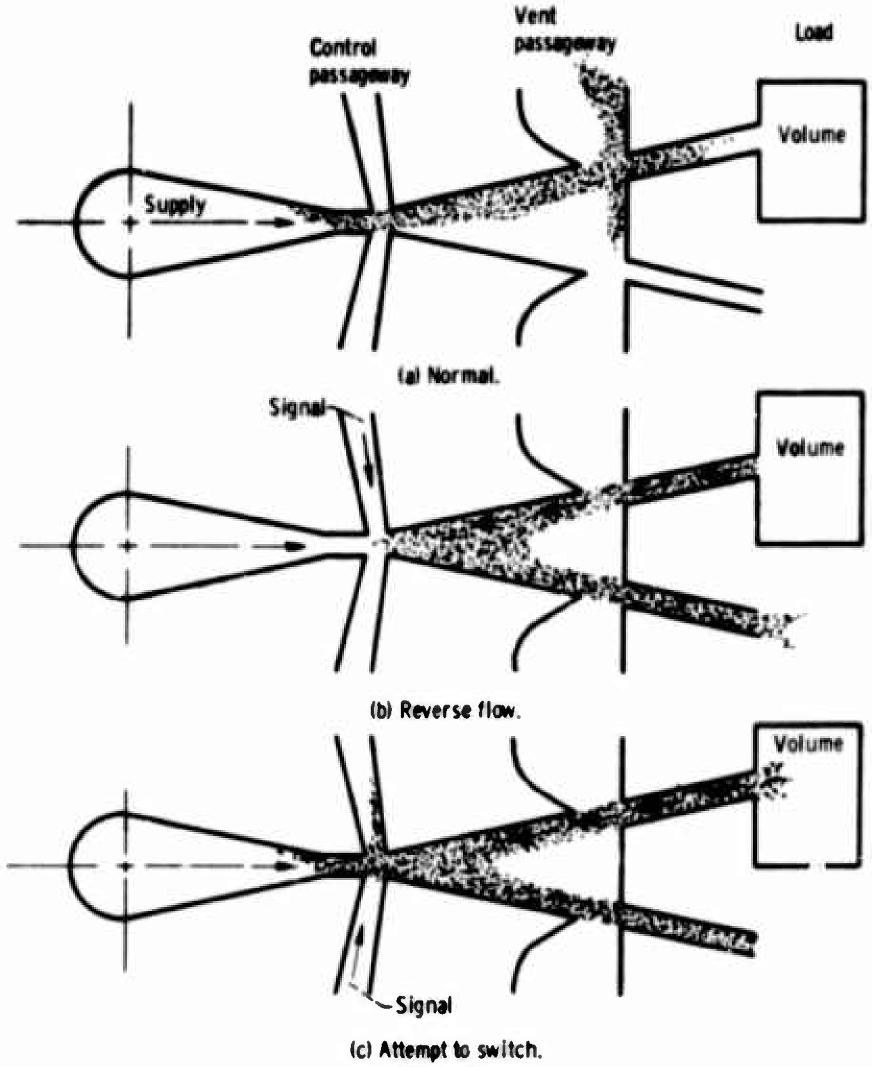

Figure 1. - Performance of standard design bistable element with various receiver loadings.

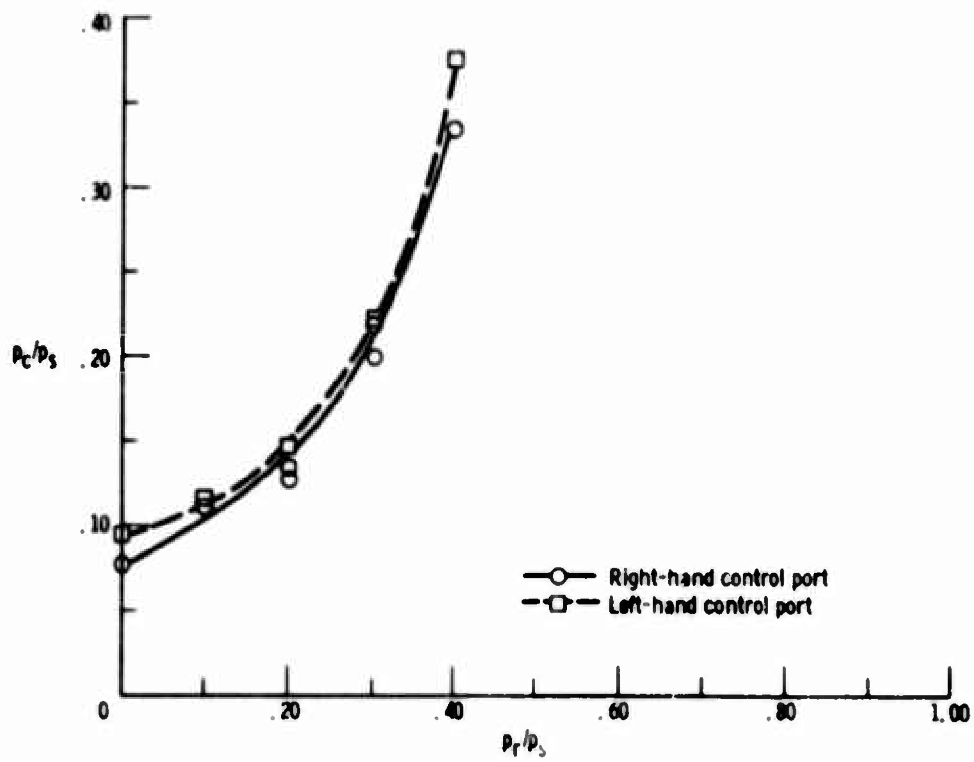

Figure 2. - Control pressures required to switch conventional fluid jet into reverse flowing receiver. Other receiver is vented to atmosphere.

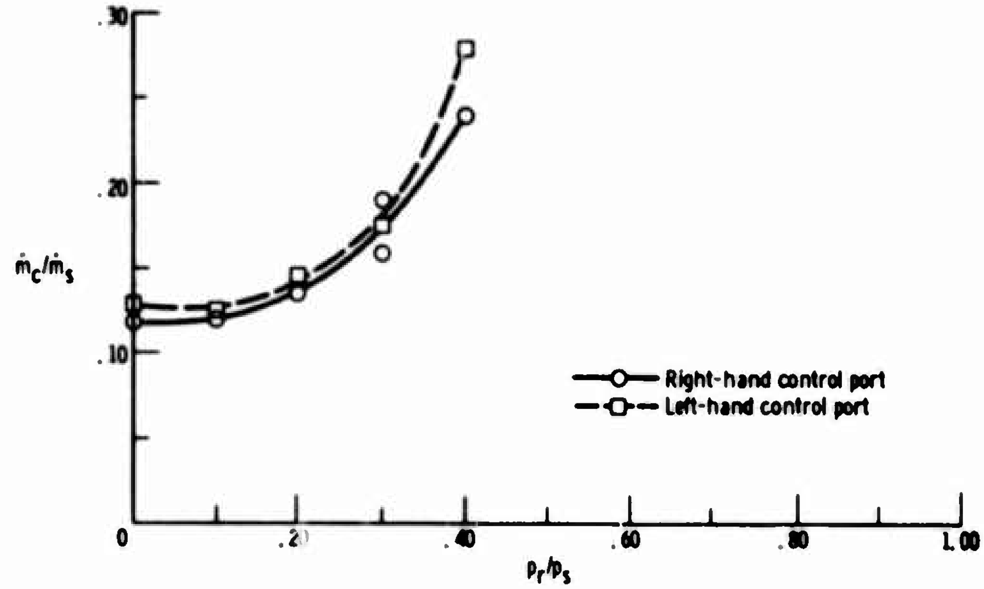

Figure 3. - Control flows required to switch conventional fluid jet amplifier into reverse flowing receiver. Other receiver is vented to atmosphere.

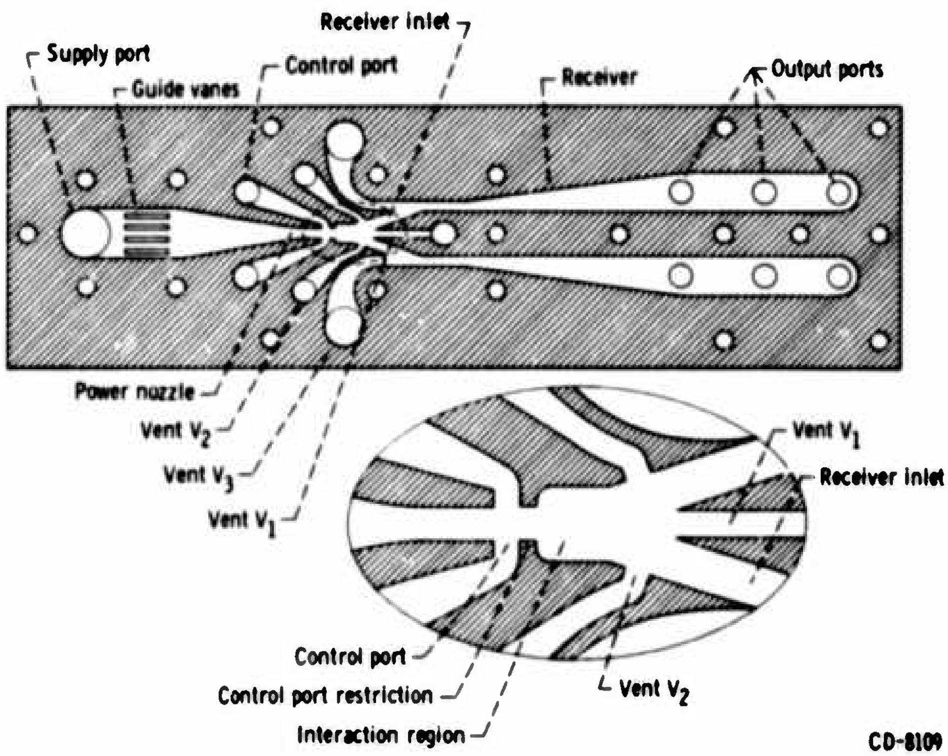

Figure 4. - NASA Model 7 fluid jet amplifier.

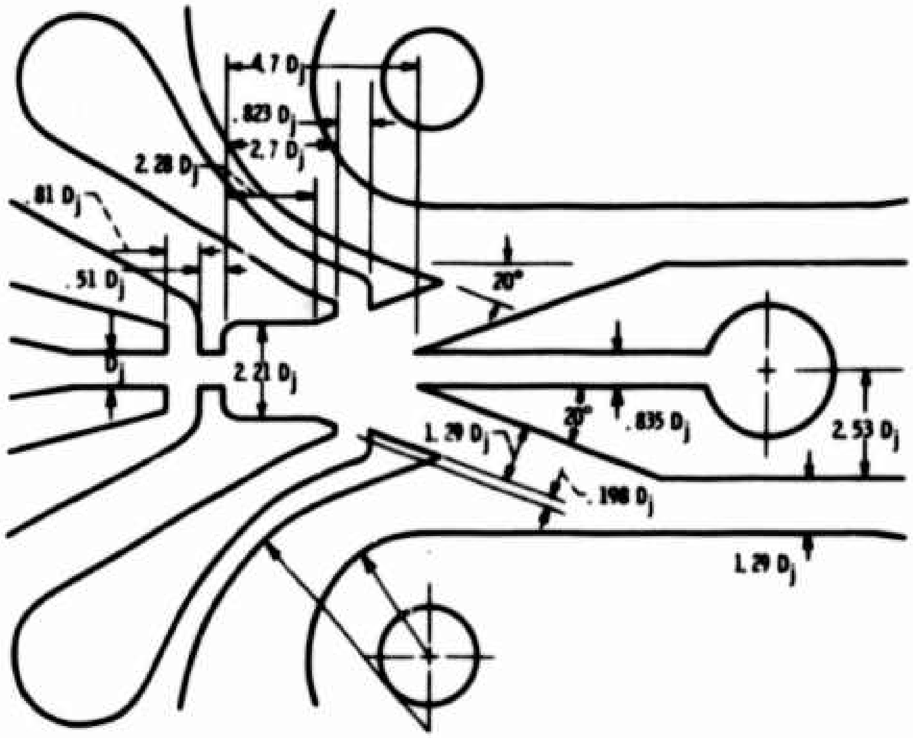

Figure 5. - Interaction region of NASA Model 7 fluid jet amplifier.

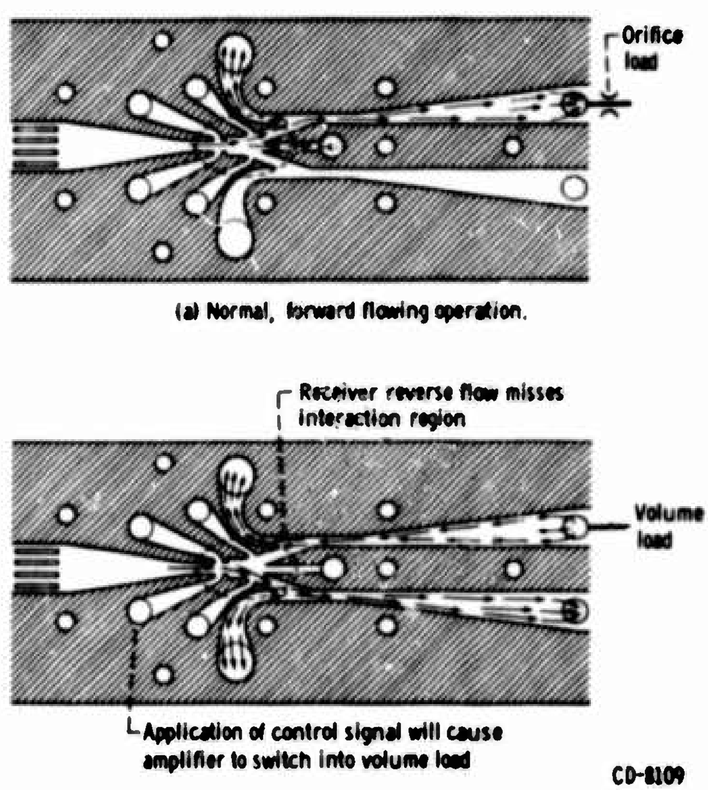

(a) Normal, forward flowing operation.

(b) Operation when receiver is reverse flowing.

Figure 6. - Performance of the NASA Model 7 fluid jet amplifier under various loading conditions.

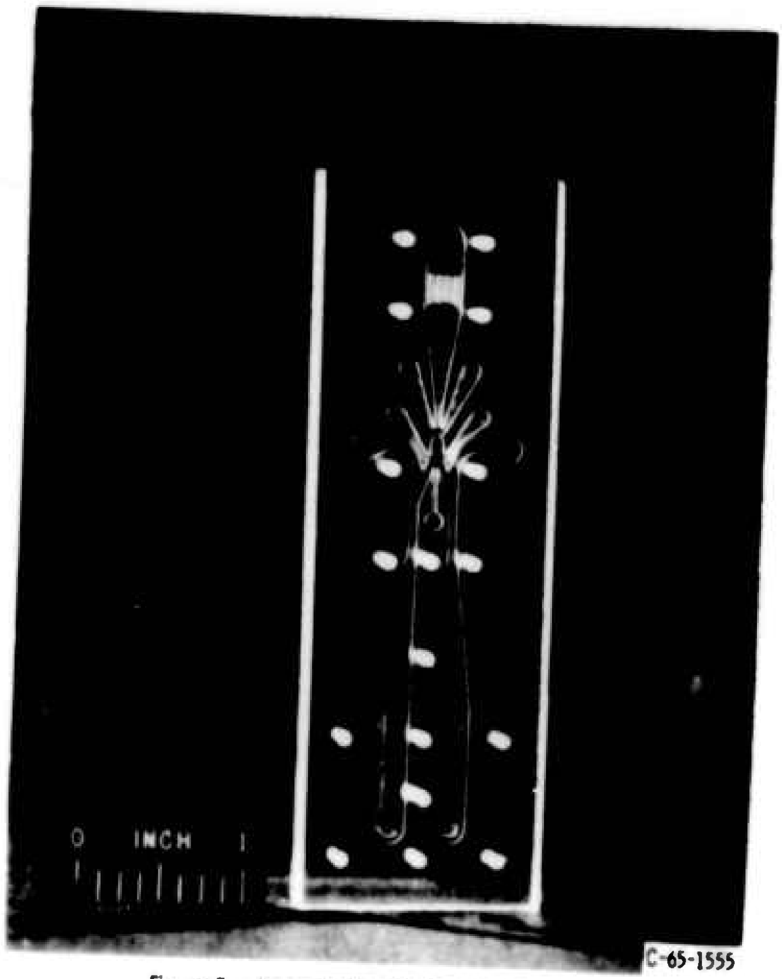

Figure 7. - NASA Model 7 fluid jet amplifier.

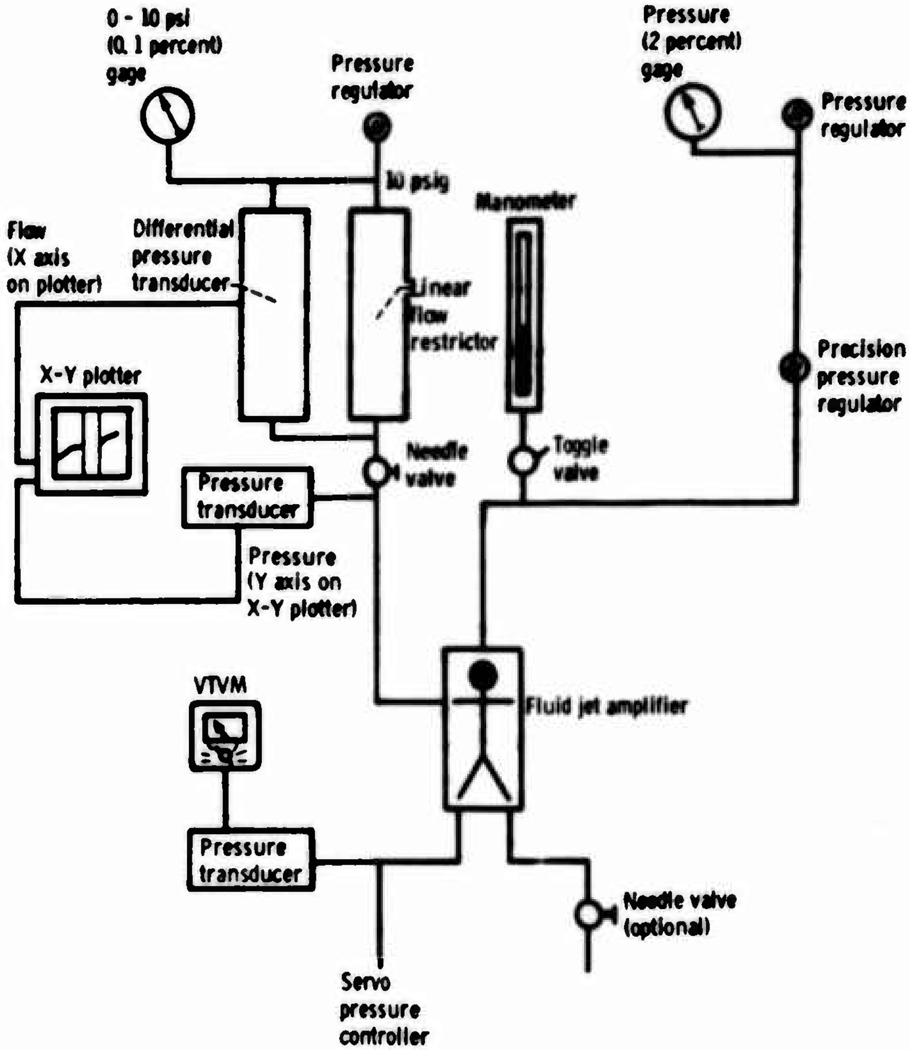

Figure 8. - Schematic of test to measure control port switching pressures and flows.

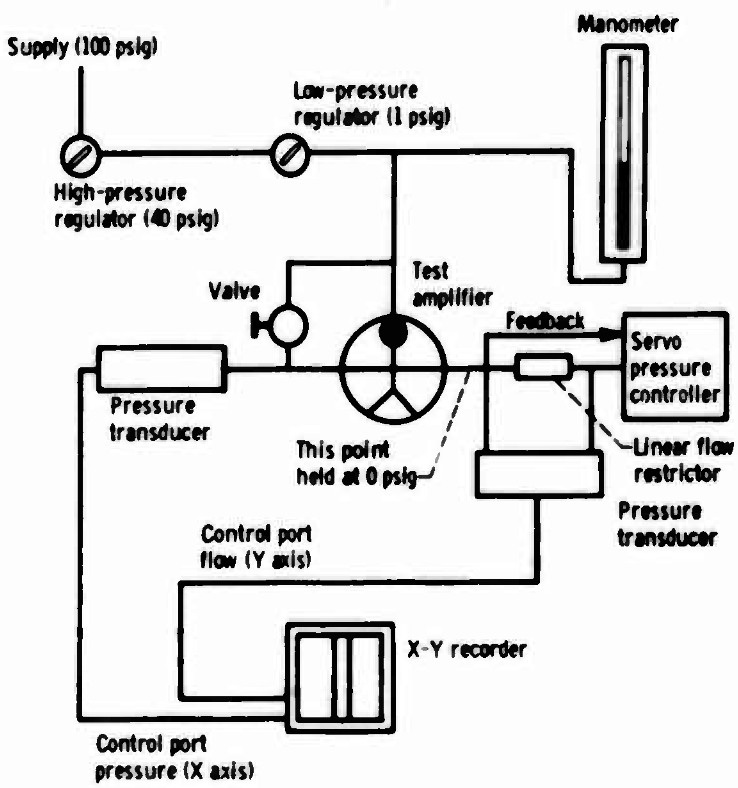

Figure 9. - Schematic of test to measure control port crossflow characteristics.

E-3119

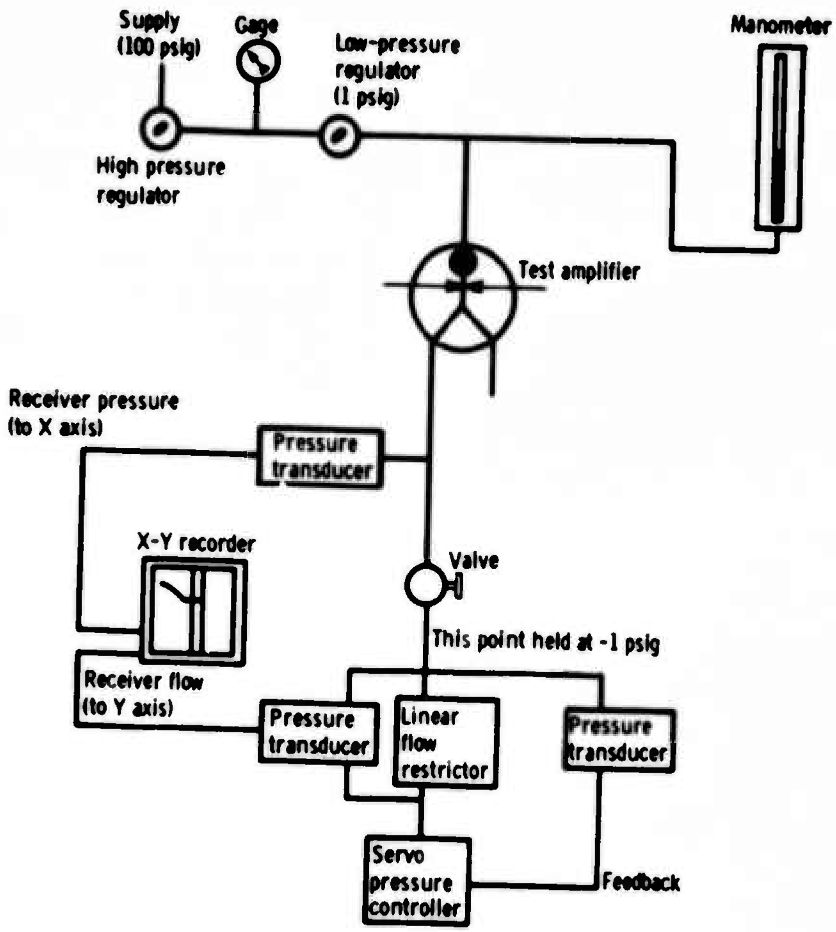

Figure 10. - Schematic for test to measure receiver characteristics.

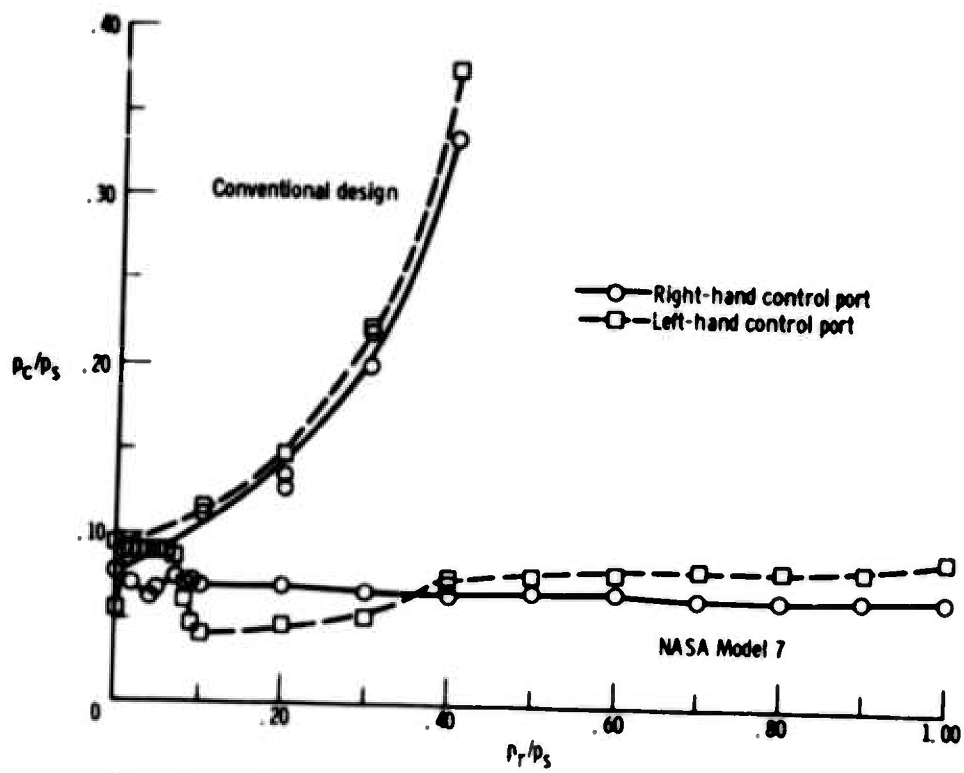

Figure 11. - Control pressures required to switch conventional and NASA Model 7 fluid jet amplifiers into reverse flowing receivers. Other receiver is vented to atmosphere.

E-3119

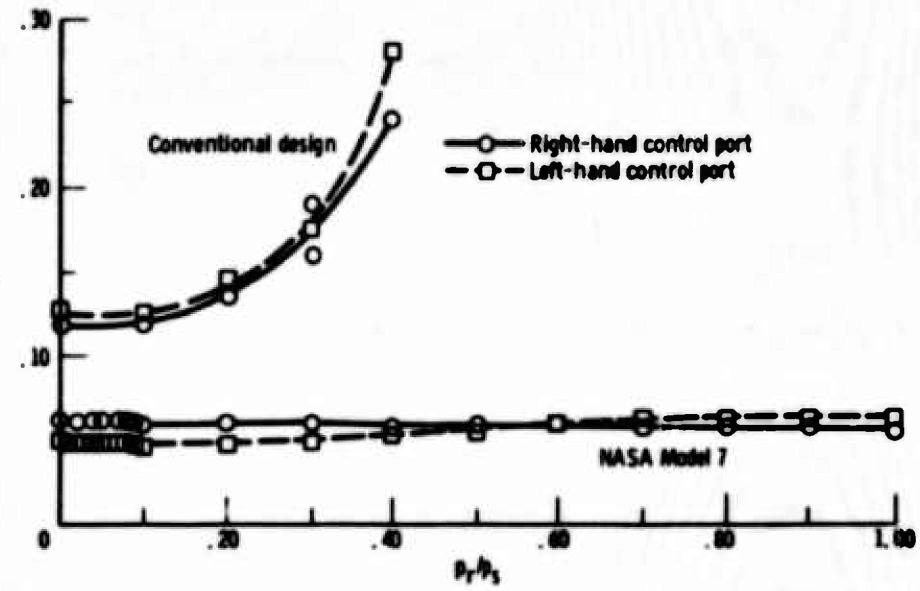

Figure 12. - Control flows required to switch conventional and NASA Model 7 fluid jet amplifiers into reverse flowing receivers. Other receiver is vented to atmosphere.

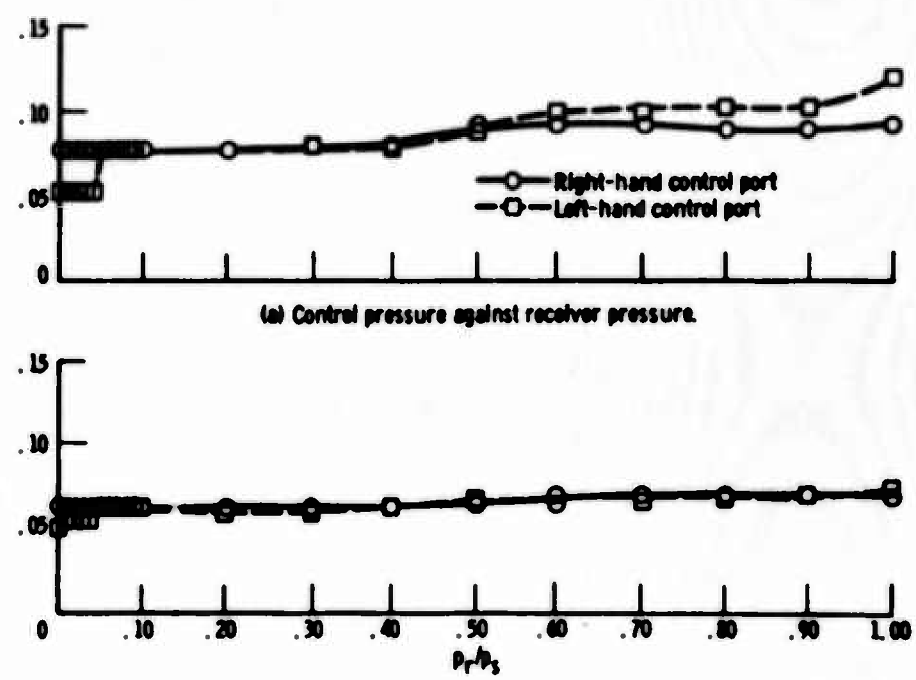

(b) Control flow against receiver pressure.

Figure 13. - Control pressures and flows required to switch NASA Model 7 fluid jet amplifier away from pressurized receiver. Other receiver is vented to atmosphere.

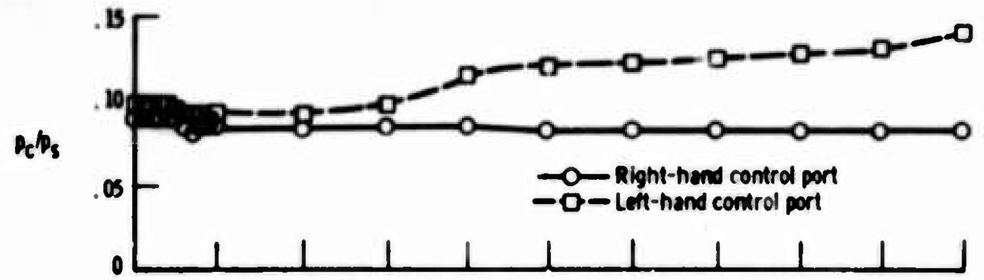

(a) Control pressure against receiver pressure.

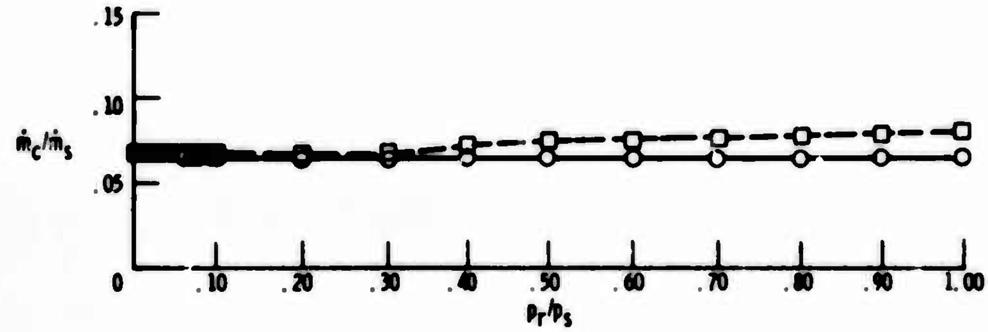

(b) Control flow against receiver pressure.

Figure 14. - Control pressures and flows required to switch NASA Model 7 fluid jet amplifier into reverse flowing receiver. Other receiver is blocked.

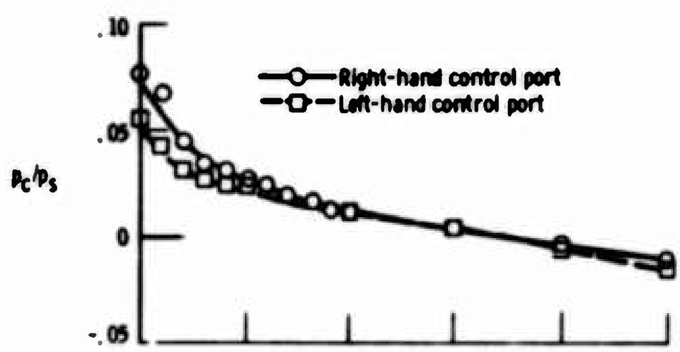

(a) Control pressure against receiver pressure.

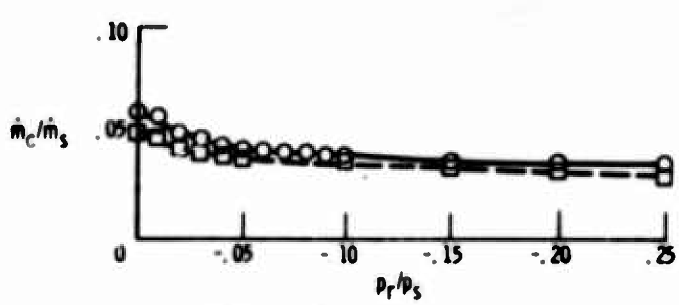

(b) Control flow against receiver pressure.

Figure 15. - Control pressures and flows required to switch NASA Model 7 fluid jet amplifier into a negatively pressurized receiver.

E-3119

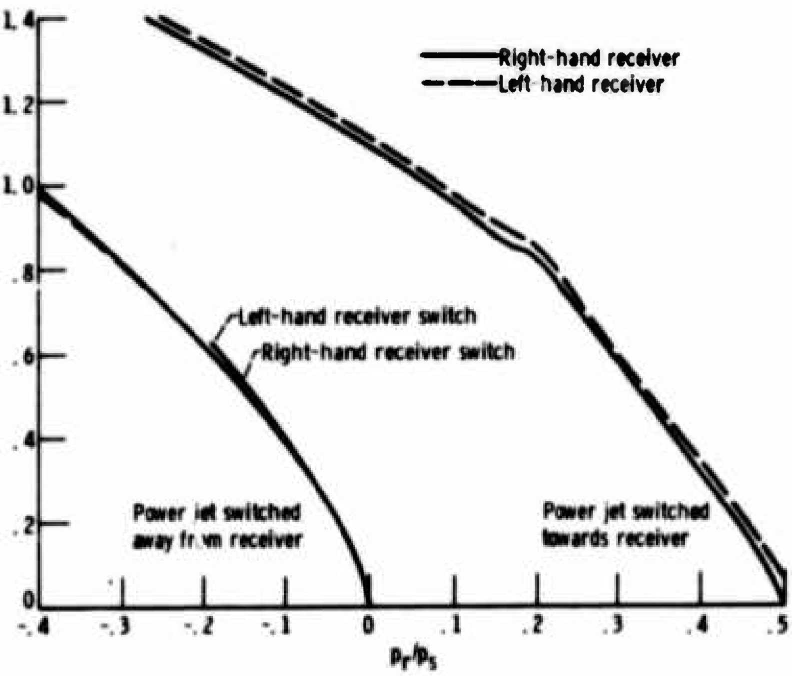

Figure 16. - NASA Model 7 fluid jet amplifier receiver pressure-flow characteristics.

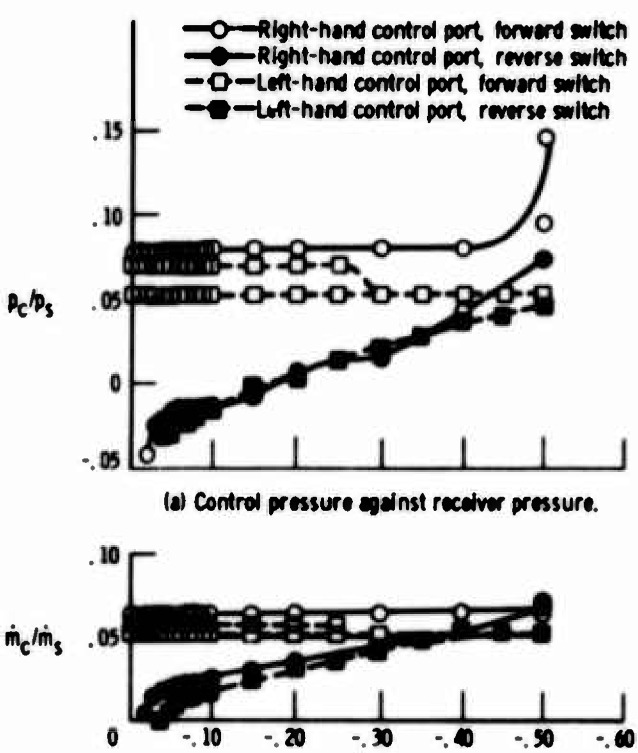

(a) Control pressure against receiver pressure.

(b) Control flow against receiver pressure.

Figure 17. - Control pressures and flows required to switch NASA Model 7 fluid jet amplifier away from negatively pressurized receiver.

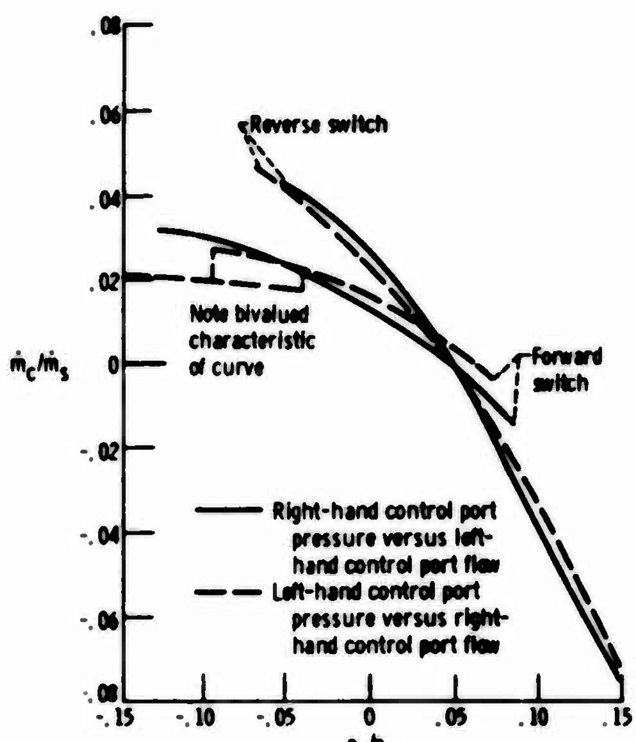

Figure 18. - NASA Model 7 fluid jet amplifier control port cross flow characteristics.

DEVELOPMENT OF A PURE FLUID NORGATE

And A

NORLOGIC BINARY TO DECIMAL CONVERTER

by

T. W. BERMEL & W. R. BROWN

of

CORNING GLASS WORKS

ABSTRACT:

A review of the empirical approach to the design and fabrication of an active, two-input, pure fluid OR-NOR Gate is presented. Performance criteria and testing methods for this device are discussed relative to a discrete standard breadboard-type component.

The breadboard assembly of a binary to decimal converter using these gates is reviewed and finally the reduction of this breadboard circuit to a three-dimensional circuit module is discussed.

INTRODUCTION

An active, two input, pure fluid OR-NOR Gate is a digital logic element with a supply pressure input, OR and NOR outputs, and two control pressure inputs. A unit having a constant supply pressure will normally generate a pressure signal from the NOR leg. If, however, a sufficient control flow is transported to either, or both, control channel inputs, the output signal will switch to the OR leg. When all control signals terminate the output will return to the NOR leg.

As non-bled fluid amplifiers must be properly sized to function in a system, thus rendering them difficult if not impossible to breadboard, only OR-NOR Gate designs incorporating bleeds at the interaction area are investigated. Closed, or non-bled, systems must be uniquely designed to accommodate specific flows and characteristics of interconnected components, therefore by incorporating bleeds in fluid element design, units of the same size and utilizing a common power source can be combined into functional systems.

Possibly the most difficult facet of designing and fabricating breadboard units, whether they be pure fluid elements or any other device utilized in logic or control circuits, is establishing and meeting certain minimum standards. The major desirable operating characteristics of an OR-NOR Gate are:

a) Fan-out capability, i.e. the ability to drive several units.

b) Load insensitivity, i.e. switch points remain constant as load is changed.

c) Operation over a broad range of supply pressures.

d) Balanced control switching characteristics.

e) Complete shutoff in the inactive output.

f) Fast response.

A number of devices were fabricated for each of the designs discussed and only typical curves are shown. Most of the data accumulated during this study have been omitted from this paper for the sake of clarity. Although substantial flow-pressure and operating range information was accumulated, it was found that these characteristics changed only slightly as the designs were changed. The recovery pressure vs. switch pressure relationship was most indicative of design parameter variations, therefore only these curves are presented.

All devices were fabricated in Fotoceram glass ceramic and cover plates of the same material were thermally fused to the etched images.

PARAMETER STUDY

It was decided that a bistable element could be altered to function as a two-input OR-NOR Gate by (a) geometrically biasing the power stream to a given attachment wall, such that in the absence of a control signal the stream would normally attach to that wall, and (b) installing a two-input control configuration adjacent to the given wall. The method of geometrically biasing a bistable unit is shown in Figure 1.

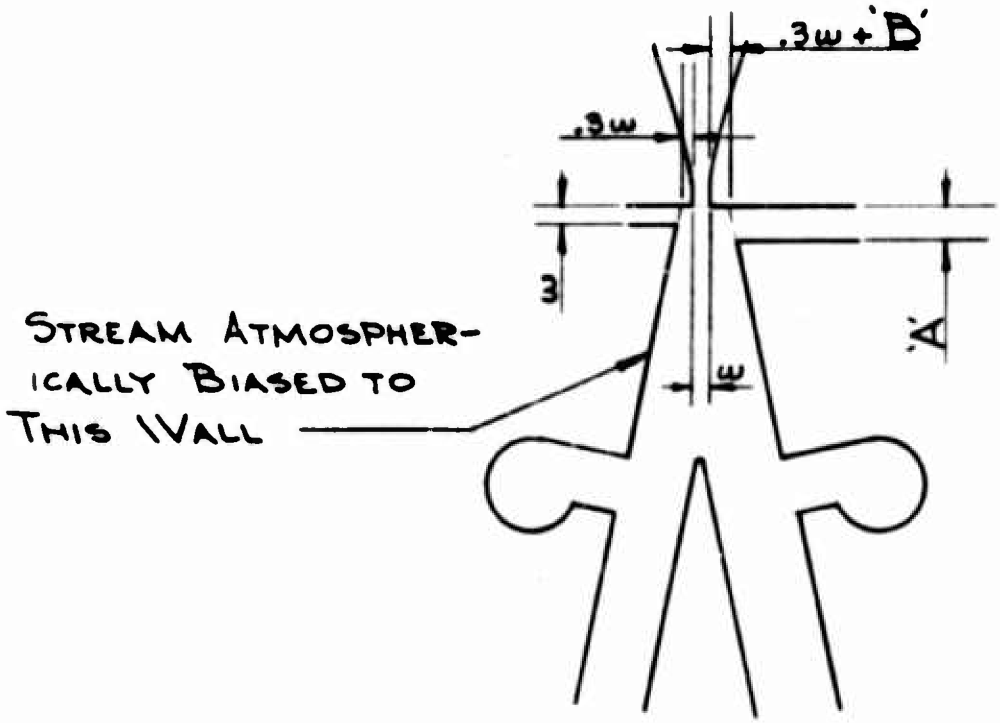

FIGURE 1

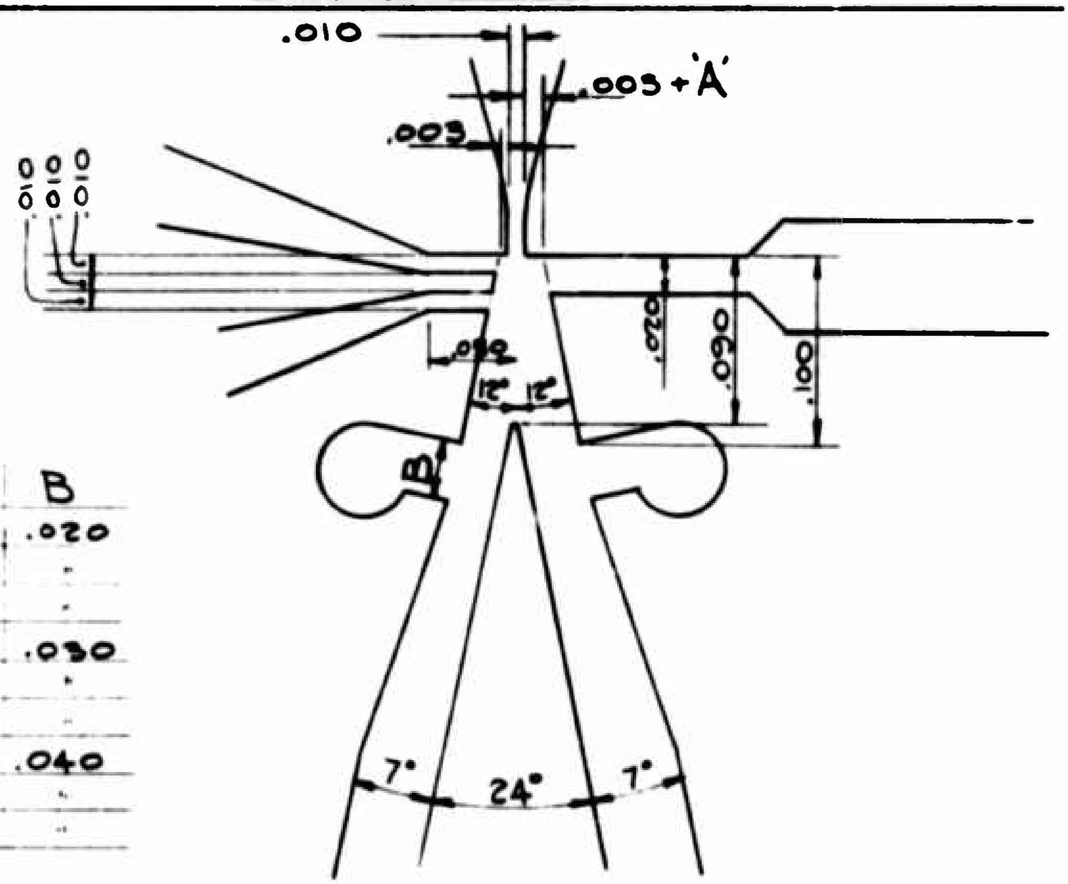

DESIGN No	A	B
1	.002	.020
2	.004	"
3	.006	"
4	.002	.030
5	.004	"
6	.006	"
7	.002	.040
8	.004	"
9	.006	"

FIGURE 2

A program was initiated to increase the control width, dimension "A", and adjacent wall setback, dimension "B", thereby increasing the tendency of the power jet to attach to the opposite wall.

The first design study is shown in Figure 2. The design of the two-input control configuration was completely arbitrary, and the OR wall offset, dimension "A", was varied in an attempt to establish an optimum bias operating condition. The effect of bleed area, dimension "B", on recovery pressure was also investigated at this time.

When designs 1 thru 9 were tested it was found that none of the elements exhibited bistability unless a substantial control differential existed. It then became quite obvious that the ratio of control width to wall length was too great to allow bistable operation. In an effort to obtain data on recovery and switching characteristics the bottom control channel was blocked, thus reducing the effective control area on the NOR side causing all of the units to bias to the proper wall and function as inverters. Typical switch curves for the top control of each design are shown in Figure 3.

The following conclusions were drawn from these curves:

a) The NOR side control area was too large (proportioning occurred when no control signal was present).

b) The greater the OR side attachment wall offset, dimension "A", Figure 2, the higher the switch pressure and the greater the tendency to proportion

SWITCH PRESSURE CURVES

RECOVERY PRESSURE, P_R VS CONTROL PRESSURE, P_C

LOWER CONTROL BLOCKED ~ SUPPLY PRESSURE, P_J = 3 PSIG

OUTPUT LOADS ON NOR LEG = ∞, 3 NOZZLE, & 4 NOZZLE

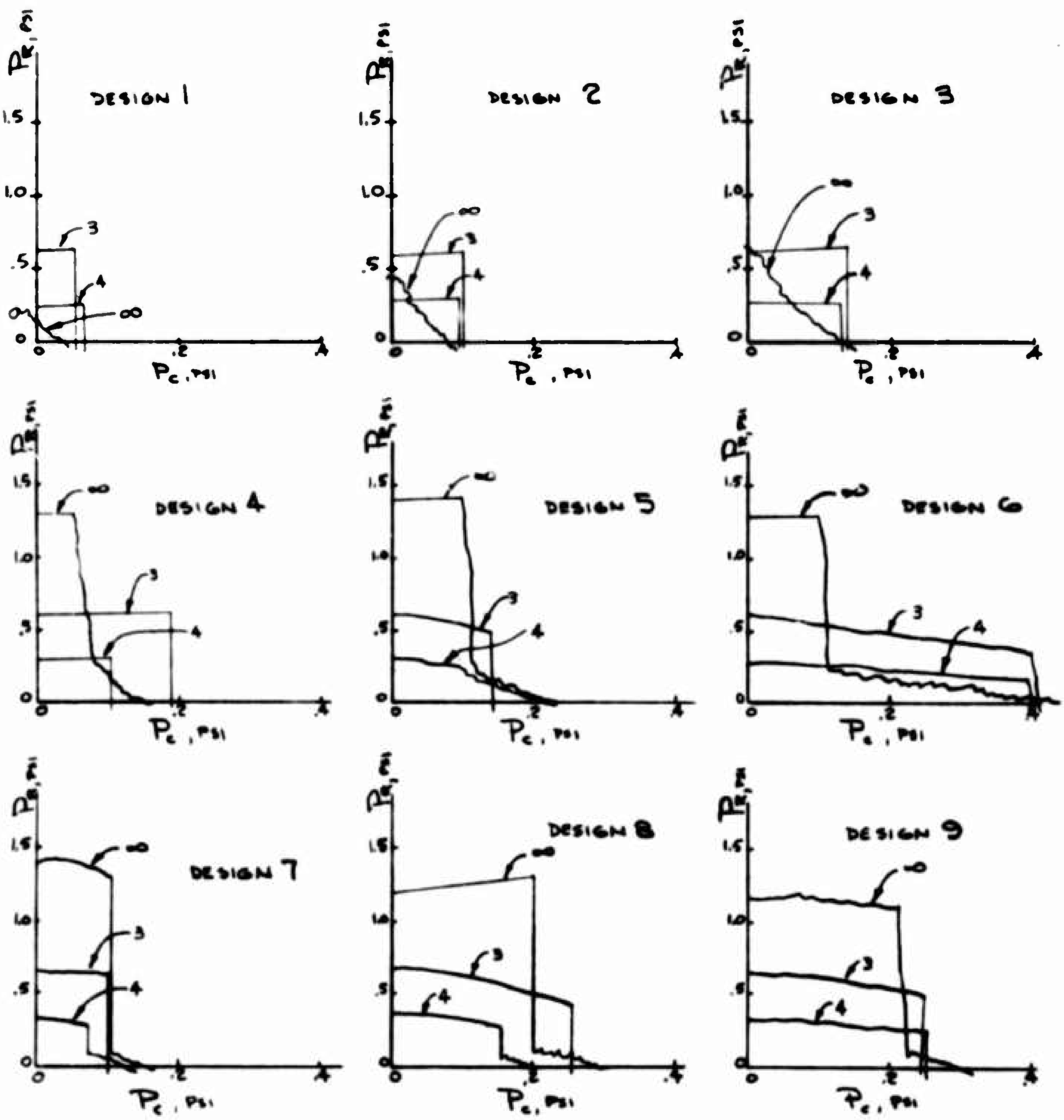

REFER FIG. 2 FOR
DESIGN DETAILS

FIGURE 3

from the "set" wall to the opposite wall during switching.

c) The bleed design did not appear to be efficient in removing all of the excess flow at high loads. Note, Figure 3, that all of the units "flood out" at the various loads. It can also be noted that the .020" wide bleeds caused extreme flood-out at high loads while there is little difference between the .030" and .040" wide bleeds.

Design #10, Figure 4, was then initiated, with the bleed design being patterned after designs discussed in a paper by R. W. Warren entitled "Bistable Fluid Amplifiers", and a two-input control again arbitrarily chosen. A typical switch curve is shown in Figure 5. The data indicated:

a) Fairly good load stability, i. e. no "flood-out" and relatively load insensitive.

b) Upper control switch pressure was high and far out of balance with lower.

c) The hysteresis loop was extremely large.

From these data it was apparent that adequate venting had been achieved, but that the control imbalance and the large hysteresis loop required further study. The switch pressures, in particular that of the upper control, were high enough to severely limit "fan-out"; and the return pressures were low enough to indicate that minor variations in manufacturing techniques or slight

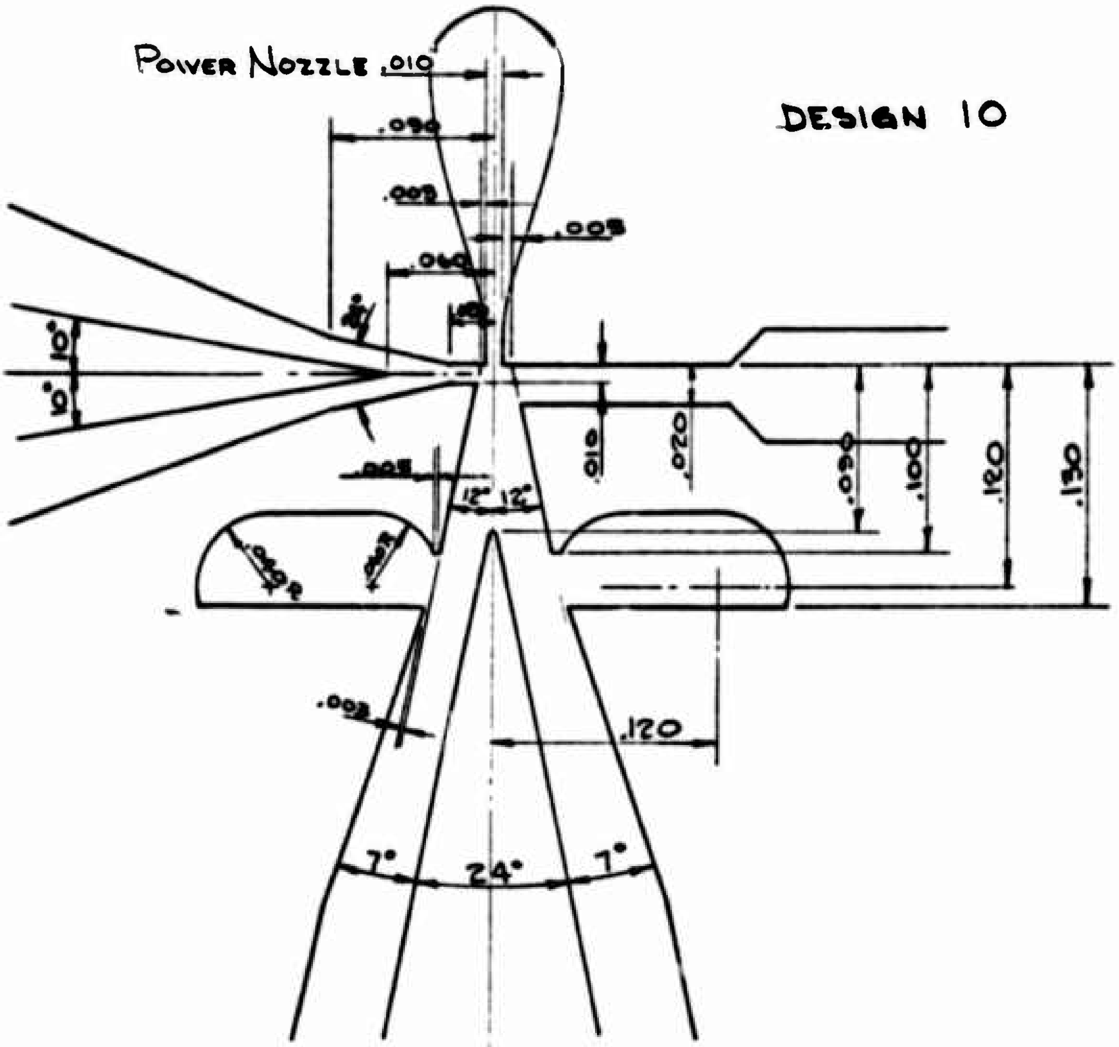

FIGURE 4

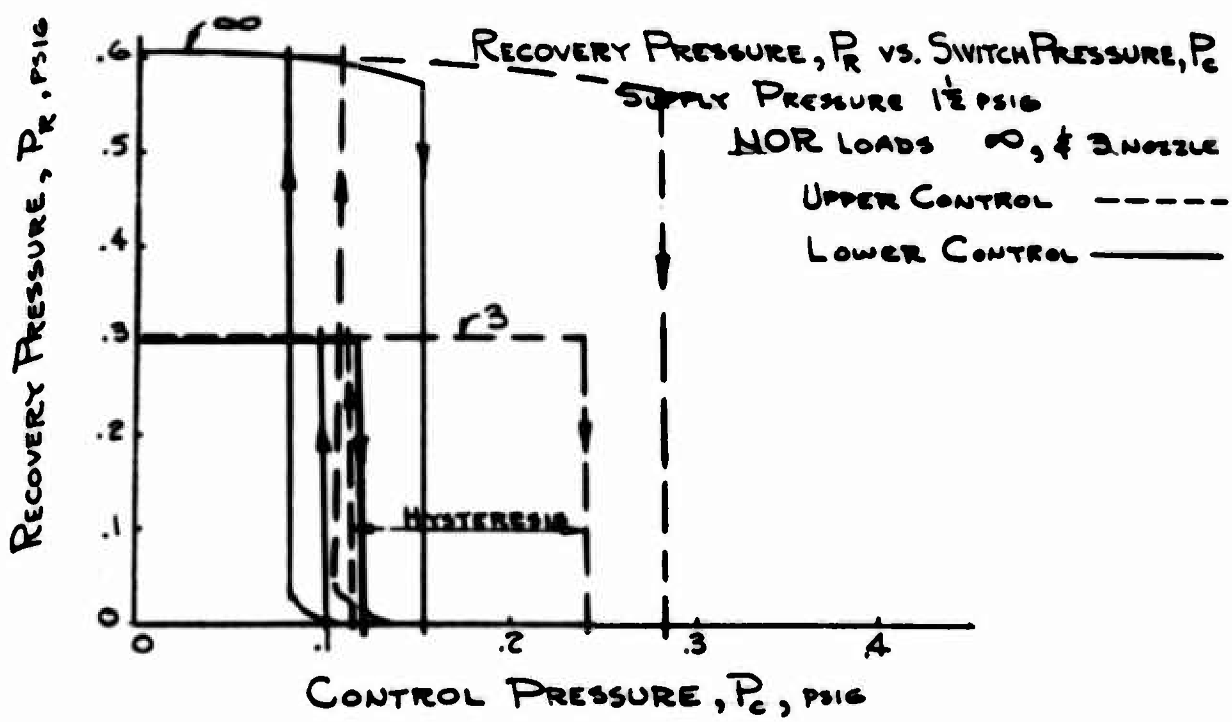

FIGURE 5

flow "spill-over" of interconnected units could result in bistability. It was decided to adjust both attachment wall locations through the ranges shown for designs 11 to 14, in Figure 6, in order to establish what effect, if any, the relative distances between the attachment walls had on the switching and return pressures. All four designs yielded approximately the same switching characteristics, as shown by the typical curve presented in Figure 7. It was concluded that the distance between walls has little effect on the switch points of this particular bistable device design and no further study is contemplated in this particular area at this time.

The most undesirable feature of design 10 is obviously the relatively high pressure required in the upper control in order to effect switching. The switch pressure level of the lower nozzle, although not optimum, was felt to be adequate; and for this reason it was decided to concentrate effort on bringing the upper control into balance with the lower, rather than decreasing the average of the two.

In an attempt to show visually the interaction of the control flows with the power stream flow, an experiment was conducted utilizing a double size image of design 10 with a transparent glass coverplate attached over the image. A container filled with smoke was then inserted in the exterior control line and a control flow passed through the container to the upper and lower controls respectively. Switching of the power stream by each control was observed. Figure 8 depicts the smoke residue formed on the transparent coverplate with vortex currents also inserted to illustrate what was believed to have been

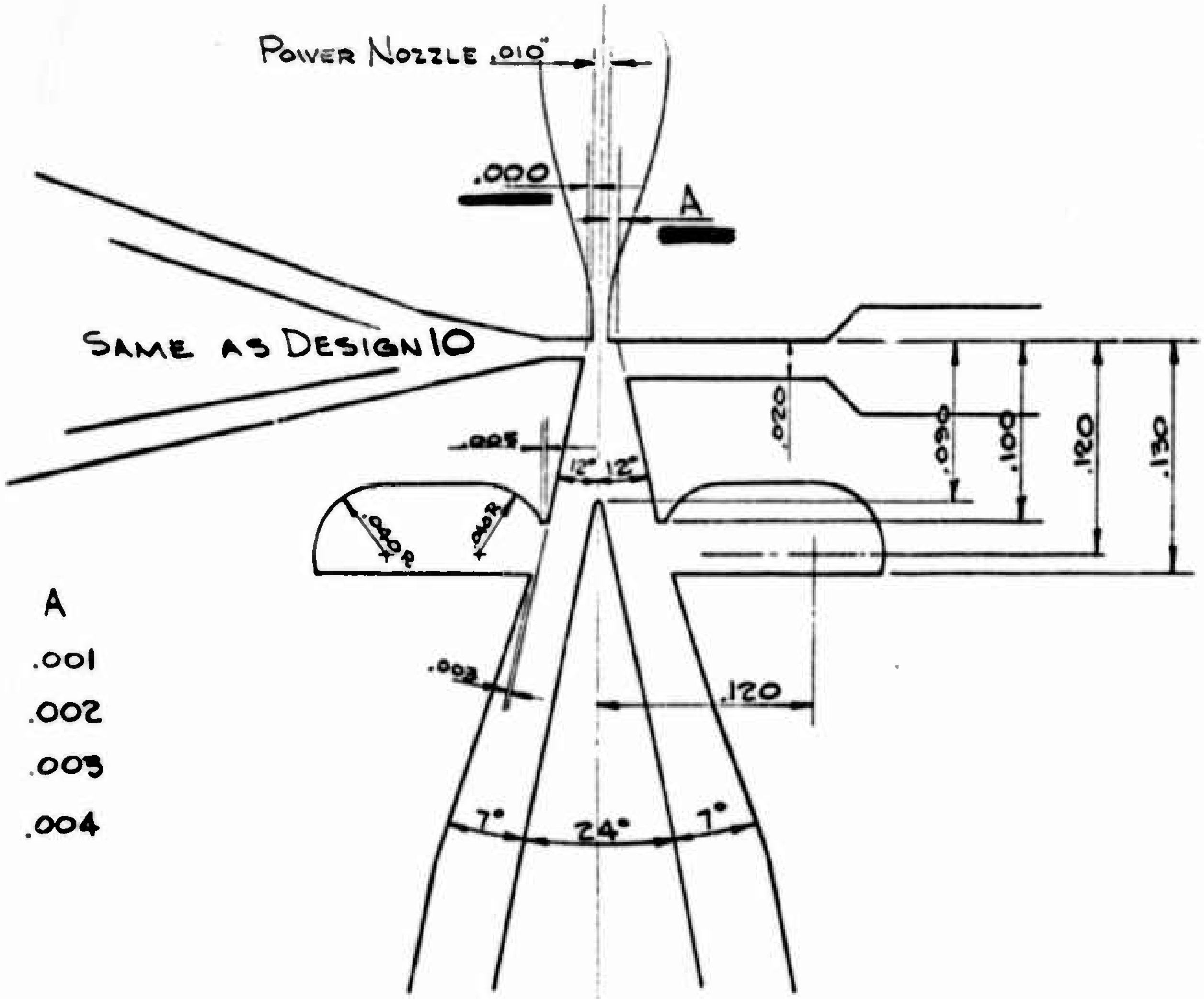

Design No.	A
11	.001
12	.002
13	.003
14	.004

Figure 6

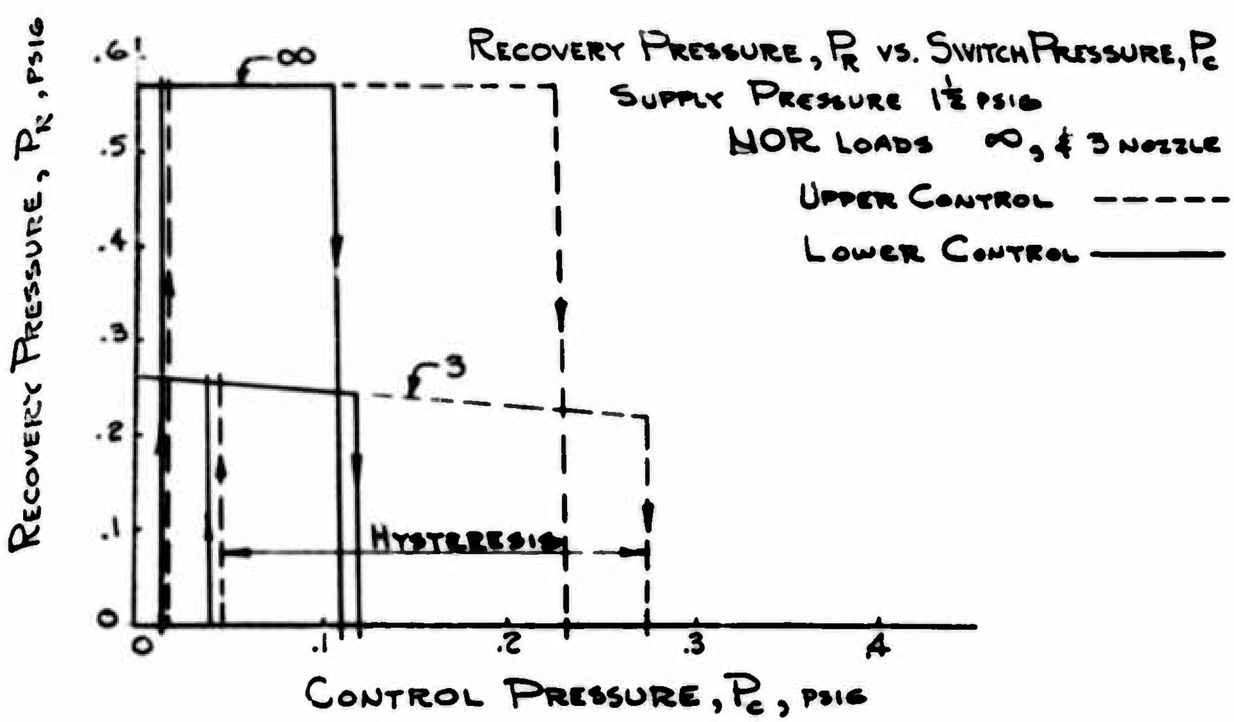

Figure 7

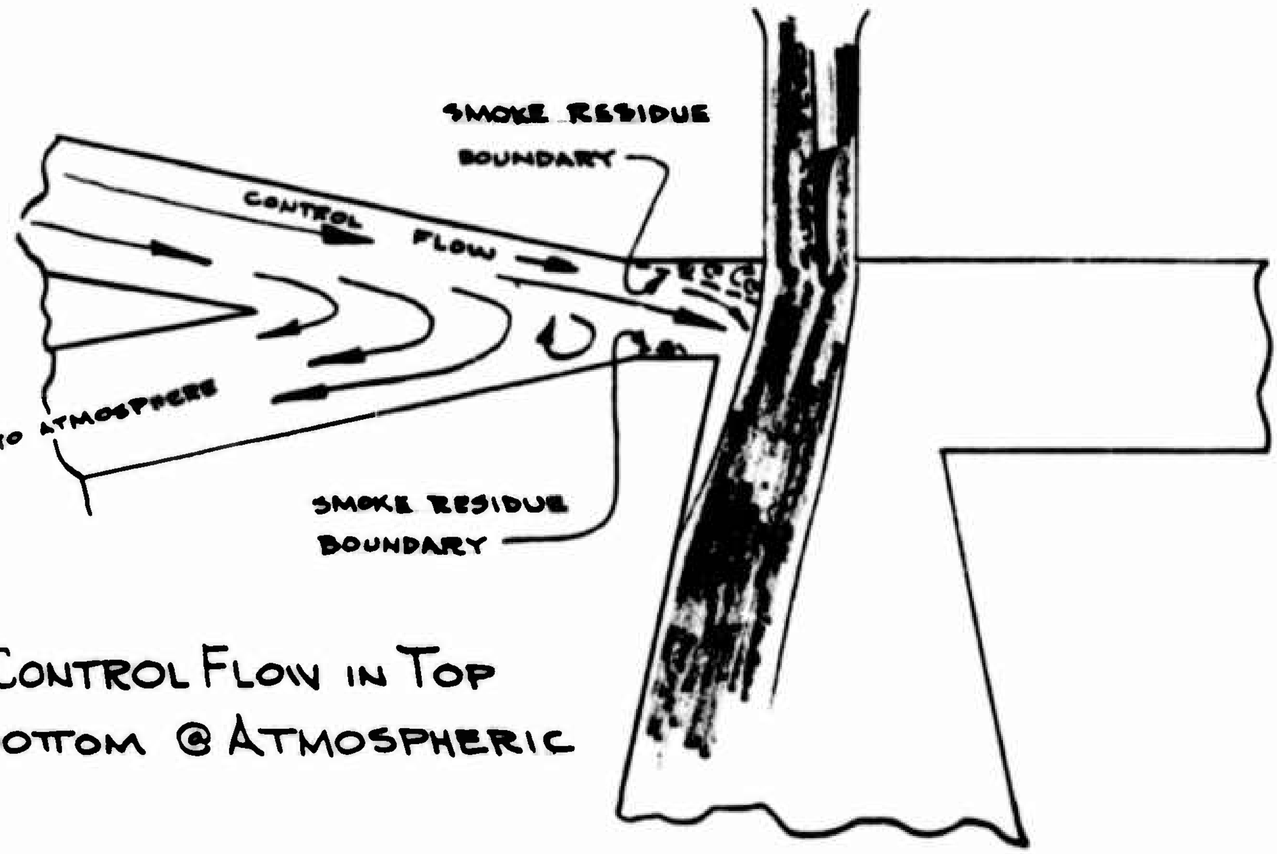

CONTROL FLOW IN TOP
BOTTOM @ ATMOSPHERIC

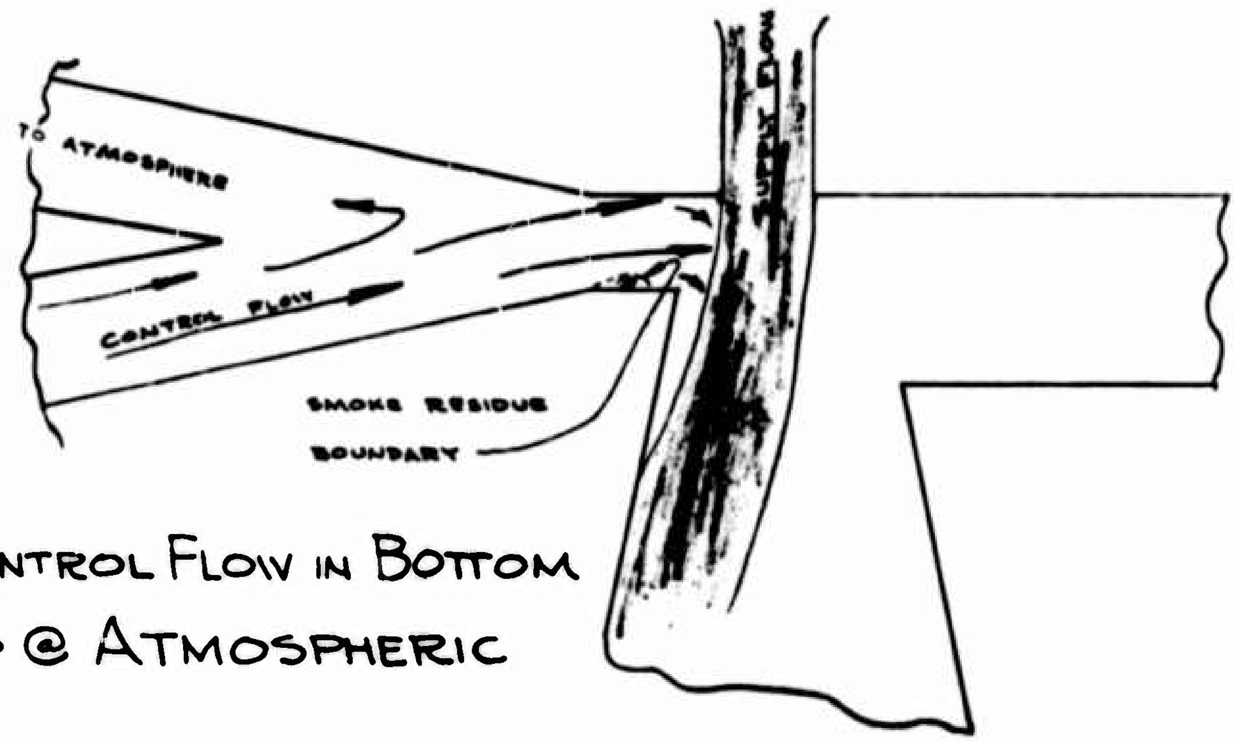

CONTROL FLOW IN BOTTOM
TOP @ ATMOSPHERIC

FIGURE 8

taking place in the critical areas. This vortex action does not appreciably effect the lower control but greatly effects the upper by apparently increasing the effective resistance at the point of impact with the power stream and allowing a relatively large amount of "waste flow" to pass out the inactive bottom control. In an attempt to minimize the effect of this phenomena three new designs were processed.

Design 15, Figure 9, moved the intersection of the two controls closer to the power stream in the belief that such a move would tend to balance the switching points. However, as noted on the curve in Figure 10, the upper control pressure actually increased, and it would appear that the closer the lower control channel to the vortex region, the more efficient it becomes in venting the control flow from the upper channel; hence the higher the pressure required to obtain enough flow to switch the power stream. Design 16, Figure 11, decreased the angle of approach between the top control channel and the power stream. From the curve in Figure 12 it is obvious that the controls were balanced rather well but that both switching points increased, indicating that the effective resistance due to the vortex phenomena in this design effected the lower control as well as the upper. The third design, #17, Figure 13, was made in an attempt to decrease the effective resistance of the control opening by removing a small amount of material from the corner between the control opening and the attachment wall. It was reasoned that this would decrease the resistance at the point of impact of the power stream and control stream by streamlining the flow at this point. The curve shown in Figure 14 not only indicates that the desired results of balancing the controls were attained but also suggests

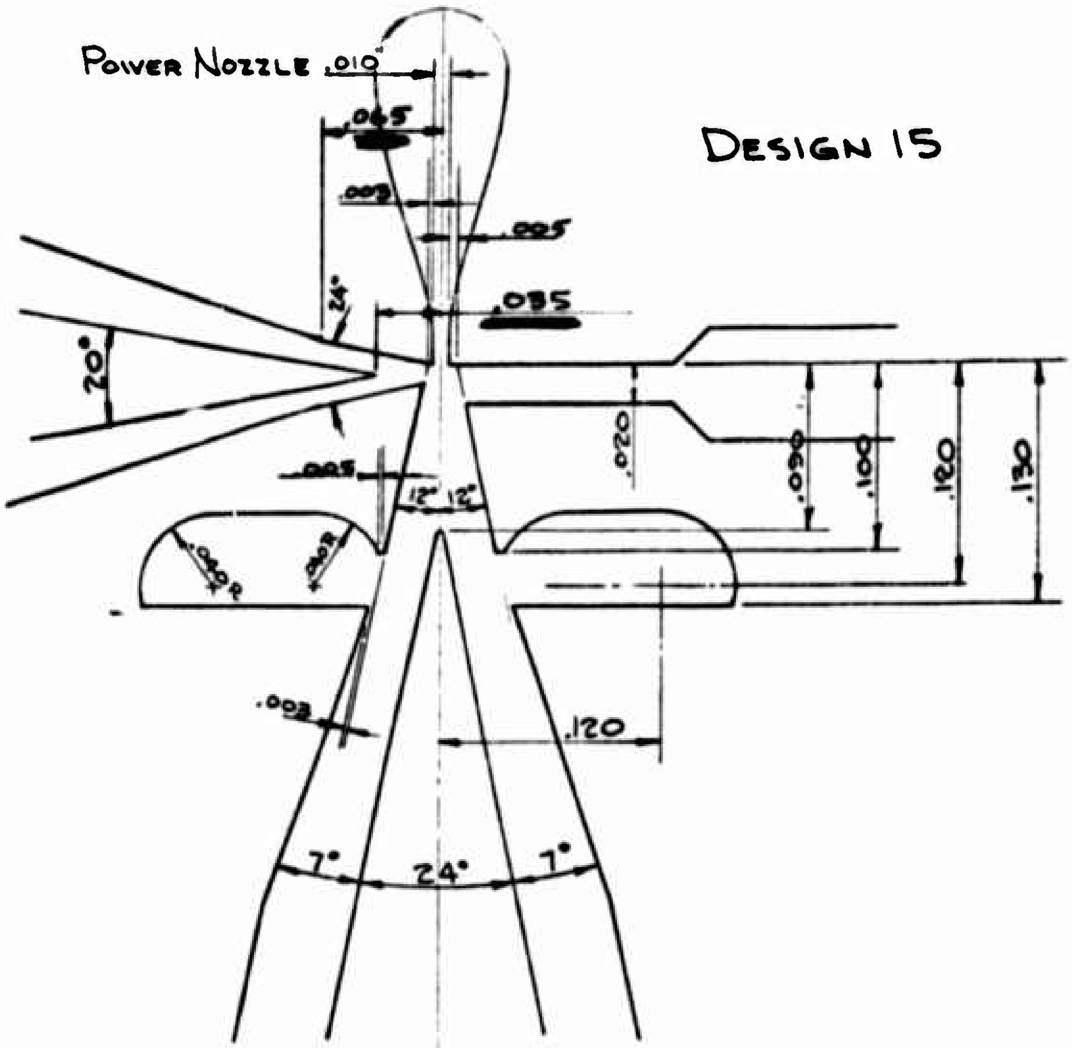

Design 15

Figure 9

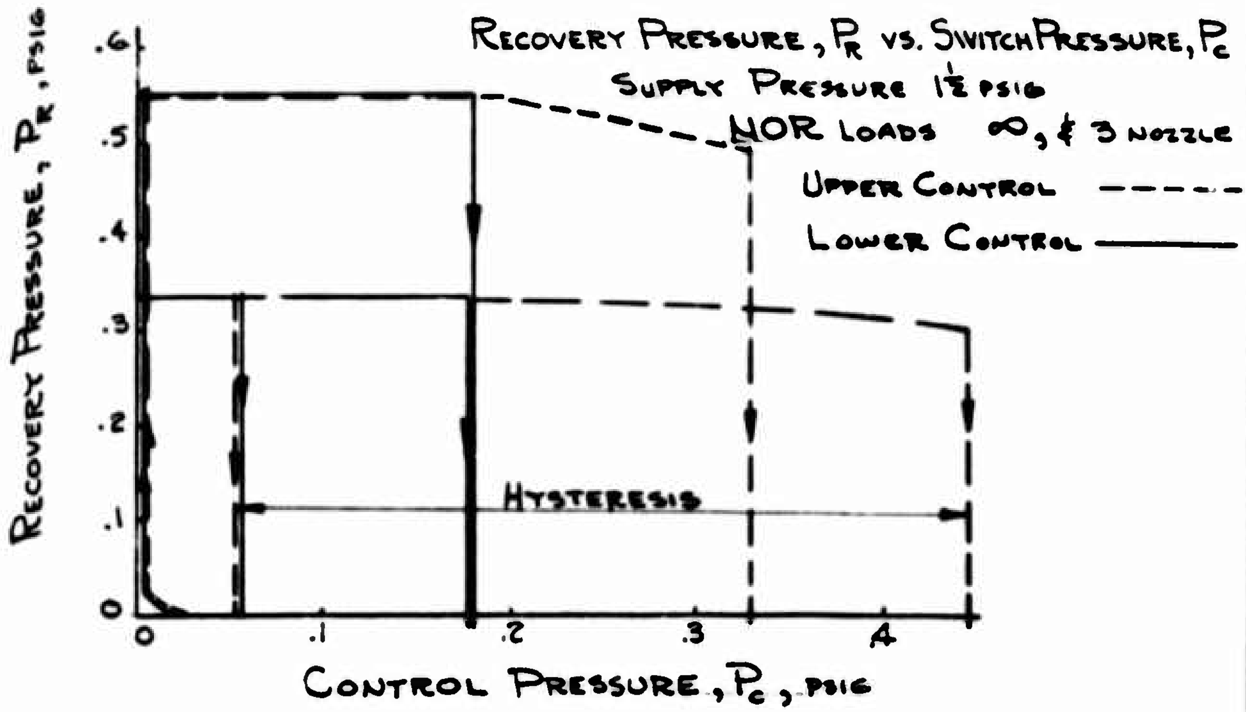

Figure 10

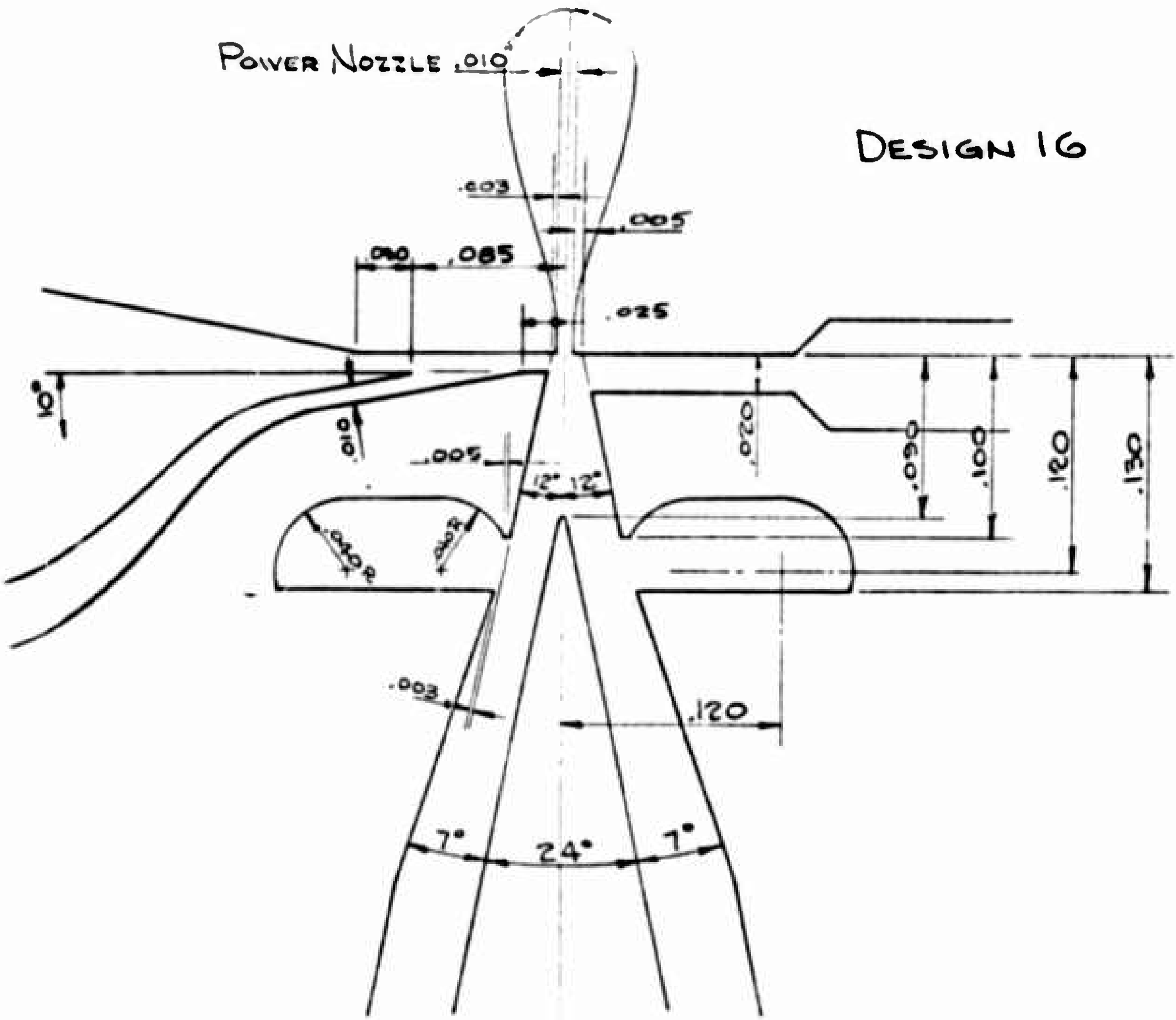

POWER NOZZLE .010
DESIGN 16
.003
.005
.010
.085
.025
10°
.010
.005
.020
.090
.100
.120
.130
12° 12°
.040R
.040R
.003
.120
7°
24°
7°

FIGURE 11

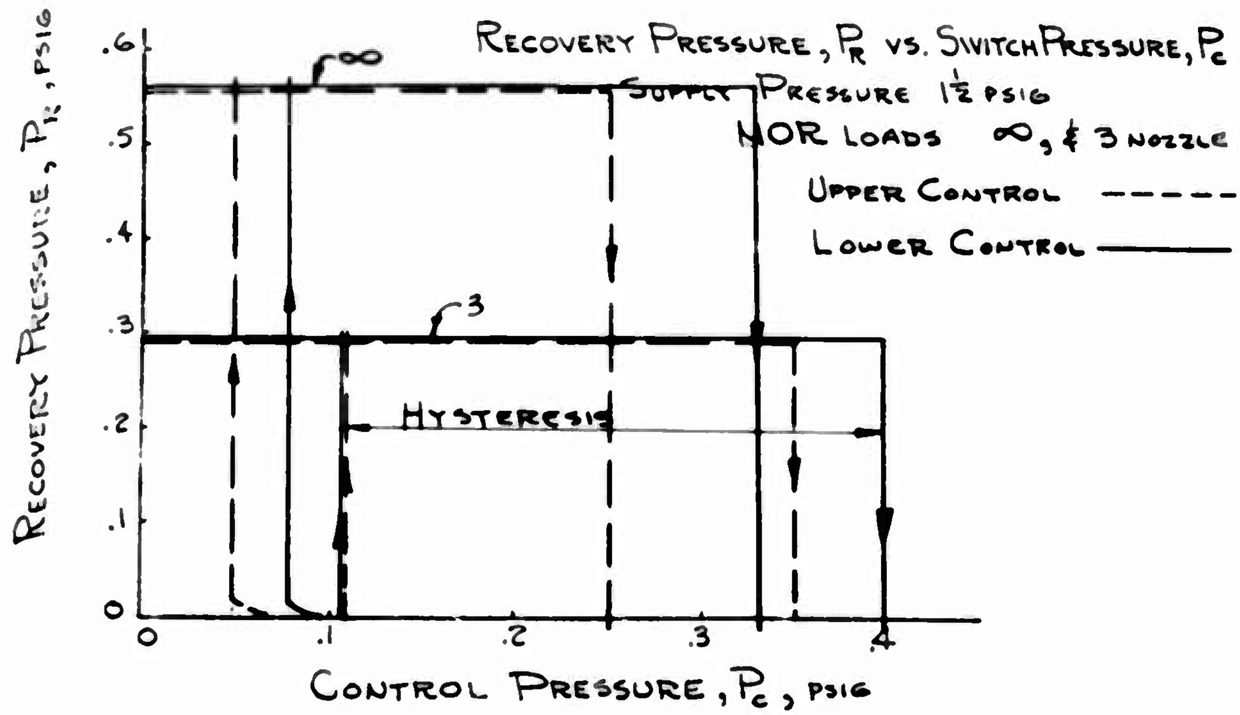

RECOVERY PRESSURE, P_R VS. SWITCH PRESSURE, P_c
SUPPLY PRESSURE 1½ PSIG
NOR LOADS ∞, & 3 NOZZLE
UPPER CONTROL
LOWER CONTROL
∞
3
HYSTERESIS
RECOVERY PRESSURE, P_R, PSIG
CONTROL PRESSURE, P_c, PSIG
0
.1
.2
.3
.4
.5
.6

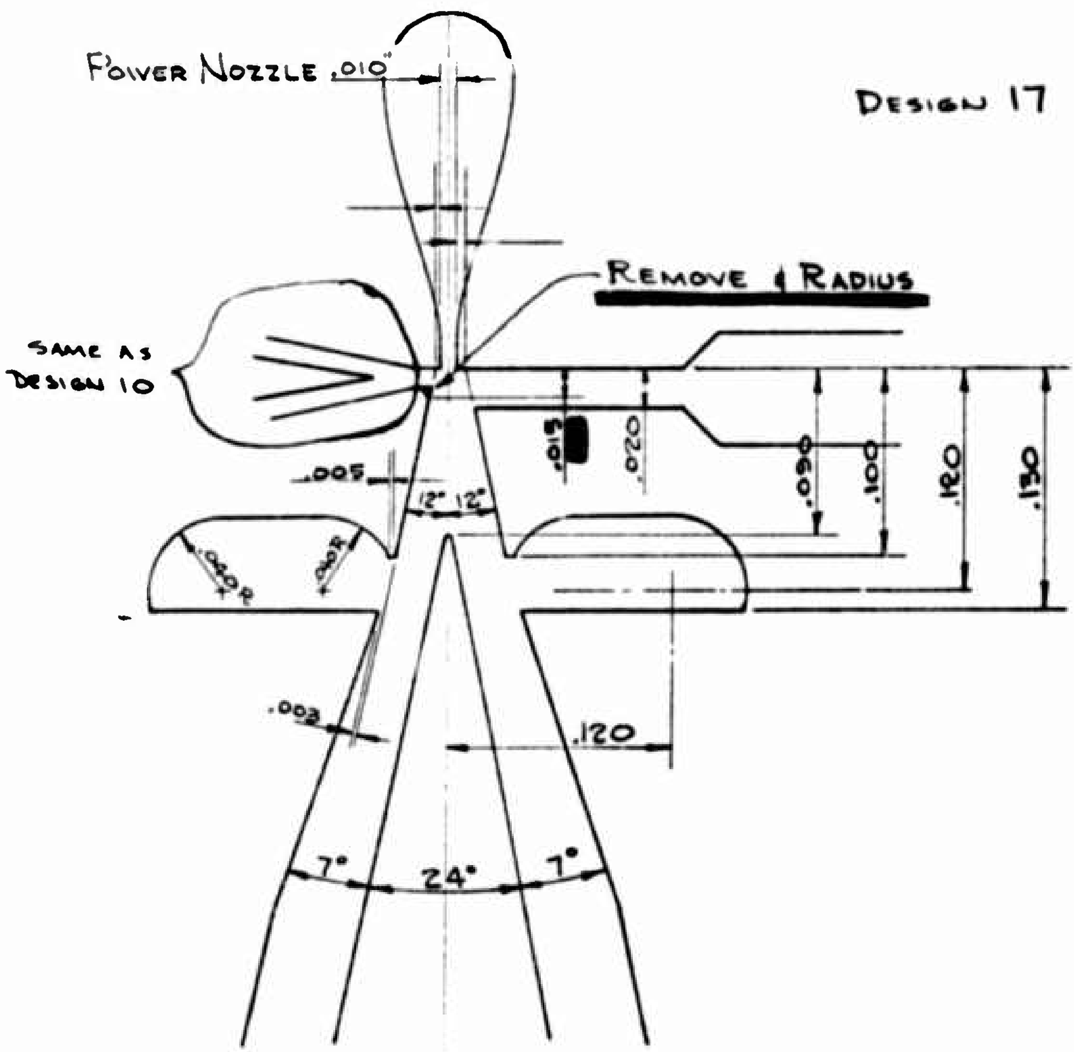

FIGURE 13

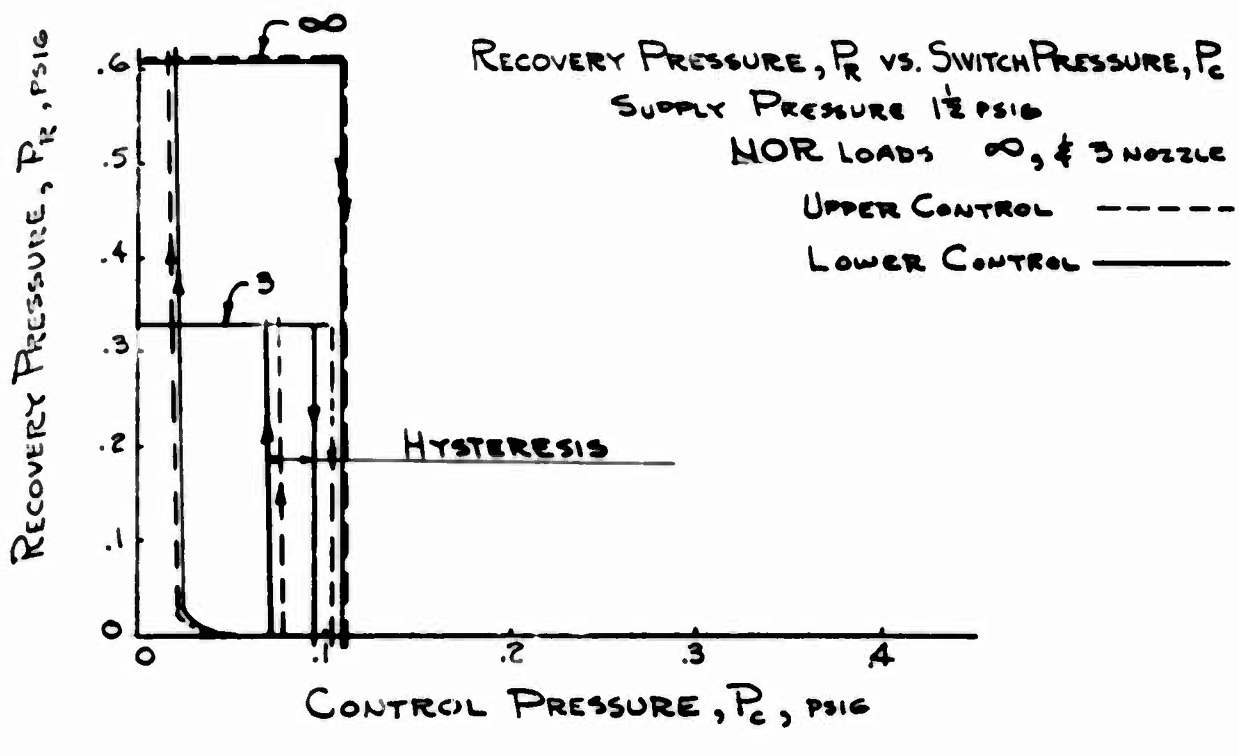

FIGURE 14

that the return pressure is increased thus decreasing the hysteresis loop.

INTERCONNECTION

Having achieved what was felt to be a reasonably stable device for use in breadboard circuits, proof of its ultimate potential required fabrication of a reasonably complex multi-layer, diffusion bonded circuit. Although the interconnection of fluid devices introduces many unique problems, most of these problems can be avoided if the circuit is designed well within the operating capabilities of the basic devices used, or conversely, if the circuit design is such that the devices included are required to operate under any marginal conditions, unexpected pressure inconsistencies combined with marginally performing gates might well result in erratic operation.

In order to establish the validity of this reasoning it was decided to design the circuit well within the capabilities of the NORgate, while, in effect, making no effort to design around potential interconnection problems. With this in mind, the following design parameters were established:

1) Fan-out - although the gate, as designed, could generally be expected to actuate six similar devices, fan-out was limited to four, to assure stable operation.

2) Complexity - the circuit should have a minimum of ten gates in a minimum of ten plates.

3) Size - all gates would have .010" wide power nozzles, and the plates would be designed to have vertical symmetry, thereby simplifying artwork preparation

and venting.

4) <u>External connections</u> - there would be no test taps, and as many devices as possible would vent into common sumps, thereby minimizing external porting. In addition, all devices would be fed from a common supply port.

5) <u>Components</u> - only two input OR-NOR gates would be included in the circuit in order to avoid malfunctions not directly attributable to the component being tested.

At the time this test was being formulated several circuits were being developed, and from these, the one selected as being most readily adaptable to the previously stated conditions was the binary to decimal converter.

BINARY TO DECIMAL CONVERTER LOGIC DESIGN

There are, of course, many basic logic designs which will accomplish the conversion from a binary number to a decimal number, one of which is that shown in Figure 15. This particular design was chosen because it utilizes only two input OR-NOR Gates with a maximum fan-out of four. The eighteen gates included could easily be laid out on ten plates.

The design is obviously negative nor logic, with the eleven gates in line representing the ten decimal numbers, plus a reset, and the seven gates in line connected to represent the four possible combinations from the one and two counters, and the three combinations required from the four and eight counters.

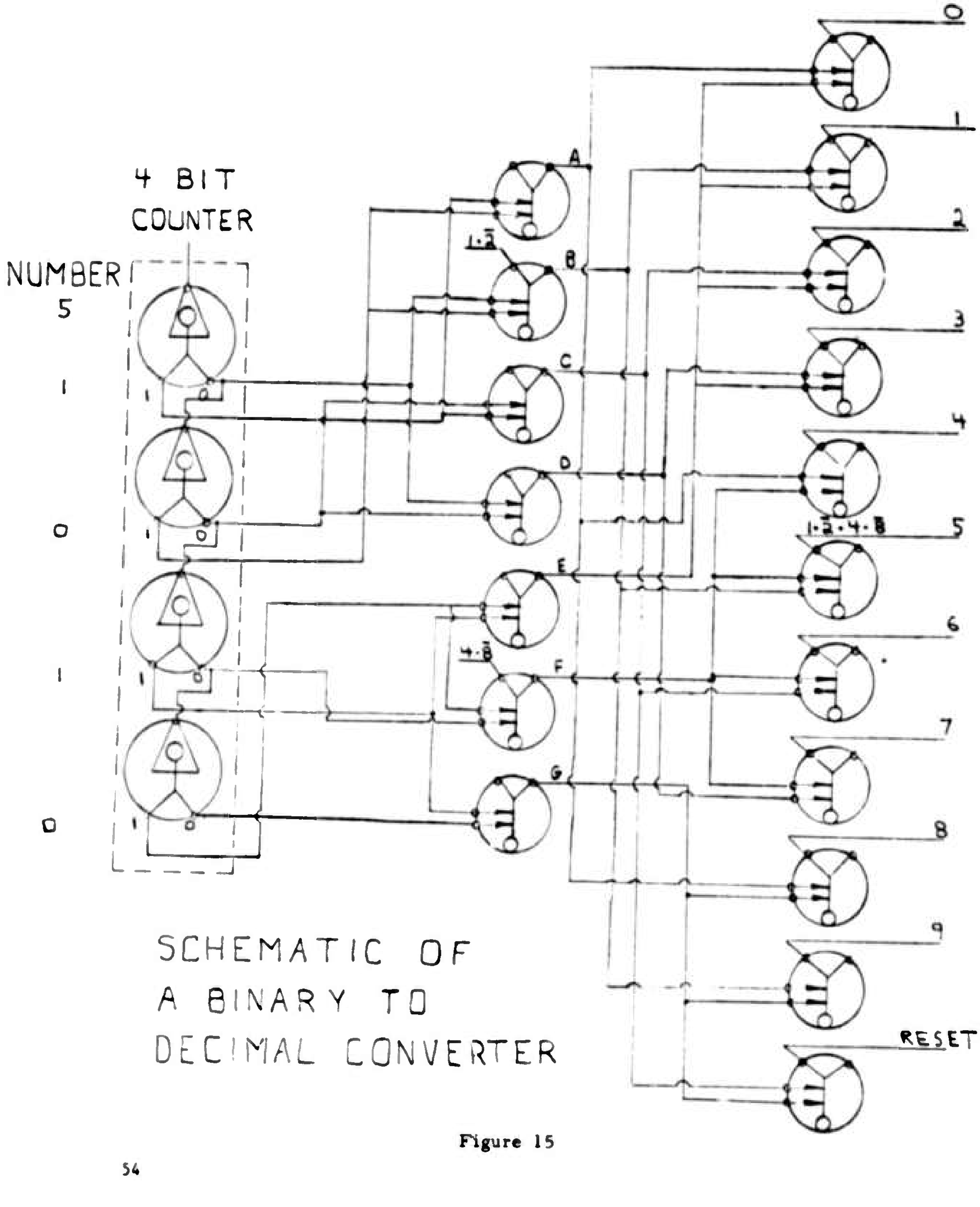
4 BIT
COUNTER
NUMBER
5
1
0
1
0
A
B
C
D
E
F
G
1·2̄
4·8̄
1·2̄·4·8̄
0
1
2
3
4
5
6
7
8
9
RESET
SCHEMATIC OF
A BINARY TO
DECIMAL CONVERTER

Figure 15

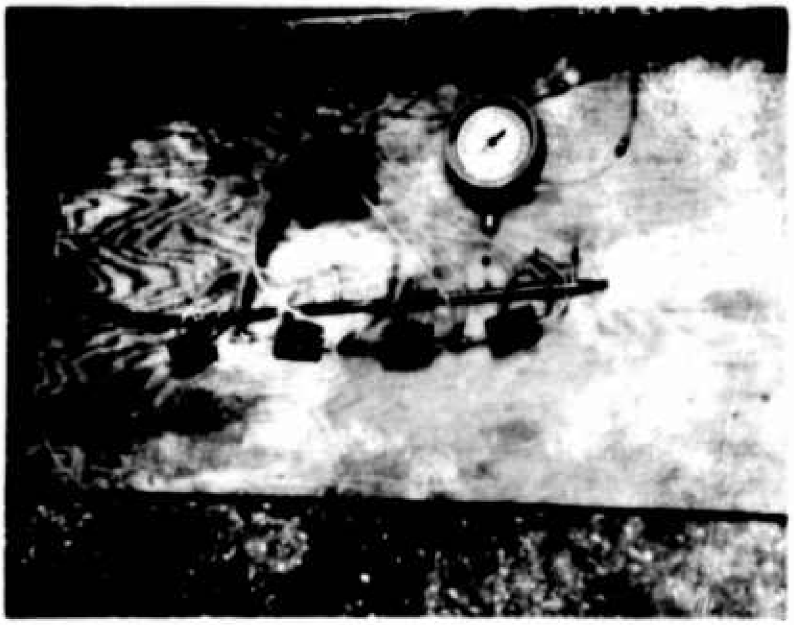

Figure 16

Figure 16 shows the converter as breadboarded prior to final design, with the counter below the manifold and the converter above, while Figure 17 shows the same layout with the converter produced in module form. The counter part of the circuit was not included in the block to avoid other than nor logic.

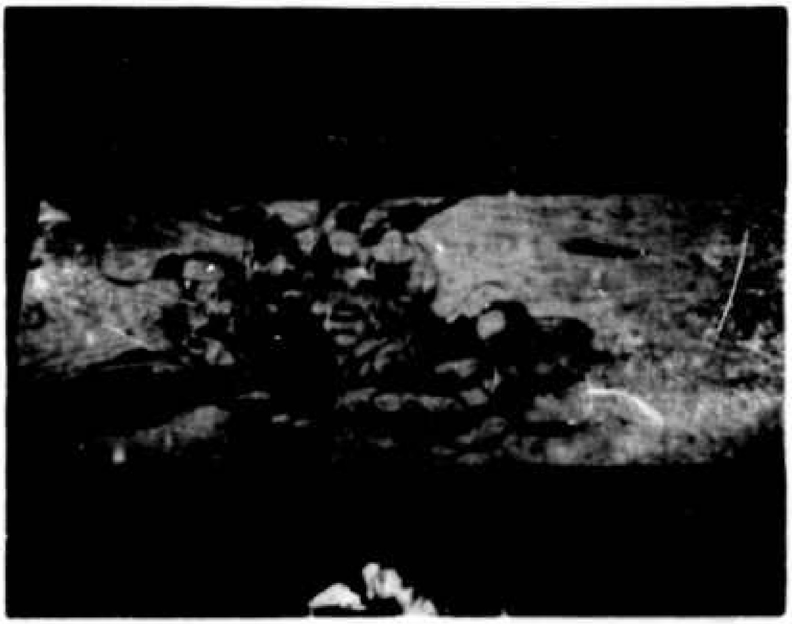

Figure 17

ASSEMBLY DESIGN

The assembly was designed with the gates placed in the same relative position on each plate, as shown in Figure 18. Although it is readily apparent that there is considerable wasted space on each plate, this design technique greatly simplifies artwork preparation and venting, and is felt to be justified until such time as size and weight become critical.

The four plates running clockwise from the top contain the seven gates which receive the signals from the counters, and the remaining five plates show nine of the eleven readout gates. One active plate and the coverplate are not shown. The device pictured in the lower left-hand corner is a standard NOR-gate of the type used in assembling the breadboard circuit.

CIRCUIT PERFORMANCE

Two converters were fabricated and stacked as shown in Figure 19, and both of them performed as intended, up to approximately 100 cps. This would certainly seem to indicate that the NORgate, as developed, is adequate for circuit fabrication as long as it is not required to function under marginal conditions. It is quite probable that this same device would malfunction if included in a circuit requiring a fan-out of five, even though designed to fan-out to six, because it is certainly not unreasonable to expect one slightly sub-standard device out of eighteen, and the fabrication techniques used do not permit replacement. Figure 20 presents the input and output characteristics of the converter.

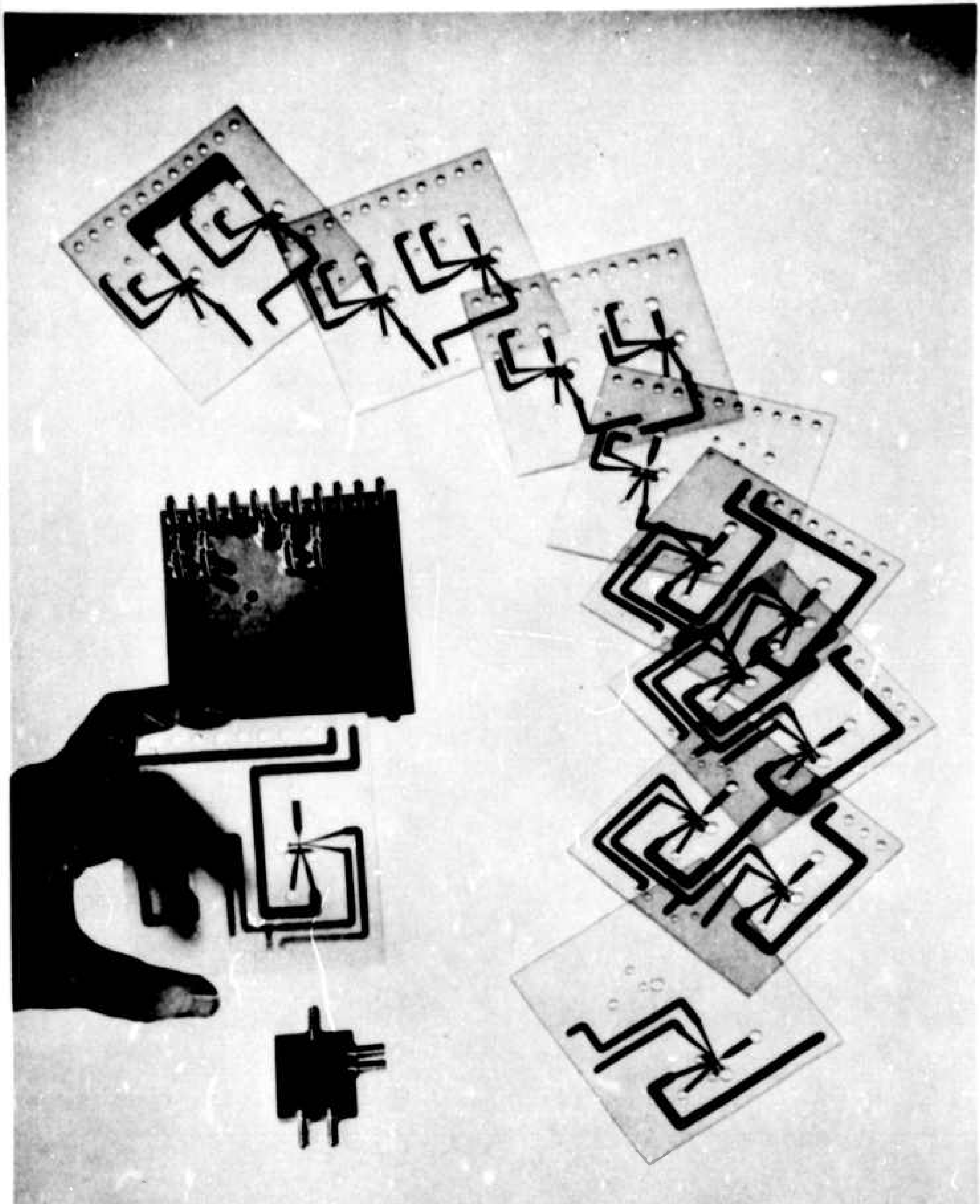

Figure 18

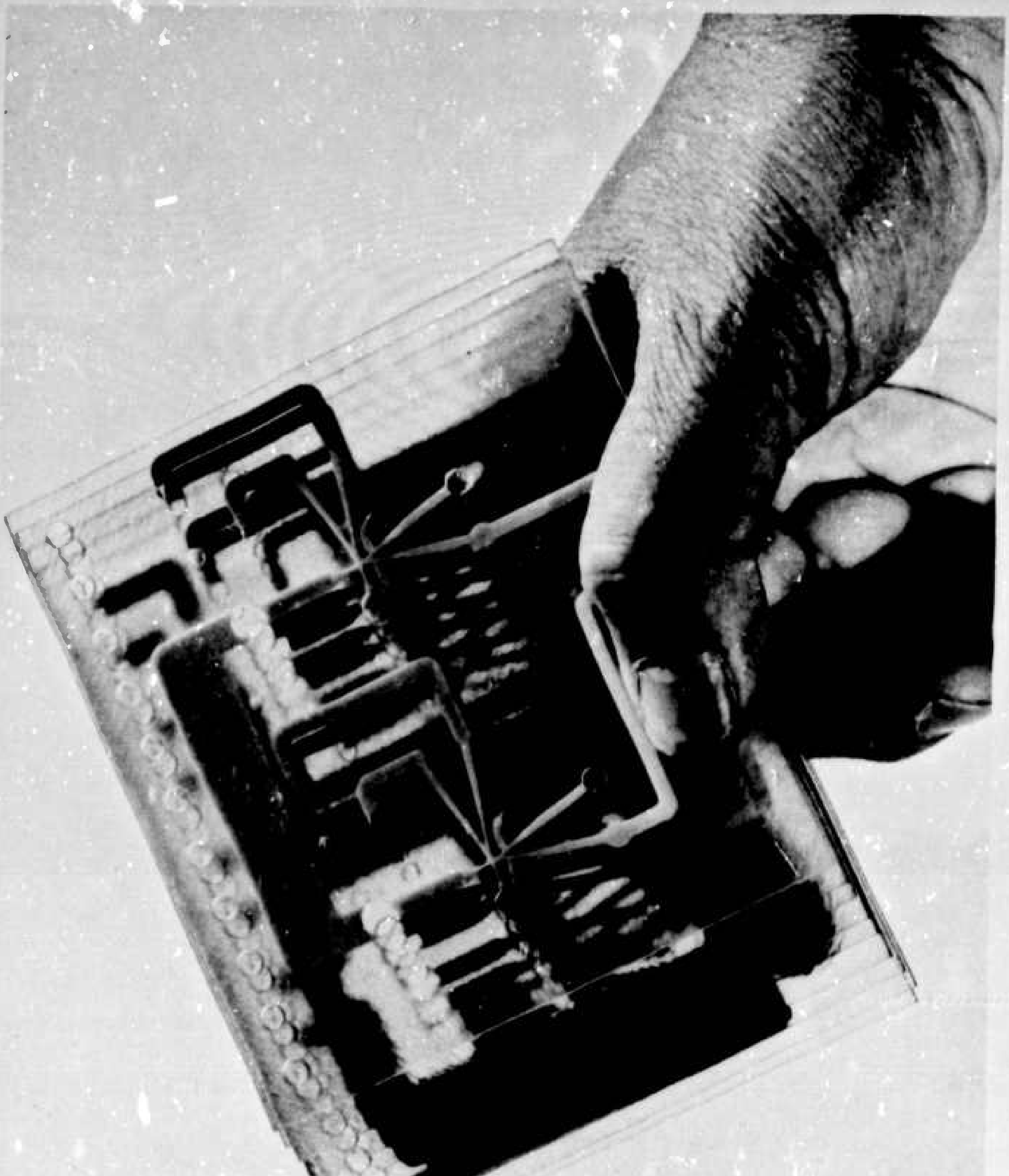

 Figure 19

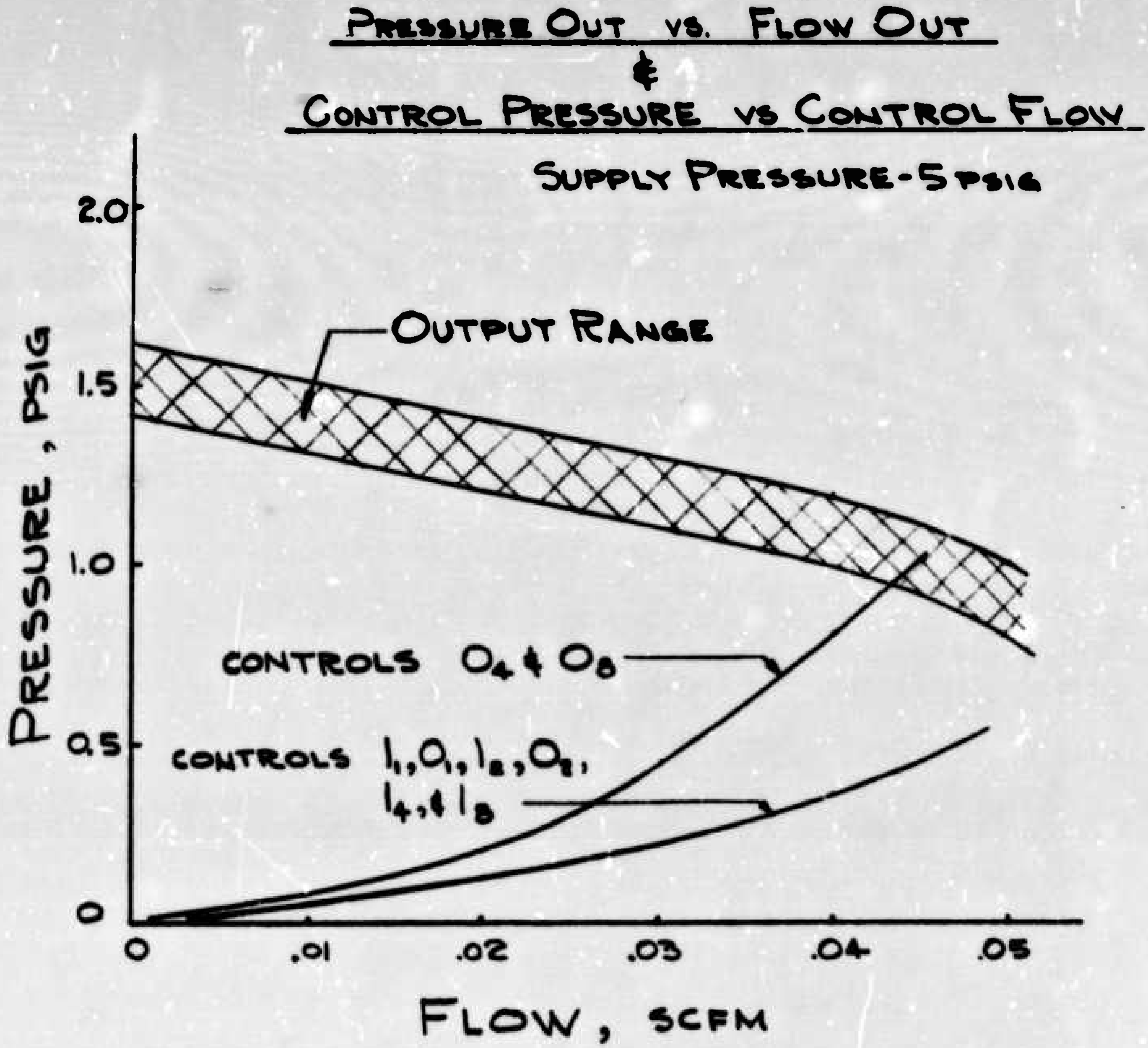
PRESSURE OUT VS. FLOW OUT
&
CONTROL PRESSURE VS CONTROL FLOW
SUPPLY PRESSURE-5 PSIG
OUTPUT RANGE
CONTROLS O4 & O8
CONTROLS I1, O1, I2, O2, I4, & I8
2.0
1.5
1.0
0.5
0
0
.01
.02
.03
.04
.05
PRESSURE, PSIG
FLOW, SCFM

Figure 20

CONCLUSIONS

It would appear that an effective method of geometrically biasing a bistable unit incorporates both a slight wall offset and an enlarged control area. Once this is accomplished and an input control width is established, 010" in this case, the operating characteristics of the unit become relatively fixed for various changes in attachment wall distances and two-input configurations. Possibly the most significant accomplishment was recognizing the apparent interaction of the control stream with the power stream and the rather elementary solution of streamlining the flow at the critical area.

The final analysis of the value of the NORgate described will not be available until data are obtained relating the fan-out of the NORgate to selection. However, the binary to decimal converter did demonstrate that fabrication of reasonably complex NOR-logic circuits in multi-layer, diffusion sealed blocks, can be accomplished.

REFERENCES

1. Warren, R. W. - "Interconnection of Fluid Amplification Elements" - Fluid Amplifier Symposium, May 1964.

2. Van Tilburg, R. W. - "Production of Fluid Amplifiers by Optical Fabrication Techniques" - Fluid Amplification Symposium, October 1962.

3. Warren, R. W. - "Bistable Fluid Amplifiers" - Fluid Amplification Seminar, June 1964.

HARRY DIAMOND LABORATORIES
WASHINGTON, D. C. 20438

A PNEUMATIC TAPE-READER

by

NORMAN A. EISENBERG

ARMY MATERIEL COMMAND DEPARTMENT OF THE ARMY

INTRODUCTION

One large class of tape-readers are those that decode paper tapes punched with holes; i.e.,the pattern of holes in the tape is translated into a typed message. Both electrical and pneumatic systems are available commercially to perform this function. The tape-reader described in this paper uses flueric devices.

Pneumatic tape-readers have been available for many years. The main use of these machines is the typing of duplicate letters. Thus businessmen are able to send apparently individually typed letters at a much lower cost than letters individually typed by a human typist. These tape-readers use a piano-roll type tape with hole positions corresponding to each character or control instruction; i.e.,there are about 50 hole positions in a tape.

Likewise electrical tape-typewriter systems have been extant for many years. The electric machines are also used to duplicate letters. In addition,the electric machines are capable of processing standard forms upon which duplicate information is to be typed together with some special information on each form; in other words, the electric machines can insert specific bits of typed information at the desired locations in a standard form. The electrical machines may also be tied in with more sophisticated business systems, which use electronic digital computers. These tape readers use an eight-hole tape; each character or control function has a combinatorial code using six bits. One hole position is used for a parity check

and the remaining position is used for the carriage return.

The system described in this paper combines the reliability of pneumatics with the flexibility of the electric system.

THE SYSTEM AS A WHOLE

The tape-reading system (fig. 1) comprises two interlocking subsystems, the main logic subsystem and the control subsystem. The primary task of translating the tape falls to the main logic subsystem, which converts the pattern of holes in the tape into pneumatic signals, amplifies these signals, feeds the amplified signals into decoding elements, and actuates the typewriter.

The control subsystem allows the operator of the tape-reader to regulate the translation process. This subsystem is responsible for advancing the tape across the reading head at the proper speed and synchronizing this motion with the main logic subsystem. Figure 2 is a photograph of the rear of the system.

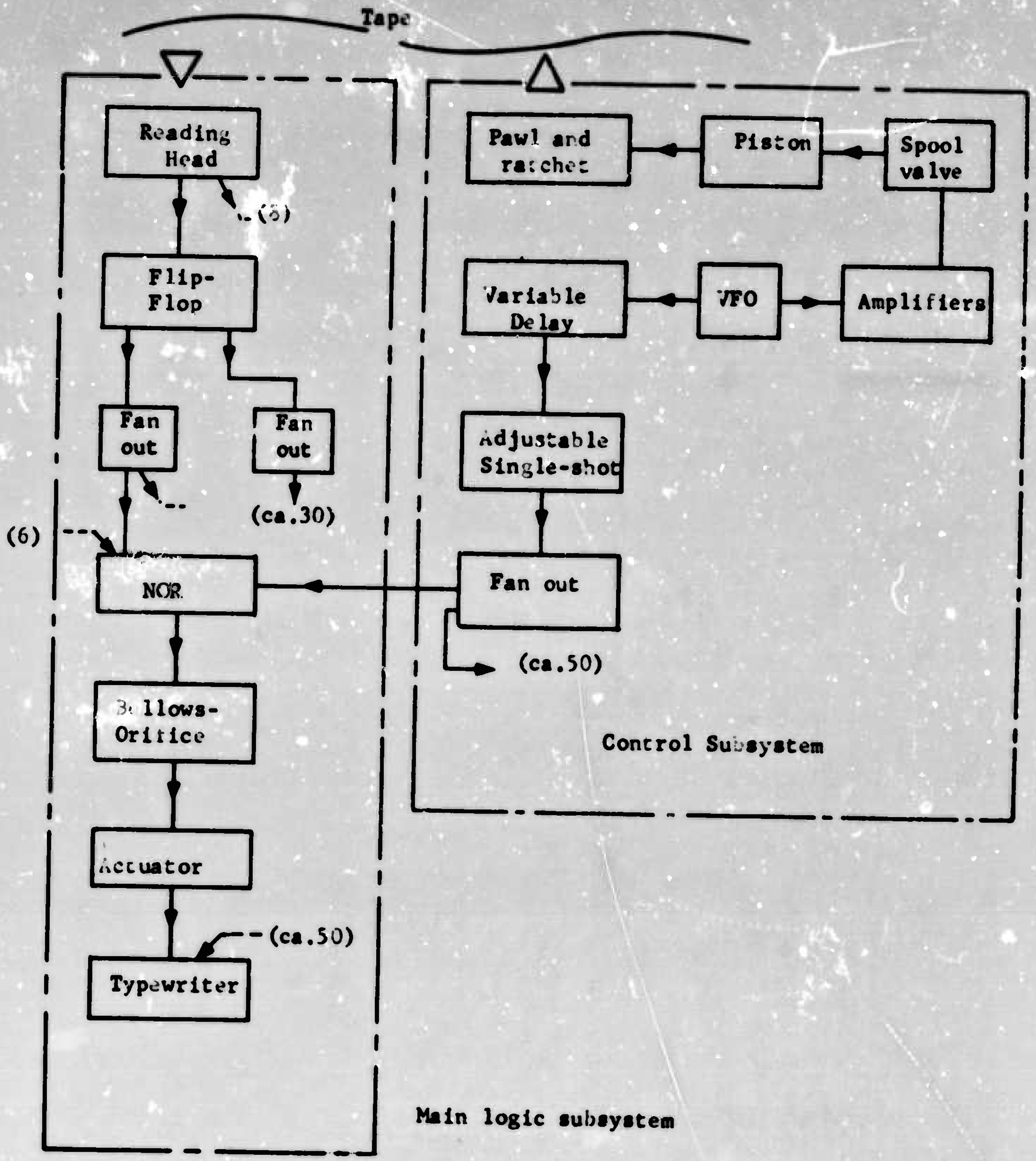

Figure 1. Block diagram of the tape-reader system

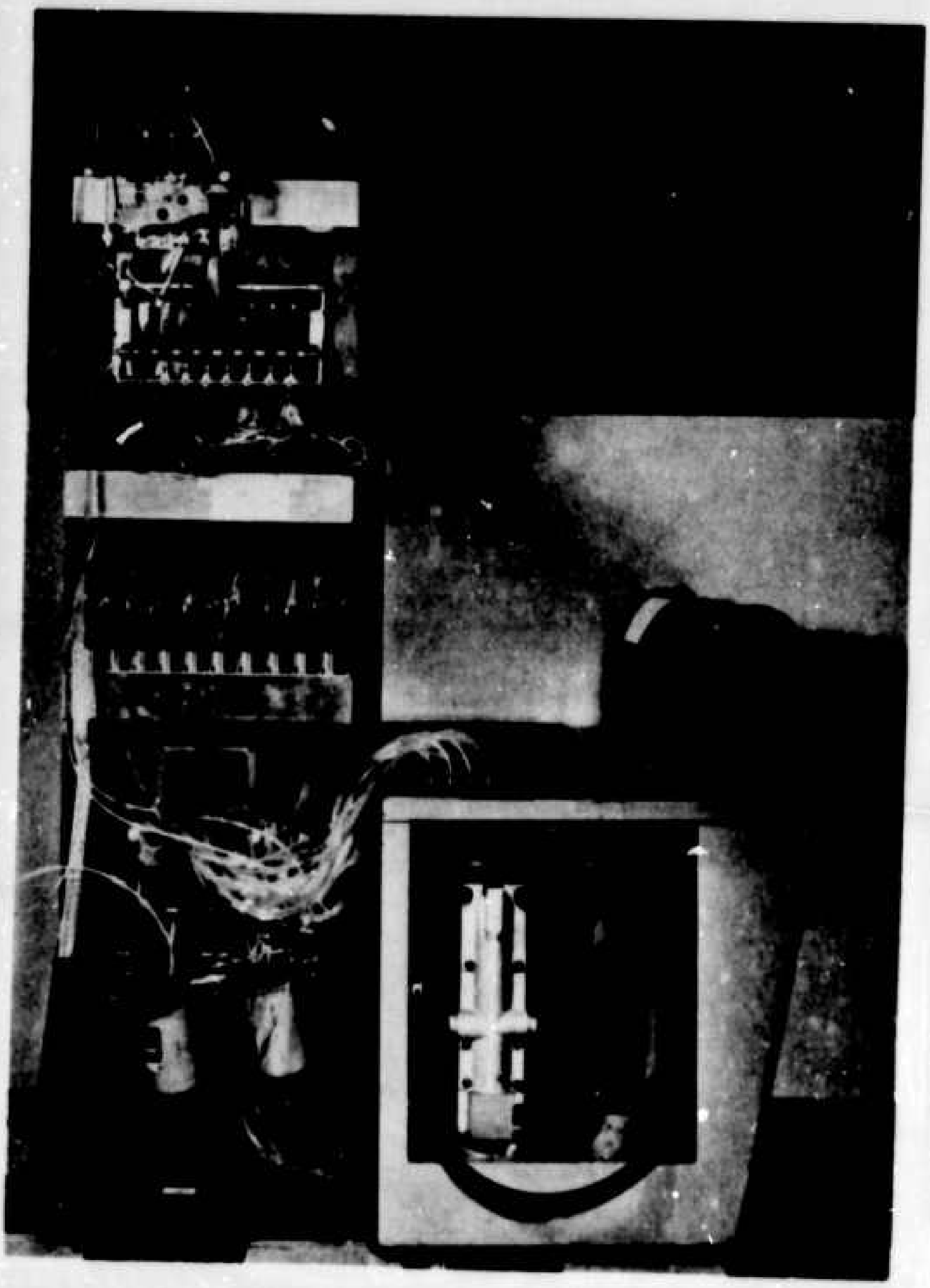

Figure 2. Rear view of assembled tape-reader system

THE MAIN LOGIC SUBSYSTEM

The first stage of the main logic subsystem is the reading head (fig. 3), which consists of two sets of eight orifices. The orifices are cut into two opposing plates between which the tape moves. The spacing of the holes in both plates corresponds to the spacing of hole positions in the paper tape. The region behind the upper plate is pressurized so that the upper set of orifices emits air jets. The orifices in the lower plate are individually connected to eight transmission tubes. As the tape moves between the plates, depending on whether or not a hole appears in a given tape position, either the transmission tubes receive a pressure step derived from the dynamic pressure of the emitted air jets passing through the hole in the tape, or the end of the transmission tube in the reading head is closed off by the paper tape.

The combinatorial logic that decodes the tape requires two types of signals: (1) signals that are high when there is a hole and low when there is not and (2) signals that are low when there is a hole and high when there is not; that is,the logic system requires a signal indicating both the presence and absence of a hole. To produce these two types of signals and also to amplify the signals originating in the reading head, the eight transmission tubes from the reading head are connected to a set of eight flueric flip-flops.

Each transmission tube is connected to one control port of a flip-flop and the other control port is left open to atmospheric pressure. When the tape position corresponding to a given flip-flop has no hole in it, the transmission tube is closed at the reading head end. Because

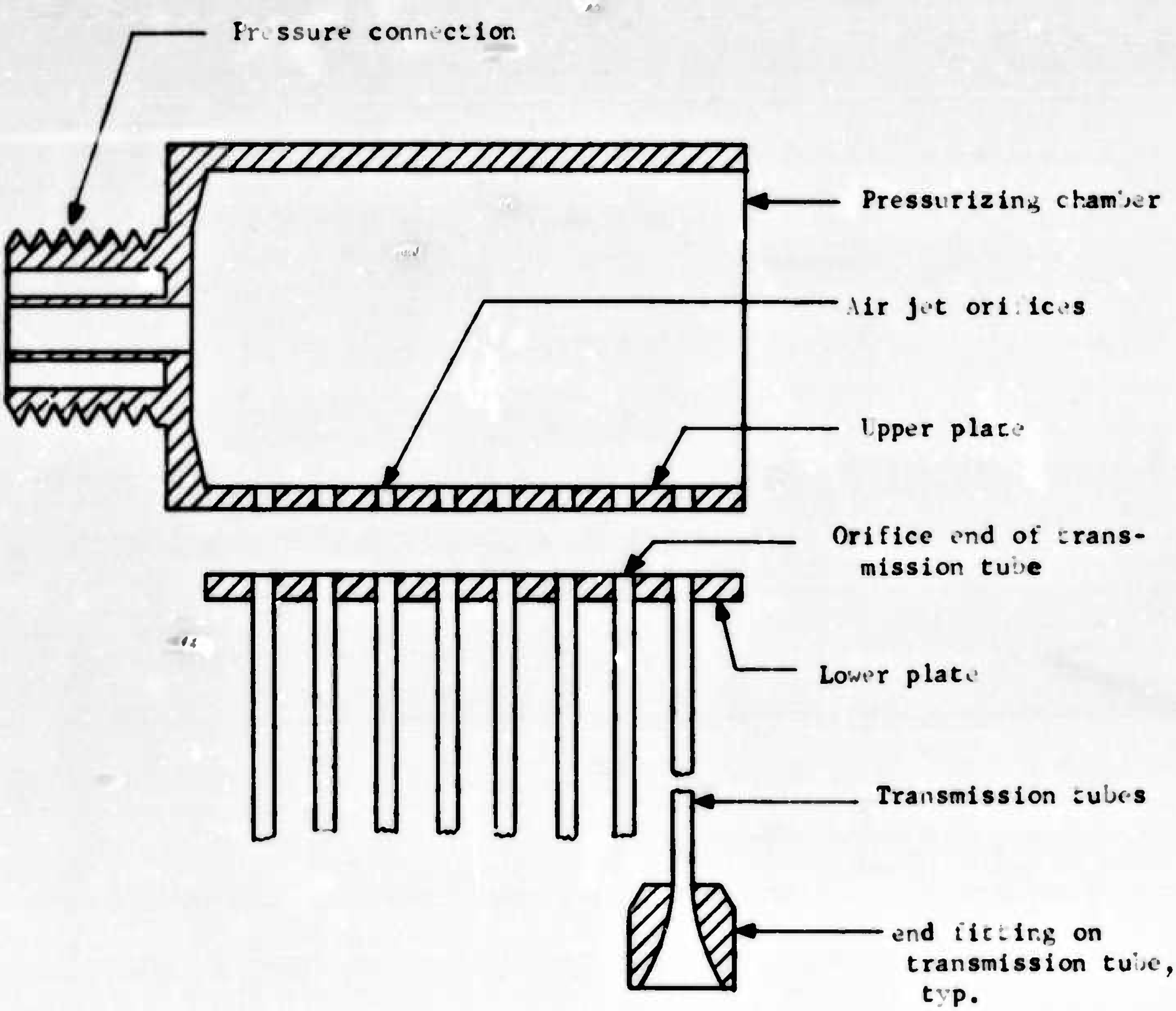

Figure 3. Schematic of the reading head

the flip-flops used are of the type in which sealing off a control port while the opposite control is open to atmosphere switches off the unit, the absence of a hole in the tape will cause the flip-flop to switch to the side connected to the reading head.

On the other hand when a hole appears in the tape position corresponding to a flip-flop, if the pressure producing the air jets in the head is sufficiently high, the pressure received in the transmission tube will cause the flip-flop to switch to the opposite side. Hence the outputs of the flip-flops are the Boolean functions X and $\bar{X}$, where X is defined as follows:

$$X = \begin{cases} 1 \text{ if there is a hole in the Xth tape position} \\ 0 \text{ if there is not a hole in the Xth tape position} \end{cases} \quad (1)$$

$\bar{X}$ is of course the Boolean complement of X.

With these two Boolean functions available for each of the eight tape positions, it is possible to produce all the combinations of inputs making up the code. The code used is one of the standard Friden Flexowriter codes. The eighth tape position is used only for the carriage return, and the fifth position is the parity bit; thus to simplify the decoding circuitry, the eighth and fifth positions were ignored and a six-bit decoding circuit was built. The parity bit is used to make an odd number of holes in the code of any character. Many erroneous codes in the tape can be detected by checking to make sure that the number of holes for any code is odd; that is, checking the parity. A parity checking circuit was not built into the present system, however, because it was not believed necessary for demonstration purposes.

Although the Boolean functions available from the flip-flops would permit the use of either AND or NOR elements for decoding, turbulence amplifiers (NOR elements) were chosen as the decoding elements (fig. 4). When there is no input to the turbulence amplifier, the output recovers a dynamic pressure from a laminar jet; when an input is received, the jet becomes turbulent, and, because of the difference in energy dissipation between laminar and turbulent flows, a much lower pressure is recovered by the output. The turbulence amplifiers used have eight input terminals. Since the turbulence amplifier behaves as a NOR element, for inputs Y_i, the output Z is

$$Z = \overline{Y_1 + Y_2 + Y_3 \; . \; . \; . + Y_k + . \; . \; .} \qquad (2)$$

However, since the code for a character is a Boolean AND function, a Boolean algebraic manipulation must be made to determine the inputs to the turbulence amplifier necessary to produce the proper response. The code for A, for example, has holes in the first, sixth, and seventh positions. Hence ignoring, as previously stated, the fifth and eighth positions

$$A = 1 \cdot \overline{2} \cdot \overline{3} \cdot \overline{4} \cdot 6 \cdot 7$$

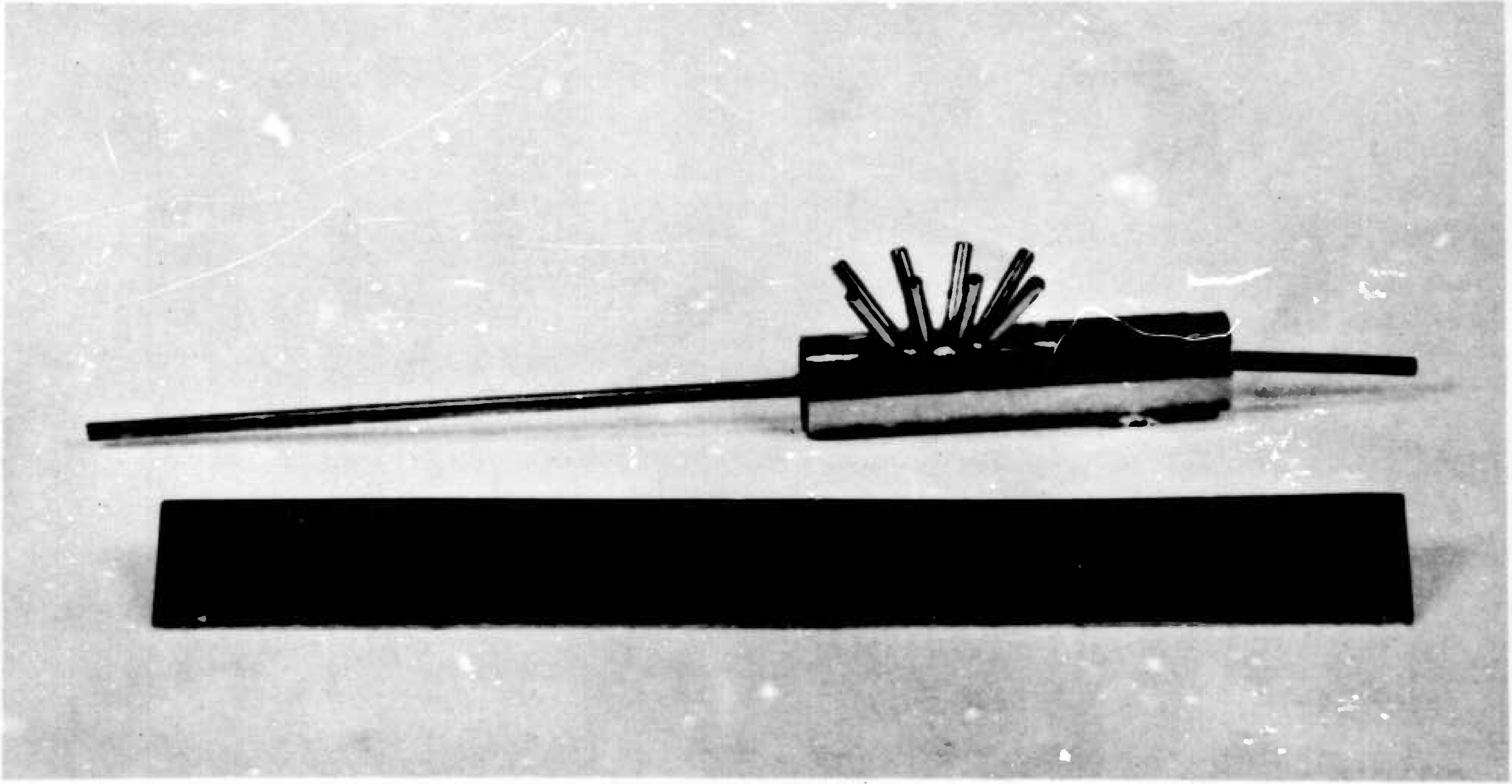

Figure 4. A single turbulence amplifier

Now, an extension of DeMorgan's Rules shows that if

$$F = U_1 \cdot U_2 \cdot U_3 \cdot U_4 \cdot U_5 \cdot U_6 \qquad (3)$$

then

$$F = \overline{\bar{U}_1 + \bar{U}_2 + \bar{U}_3 + \bar{U}_4 + \bar{U}_5 + \bar{U}_6} \qquad (4)$$

where, as is customary, · is the Boolean AND operation, + the Boolean OR operation, and - is the Boolean inversion.

A comparison of (2), (3), and (4) shows that if

$$F = U_1 \cdot U_2 \cdot U_3 \ldots$$

then the variables $\bar{U}_1$, $\bar{U}_2$, and $\bar{U}_3$ . . . must be supplied to the inputs of a turbulence amplifier so that its output will be F.

Since the same variables are required as inputs to several NOR elements, fanouts are necessary at the outputs of the flip-flops. The fanouts used are manifolds in which the supply and output ports are mounted axially in order to reduce losses. Each fanout has 30 outputs through 0.032-in. I.D. brass tubes about 4 in. long.

Appendix I shows that if the supply pressure to the flip-flops is greater than 57.4 cm H_2O, then the steady-state operation of the main logic circuit is assured. (The dynamic problems will be treated shortly.) Thus, whenever a particular code appears in the reading head, the corresponding turbulence amplifier delivers an output pressure signal.

The remaining task of the translating system is the conversion of this pressure output into the movement of the typewriter keys. Because the primary objective was the demonstration of flueric logic devices in a complex system, the development of pneumatic-to-mechanical transducers was not considered. Instead provision was made to utilize an existing system.

The existing 50-hole tape reading system contains actuators requiring a vacuum supply. In this system the control port of the actuator is connected directly to the reading head; thus as the piano-roll tape rides over the reading head the holes in the tape allow the control port to be exposed to atmospheric pressure. When a control port is connected to atmospheric pressure, the actuator activates a typewriter key through a series of levers. The compatibility of this actuating system with several popular models of typewriters made its use in the main logic subsystem very desirable.

Because the output of the turbulence amplifiers is a pressure step above atmosphere and the input to the actuators is the partial release of a vacuum, a bellows-controlled orifice arrangement (fig. 5) was used to couple the two sets of devices. When the orifice is uncovered the actuator connected to it will pull a key on the typewriter

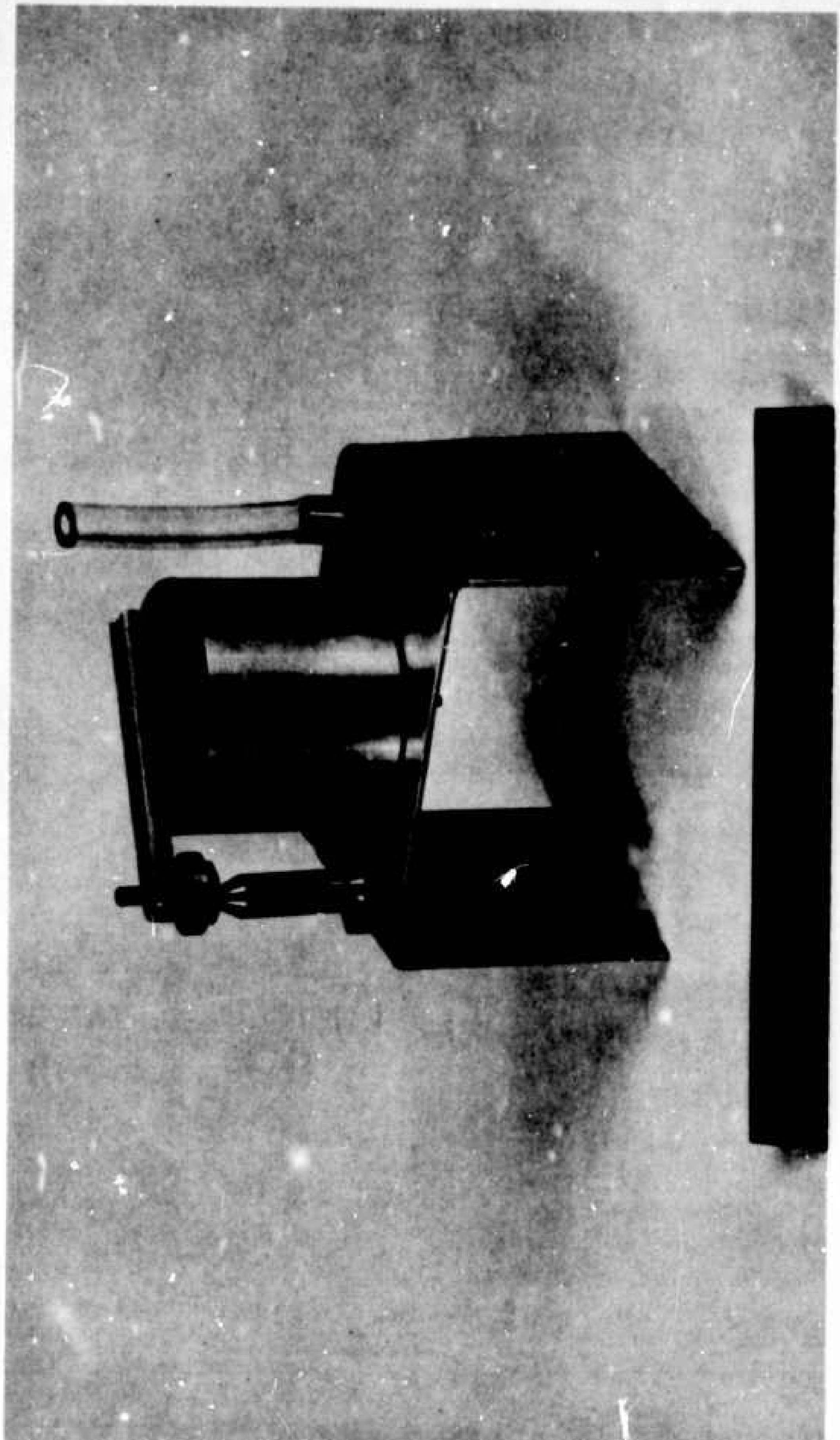

Figure 5. The assembled bellows-orifice arrangement

down. When the orifice is covered the key is released.

All the dynamic problems center around the synchronization of the pneumatic input signals to the NOR elements. The requirement is that all inputs to all NOR elements must change simultaneously for proper operation of the system described above.

Since changes in the various inputs to a NOR element cannot be made to arrive simultaneously, a means of eliminating the transient errors was developed. Because only six of the eight inputs to the NOR units are used for decoding, one of the remaining inputs is used to receive a blanking pulse. A pulse of air delivered to a NOR unit will prevent it from firing; thus a blanking pulse delivered to all the NOR units, during the time that the inputs are still changing, will prevent errors caused by the transition. The blanking pulse would be required to arrive at the NOR element a short time before a change occurs and to cease a short time after all changes in the inputs are completed; in other words, the blanking pulse would completely mask the transition period. Because the blanking pulse must be synchronized with the tape motion, the pulse originates in the control circuit and passes through a fanout to all the decoding NOR elements.

THE CONTROL SUBSYSTEM

The central component of the control subsystem is a two-output flueric trigger (fig. 6). The two outputs of the flueric trigger (ST) are Boolean complements of each other. When the input to the ST reaches a threshold level, the normally high output becomes low, and the normally low output, high. When the input reaches some lower threshold level, the outputs return to normal. The normally high output is sometimes called the low side, and the normally low output is called the high side: i.e., the outputs of the ST are named for their condition in the activated state. This type of device has been identified by the nonstandard nomenclature OR-NOR.

The ST's used in the control subsystem have integral Y connectors in the control and two outputs. The device was designed by tilting the power jet of a bistable unit (flip-flop) until it became monostable. The device has a built-in fanout of two, but the use of external Y connectors permits a fanout of five.

The control subsystem must advance the tape and provide a synchronized blanking pulse to the translating system. Because of its purposes, the control subsystem naturally separates into three main parts: (1) a central oscillator, (2) the blanking circuit, and (3) the advancing circuit. The advancing circuit contains both moving-part and no-moving-part pneumatic components, whereas the oscillator and blanking circuits are entirely fleuric.

The central oscillator is a resistance-capacitance, feedback type. Varying the value of the feedback resistor with a needle valve varies the frequency of oscillation. The frequency can be varied continuously from 5 to 11 cps. The output of the oscillator is a square

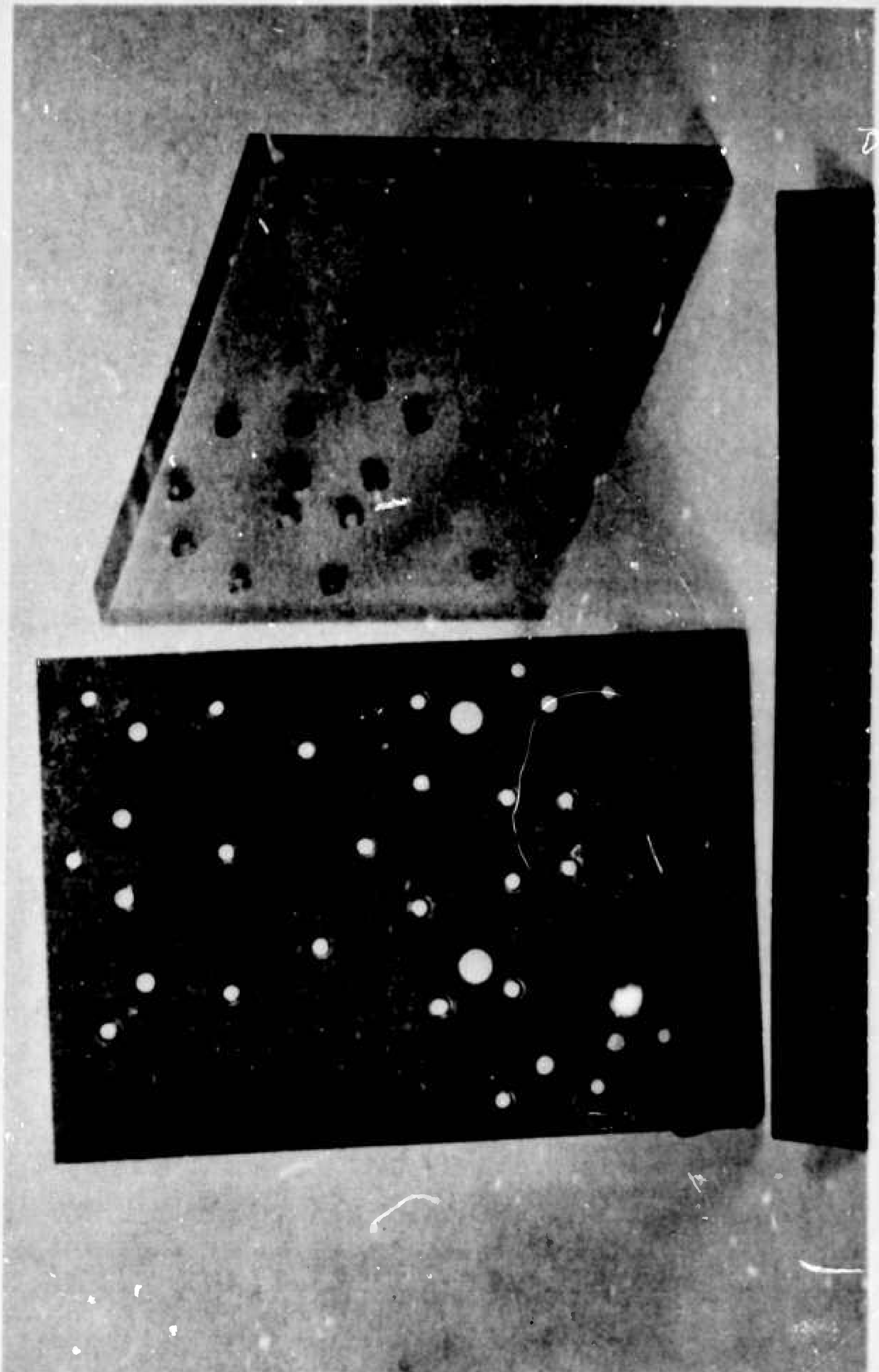

Figure 6. Disassembled flueric trigger

wave. Since it is desirable to be able to stop the system at any time, an input is provided to lock the oscillator in one position. The output of the oscillator is fed into the tape advance and blanking circuits.

The tape advance circuit amplifies the clock pulse from the oscillator and uses it to drive a piston. The piston drives a tape-advancing sprocket through a pawl and ratchet assembly.

The blanking circuit contains a variable time delay, an adjustable single-shot multivibrator, and a pulse power output (fig. 7). The variable time delay is necessary to compensate for the many delays in the advancing circuit. Adjustment of the variable delay will cause the blanking pulse to coincide with the change of tape position. The variable delay is effected by passing the output of the oscillator through a series tank and valve combination into ST. Adjustment of the valve varies the time delay, because the time required for the pressure in the tank to reach the switching pressure of the ST depends on the series resistance.

The adjustable single-shot multivibrator (SS) varies the on-time of the periodic step-function output. This feature is necessary, because the duration requirement for the blanking pulse changes with frequency. If the blanking pulse is too short, the NOR logic will erroneously decode the transient input states, since not all the transient states will be blocked. If the blanking pulse duration is too long, the NOR elements will not have enough time to come to a fully on-state, and the bellows-orifice mechanisms will not actuate, because of the lack of sufficient pressure.

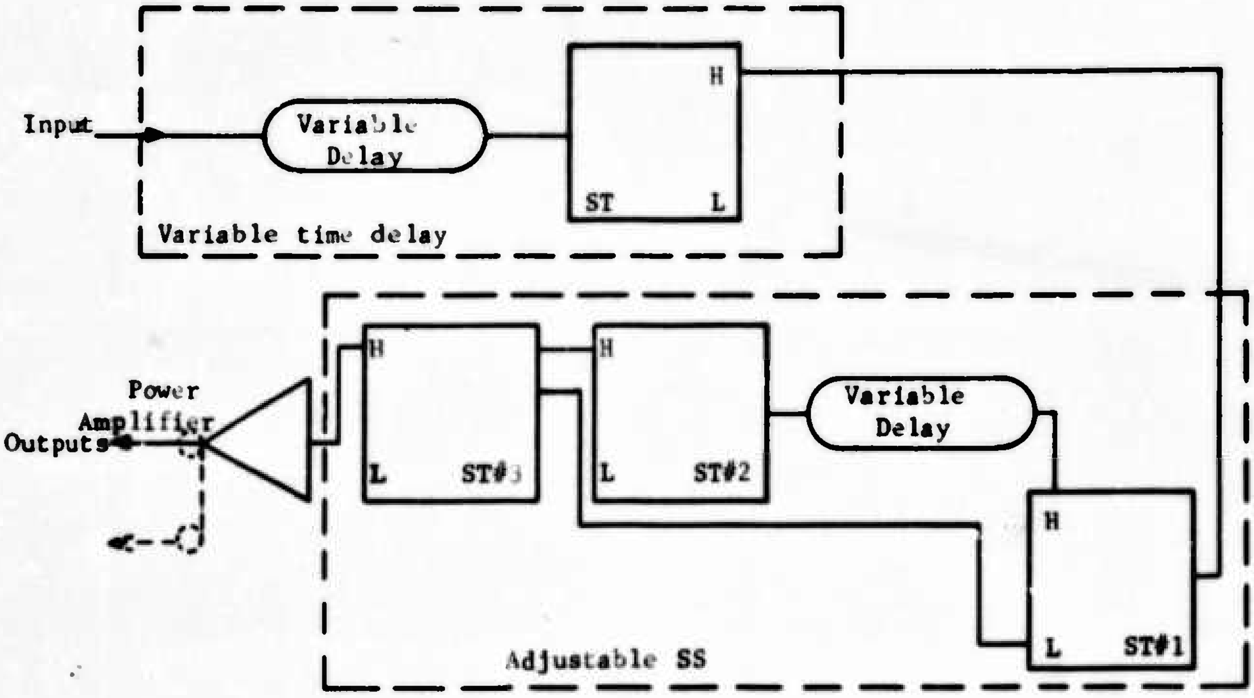

Logic Circuit

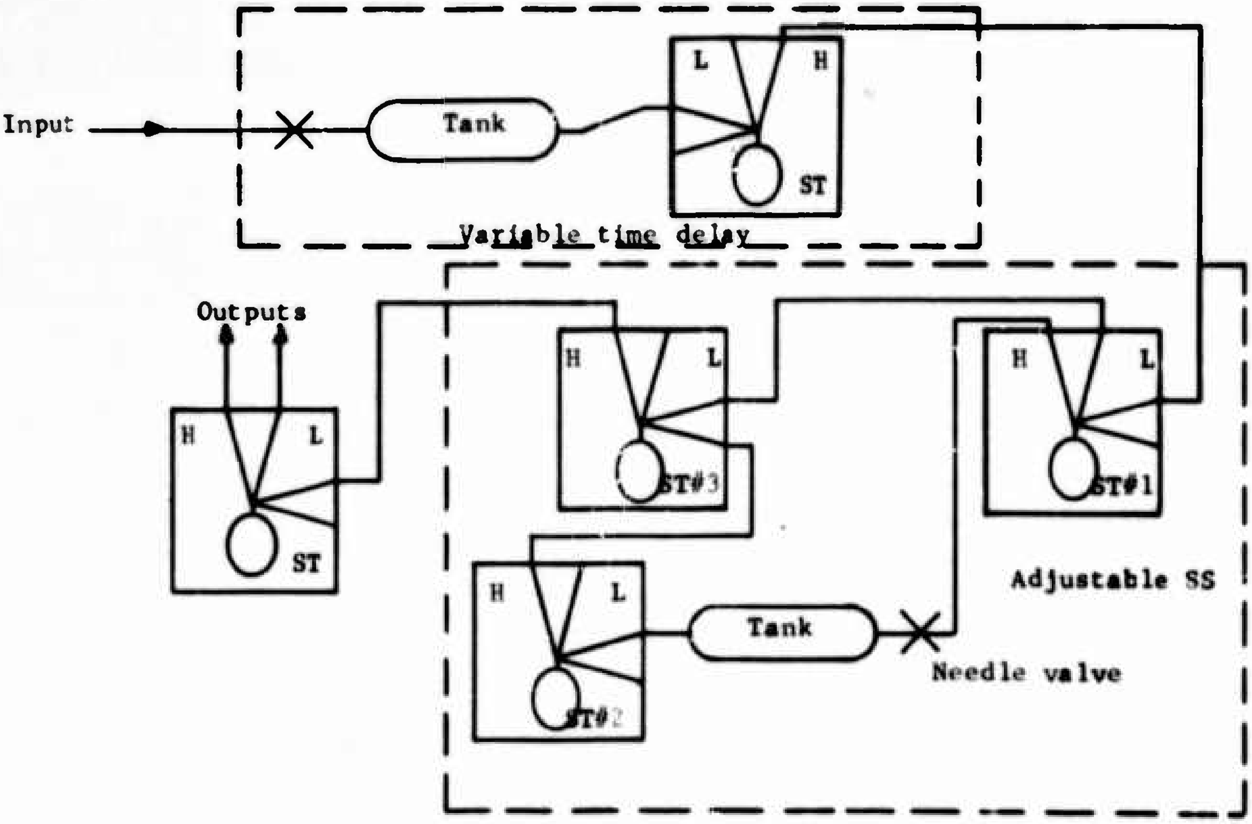

Equivalent Pneumatic Circuit

Figure 7. The blanking circuit

The adjustable SS uses three ST's and a series valve-tank combination. ST 3 has inputs from the high side of ST 2 and the low side of ST 1. In the quiescent state, with no input from the delay circuit to ST 1, the low side of ST 1 has an output, so that ST 3 is in the activated state, and no output occurs on its low side. When an input comes into ST 1, the low side no longer has an output and ST 3 goes to an unactivated state with an output on the low side. Since the high side of ST 1 is connected to the input of ST 2 through a valve-tank combination, ST 2 switches to an activated state after a time delay depending on the valve setting. When ST 2 switches, it deactivates ST 3. Thus the low side of ST 3 has an output that starts when there is an input to ST 1, and stops after a delay time dependent on the valve setting. Thus a variable pulse width is achieved without affecting frequency. By choosing one or another of the outputs of ST 3, pulse widths of 5 to 95 percent of the period of oscillation are available.

The output of the SS is fed into an ST with a higher power jet pressure than the ST's in the SS. This power amplified signal is then delivered to a fanout that feeds all the NOR elements. Adjustments of pulse width and time delay are made while observing simultaneously the output of the masking pulse fanout and the other inputs to the NOR decoders. In this manner the blanking pulse is adjusted to the proper width and the correct time relationship to the changing inputs.

PERFORMANCE

In general the performance of the tape-reader was good. Tapes could be read at about ten characters per second with few errors. This is about twice the speed of existing pneumatic tape readers and about the normal operating speed of electric tape readers. The causes of the errors are known.

One type of error occurs when the carriage is returned. The time for the carriage to return is greater than the period of oscillation, especially for long lines of type. At 10 cps, the carriage return for a full line of type takes about four periods. Hence, while the carriage is still in reverse motion, the initial letters on the next line will be typed, causing them to appear erroneously in the middle of the page. To eliminate these errors the tape must not advance while the carriage is returning. An obvious solution is to lock the oscillator for a few periods by a signal from the eighth (carriage return) flip-flop. This solution will not work because the delay between the oscillator and tape advance ratchet is greater than a period of oscillation; hence, even if the oscillator were shut down, the signal still in the lines would make the tape advance. Another possible solution is to pre-sense the carriage return hole by a separate reading head and thereby shut off the oscillator enough in advance so that the stopping of the tape-advancing sprocket will coincide with the return of the carriage.

Another type of error occurs when a double letter is coded. The action of the bellows-orifice arrangements, although fast enough for effective single operation at high speeds, is not fast enough to

respond to two consecutive signals. Nothing short of redesigning the bellows-orifice arrangements will solve this problem. However, if the reading speed is reduced slightly, the present arrangements will respond fast enough.

APPENDIX I

CONDITION FOR EFFECTIVE STEADY-STATE OPERATION

The flip-flop, fan-out, turbulence amplifier circuit is as follows:

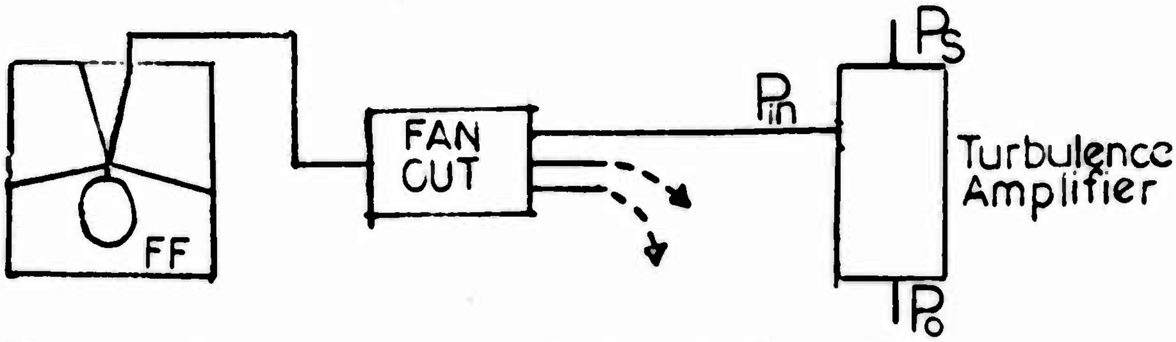

This circuit can be represented schematically as follows:

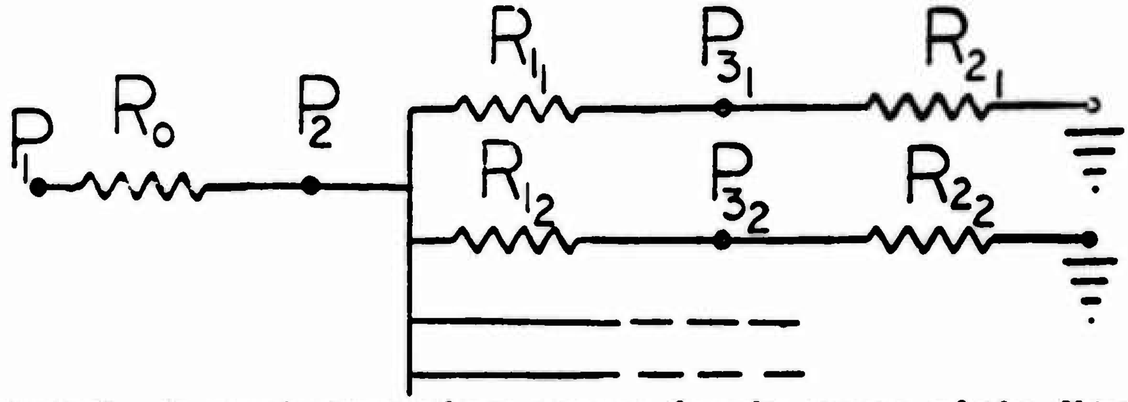

where P_1, R_o is the equivalent circuit for the output of the flip-flop (P_1 is either a constant pressure dependent on the supply pressure to the flip-flop or is zero pressure when the flip-flop is switched off, and R_o is a square law resistance.

The R_{1i} are the resistances of the separate branches of the fan-out. The R_{2i} are the input resistances of the turbulence amplifiers. Both the R_{1i} and R_{2i} are linear resistances.

Now the circuit must be arranged so that when the flip-flop is on, P_3 is large enough so that the turbulence amplifier is shut off. Figure A1 shows that although the turbulence amplifier never shuts off entirely, a suitably low output pressure level is reached when

$$P_{in} = .25\ P_o \qquad \begin{array}{ll} P_{in} & = \text{P input pressure} \\ & \quad (\text{cm } H_2O) \\ P_o & = \text{output pressure} \\ & \quad (\text{cm } H_2O) \end{array} \qquad (1)$$

Figure A2 shows that

$$P_o = .319\ P_s - 3.19 \qquad 20 \leq P_s \leq 55 \qquad (2)$$

where P_s is the supply pressure.

Since it is desired to have as high an output as possible from the turbulence amplifiers without sacrificing stability, P_s is set nominally at 50 cm H_2O. Thus $P_o = 12.75$ cm H_2O, and for effective operation $P_{in} \geq 3.19$ cm H_2O.

The circuit components must then be adjusted to effect this condition. Since R_o, R_{1i}, and R_{2i} are all fixed, P_1 is the only adjustable parameter. P_1 may be changed by varying the supply pressure to the flip-flop. From figure A3 it is seen that

$$P_1 = .533\ P_j \qquad (3)$$

where P_j is the supply pressure of the flip-flop.

Steady-state equations for the circuit can be written by applying the resistance laws and the continuity equation for one-dimensional incompressible flow.

Figure A1. Output and input pressures for a turbulence amplifier with different supply pressures.

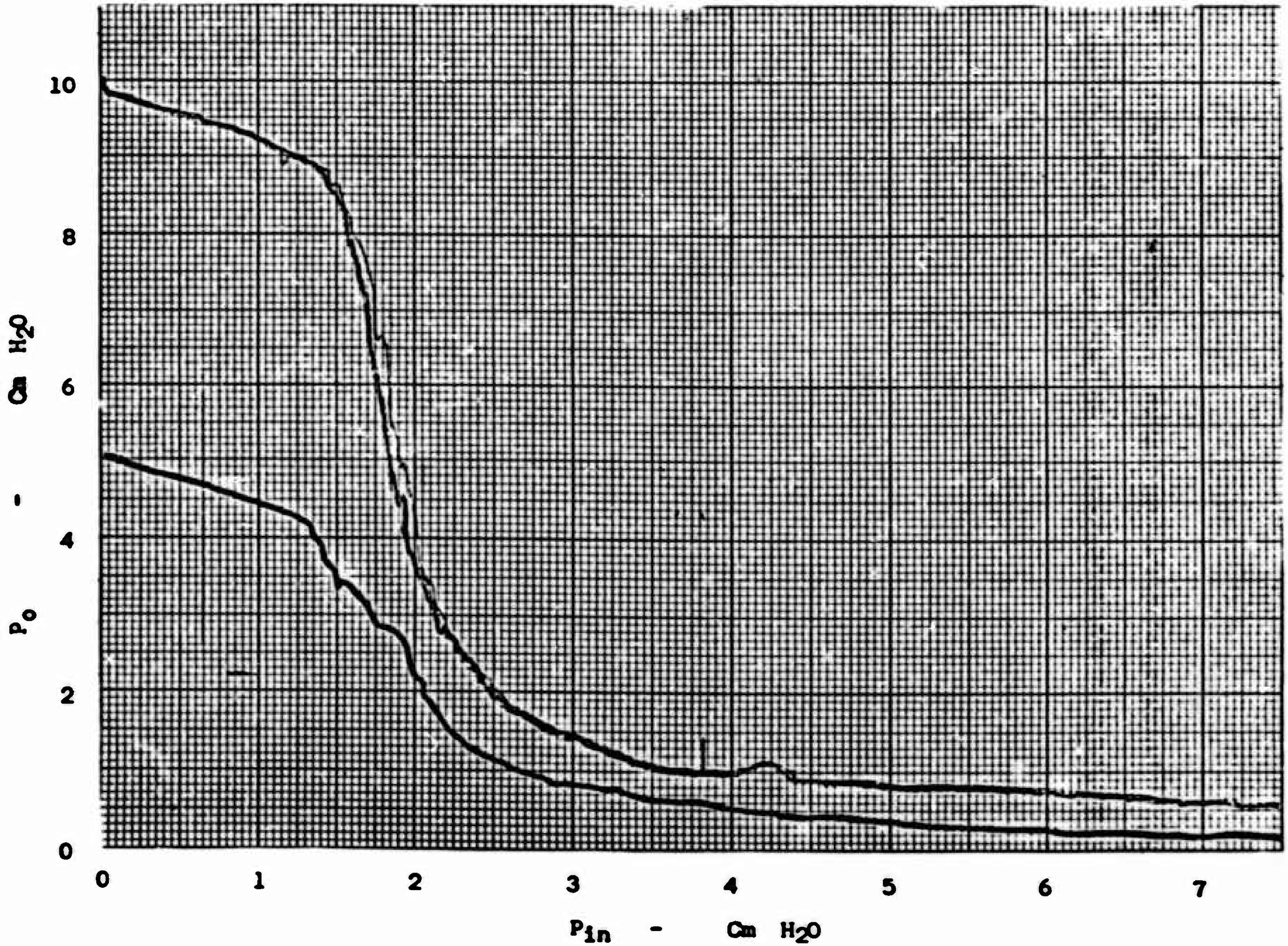

Figure A2. Output and supply pressures for a turbulence amplifier with no input.

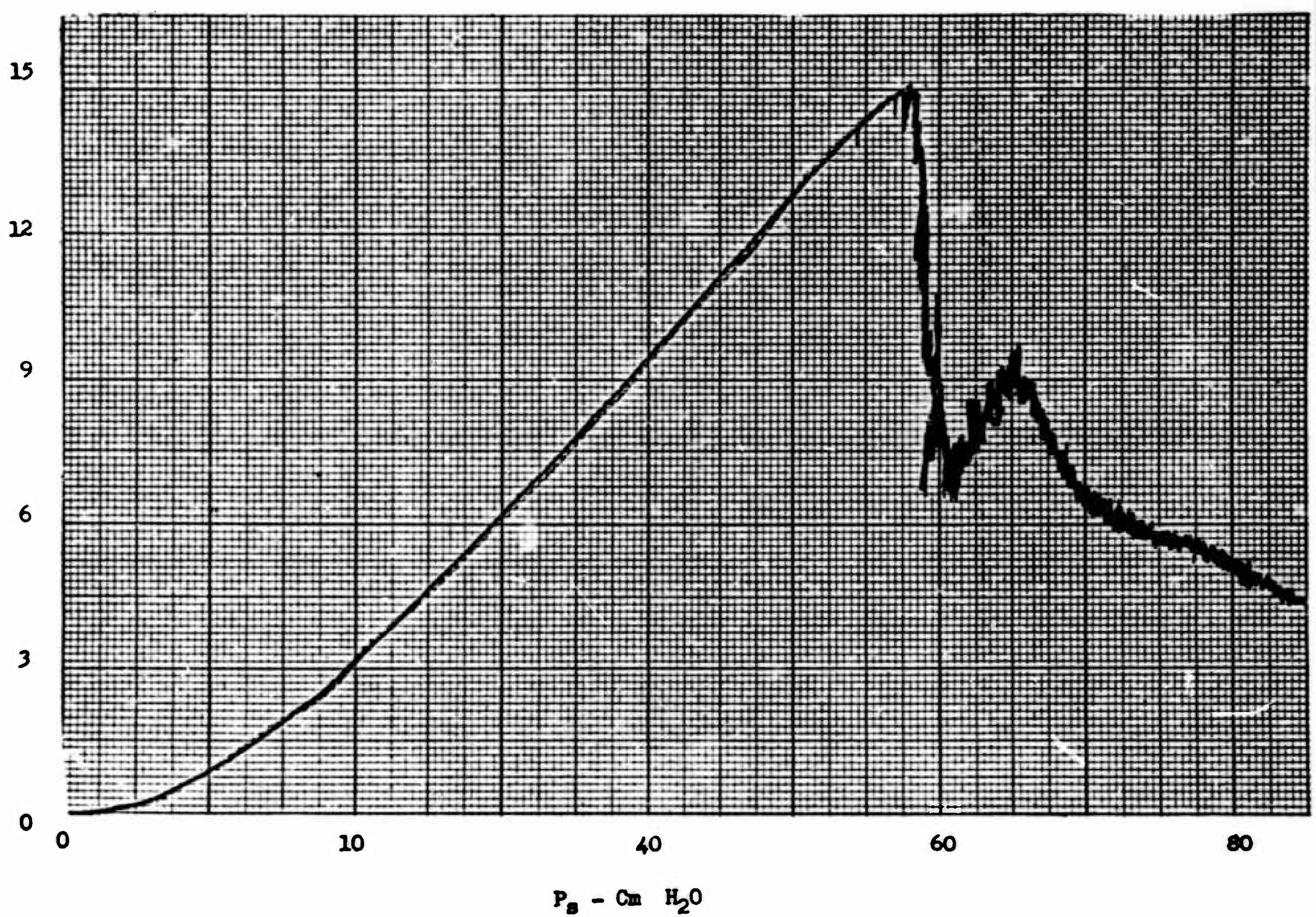

Figure A3. Output and supply pressures for a flip-flop.

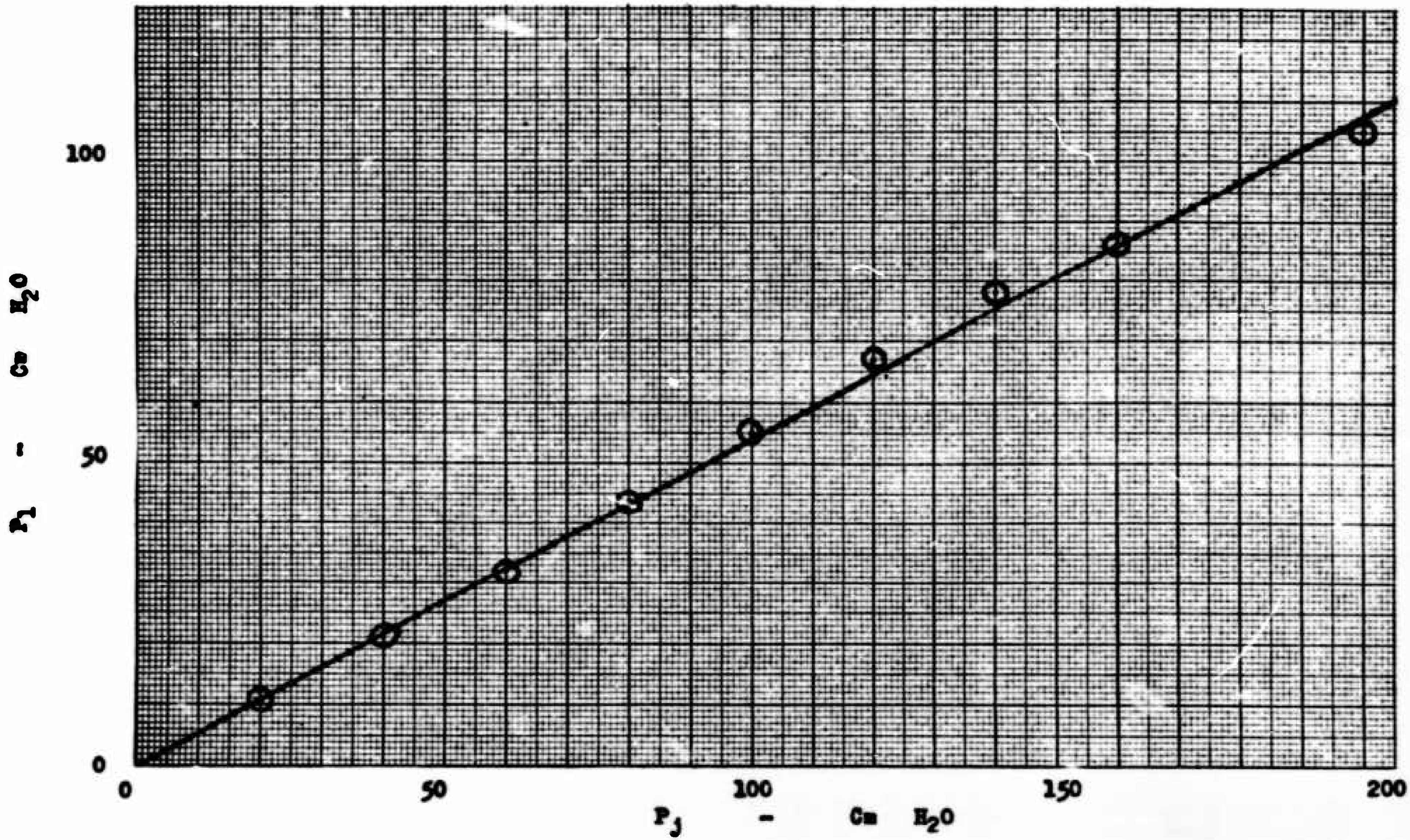

Since

$$R_{11} = R_{12} = \ldots\ldots\ldots\ldots\ldots\ldots = R_{1i} = \ldots\ldots\ldots\ldots$$

and

$$R_{21} = R_{22} = \ldots\ldots\ldots\ldots\ldots\ldots = R_{2i} = \ldots\ldots\ldots\ldots$$

We may write

$$P_{31} = P_{32} = \ldots\ldots\ldots\ldots\ldots\ldots = P_{3i} = \ldots\ldots\ldots\ldots$$

$$Q_{11} = Q_{12} = \ldots\ldots\ldots\ldots\ldots\ldots = Q_{1i} = \ldots\ldots\ldots\ldots$$

$$Q_{21} = Q_{22} = \ldots\ldots\ldots\ldots\ldots\ldots = Q_{2i} = \ldots\ldots\ldots\ldots$$

Thus it is possible to speak of R_1, R_2, P_3, Q_1, and Q_2. The resistance laws give

$$P_1 - P_2 = Q_o{}^2 R_o \tag{4}$$

$$P_2 - P_3 = Q_1 R_1 \tag{5}$$

$$P_3 = Q_2 R_2 \tag{6}$$

The continuity equation yields

$$Q_1 = Q_2 \tag{7}$$

$$Q_o = NQ_1 \tag{8}$$

where N is the number of fan-outs.

Combining (5), (6), and (7)

$$P_2 = Q_1 (R_1 + R_2) \tag{9}$$

Combining (9), (4), and (8)

$$P_1 = N^2 Q_1{}^2 R_o + Q_1 (R_1 + R_2)$$

or

$$N^2 Q_1{}^2 R_o + Q_1 (R_1 + R_2) - P_1 = 0$$

hence

$$Q_1 = \frac{-(R_1 + R_2) \pm \sqrt{(R_1 + R_2)^2 + P_1 N^2 R_o}}{2N^2 R_o} \qquad (10)$$

Obviously the positive root should be taken, hence

$$Q_1 = \frac{-(R_1 + R_2) + \sqrt{(R_1 + R_2)^2 + P_1 N^2 R_o}}{2N^2 R_o} \qquad (11)$$

Combining (11), 6, and 7

$$P_3 = \left\{ \frac{\sqrt{(R_1 + R_2)^2 + P_1 N^2 R_o} - (R_1 + R_2)}{2N^2 R_o} \right\} R2 \qquad (12)$$

Substituting the appropriate values in equation 12

$$P_3 \geqq 3.19 \text{ cm } H_2O$$

$$R_1 = 3.3 \times 10^{-2} \frac{\text{cm } H_2O}{\text{cc/min}}$$

$$R_2 = 8.0 \times 10^{-2} \frac{\text{cm } H_2O}{\text{cc/min}}$$

N = 35 (an upper bound for the fan-out of a single variable for the code used; see figure 3)

$$R_o = 1.61 \times 10^{-6} \frac{\text{cm } H_2O}{(\text{cc/min})^2}$$

one concludes that for proper operation

$$P_1 \geqq 30.6 \text{ cm } H_2O$$

hence by relation (3)

$$P_J \geqq 57.4 \text{ cm } H_2O$$

ACKNOWLEDGEMENT

The assistance of Frank Weiser in the construction of this tape-reader is gratefully acknowledged. Mr. Weiser designed and built many of the mechanical parts of the tape reader. His skill and experience were invaluable in the speedy fabrication of many complicated devices.

FLUID STATE HYBRID CONTROL SYSTEMS

by

P.A. Orner
Giannini Controls Corporation
Malvern, Pennsylvania

and

J.N. Wilson
University of Saskatchewan
Saskatoon, Saskatchewan

ABSTRACT

This paper assesses the simultaneous use of both proportional and bistable fluid state devices in synthesizing closed loop control systems. In particular, the desirable features of systems using proportional devices in the power amplifier and actuator sections of the system and digital devices in the feedback and compensating sections are presented. The advantages of typical systems are evaluated with respect to accuracy, speed of response, compensation, stability, impedance matching, and efficiency. Preliminary experimental results are reported.

A Paper Prepared For
The Third Fluid Amplification Symposium
Harry Diamond Laboratories, Washington D.C.

October 1965

FLUID STATE HYBRID CONTROL SYSTEMS

by

P.A. Orner - Giannini Controls Corporation
Malvern, Pennsylvania

J.N. Wilson - University of Saskatchewan
Saskatoon, Saskatchewan

INTRODUCTION

Past and present research and development in fluid state devices has resulted in several types of proportional and bistable fluid amplifiers with widely varying performance characteristics. While initial efforts were directed towards development of individual elements, more recent investigations have been concerned with synthesis of practical systems. The inherent advantages of fluid state devices immediately suggest applications to closed loop control systems.

However, when one encounters the design of control systems employing exclusively fluid state devices, a number of decisions must be made, viz.:

1. How can the controlled variable be monitored with sufficient accuracy over the maximum expected excursion?

2. How can the command or reference information and perhaps adaptation information be reliably and accurately read into the system?

3. How can the system best be compensated to meet stability and dynamic design requirements?

4. How can the power amplification and mechanical actuation functions in the forward loop be executed most reliably and efficiently?

Considerations such as those noted above lead the authors to believe that hybrid fluid state systems employing bistable and proportional devices in appropriate portions of a control system

offer several advantages.

At the present level of development in fluid state technology, it is worthwhile to examine the most advantageous applications of fluid state devices (both proportional and bistable) in the various parts of the control loop.

TRANSDUCTION AND COMPUTATION

First, let us examine the problem of measuring the controlled variable. The main advantage of using digital transduction is the capability to measure large excursions of the controlled variable and yet preserve resolution. Coupled with this is the fact that digital logic elements are relatively insensitive to noise. Consequently, noise generated in the transduction process is not transmitted through the system. Another advantage of digital transduction is the insensitivity to reference variations and parameter changes.

A good example of the case in point is the pneumatic gauge (essentially a flapper valve used for analog position measurement). Such a device is capable of measuring position accurately, providing the controlled variable executes only small excursions from the null point. In addition the device's performance characteristics change with variations in operating pressure, geometrical design, and fluid properties. Admittedly, not all analog transduction devices operate on the pneumatic gauge principle but it is felt that sensitivity to reference variations and parameter changes are two characteristics of nearly all analog transduction means which tend to degrade control system performance. No doubt, applications exist in which analog transduction may be the only means possible due to economic or practical considerations.

Turning now to the feedback and computational portions of the system, one desirable feature of using digital devices is their inherent insensitivity to noise. Large noise-to-signal ratios, which proportional devices at the present state-of-the-art are prone to exhibit[1,2], tend to result in saturation and reductions in sensitivity especially if several stages of amplification are used. One further drawback to the use of proportional devices in the feedback and computational portions of the system is their rather high sensitivity to geometry (introduced during fabrication), often resulting in asymmetrical or nonlinear operation[2].

There are, however, certain features of the use of proportional amplifiers which are superior to digital devices so far as

feedback and computation are concerned. The first is their frequency response. Proportional devices have a response time an order of magnitude faster than digital devices. Furthermore, in many control systems, the number of proportional elements used will be considerably less than the number of bistable devices to accomplish the same function. In other words, it appears that fluid state analog systems possess the potential for considerably faster operation than digital systems.

COMMAND INPUTS

A very important aspect of the use of digital devices for the computational parts of the system is the ease with which command information can be read into the system. As an example, command information could be read into a fluid state digital system on punched tape or as a train of fluid pulses. For very high performance continuous systems, the analog reference signal generators would have to generate signals to an accuracy at least as high as that expected of the system. This could be a feat in itself, especially for variable set-point systems.

DYNAMIC COMPENSATION

The compensation of control systems generally reduces to one of designing suitable lead-lag networks or combinations thereof. For integration, proportional devices have been shown to be sensitive to asymmetries in geometry[3] which results in unpredictable reset rates as well as drift. While a counter will perform the integration function very effectively digitally, it does require more elements and invariably will have a limit on the maximum rate of integration due to the dynamics of the digital amplifiers.

In regard to lead circuits, the most undesirable feature of proportional devices is their tendency to generate noise[1,2] – an undesirable signal to pass through any differentiator. Digital differentiation, though possible, adds to circuit complexity and results in essentially a sampled data subsystem. Gaither and Taft[4] have developed an interesting technique of digital lead compensation which appears particularly attractive for use with fluid state digital devices. Two features of this technique which are claimed superior to conventional lead compensation are (a) the magnitude and duration of the compensating signals can be easily controlled with a minimum of logic as well as be gated in or out at will and

(b) the lead compensation does not amplify noise produced in the main control and is independent of the level of the D.C. error signal. Although this technique has been implemented with electronic circuitry, it has not as yet been evaluated with fluid state digital circuitry.

POWER AMPLIFICATION AND MECHANICAL ACTUATION

In general, the power amplifier must accept a low power level signal from a high impedance source (i.e. a signal amplifier), and in turn deliver relatively large amounts of power to the mechanical actuator. Since fluid amplifiers are essentially "open-center" devices, some pneumatic servosystems utilize fluid amplifiers for computation, but employ conventional spool valves for power amplification. When standby power consumption is of overwhelming importance, this approach seems valid. If all the advantages of a true "no moving parts" approach are to be fully realized, however, the power amplification should also be achieved with a pure fluid device. The optimal pure fluid amplifier would therefore possess an infinite control input impedance, and a sufficiently low output impedance to properly mate with the actuator.

If the actuator is a piston device, a vane motor, etc., its static (zero load velocity) input impedance is infinite, but its dynamic input impedance is finite and variable, the magnitude and sign depending on the instantaneous load velocity. "Blocked load" and flow reversal instabilities often arise when coupling high power level proportional fluid jet devices to such loads. An impulse turbine presents a relatively low input impedance, independent of the mechanical load behavior. A turbine-type actuator is thus desirable from the amplifier loading viewpoint. Further, if the pneumatic supply source for the fluid jet power amplifier is power-limited, a low pressure-high flow turbine actuator will require no more source power than an equivalent-power-output high pressure-low flow positive displacement motor.

PROTOTYPE SYSTEM

In order to evaluate the performance and relative merits of fluid state devices for control system applications, the authors undertook the initial stages of development of a fluid state incremental digital position control system at the Case Institute of Technology, Cleveland Ohio[5,6]. A block diagram of the complete system is presented in Figure 1. The portions of the system described

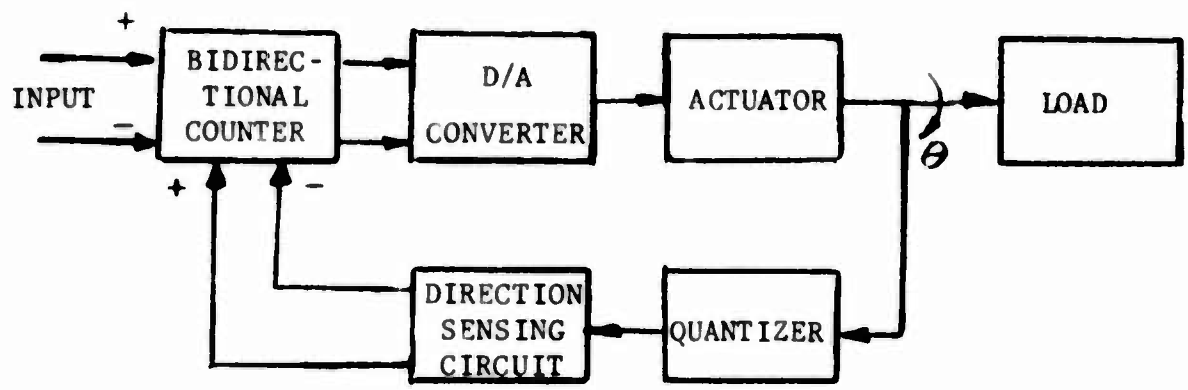

FIGURE 1. BLOCK DIAGRAM OF FLUID DIGITAL CONTROL SYSTEM

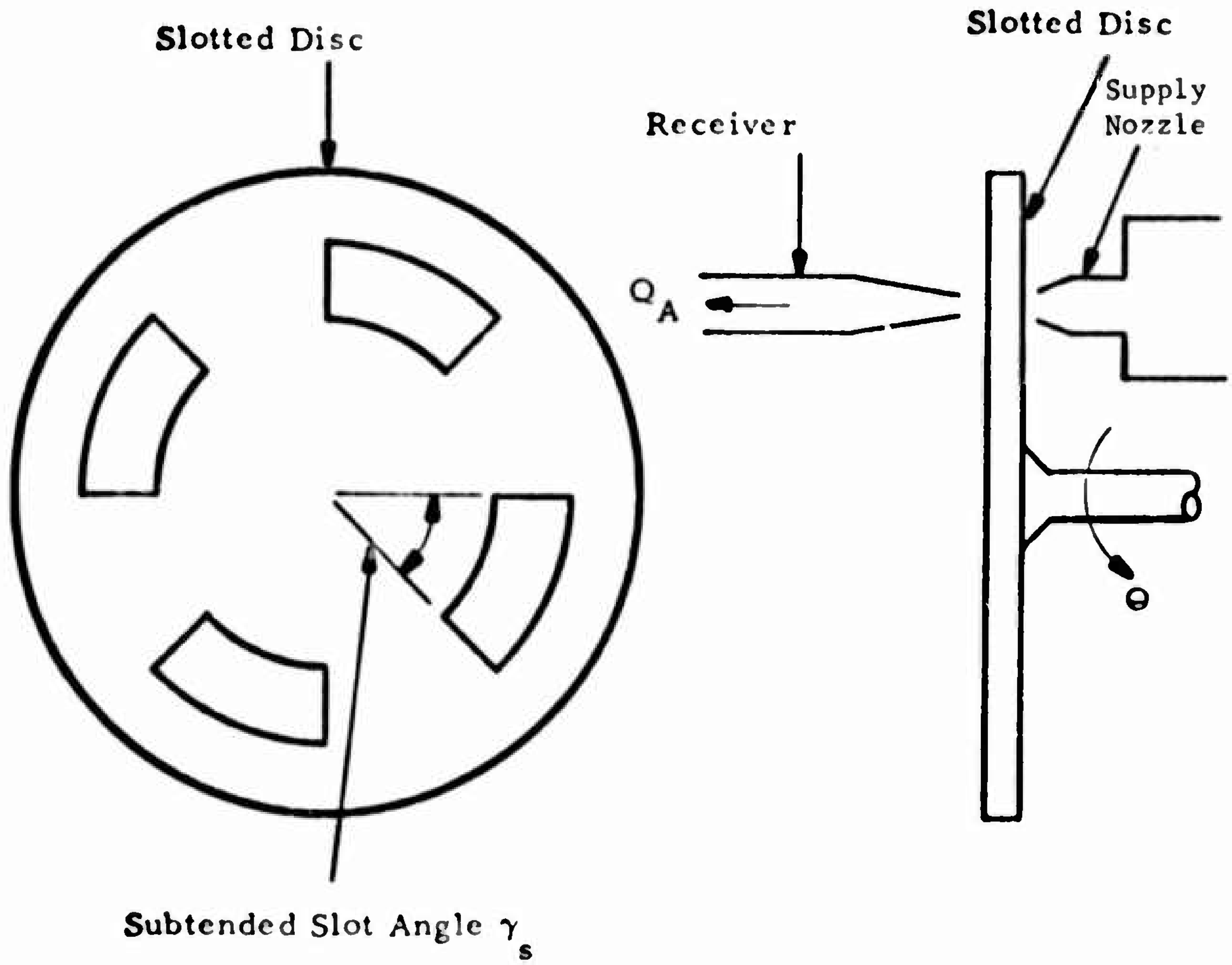

FIGURE 2. SCHEMATIC OF FLUID QUANTIZER

herein are the power amplifiers and actuator of the forward loop, the digital position transducer, the feedback, and the computational sections. The design and the evaluation of the digital-analog converter which closed the control loop is discussed in another report[7].

The scheme of digital position transduction used was the slotted disc quantizer reported previously[8]. A schematic of the device is shown in Figure 2. The geometry of the device investigated experimentally is shown in Figure 3. Typical normalized receiver load characteristics, considered to be one of the most important performance criteria of the device, are depicted in Figure 4. (Note the saturation effects for both small and large values of the slot displacement or area of common communication between the supply nozzle and receiver.) This method of quantization using a fluid as the information transmission medium is very effective. The accuracy or resolution obtainable is determined by two physical considerations — the widths of the slots which will be limited by manufacturing techniques and the radius at which the slots are located. Even a relatively crude device with a slot width of 0.010 inch at a radius of one inch gives the capability of measuring angular position (or any controlled quantity which can be expressed as an angular position) to 1 part in more than 600.

The direction sensing circuit, which determines the polarity of the controlled variable, is shown in Figure 5. The technique used in implementing this circuit is similar to that employed in corresponding electronic systems, viz.: two supply nozzle-receiver sets are located (n + 1/2) slot widths circumferentially to introduce a phase difference between the two receiver signals. Logical gating may then be used to generate signals indicative of the direction of rotation of the controlled variable.

The circuit for the four-stage binary bidirectional counter, the comparator of the system, is depicted in Figure 6. The asynchronous mode of operation was adopted because of the circuit simplifications afforded[5].

The feedback and computational parts of the system operated reliably at over 100 cycles per second. (Supply pressures to active elements ranged from 8 to 20 inches of water. Supply nozzle widths were nominally 1/32".) This frequency is not considered an upper limit for a system of this type. Miniaturization of devices, refined designs, and increased supply pressures would all contribute to an increase in speed of operation.

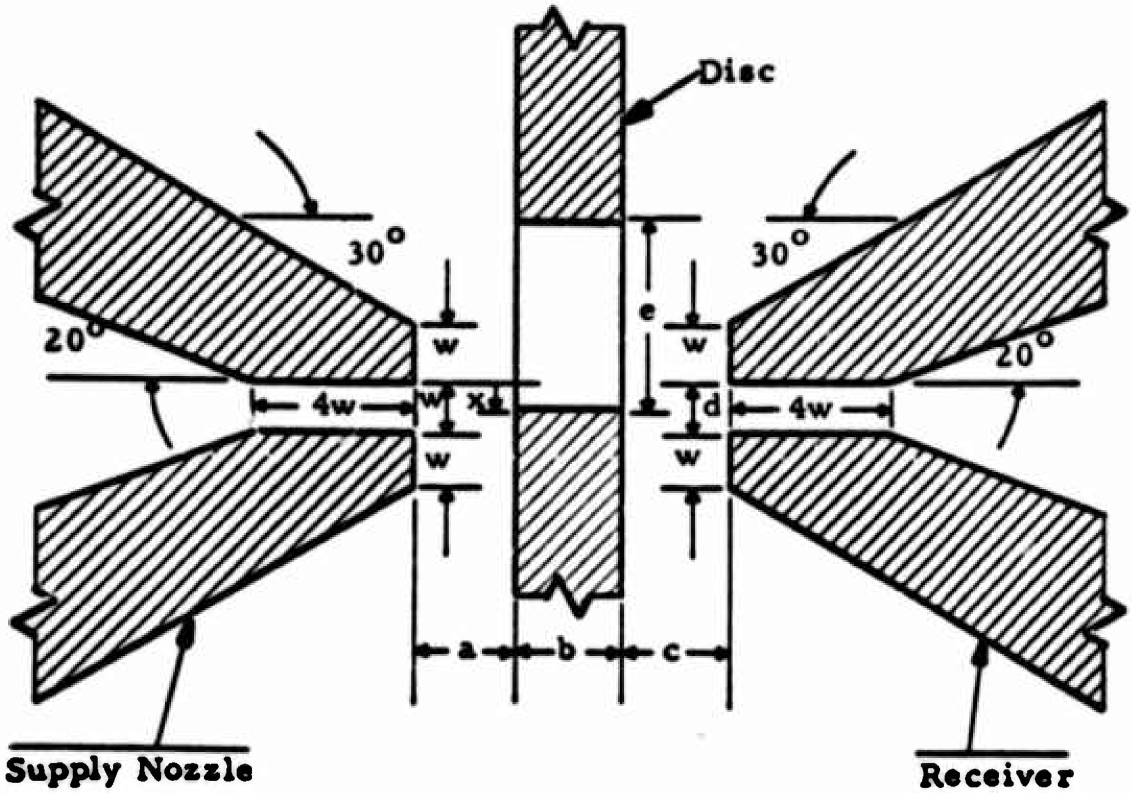

w = .030"

FIGURE 3. SUPPLY NOZZLE, RECEIVER, AND QUANTIZER DISC

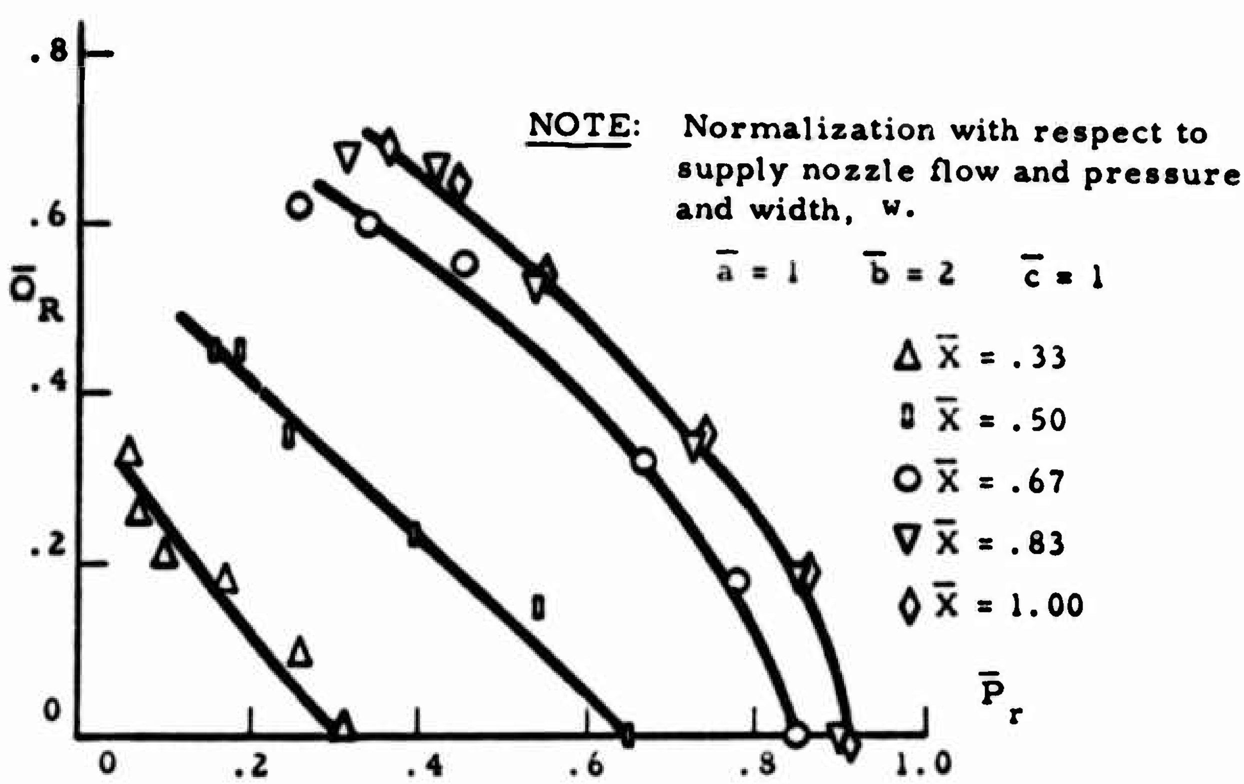

FIGURE 4. NORMALIZED RECEIVER LOAD CHARACTERISTICS

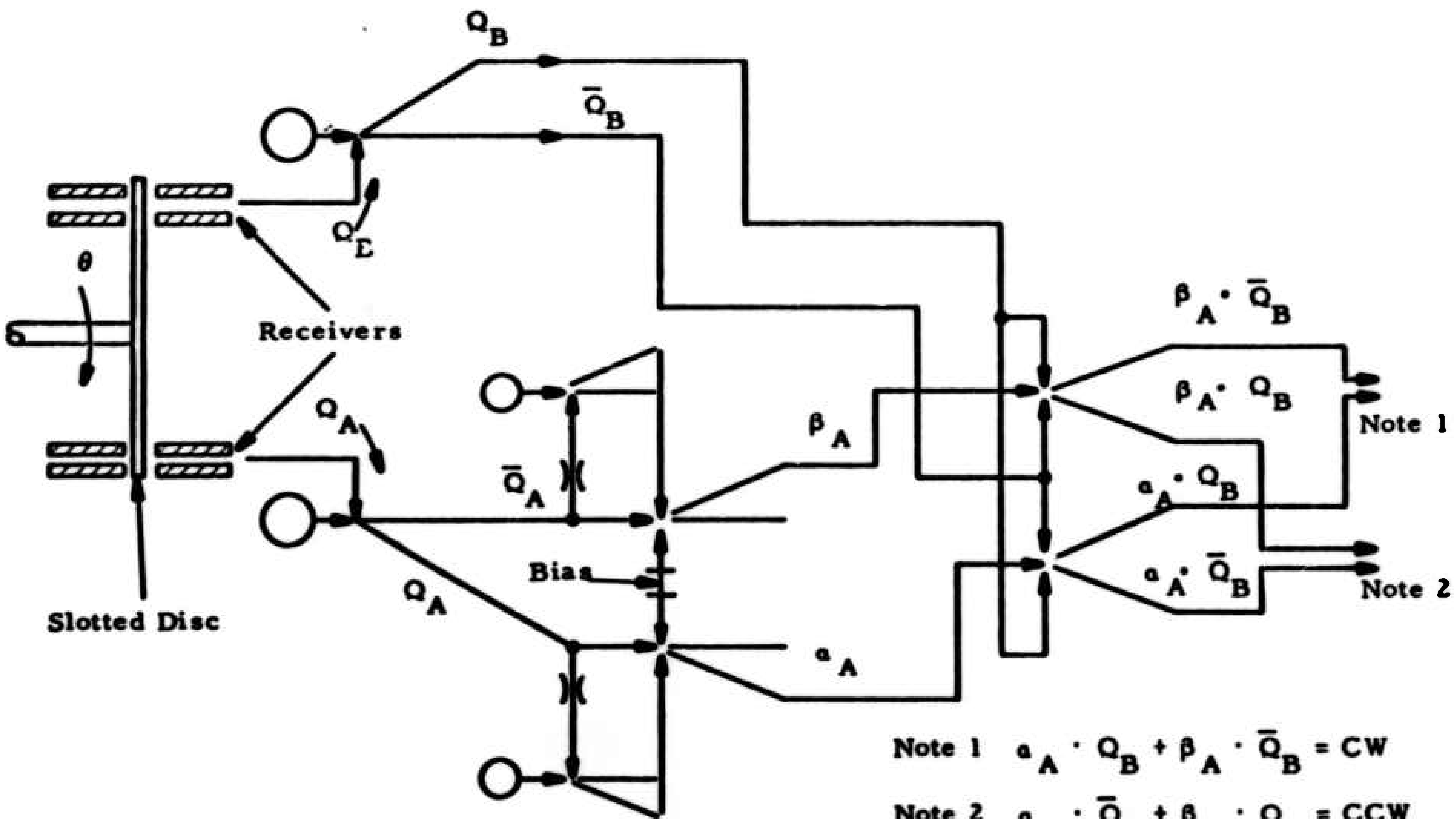

Note 1 $\alpha_A \cdot Q_B + \beta_A \cdot \bar{Q}_B = CW$

Note 2 $\alpha_A \cdot \bar{Q}_B + \beta_A \cdot Q_B = CCW$

FIGURE 5. SCHEMATIC DIAGRAM OF DIRECTION SENSING CIRCUIT

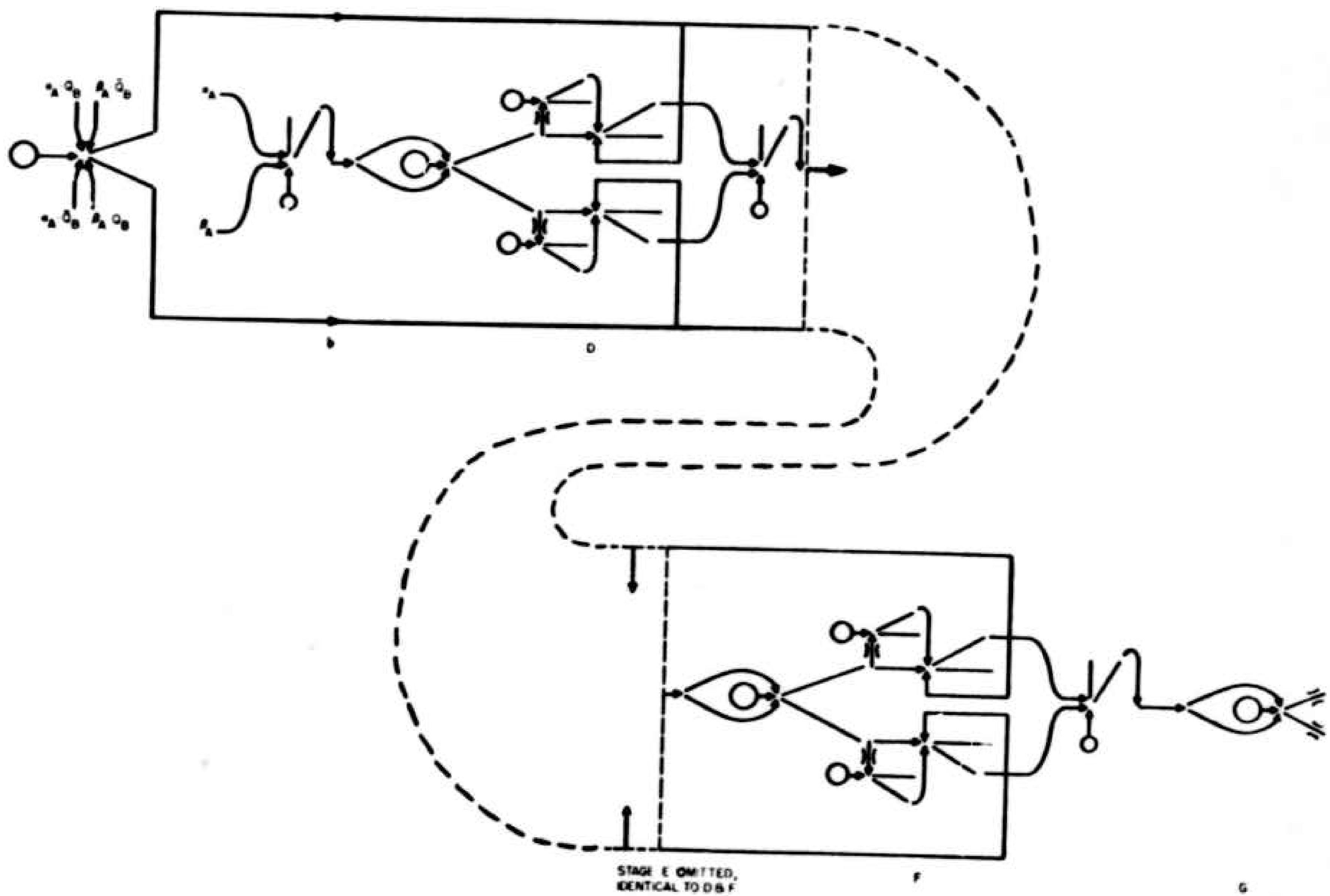

FIGURE 6. SCHEMATIC DIAGRAM OF BIDIRECTIONAL COUNTER (INCL. BUFFER AMPLIFIER)

The power amplifier is shown in Figure 7. The operating principle is the forced separation of a two-dimensional power jet from a curved surface[6]. The control signal is the separation-inducing flow through a number of slots on the curved surface. The average power gain was approximately 80:1 over the dynamic range from zero to maximum output flow. Nearly infinite input impedance operation was attained over reduced dynamic ranges by specific designs of the control flow slots, resulting in incremental power gains on the order of 1500:1.

The actuators were small, two-stage, axial-flow impulse turbines with a maximum output of approximately one-tenth horsepower when coupled to the power amplifiers. A pair of power amplifier-turbine packages was used in the push-pull circuit shown in Figure 8. An analog loop was closed with conventional beam deflection amplifiers, resulting in a rotary position servo with better than one cycle per second bandwidth at a system supply pressure of 3 psig[6]. The digital loop was implemented by removing the analog feedback valve, input amplifier, and feedback summing amplifier; and replacing them with the quantizer, bidirectional counter, and digital-analog converter. The performance of the digital loop is presented in the paper by Turnquist and Taft[7].

SUMMARY AND CONCLUSIONS

This paper has assessed, from a control system viewpoint, the use of fluid state digital and proportional devices in feedback circuits. Based on the present knowledge of the performance of fluid state devices, it appears that several advantages are to be gained by using digital feedback and computation in the system, and allowing the power amplification and actuation functions to be analog. It also appears that the compensation can be achieved digitally with several attendant desirable features.

Preliminary experimental data obtained during the development of a complete incremental digital position control system, employing exclusively fluid state devices, demonstrate the feasibility of fluid state digital measurement, feedback, and computation; and also demonstrate the practicality of an analog power amplifier and turbine actuator combination.

FIGURE 7. BOUNDARY LAYER POWER AMPLIFIER

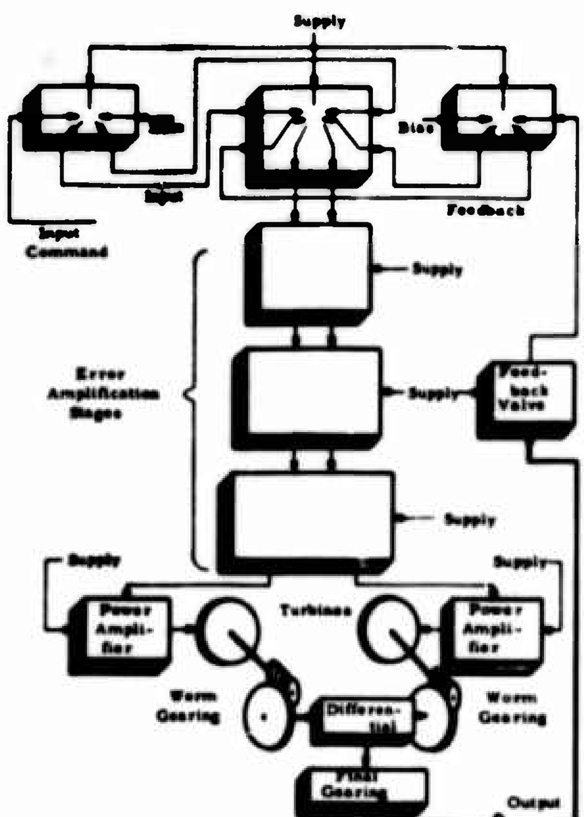

FIGURE 8. ANALOG CLOSED LOOP POSITION CONTROLLER (SHOWING TURBINES AND POWER AMPLIFIERS)

ACKNOWLEDGMENTS

The development of the quantizer, feedback, and computational parts of the system was sponsored by the Harry Diamond Laboratories under Contract Number DA-49-186-AMC-79(D).

Portions of the development of the turbine actuator were sponsored by the Aro Corporation (Bryan, Ohio) and the Rotor Tool Company (Euclid, Ohio).

The work was conducted under the supervision of Professor C.K. Taft, Engineering Design Center, Case Institute of Technology. The authors would also like to thank Mrs. M.R. Greenberg for the patient and skillful typing of this report.

REFERENCES

1. Jet Interaction Noise
   F.A. Moynihan
   Proc. Fluid Amp. Sym. Volume I, May 1964.
   Harry Diamond Laboratories, Washington D.C.

2. The Staging of Pressure Proportional Amplifiers to Provide Stable, Medium Gain, Dual Control, Single Output Pure Fluid Systems
   W.L. Cochran and R.W. Van Tilburg
   Proc. Fluid Amp. Sym. Volume II, May 1964.
   Harry Diamond Laboratories, Washington D.C.

3. Experiments in Analog Computation with Fluids
   S. Katz, J.M. Goto, and R.J. Dockery
   Proc. Fluid Amp. Sym. Volume II, May 1964.
   Harry Diamond Laboratories, Washington D.C.

4. Digital Lead Compensation of Pulse-Data Control Systems
   P.H. Gaither and C.K. Taft
   Report EDC 1-63-17, 1963.
   Case Institute of Technology, Cleveland Ohio.

5. A Fluid Analog-Digital Conversion System
   J.N. Wilson
   Report EDC 7-64-4, September 1964.
   Case Institute of Technology, Cleveland Ohio.

6. <u>A Fluid Amplifier Controlled Pneumatic Turbine Servomechanism</u>
P.A. Orner
Report EDC 7-64-5, October 1964.
Case Institute of Technology, Cleveland Ohio.

7. <u>Fluid State Digital-to-Analog Converter</u>
C.K. Taft and R.O. Turnquist
Proc. Fluid Amp. Sym., October 1965.
Harry Diamond Laboratories, Washington D.C.

8. <u>A Fluid Encoding System</u>
C.K. Taft and J.N. Wilson
Proc. Fluid Amp. Sym. Volume IV, May 1964.
Harry Diamond Laboratories, Washington D.C.

A FLUID STATE DIGITAL TO ANALOG CONVERTER

by

Dr. Charles K. Taft

Ralph O. Turnquist

Case Institute of Technology

Cleveland, Ohio

A FLUID STATE DIGITAL TO ANALOG CONVERTER

Introduction

Research in fluid state systems at Case Institute of Technology is concerned with the design of servos using pure fluid elements. Part of this research has been concerned with the application of fluid state devices in the design of a complete fluid state digital pulse data control system. The design of this kind of control system was undertaken because it provides a suitable vehicle for evaluation of the applicability of fluid state devices to the following wide range of control system design problems:

1. Digital measurement
2. Digital data handling
3. Digital to analog conversion
4. Preamplification
5. Power amplification
6. Pneumatic-mechanical energy conversion
7. Input data handling
8. Compensation

The research results for items 1 and 2 have been published by Wilson[1,2], and the research results for items 4,5,and 6 have been published by Orner[3,4]. This paper presents the research results for item 3 and also presents typical test results for the complete fluid state digital pulse data control system.

Function of a Fluid State D/A Converter

To understand the function which a fluid state D/A converter must perform, refer to the block diagram of the fluid state digital pulse data control system shown by Figure 1.** In such a system, the state* of the bidirectional counter is an indication of the error in the system. At a given instant of time the difference between the actual counter state and some reference counter state (set point) is the number of quanta by which the angular rotation of the output shaft of the system is in error. By definition, one quantum is the angular rotation of the output shaft required for the quantizer to generate successive feedback pulses.

* Counter state is the binary number represented by the state of the T (or trigger) elements which serve as the memory bits of the fluid state counter. Flow at one specified outlet of the T memory element is designated as the "1" state. No flow at this outlet is designated as the "0" state.

**Figures appear on pages 121 through 130.

However, the system error represented as a binary number by the state of the counter is not useful information to the system in this form. The binary number must be converted to an analog fluid signal which can command the system prime mover to drive the system output shaft (in the appropriate direction) so that when an error exists, it will be reduced to a minimum as quickly as possible. Transforming the binary numbers represented in the counter by a combination of flows ("1"'s) and no flows ("0"'s) into an analog fluid pressure is the function of the fluid state digital to analog converter. Specifically, the magnitude of the output pressure of the digital to analog converter should increase when the binary number represented by the state of the counter increases. Because the counter and preamplifier both operate at "signal" pressure levels (less than 1 psig), the fluid state D/A converter should also operate at "signal" pressure levels.

Design Requirements for a Fluid State Digital to Analog Converter

Having described the function which the D/A converter must perform as part of the complete system, it is now meaningful to present the design requirements which were established for this device.

1. Should produce an output pressure (while "driving" the control port of a proportional amplifier) which is a function of the binary combination of fluid signals (either "1"'s and/or "0"'s) which exist at the "1" outlets of the T memory elements of the fluid state counter.
2. Should operate using signals only from the "1" outlets of the counter T memory elements. This implies the use of monostable (NOR) type elements in the D/A converter. Thus only one connecting line is required from the outlet of each T memory element to the D/A converter.
3. Should operate directly with fluid signals of equal magnitude from all counter T memory elements. No additional amplifying elements should be required between the counter and the D/A converter. If signals are of equal magnitude, the loading effects by the D/A converter will be the same for all T memory elements.
4. Should have satisfactory dynamic response at operating speeds of fluid state counter.
5. Should have no mechanical moving parts.
6. Should be readily manufactured utilizing materials and techniques commonly employed for fluid state systems.

Choosing a Design Consistent with Design Requirements

Initially two techniques commonly used for electronic digital to analog conversion were studied to determine if their fluid analogs could be implemented. These techniques are the current source ladder network[5] and the voltage source ladder network.[5] However, these techniques require that the impedance* of the load being "driven" be either infinite, or else very high. The load driven by a fluid state D/A converter is the control port of a proportional "beam deflection type" amplifier which has a relatively low input impedance. Therefore, it was considered unfeasible to implement the fluid analogs of the electronic D/A techniques. Instead, fluid flow devices capable of driving low impedance loads were considered for use in fluid state digital to analog conversion and a slightly different type of D/A converter scheme was devised.

A flow device suitable for fluid state D/A conversion is shown by Figure 2. It includes a flow collector, input stages consisting of identical monostable type elements, and a single output. Every input stage either delivers "flow to" or receives "flow from" the flow collector. It provides "flow to" the collector if the T memory element which controls it is in the "1" state; "flow from" if the T memory element which controls it is in the "0" state. The binary weighting factor (2^0, 2^1, 2^2, ...2^8) associated with each T memory element in the counter is incorporated into the D/A device by using one orifice of area A_1 in the stage controlled by the T memory element of "weight" 2^0; two orifices of area A_1 in the stage controlled by the T memory element of "weight" 2^1; etc.

This scheme for fluid state D/A conversion simply accepts a set of fluid control signals (or absence thereof) which represent a binary number, and from this information produces a single output pressure which is proportional to the binary number.

A general expression for calculating the discrete theoretical static output pressures of this fluid state D/A converter as a function of counter state (binary n) can be obtained from flow continuity considerations if the following assumptions are used.

1. That the receiver pressures of all stages are binary in nature, i.e. either $P_r = P_{r_1}$ when switched "on", or $P_r = P_{r_0}$ (atmospheric) when "off".

---

* In electronic devices static impedance refers to resistance, that is $\frac{V}{I}$. In fluid state devices, static impedance is defined as resistance to the flow of the working fluid and may be expressed mathematically as Q/P.

2. Incompressible flow. This is valid because pressure differences used are less than 1 psig.
3. The flow discharge coefficients of receiver outlet orifices and the load orifice are equal. This is valid because all receiver outlet orifices are of the same diameter.

The general expression is

$$P_n^* = \frac{1 + \dfrac{(A_L/A_1)^2}{(2^s - 1)^2}}{1 + \left[\dfrac{(2^s-1-n) + \left(\dfrac{A_L}{A_1}\right)}{n}\right]^2}$$

where $P_n^* = P_n / P_{2^s-1}$ and $P_o^* = 0$

$n = 1,2,3,\ldots(2^s-1)$
s = number of input stages
A_1 = Area of receiver outlet orifice in input stage 2^0
A_L = Area of load orifice

The sixteen discrete theoretical static output pressures P_n^* for a four input stage fluid state D/A converter are shown as a function of counter state by Figure 3. Even though the flow-pressure characteristics of all receiver outlet orifices are nonlinear, the static output pressure characteristic P_n^* is reasonably linear with respect to counter state. It is particularly fortunate that P_n^* is linear for the counter states $6 < n < 12$. This is true because the set point counter state of a pulse data control system will be within this range. Therefore, the D/A output pressure (system error) will change in steps of equal magnitude about the set point state of the system if this D/A converter design is used.

Additional study of the fluid state D/A flow device determined that it is possible to achieve a nearly linear output pressure characteristic if <u>two changes</u> are incorporated into the flow device.

1. Use outlet orifices in each stage which have linear flow-pressure characteristics.
2. Add an additional stage which always delivers flow to the flow collector, i.e. a bias stage.

Linear orifices can be realized in practice if the following two requirements are both satisfied[6].

1. The Reynolds No. (N_r) of the flow thru the orifice is less than 2000.
2. The minimum length (L) of the orifice satisfies the relation $L = .058\ N_r D$, where D is the diameter of the orifice.

The bias stage provides a positive D/A output pressure at a counter state of binary 0. As shown by Figure 4, this eliminates the most non-linear portion of the load orifice flow-pressure characteristic from the range of values of P_n*. Therefore, the load orifice characteristic is essentially linear as far as the D/A converter is concerned. This in conjunction with the linear receiver outlet orifices results in a nearly linear output pressure characteristic.

The general expression for calculating the discrete theoretical static output pressures of this fluid state D/A converter design as a function of counter state is

$$P_n^* = \frac{(2YVP_{r_1} + T^2) - \sqrt{(2YVP_{r_1} + T^2)^2 - 4Y^2V^2P_{r_1}^{\ 2}}}{2V^2 \quad P_{2^s-1}}$$

where $Y = n + (A_B/A_1)$

$V = 2^s - 1 + (A_B/A_1)$

$$T = \frac{RA_L C_{dL}\sqrt{2}}{A_1\sqrt{.0361\rho}}$$

A_B = Area of orifices in bias stage

C_{dL} = Load orifice flow discharge coefficient

A_L = Area of load orifice

A_1 = Area of outlet orifice in D/A input stage 2^0
R = $32 \mu L/D^2$ ("resistance")
μ = Absolute viscosity
ρ = Density
s = Number of D/A input stages (not including bias stage)
n = $0, 1, \ldots, (2^s - 1)$

The sixteen discrete theoretical static output pressures P_n* for a 4 input stage -1 bias stage "linear" D/A converter are shown as a function of counter state in Figure 5.

Two fluid state D/A converter designs have been presented. The first design uses nonlinear thin plate orifices and produces a reasonably linear static output pressure characteristic as shown in Figure 3. The second design uses linear orifices (subject to Reynolds number and L/D constraints) and a bias stage. However, it produces a nearly linear static output pressure characteristic as shown in Figure 5.

Development of Monostable Element for Fluid State D/A Converter

In order to implement either of the two fluid state D/A converter designs, it was necessary to develop a monostable element suitable for use at the input stages which satisfied these requirements:

1. When the monostable element of any input stage is switched "on"*, its "on" receiver pressure P_{r1} should always have approximately the same constant value (in any input stage) regardless of changes in either D/A output pressure P_n or in "on" control pressure P_{c1}. The output pressure P_n takes on a wide range of values as the counter state changes; P_{c1} increases approximately 17% (in the bidirectional counter design used) when counter operation changes from "increasing count" to "decreasing count". Also in any other binary "driver" there will be some variations in the binary control signals.
2. When the monostable element of any input stage is "off"**, its "off" receiver pressure P_{ro} should always be approximately atmospheric (in any input stage) regardless of changes in D/A output pressure P_n.

* Monostable element switched "on" means that its receiver delivers flow to the flow collector.
** Monostable element "off" means that its receiver receives flow from the flow collector.

3. Control nozzle size must be small so that "on" control nozzle flow Q_{c_1} is small. This is necessary so that sufficient flow remains for correct operation of the interstage pulse forming circuits of the counter.

Figure 6 is a drawing which defines the monostable element developed for use at the input stages of either of the two fluid state D/A converter designs. The final configuration of the element was established from experimental test results obtained using an adjustable test model.

As shown by Figure 7, this element can only approximately satisfy the requirement that the "on" receiver pressure P_{r_1} of the element remain constant regardless of changes in D/A output pressure P_n. Furthermore, the change in P_{r_1} with P_n increases as the number of outlet orifices increases. However, it was found that "dummy" receiver outlet orifices discharging to atmosphere could be used to make the average "on" receiver pressures from stage to stage more uniform. Thus it was possible to obtain experimental static output pressure characteristics closely approximating those predicted by theory.

The effect of a 66% change in $\bar{P}_{c_1}$ is to change $\bar{P}_{r_1}$ approximately 3.96%. In the actual counter used $\bar{P}_{c_1}$ changes approximately 17%. For this change in $\bar{P}_{c_1}$, the change in $\bar{P}_{r_1}$ is only 1.02%.

Experimental Static Test Results

Both fluid state D/A converter designs were built and tested. Figure 8 shows a 4 input stage "nonlinear" D/A design and Figure 9 a 4 input stage—1 bias stage "linear" D/A design. The actual static output pressure characteristic for the 4 stage "nonlinear" unit is shown by Figure 10; the static output pressure characteristic for the "linear" unit by Figure 11. The static output pressure characteristic for a 5 stage "nonlinear" unit is shown by Figure 12.

Experimental Dynamic Test Results

The four bit fluid state bidirectional counter designed by Wilson(1,2) was used to dynamically test both fluid state D/A converter designs.

In order to correctly interpret the dynamic test results, it is necessary to understand the sequential nature of the counter operation. Every pulse (either input or feedback) fed into the counter goes to the T memory element of least significance (2^0) causing it to always switch its outflow to the opposite outlet. If the change in counter state associated with a given pulse involves the switching of additional T memory elements, this occurs at time intervals of .008 sec. per suc-

ceeding T memory element.

For example, assume that the counter state is binary 7 and increasing. The next pulse into the counter changes its state to binary 8. The sequential manner in which this change of state occurs is:

Elapsed Time	Counter State	Comment
0	0111	pulse arrives
.002	0110	2^0 T switches
.010	0100	2^1 T switches
.018	0000	2^2 T switches
.026	1000	2^3 T switches

Note that the counter state actually goes from binary 7 to binary 6, then binary 4, then binary 0 before the state binary 8 is realized. Since the D/A converter follows the counter state closely, the D/A output pressure will have "decrease-increase" spikes whenever a change in counter state requires more than the 2^0 T element to switch. However, the spike of greatest time width occurs when all T elements must switch (transition from binary 7 to binary 8).

If the counter state is at binary 8 and decreasing, the situation is reversed. The counter state now actually goes from binary 8 to binary 9, then binary 11, then binary 15 before the state binary 7 is realized. Now "increase-decrease" spikes occur on the D/A output pressure. Again the spike of greatest time width occurs when all T elements must switch. If these "spikes" in the D/A output pressure should be objectionable to downstream circuitry, they could be eliminated by introduction of suitable time delays between the counter and D/A converter.

One other factor which must be considered is the maximum rate at which pulses may be fed to the counter. Because the counter transitions from binary 7 to binary 8, or vice versa, require .026 seconds to complete, pulses fed into the counter must not be less than .026 seconds apart. Therefore, the pulse rate to the counter must not exceed 1/.026, or 38.4 pulses per second. If higher pulse rates are used, the 2^0 T element will switch again before the 2^3 T element switches (binary 7 to binary 8 transition).

Figure 13 shows typical dynamic test results for a 4 input stage "nonlinear" D/A converter. Figure 14 shows typical dynamic test results for a 4 input stage -1 bias stage "linear" D/A converter.

Theoretical Dynamic Capability of Fluid State D/A Converters

Although dynamic testing is limited to pulse rates less than 38.4 pps, because of the carry propogation time of the counter, it is possible

to theoretically predict the maximum speed of operation from the transfer function. For a nonlinear D/A converter it is not possible to derive a linearised transfer function because of the nonlinear receiver outlet orifices. However, it is possible to derive the transfer function for the linear D/A converter which describes the change in output pressure for a single change in counter state. The transfer function is

$$\Delta P_n(s) = \frac{K(n)\, e^{-(T_{sp} + T_j)\, s} \left[\quad\right] (Q_{c_1} - Q_{s_o})(s)}{s^2 + 2\,\zeta w_n s + w_n^2}$$

where $\left[\quad\right] = \pm 8\, K_{c8}\, K_{r8} \pm 4\, K_{c4}\, K_{r4} \pm 2K_{c2}\, K_{r2} \pm K_{c1}\, K_{r1}$

$$K(n) = \frac{1}{\tau_r\, \tau_c(n)\, C_{(n)}}$$

$$\tau_r = \frac{R\, V_r}{A_8 B_s}$$

$$\tau_c(n) = \frac{RV_c}{C(n) A_1 B_s}$$

$$C(n) = \frac{RA_L C_{dL}}{A_1 \sqrt{2\rho P_{n_o}}} + 19$$

T_{sp} = attachment wall separation time

T_j = nozzle to receiver transport time

$K_{ri} = \dfrac{R}{\bar{X}_i}$ $\quad i = 8, 4, 2$ or 1

K_{ci} = Flow gain from control nozzle to receiver inlet $i = 8, 4, 2$ or 1

$$\zeta = \frac{\tau_r + \tau_c(n)}{2\tau_r\, \tau_c(n) w_n}$$

$$\omega_n = \left[\frac{R A_L \, C_{dL}}{\tau_r \tau_e(n) \, C(n) \, A_1 \, (2\rho P_{ne})^{1/2}} \right]^{1/2}$$

$$R = \frac{32 \mu L}{D^2}$$

By evaluating the natural frequency ω_n and the damping ratio ζ, it is possible to predict the dynamic capabilities of the linear D/A converter. For the unit designed the calculated values are

$$\omega_n = 1880 \text{ rad/sec}$$

$$\zeta = 11.7$$

Substituting these values into the denominator of the transfer function and factoring gives the two real roots

$$(s+81)\ (s + 43.900)$$

The effect of the largest root on overall dynamics will be extremely small and can be neglected. Therefore, the linear D/A dynamics can be approximated by a first order transfer function as follows:

$$\Delta P_n(s) = \frac{K(n)\, e^{-(T_{sp} + T_j)s} \boxed{} (Q_{c1} - Q_{co})(s)}{81\ (\tau s + 1)}$$

where $\quad \tau = \frac{1}{81} = .0123$ seconds = dominant time constant

It is difficult to determine the maximum operating speed of the D/A converter since this depends on the desired analog waveform. However, for a dominant time constant of .0123 seconds, the output pressure of the linear fluid state D/A converter built will become attenuated and delayed for counter operating speeds greater than 1/.0123, or 81 pps. This is illustrated in Figure 15 where two types of bidirectional counter behavior are examined and the effects of D/A dynamics are noted. In Figure 15a it is assumed that a pulse train of constant frequency enters the "up" line of the bidirectional counter and a second pulse train, 90° out of phase, enters the "down" line of the bidirectional counter. This situation is a common one during steady-state operation of a pulse data system in response to a ramp input. The effect of the switching and transport delay $T_{sp} + T_j$ is to delay the response of the D/A converter. The effect of τ is to attenuate

the "ripple" in the D/A converter output pressure. As T/τ the ratio of bidirectional counter oscillation period to D/A time constant approaches zero, the output ripple e_o approaches zero. Thus for this bidirectional counter behavior the effect of increasing τ is to reduce output ripple.

If the bidirectional counter state is increasing at a constant rate as shown in Figure 15b a different effect is displayed. In this case a pulse data system and the postulated bidirectional counter behavior could represent the situation where, at the start of the transient, no feedback pulses have been generated. If the bidirectional counter state is decomposed into a ramp and a ripple, it can then be shown that the D/A converter dynamics cause its output to lag behind the ramp portion of the bidirectional counter state by an amount equal to the lag $T_{s_D} + T_i$ plus the D/A time constant τ. It is obvious that this will have a destabilizing effect on the pulse data control system where this combination of bidirectional counter and D/A converter is used. In fact it is difficult to determine the maximum allowable rate at which the bidirectional counter can change state based on the D/A converter dynamics, because this depends on the waveform of the counter state changes.

The D/A converter dynamics, however, contribute directly to the stability of a pulse data control system which uses this element. In general this effect depends on the topology of the particular system in question, but if the D/A converter output is used as the control, then D/A converter dynamics can be combined with the dynamics of the subsequent system stages to determine stability. Since stability will determine overall system gain and bidirectional counter capacity, and gain will determine the maximum system operating rate, D/A converter dynamics can determine the maximum system operating rate indirectly. However, for the present state of the art, the bidirectional counter is the limiting factor in determining maximum system operating rate.

Anticipating the design of bidirectional counters with higher operating speeds it is of interest to determine if this fluid state D/A converter design can be modified such that attenuation of its output pressure occurs only for counter operating speeds greater than the 81 pps previously cited.

The dominant time constant τ is a function of ζ and ω_n, both of which are functions of the receiver volume V_r and the flow collector volume V_c. If the flow collector volume of the design built is decreased by a factor of three fourths, the dominant time constant becomes .0067 seconds. Now the output pressure of the D/A converter will only become attenuated for counter operating speeds greater than 1/.0067, or 150 pps. Even higher counter operating speeds before attenuation occurs could be obtained by decreasing the receiver volume of the input stages. However, this would have to be accomplished without changing

the receiver loading characteristics (See Figure 7).

There is one additional factor which should be considered in predicting the maximum speed of operation of the linear fluid state D/A converter. This factor is the magnitude of the supply jet separation time T_{sp} and the magnitude of the supply jet to receiver transport time T_j of the monostable element input stages. For the monostable element design used, the sum of the two was experimentally measured to be on the order of .008 seconds. This, therefore, limits maximum operating speed of the design built to approximately 1/.008, or 125 pps. However, miniaturization of the monostable element input stages would allow a significant increase in this value.

System Test Results

Figure 16 shows the operation of the linear D/A converter in the prototype fluid state digital pulse data control system. A step input was applied to the system by resetting the counter from its set point state (binary 8) to binary 0. Each feedback pulse generated by the quantizer increases the counter state by one until the set point state is reached. Note the reduced overshoot and increased stability when digital lead compensation is incorporated.

Conclusions

Design requirements were established for a fluid state D/A converter to be used in a fluid state digital pulse data control system. Two D/A converter designs satisfying these requirements were built and tested. One design used simple nonlinear thin plate orifices and produced a reasonably linear static output pressure characteristic. The other design used linear orifices and a bias stage and produced a linear static output pressure characteristic. Both designs were tested statically and dynamically. Static test results were in good agreement with those predicted by theory. Dynamic testing was limited to fairly low counter pulse rates, but it was possible to predict the dynamic capability of the linear orifice design from its transfer function. It is anticipated that the dynamic capabilities of the nonlinear orifice design will not be significantly different. Both designs performed satisfactorily in a complete fluid state digital pulse data control system.

References

1. Wilson, J. N., "A Fluid Analog to Digital Conversion System", Doctor of Philosophy Thesis, Cleveland: Case Institute of Technology, 1964.

2. Wilson, J. N., "Fluid Analog to Digital Conversion System", Fluid Amplification Report No. 13, Harry Diamond Laboratories, Washington, D. C.

3. Orner, P. A., "A Fluid Amplifier Controlled Pneumatic Turbine Servomechanism", Doctor of Philosophy Thesis, Cleveland: Case Institute of Technology, 1964.

4. Orner, P. A., Taft, C. K., "Development of a Pure Fluid Power Amplifier", Prodeedings 1965, Joint Automatic Control Conference.

5. Susskind, Alfred K. (ed.), "Notes on Analog-Digital Conversion Techniques", New York: John Wiley and Sons, 1957.

6. Langhaar, H. L., "Steady Flow in the Transition Length of a Straight Tube", Journal of Applied Mechanics, Vol. 9, pp 55-58, 1942.

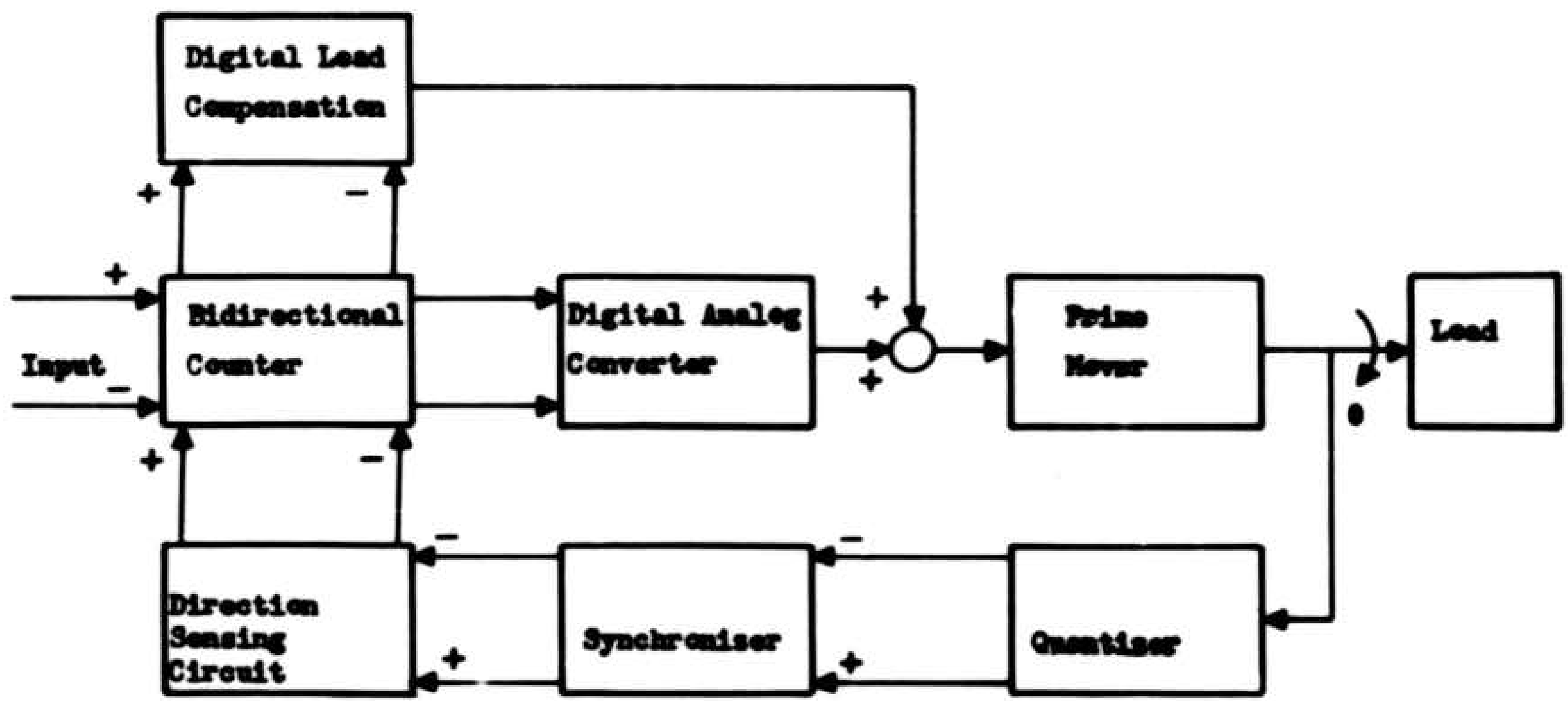

Figure 1 Block Diagram of Fluid State Digital
Pulse Data Control System

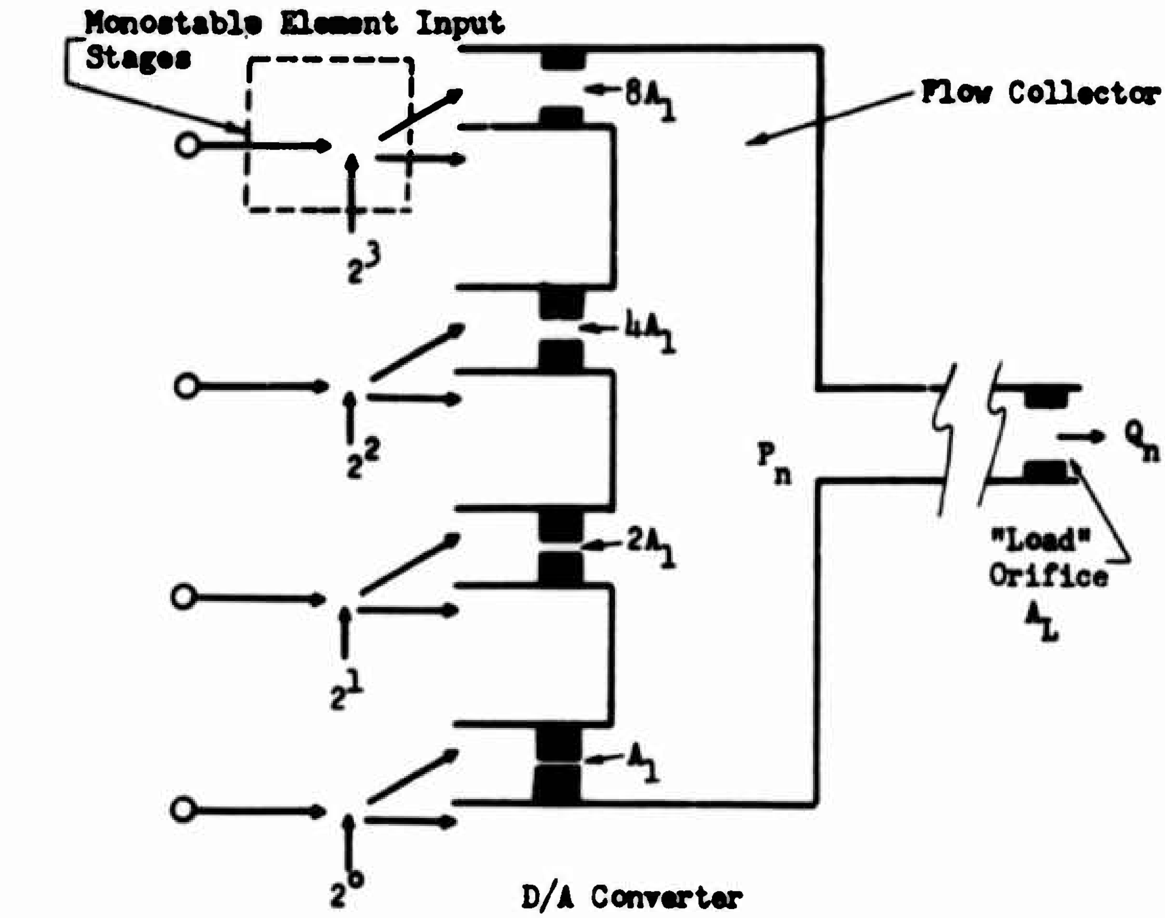

D/A Converter

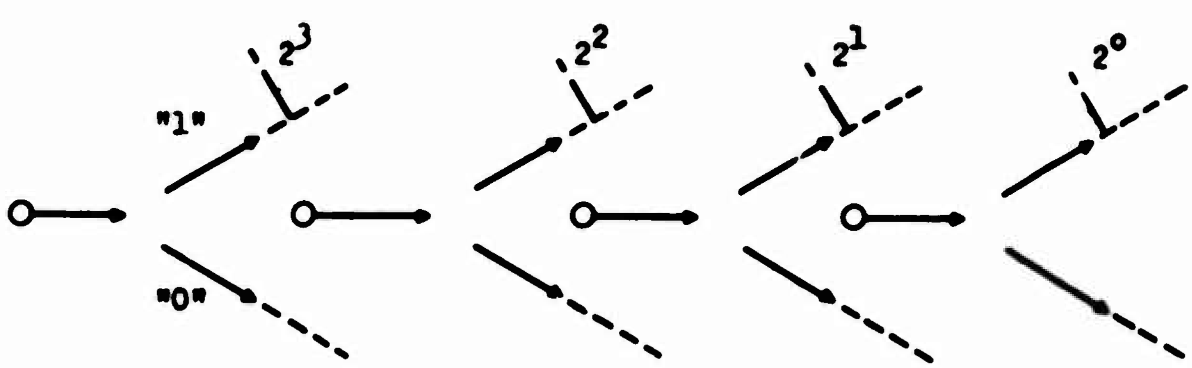

Memory Portions of T Memory Elements Located

In Bidirectional Counter

Figure 2 Fluid State D/A Converter

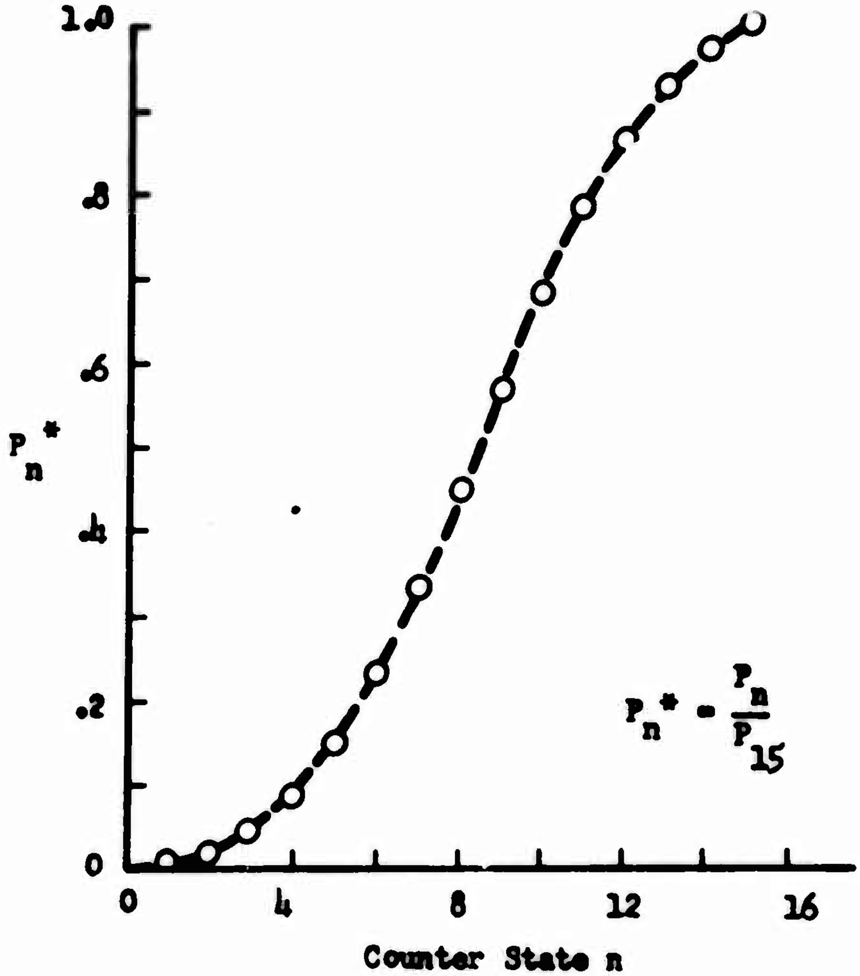

Figure 3 Theoretical D/A Output Pressure Characteristic

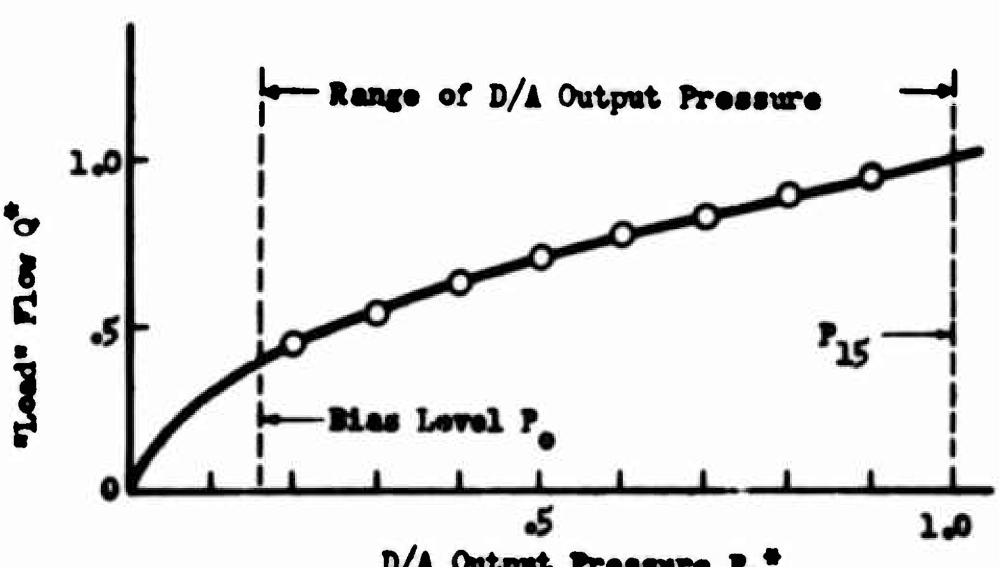

Figure 4 Effect of D/A Bias Stage

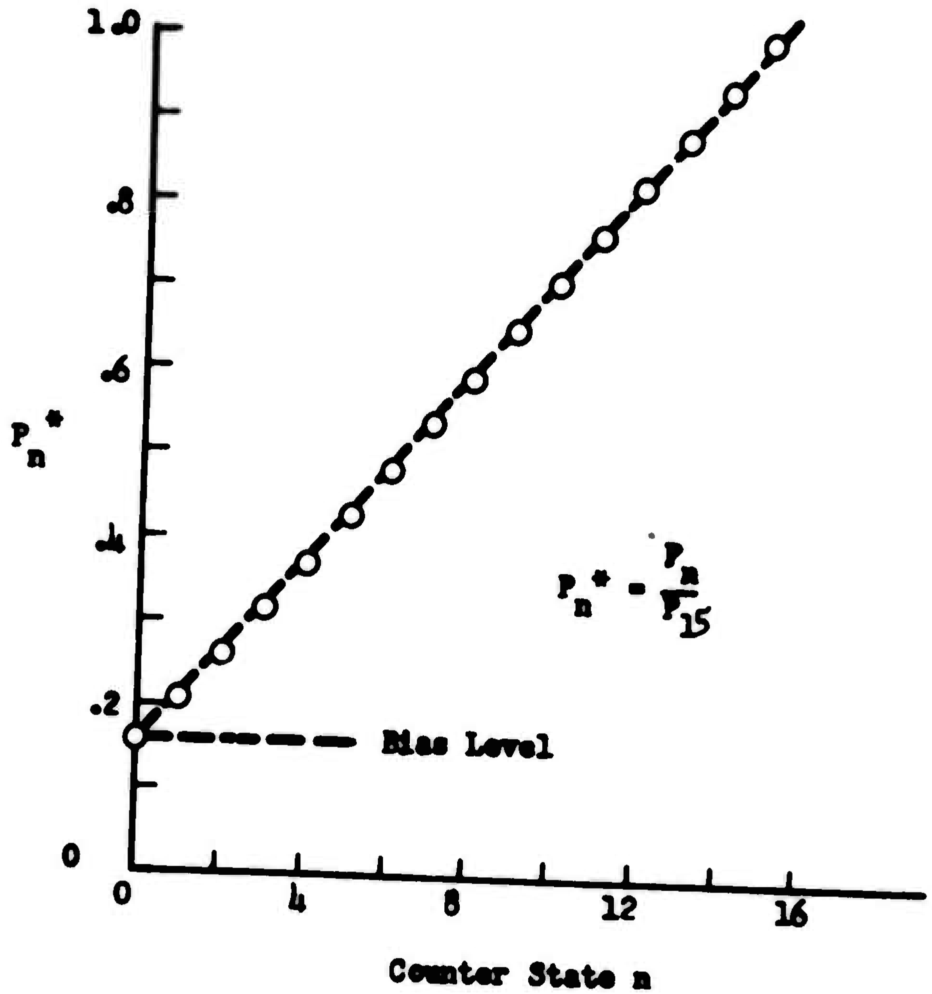

Figure 5 Theoretical "Linear" D/A Output

Pressure Characteristic

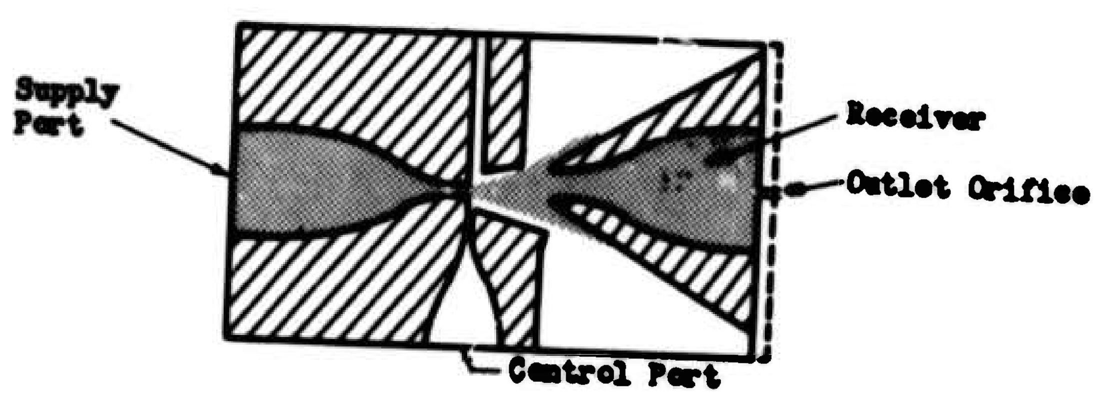

Figure 6 Monostable Element for Fluid State

D/A Converter

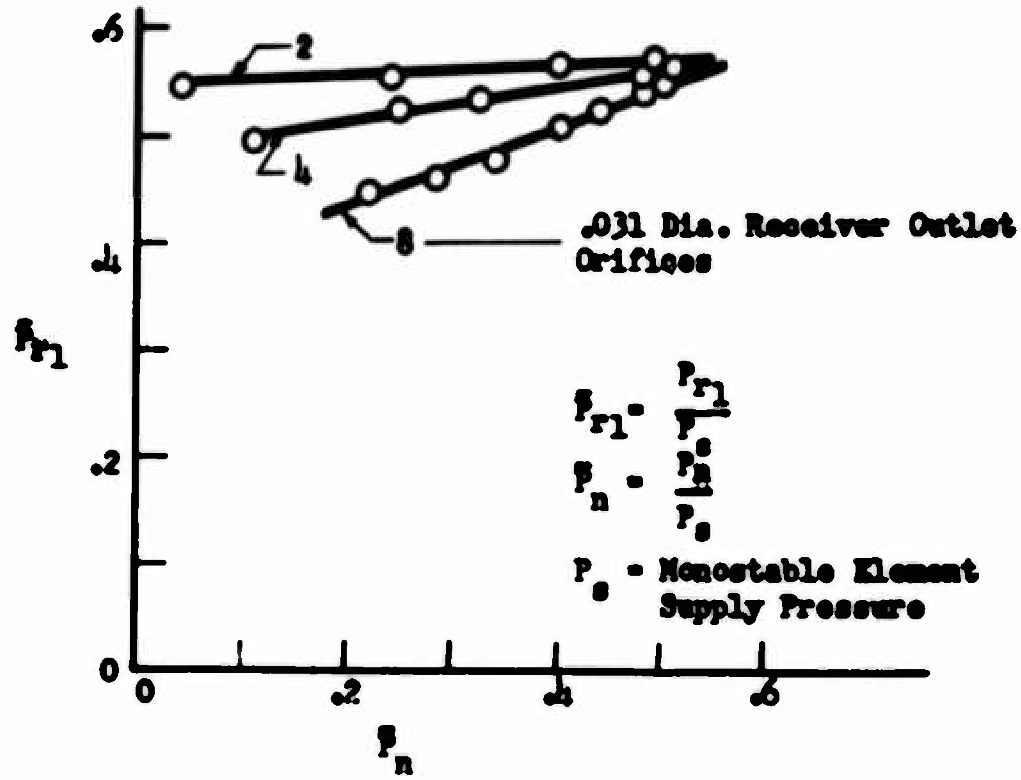

Figure 7 Receiver Loading Characteristics

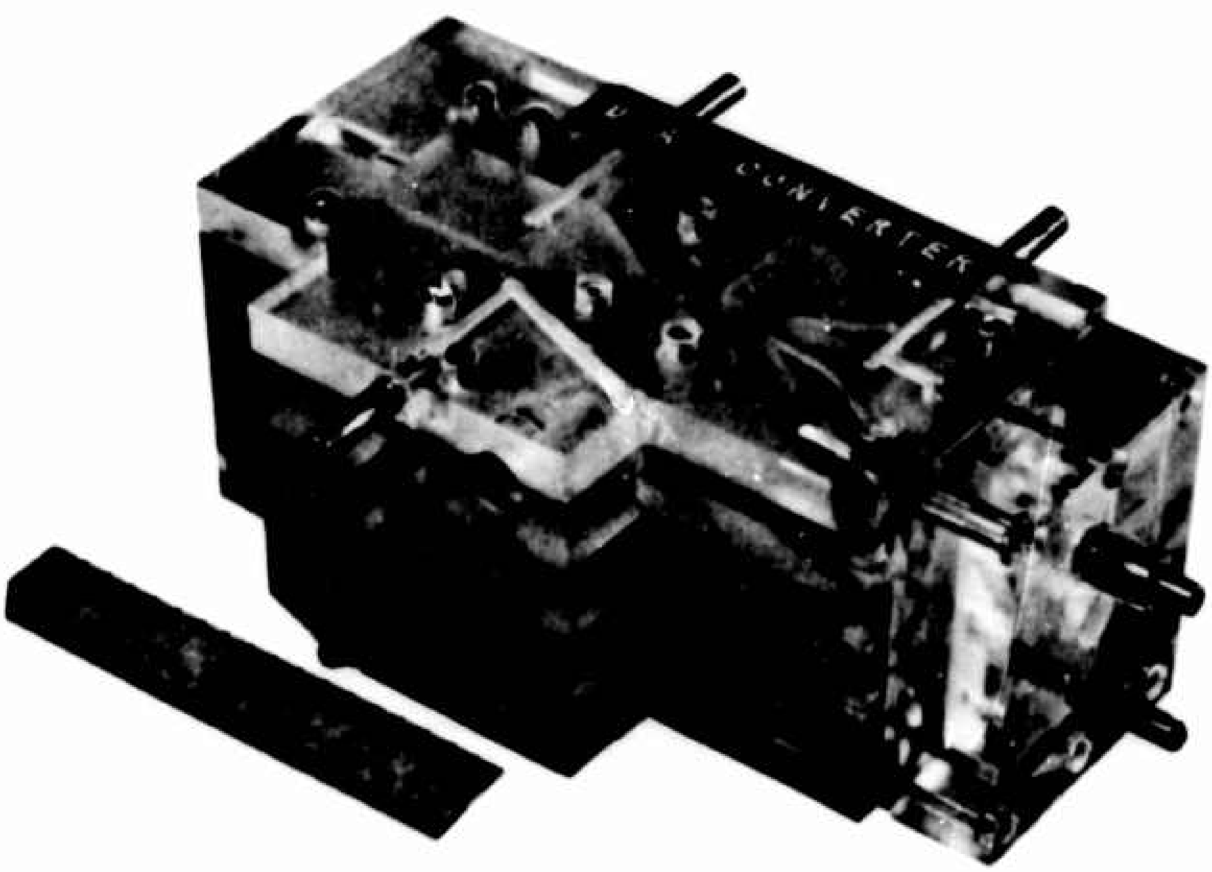

Figure 8 "Nonlinear" D/A Converter

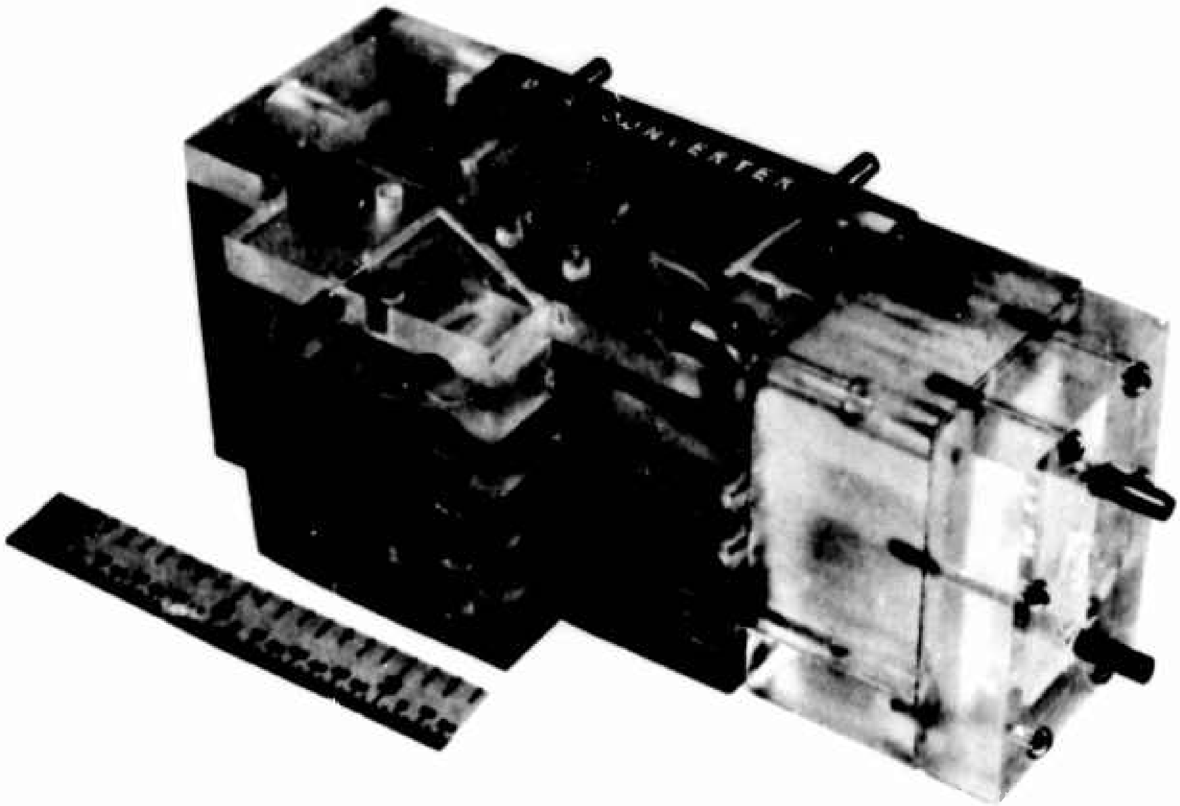

Figure 9 "Linear" D/A Converter

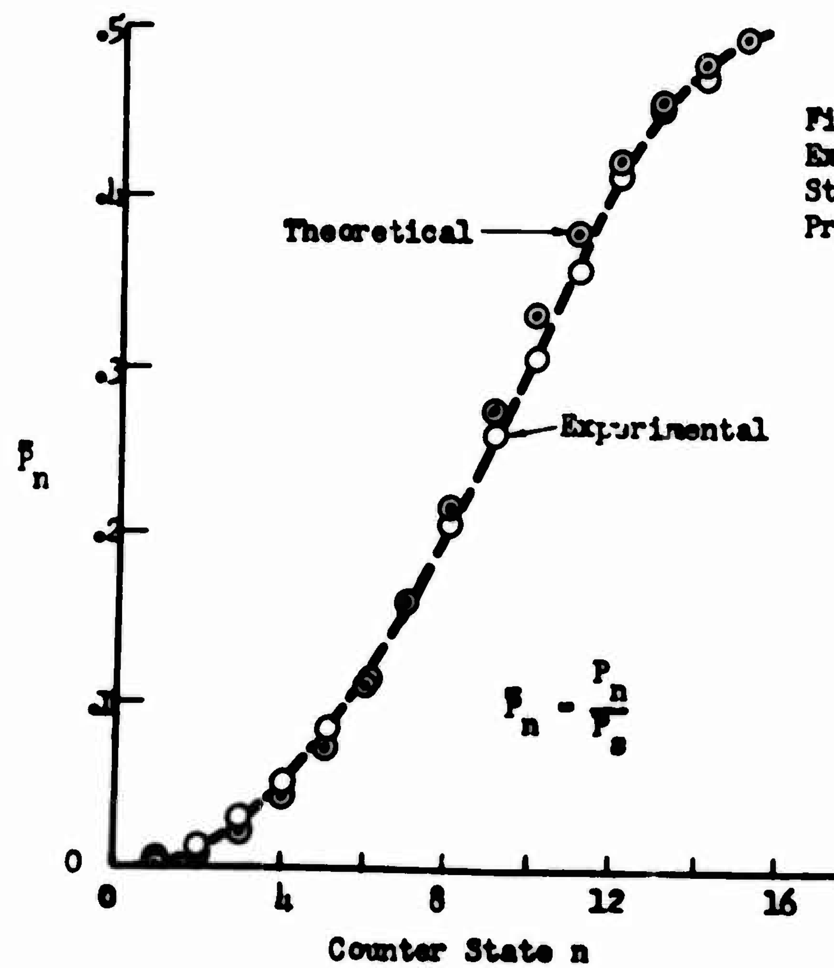

Figure 10
Experimental
Static Output
Pressure

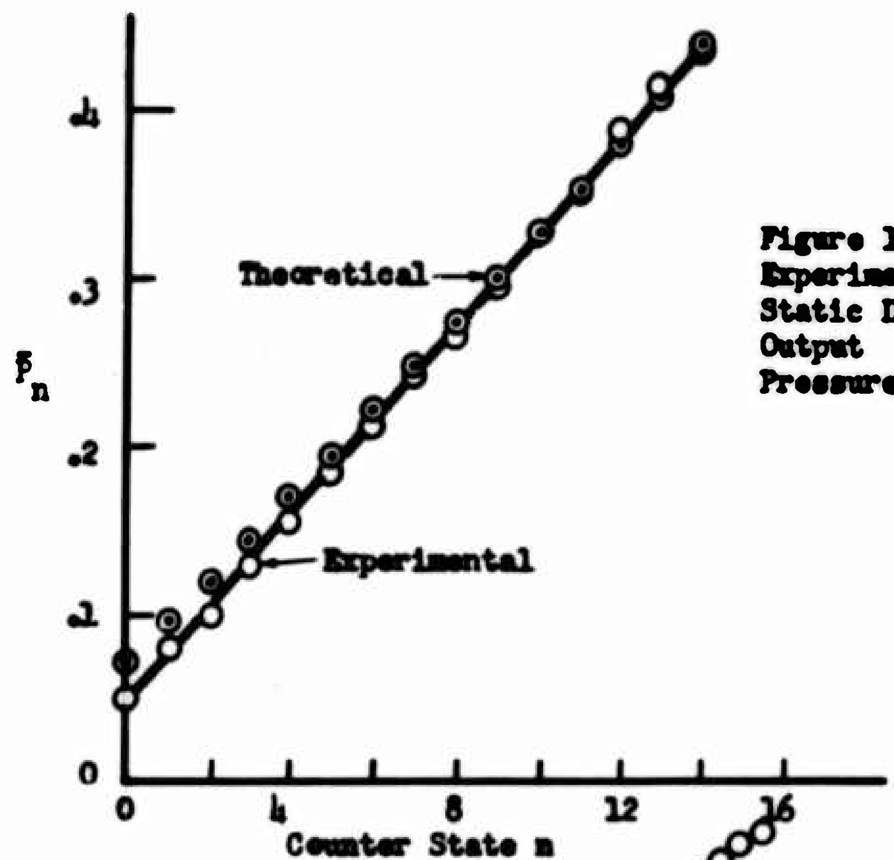

Figure 11
Experimental
Static D/A
Output
Pressure

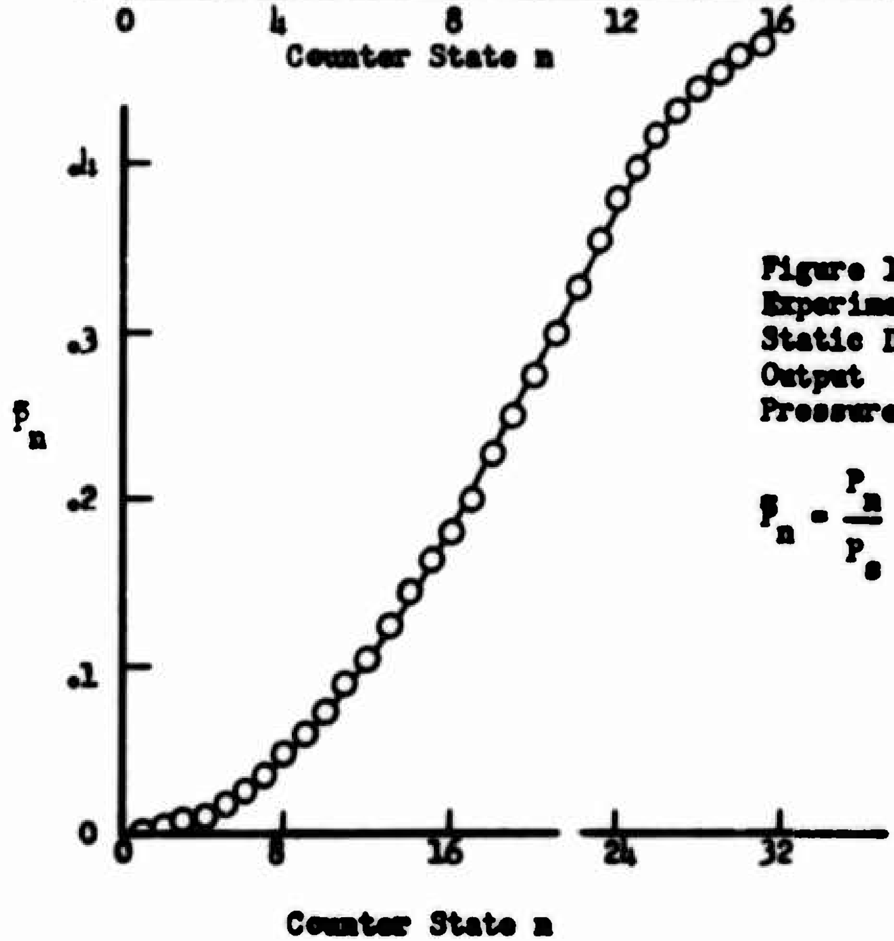

Figure 12
Experimental
Static D/A
Output
Pressure

$$\bar{P}_n = \frac{P_n}{P_s}$$

well with all three capacitances. Figure 14 is a plot of flow output as a function of control flow input. The solid line represents change in output flow without any screw (bias) adjustments. This curve shows that the jet does not split equally between the two outputs. The dotted line is the same curve taken after the screws on the oscillator have been adjusted to obtain a flow balance. From the dotted graph it is evident that a proportional flow gain of about 500 is obtained. The pulsating flow was measured by using two minimum orifice-type flow meters, one placed at each output. Hence a change in output flow due to change in control flow could be constantly monitored.

A laboratory rocket model was built (fig. 15), and the whole system was placed in it. An autopilot of the bank and climb type was obtained and connected directly to the system. The gyroscope output is in the form of a proportional signal for any deviation from a preset position. The whole missile was free to rotate about its center of gravity. Whenever a change in its preset position occurred, the gyro commanded the pneumatic system to exert thrust in a direction opposite to the missile displacement. The two knobs on the stand were provided for manual control by eliminating the gyroscope from the circuit. The input signal in the manual control was provided directly from the atmosphere since the pressure in the control port is below atmosphere.

At this particular time the work is being directed toward using the system as a control for a ballistic-type missile. A supersonic last stage has been developed to obtain the thrust necessary for control, and

a vortex gyroscope is in the process of development to be used as the sensor. In this manner, a whole pneumatic control system with no moving parts will be constructed.

4. CONCLUSION

A reaction control system is quite useful for attitude control for vehicles in which ordinary control surfaces cannot be employed (ref. 3). The use of a proportional reaction-type control system is more effective than the on-off type, and higher performance can be achieved. The reaction control discussed produces a differential thrust, by means of a combination of d-c shift and pulse width modulation, that is proportional to a steady differential signal applied to the control ports. The size of the control signal in terms of power necessary to produce full deflection is 0.74 watts at 24psig (or 165.5 KN/m^2) input pressure; the output is the equivalent of 1627w. The pressure or flow differential at the control can come directly from a pneumatic gyroscope or a non-moving-part rate gyroscope of the vortex type. In the latter case, the pitch rate or yaw rate can be controlled by jet reactions in response to command signals from the vortex gyroscope.

5. ACKNOWLEDGMENT

The authors are greatly indebted to John M. DeLawter for having assisted in the construction of the system. The authors wish to thank Mr. George A. Gray and A. L. Notestine for providing great accuracy in the machining of the various components. The authors are indebted to W. J. Kehres who helped in setting up the apparatus for gathering data for the various tests.

REFERENCES

1. Kadosch, M. Contribution au freinage des avions a reaction par deviation du jet propulsif. Bulletin de la Societe francaise des Macaniciens, 1955, No. 16, pp. 41-50.

2. Campagnuolo, C. J., "A Three-Stage Digital Amplifier," TR-1106, Harry Diamond Laboratories, Army Materiel Command, Washington, D.C. 20438.

3. Wai Chao, W. "Hot-Gas Systems Control Attitude in Extreme Environment," Aerospace Engr. March 1961, pp. 65-69.

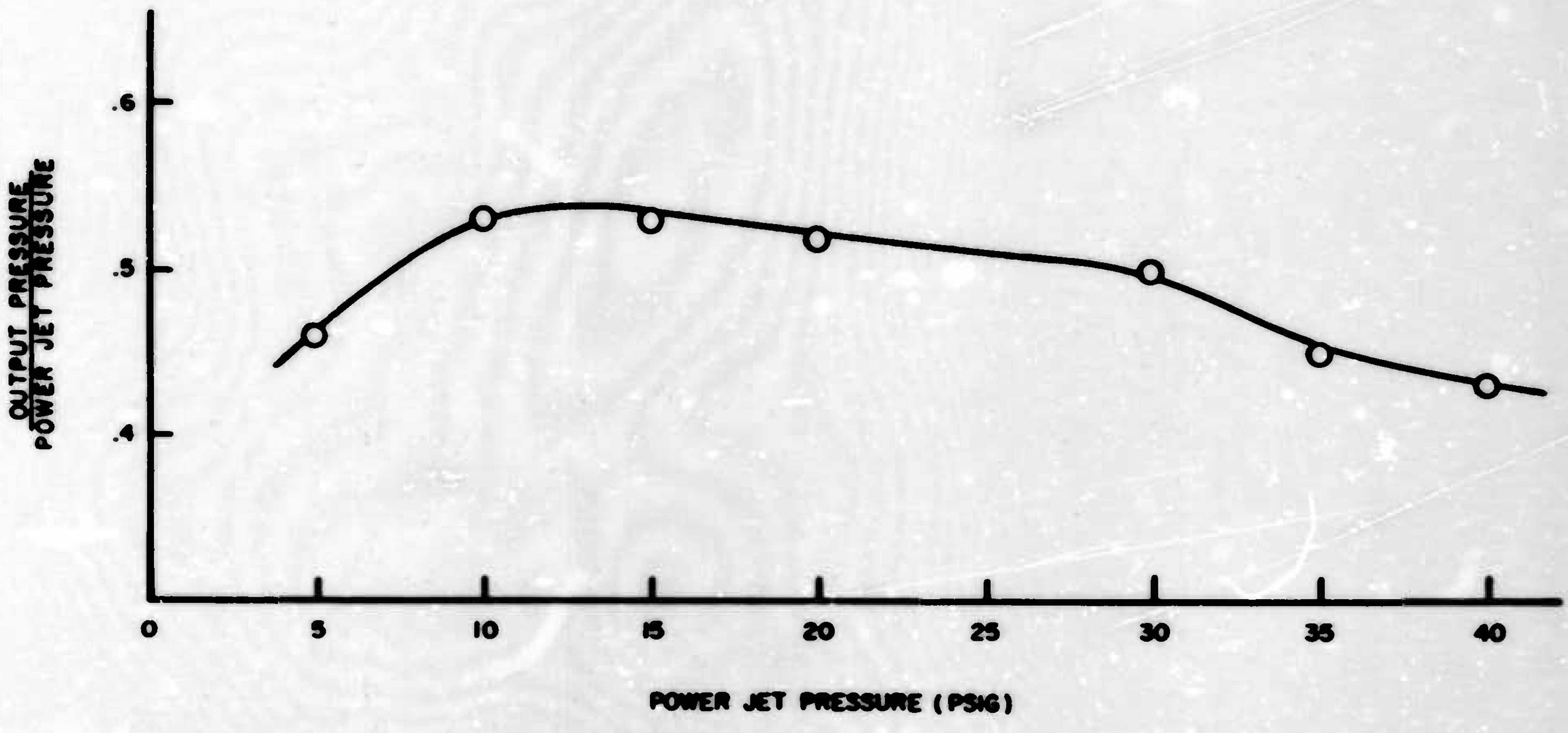

601-65

Figure 1. Pressure recovery of three-stage digital amplifier versus power-jet pressure.

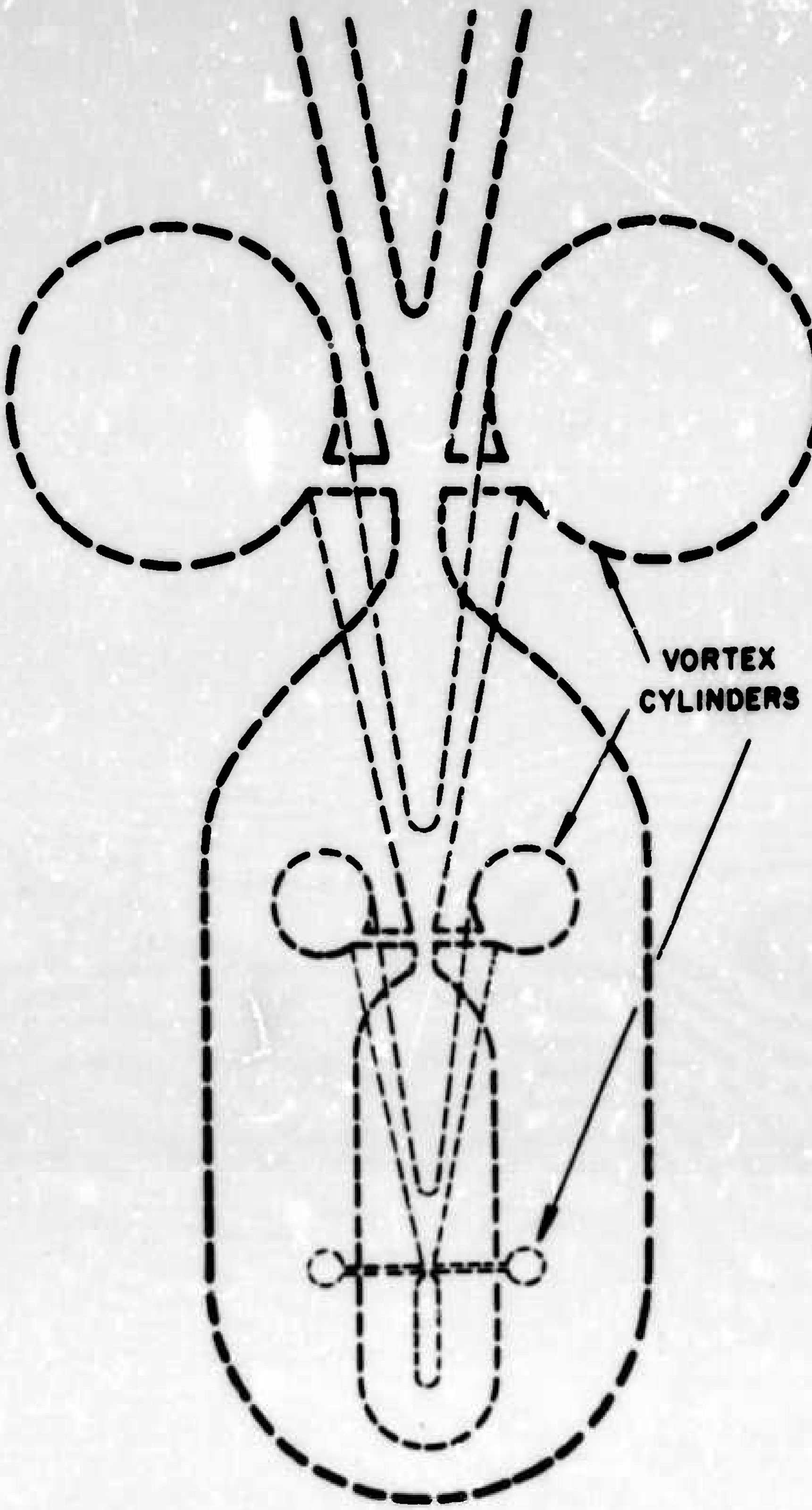

Figure 2. Schematic diagram of three-stage digital amplifier.

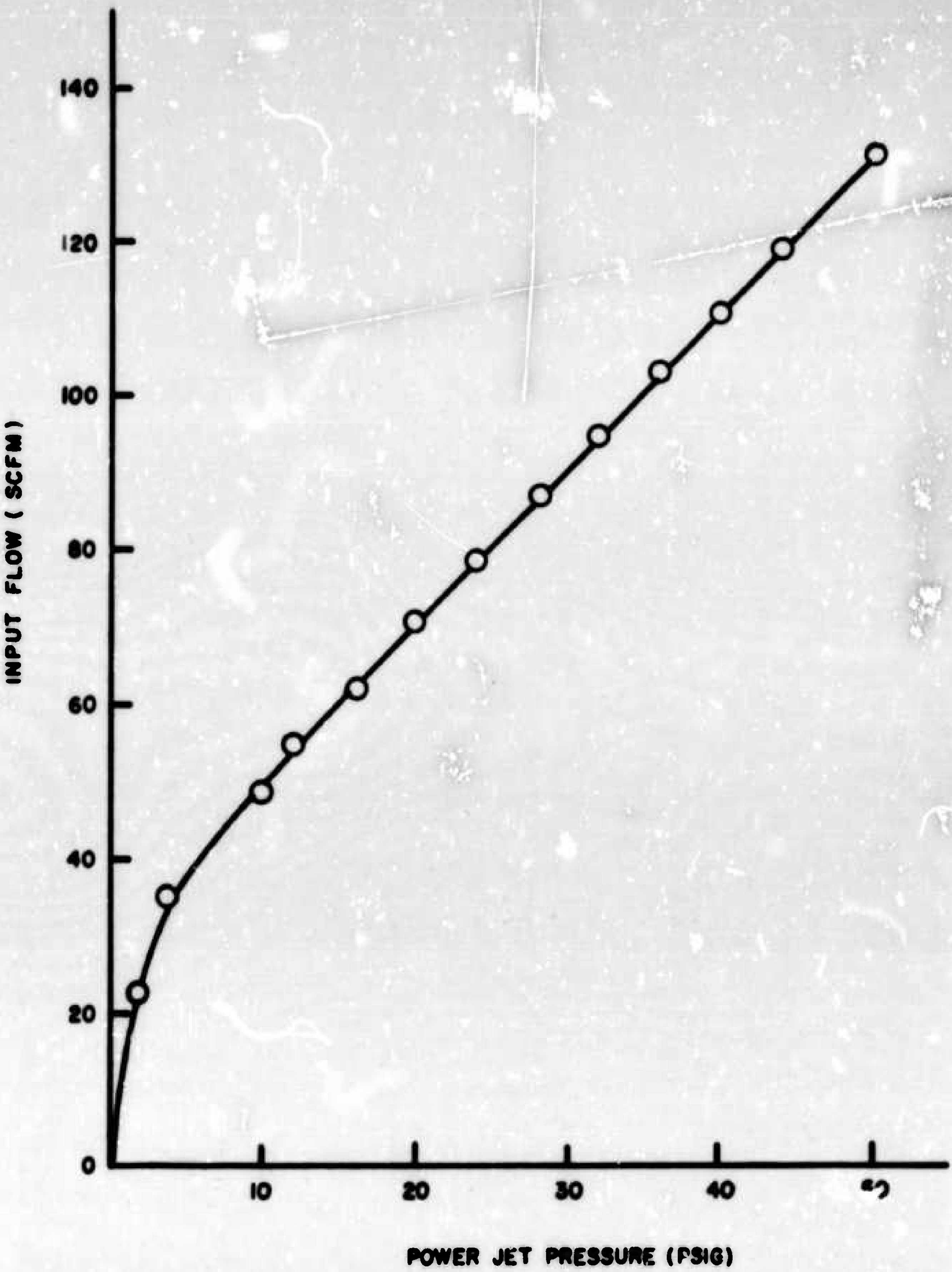

593-65

Figure 3. Input power jet flow versus input pressure for three-stage digital amplifier.

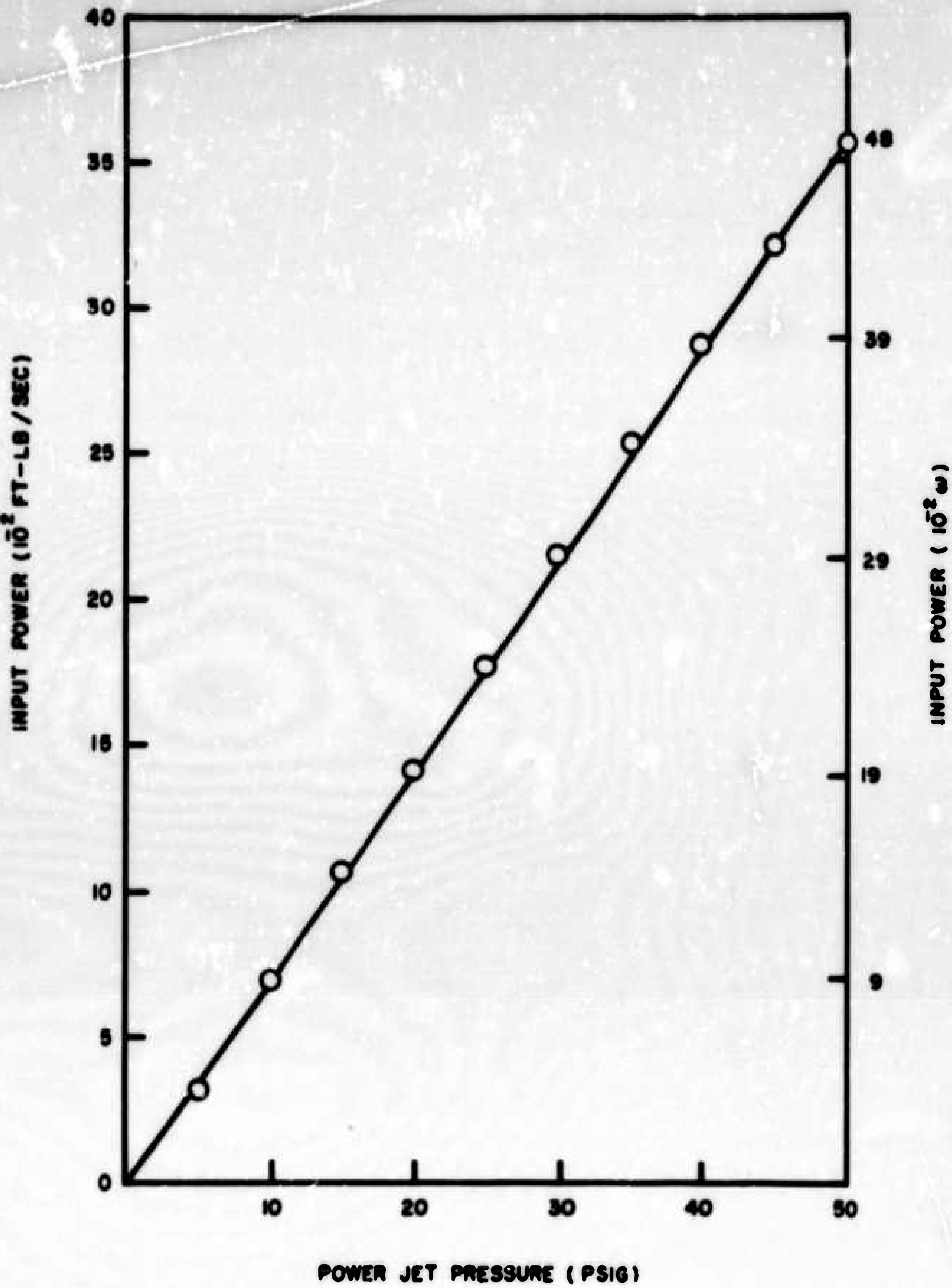

595-65

Figure 4. Input power jet power as a function of input pressure of three-stage digital amplifier.

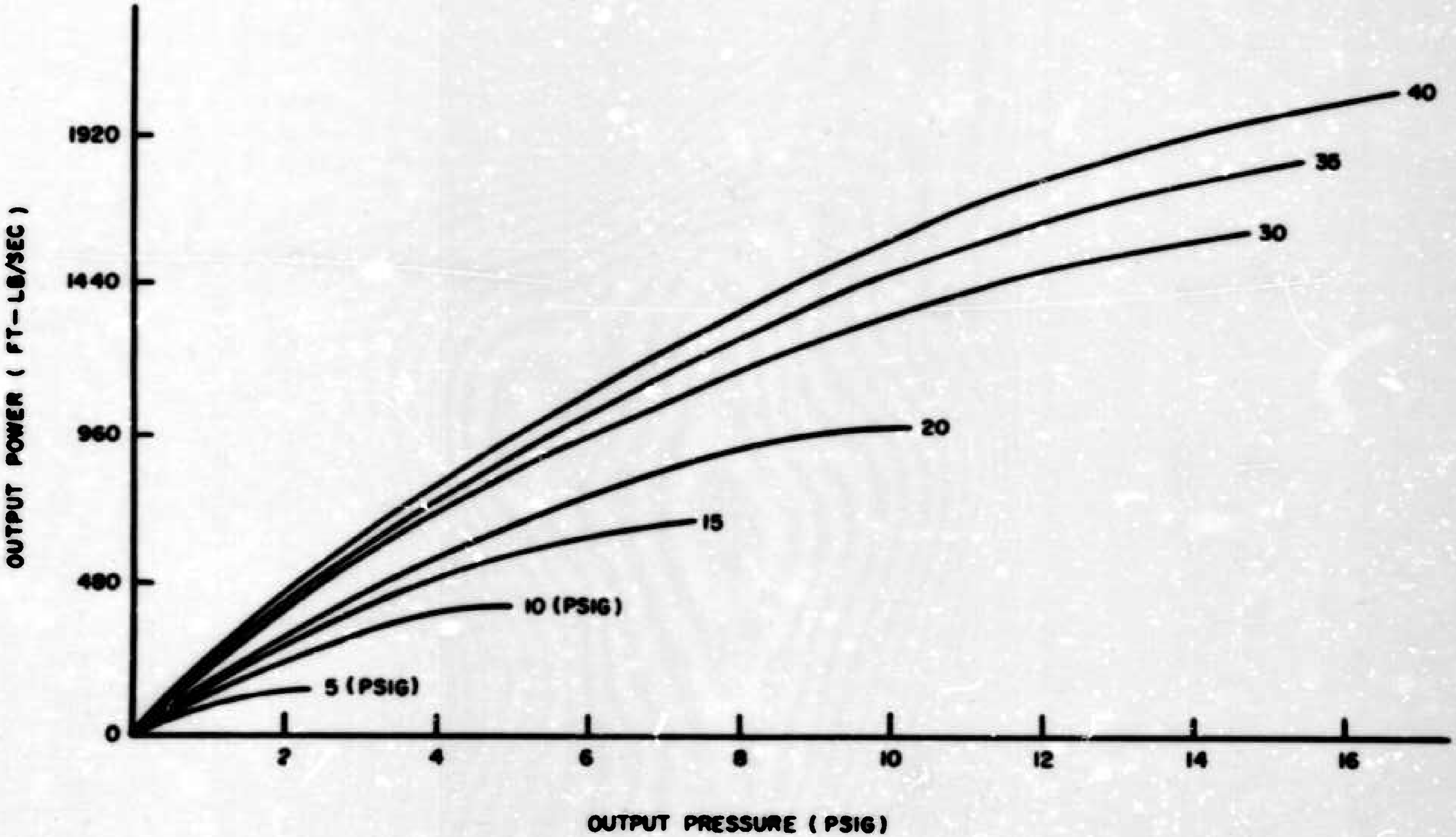

602-65

Figure 5. Load curves for three-stage digital amplifier for various power jet pressures.

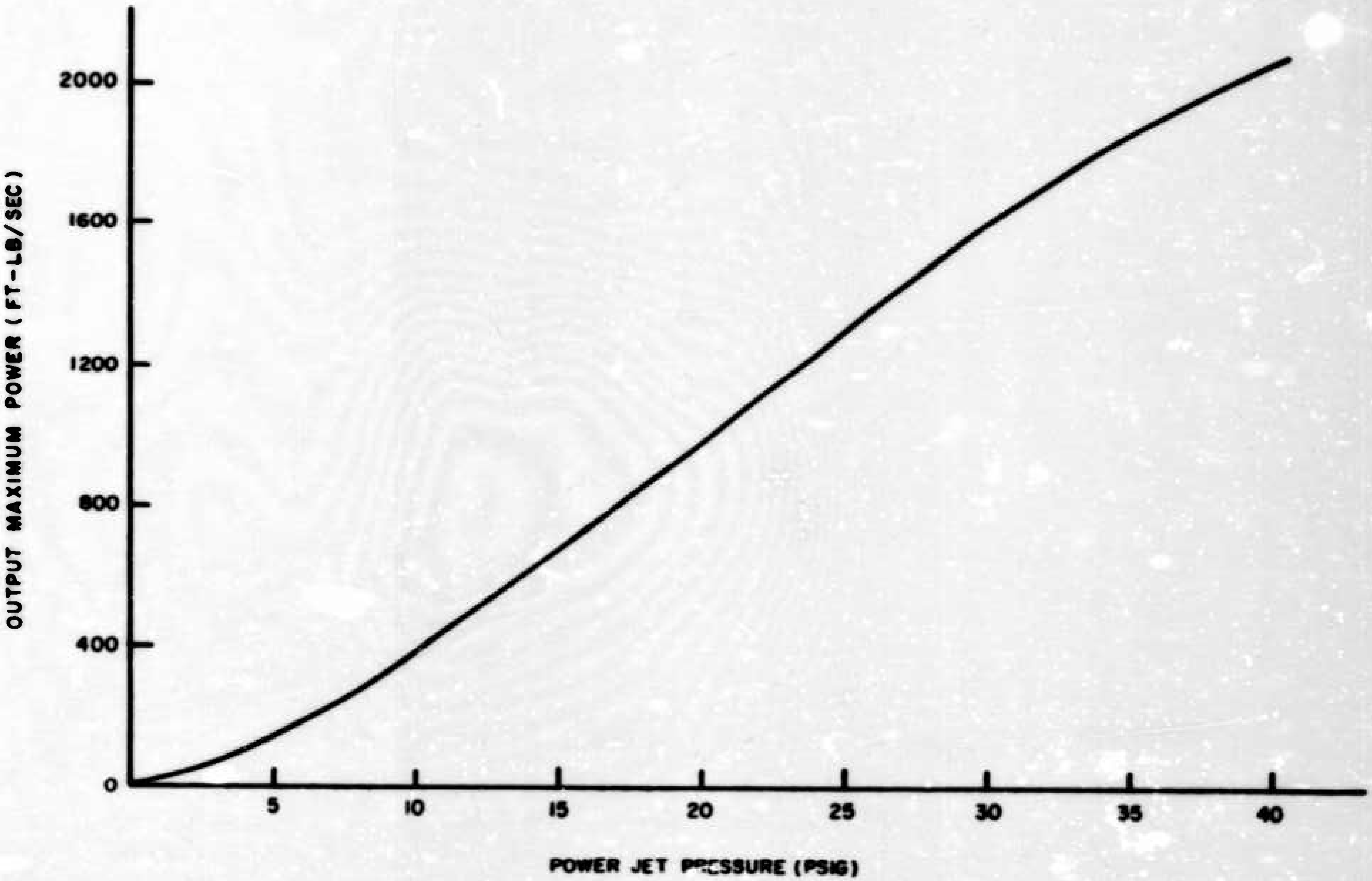

600-65

Figure 6. Maximum output power of three-stage amplifier versus power-jet supply pressure.

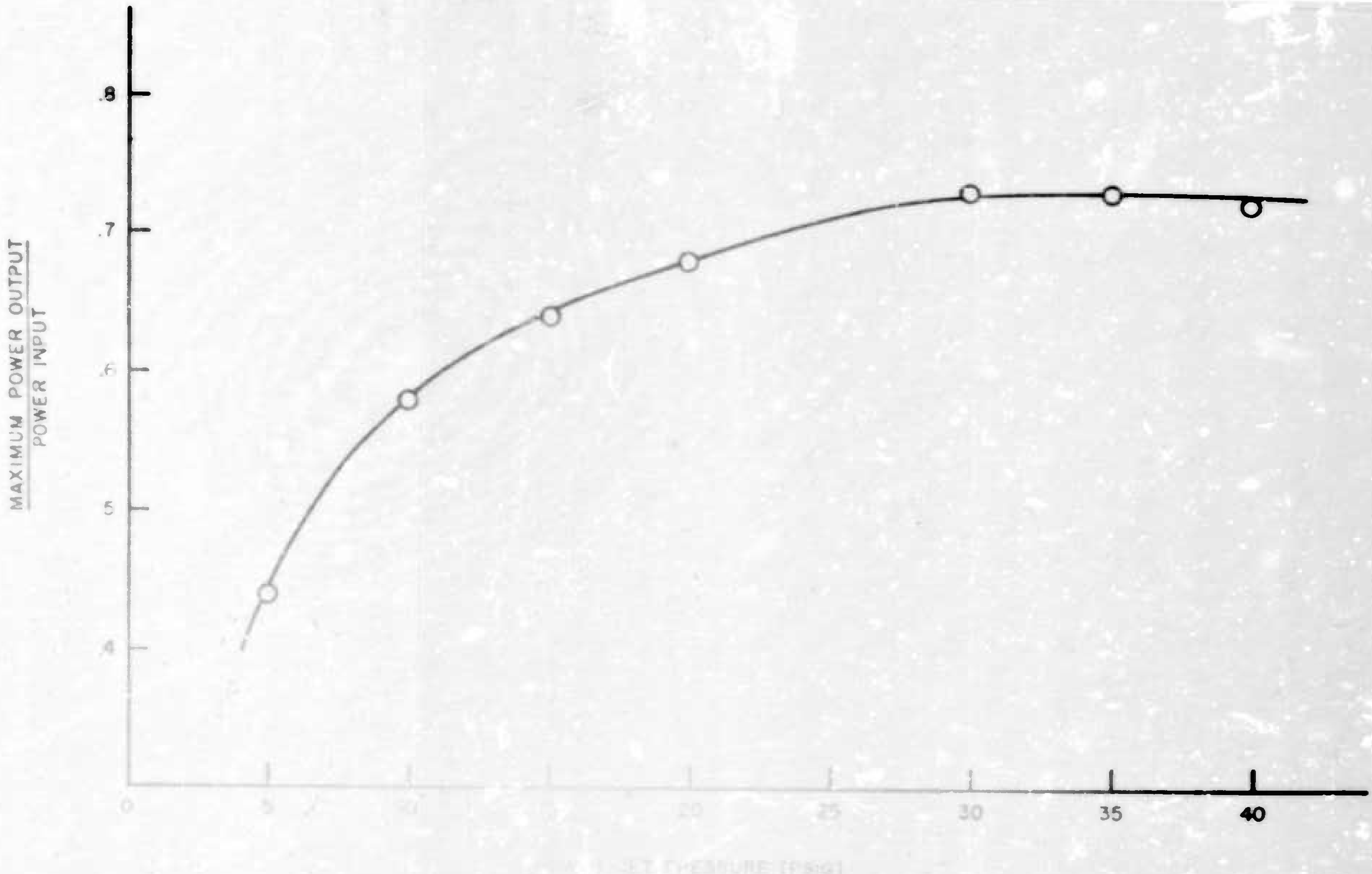

599-65

Figure 7. Power efficiency of three-stage digital amplifier versus power-jet supply pressure.

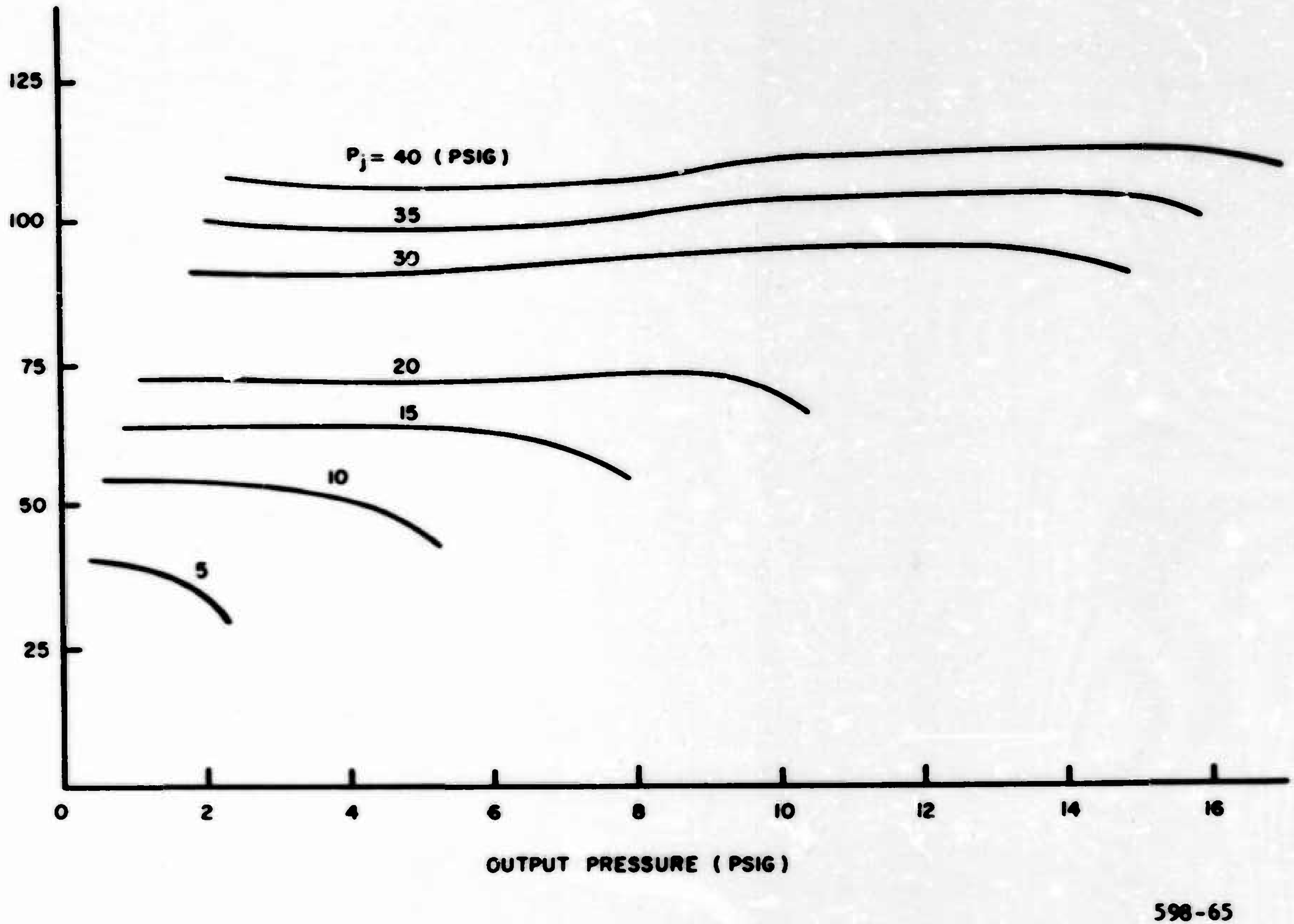

Figure 8. Output flow versus output pressure of three-stage digital amplifier for various power jet pressures.

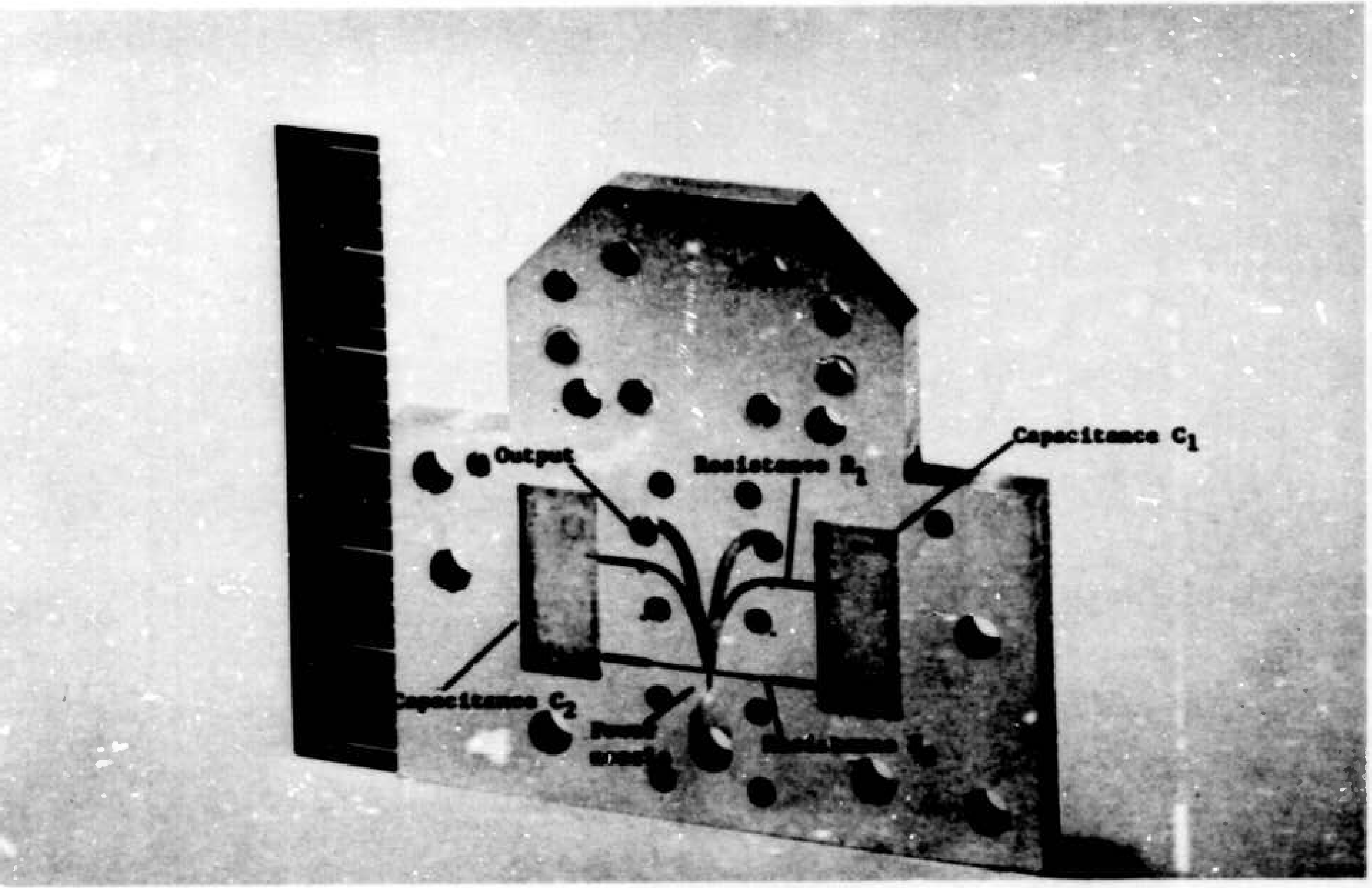

Figure 9. Relaxation oscillator. 1840-64

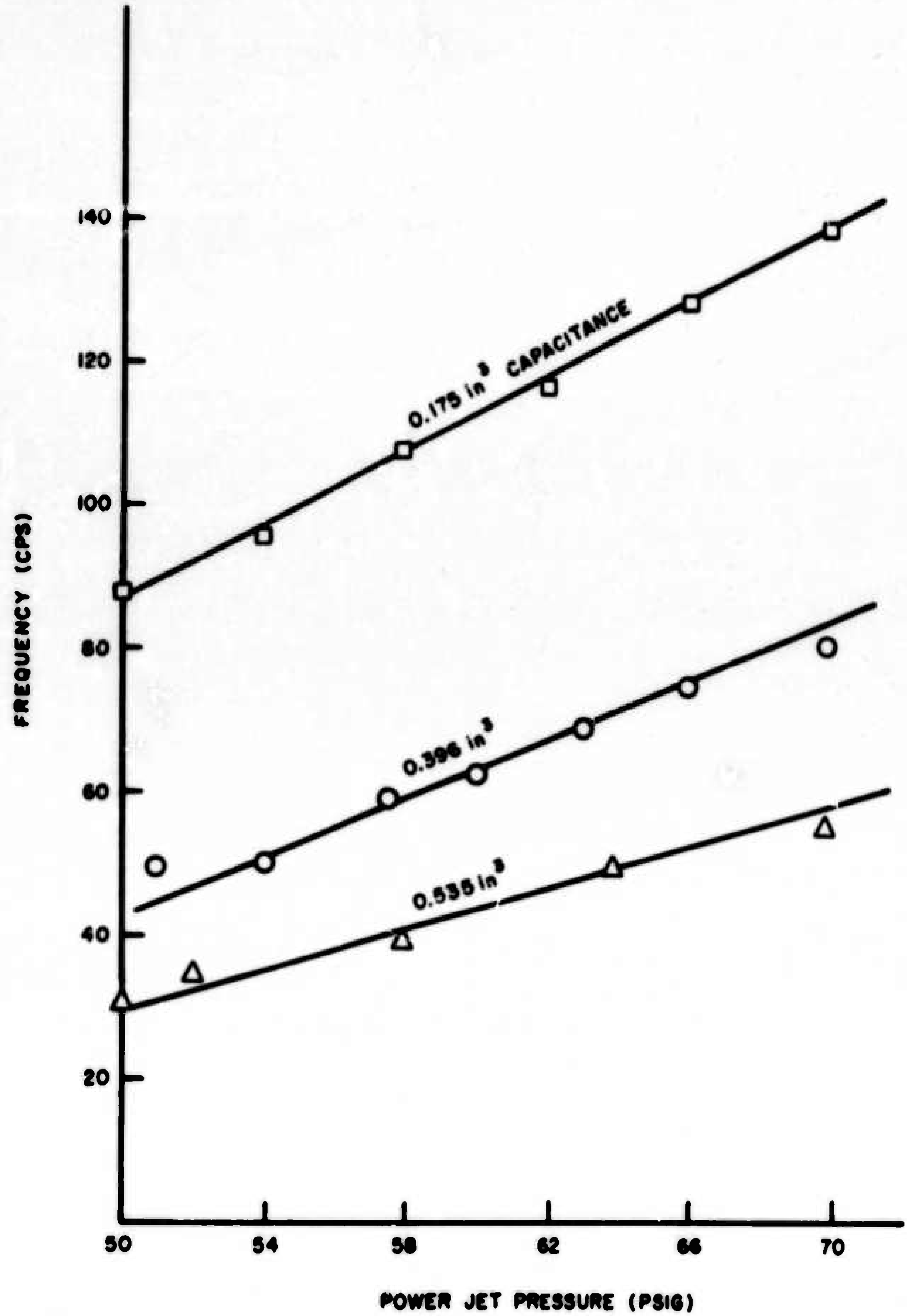

FREQUENCY (CPS)
140
120
100
80
60
40
20
0.175 in³ CAPACITANCE
0.396 in³
0.535 in³
50
54
58
62
66
70
POWER JET PRESSURE (PSIG)

596-65

(a)

p_j = 58 psig

freq = 40 cps

(b)

p_j = 64 psig

freq = 50 cps

(c)

p_j = 70 psig

freq = 55 cps

555-65

Figure 11. Traces from the output flow of Rc relaxation oscillator

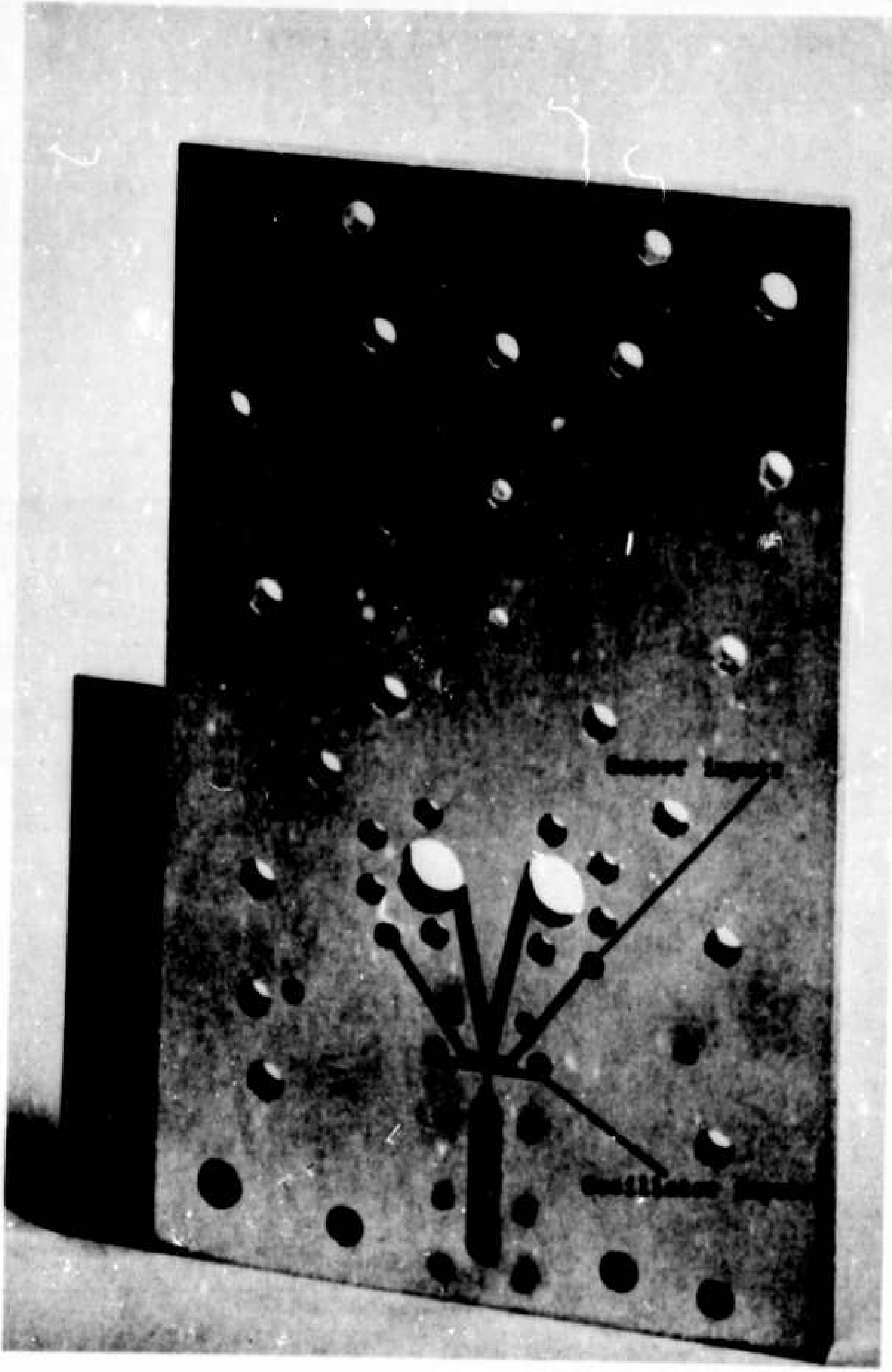

Figure 12. First-stage of digital system. 1842-64

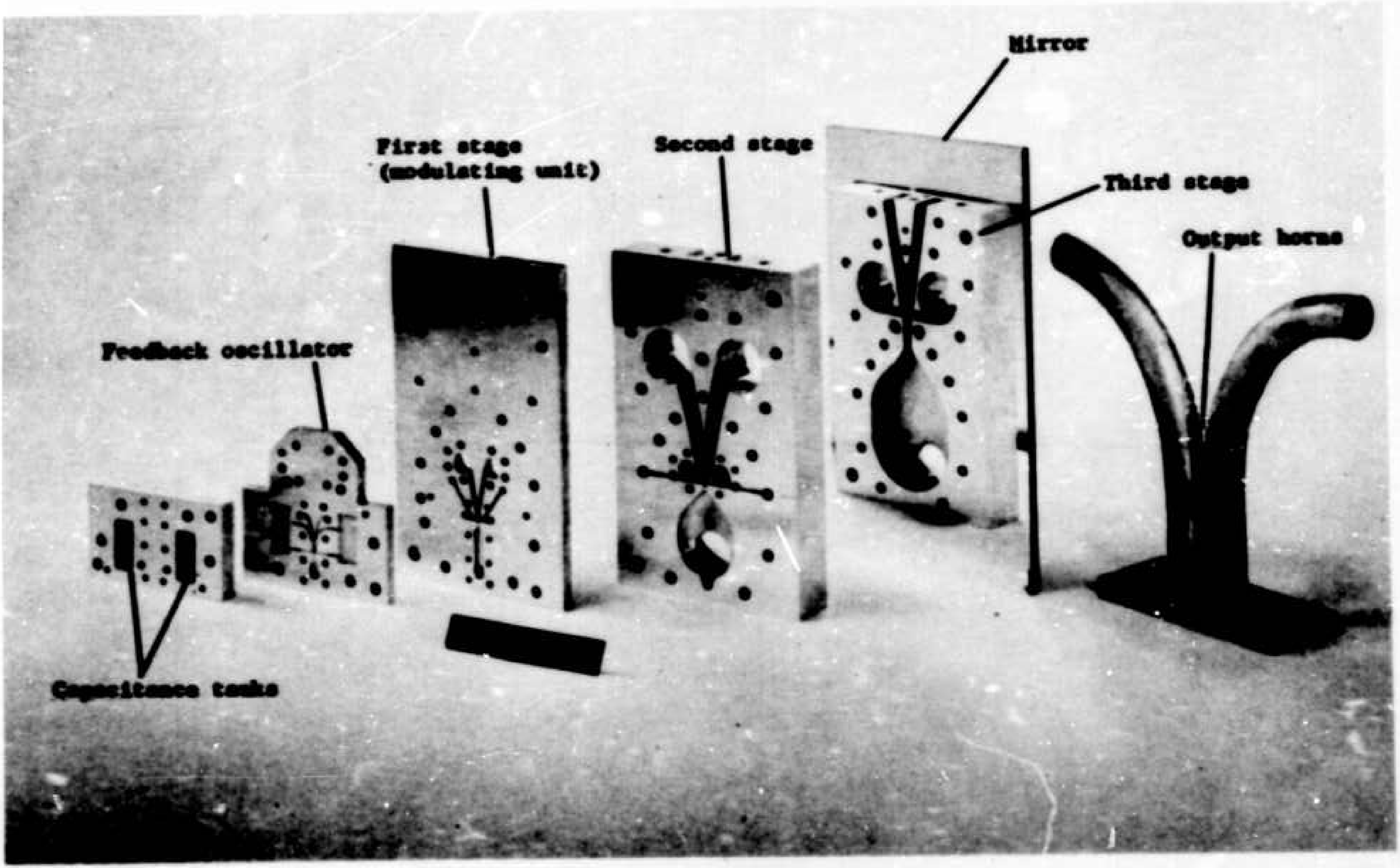

Figure 13. Digital proportional system. 1843-64

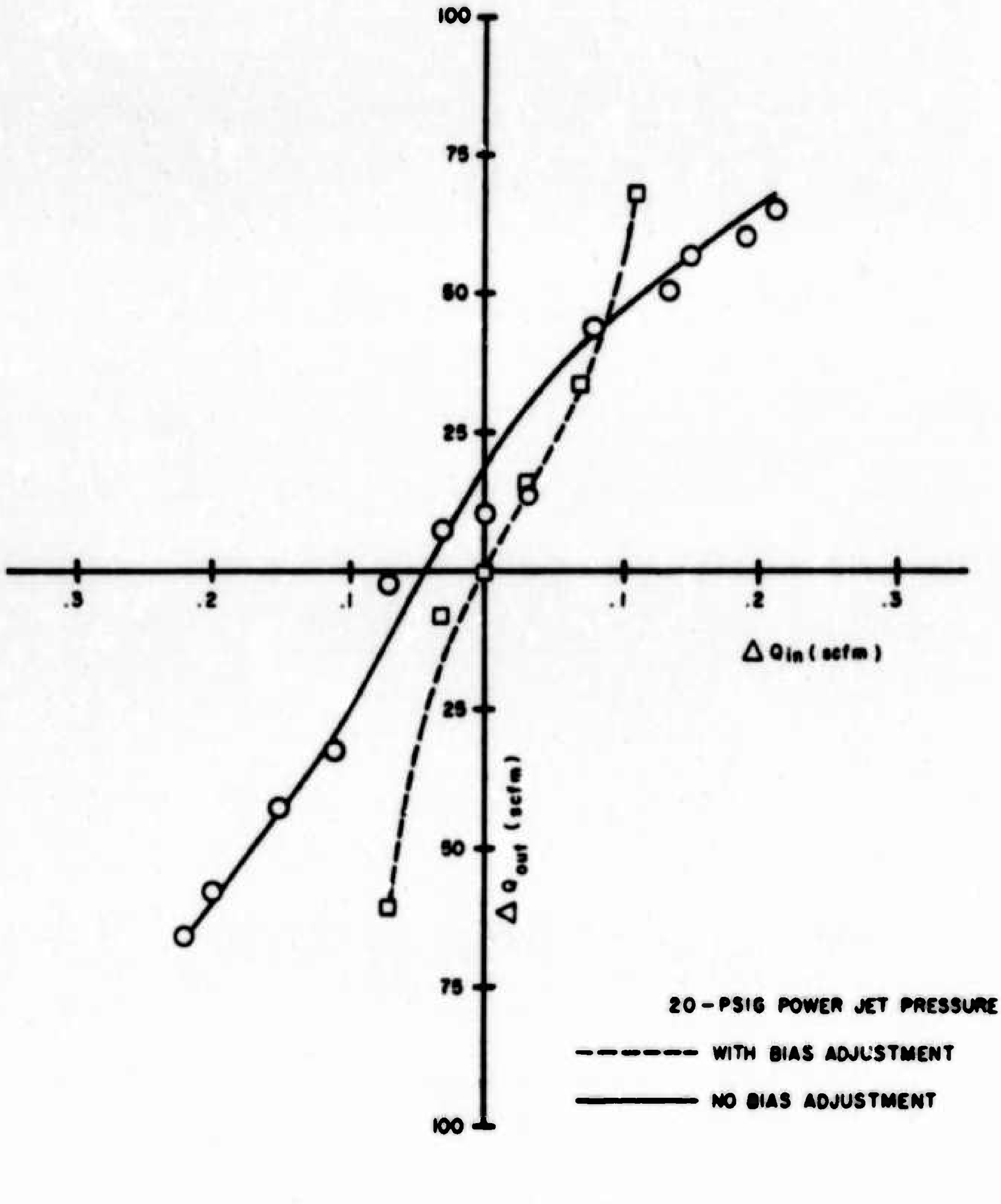

597-65

Figure 14. Differential flow gain curves for hybrid system.

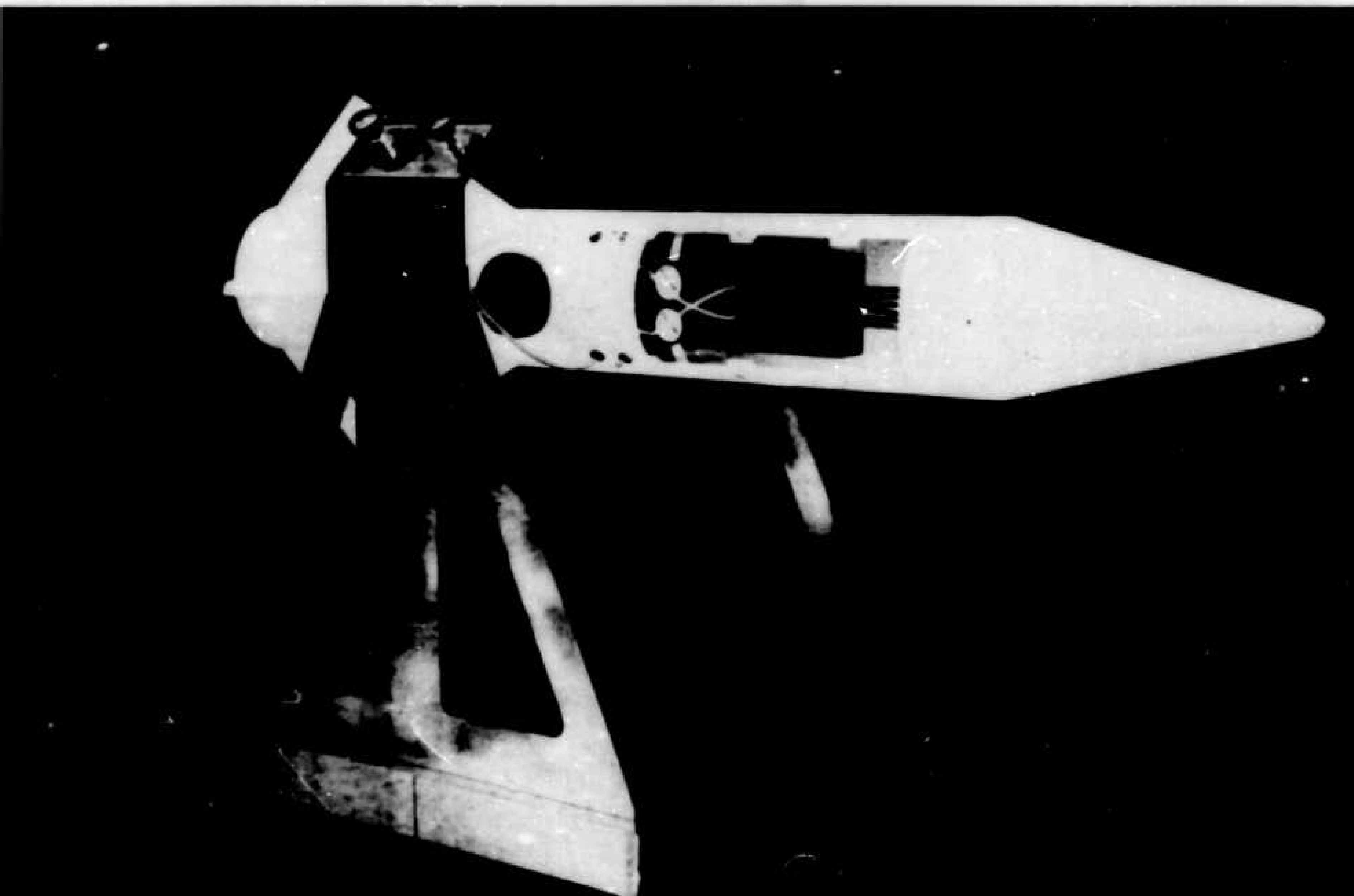

2008-64

Figure 15. Display model containing pneumatic gyroscope and fluid control system.

HARRY DIAMOND LABORATORIES
Washington, D. C. 20438

A DEVELOPMENT REPORT ON A FLUID AMPLIFIER ATTITUDE CONTROL VALVE SYSTEM

by

Allen B. Holmes
John E. Foxwell

ABSTRACT

A digital hot gas fluid amplifier attitude control valve system has been built at HDL. The control system consists of a fluid amplifier reaction-jet valve, four solenoid actuators, a solid-propellant hot gas generator, and a regulated control air supply. The control hardware has been packaged in a Test Instrumentation Missile (TIM) and is scheduled for flight testing at the Redstone Arsenal Missile Test Range in May 1965. This report describes the evaluation, design, and specifications of the hybrid fluid valving system that is to be employed in this flight test.

1. INTRODUCTION

The HDL fluerics development section was formed in September 1964, and one of its first major missions was a flight demonstration of the applicability of a fluid amplifier valve for use in a missile attitude control system. During the previous year, a large number of fluid amplifier valves were designed and evaluated for use in both secondary-injection thrust vector control systems and reaction-jet control systems. These valves operated successfully at supply pressures in excess of 1000 psi and at temperatures up to 5300°F (ref 1 and 2).

Based upon these studies, it was proposed that a fluid amplifier control system be built, evaluated, and flight tested on a Test Instrumentation Missile (TIM). The output reaction thrust from the amplifier would be programmed to guide the missile along a predetermined trajectory and to perform a series of in-flight maneuvers.

2. DESCRIPTION

Two fluid amplifier valve configurations were evaluated to determine the optimum valving concept to be used in the attitude control of a spin-stabilized missile. Digital devices were chosen because they provide a higher gain than do similar proportional devices. Proportional output from digital devices can be approximated by using an oscillating control signal. An oscillatory control mechanism was used with both valving concepts because this mode of control provides valuable data that can be applied to future flights using pulse duration modulation or similar techniques. We chose a 30-cps control signal frequency because it was several times higher than the natural frequency of the missile, and hence the missile could not respond to its output.

2.1 Dual Axis Double Nozzle Attitude Control System

This reaction-jet system calls for two two-way fluid amplifier valves to provide attitude control in both the pitch and yaw planes of a spin-stabilized missile (fig. 1). In this system, both fluid amplifier valves are actuated by a 30-cps pneumatic control signal. This is considered to be the null or zero control condition. Control in either the pitch or yaw plane is achieved by overriding the 30-cps zero control signal with an appropriate d-c pneumatic signal of time duration Δt in seconds. The magnitude of Δt is determined by the amount of control desired (fig. 1).

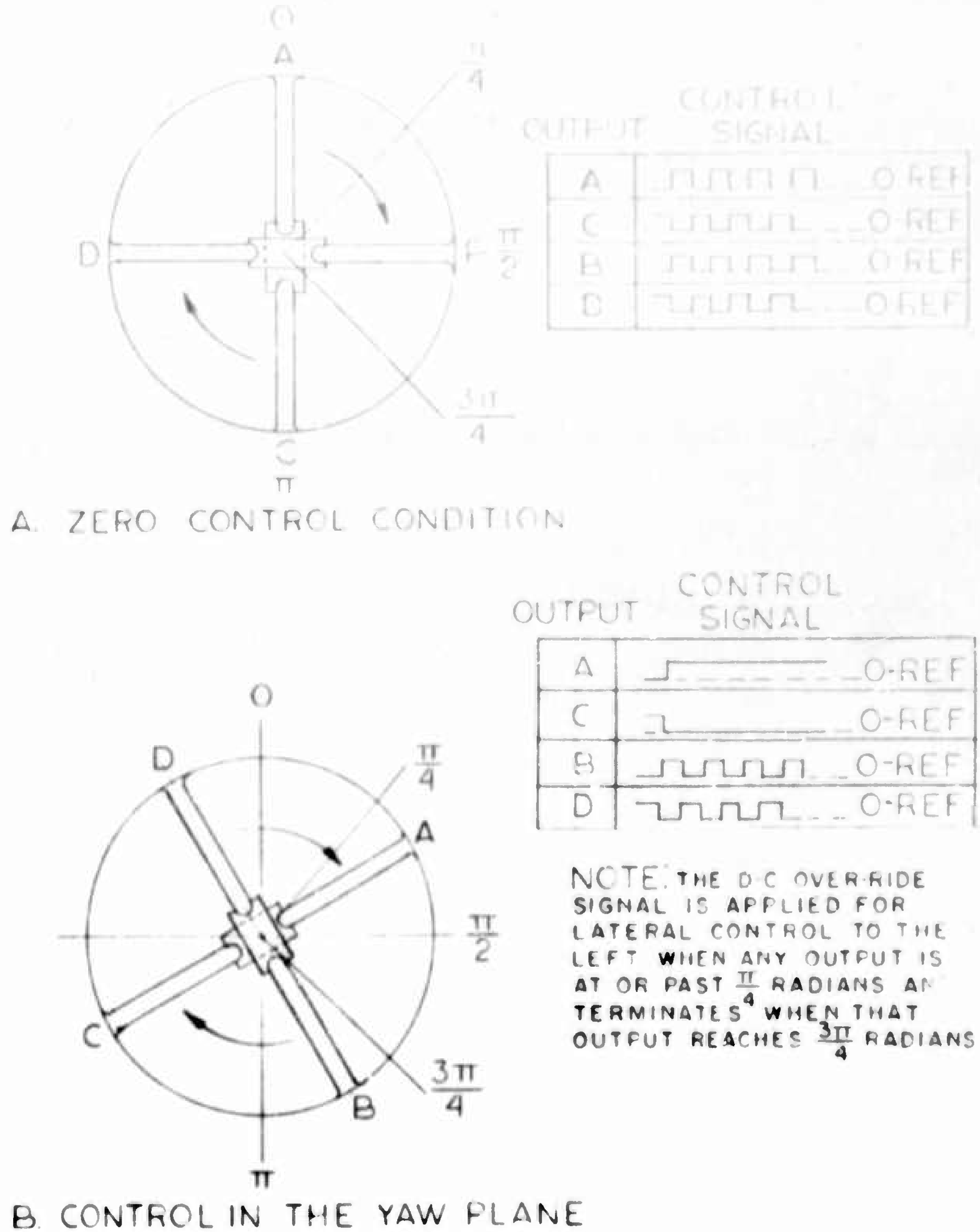

FIGURE 1. MISSILE CROSSECTIONAL SCHEMATIC SHOWING TRANSITION FROM ZERO CONTROL CONDITION TO CONTROL IN THE YAW PLANE FOR A DOUBLE NOZZLE ATTITUDE CONTROL SYSTEM.

Since control in the pitch plane is exactly the same as control in the yaw plane, it is sufficient for a system efficiency analysis to consider control in the yaw plane only. Maximum yaw plane control to the left, for example, occurs when the d-c override signal is applied to any output when it reaches the $\pi/4$ position and terminated when that output reaches the $3\pi/4$ position. At exactly this moment, the "following" output will be at the $\pi/4$ position and a d-c override signal will be applied to it (fig. 1B). In this manner, there will always be a minimum of 0.707 of the output thrust T of one amplifier value directed laterally to the left, independent of the rate of missile spin.

Integration between the limits $\pi/4$ and $3\pi/4$ shows that 90 percent of the output thrust and/or impulse of the amplifier is available for lateral control to the left. The entire output energy of the noncontrol amplifier is wasted. These two conditions limit the maximum theoretical operating efficiency η_{TH} of the two two-way fluid amplifier system to

$$\eta_{TH} = (1/2)(0.9) + (1/2)(0) = 0.45 \qquad (1)$$

A two-way fluid amplifier valve operates at an efficiency approximately 65 percent of the theoretical isentropic thrust and/or impulse available. This limits the actual operating efficiency η_{ACT} of the two-way amplifier system to

$$\eta_{ACT} = (1/2)\ (0.9)(0.65) + (1/2)(0)(0.65) = 0.292 \qquad (2)$$

2.2 Dual Axis Single Nozzle Attitude Control System

A novel four-output fluid amplifier valve was conceived and built at HDL during the preliminary testing stages of the above double nozzle attitude control system in an attempt to eliminate the low system operating efficiency and to significantly reduce packaging and balancing problems.

The four-output fluid amplifier valving system utilizes a single supersonic nozzle flowing into a fluid amplifier with four equally spaced output ducts. If no control signal is given to the four control ports, the amplifier output flow splits equally among the four output ducts and the directed thrust and/or impulse is zero. A zero control condition can also be obtained by cycling any two opposing control ports (fig. 2A and 2B). The double nozzle control procedure is also used for the single nozzle attitude control system.

If the amplifier flow is directed to output duct A in figure 2C, there is some flow equally divided in ducts B and D. The magnitude of this uncaptured flow is approximately 15 percent of the total flow through

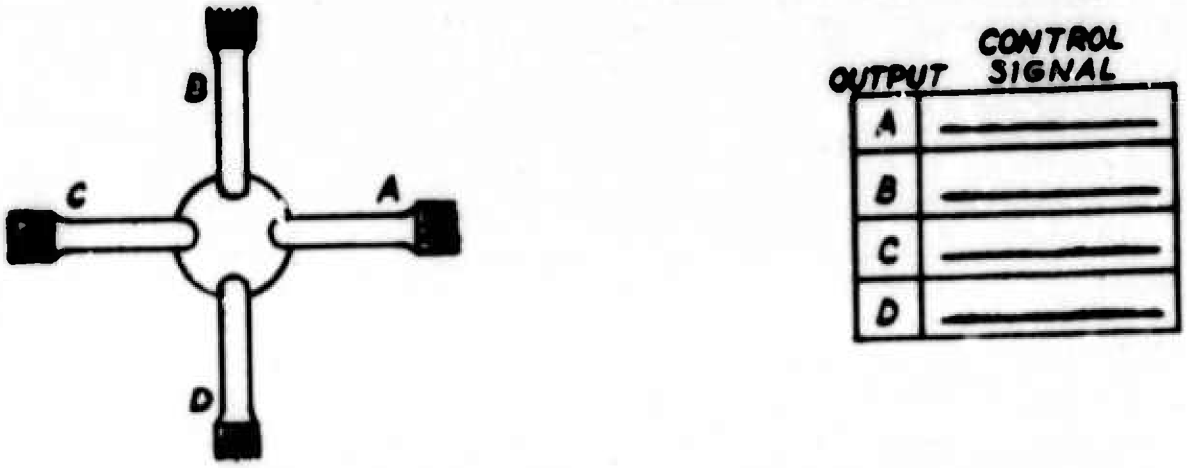

A. ZERO CONTROL CONDITION

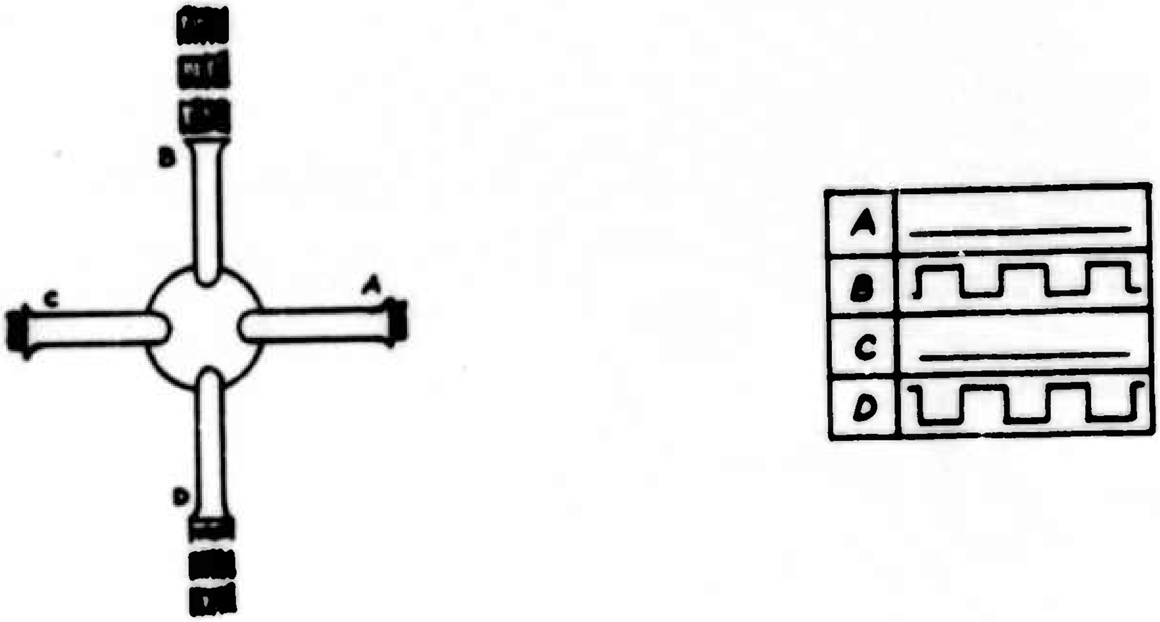

B. ALTERNATING ZERO CONTROL

C. FULL CONTROL

FIGURE 2. ILLUSTRATION OF ZERO AND FULL CONTROL CONDITIONS FOR A DUAL AXIS SINGLE NOZZLE ATTITUDE -

the amplifier. The directed thrust and/or impulse resulting from this uncaptured flow is zero because the directions the flow assumed are opposite and the magnitudes are equal. Therefore, system efficiency calculations must take into account that only 85 percent of the amplifier flow is available for directed thrust and/or impulse.

As in the double nozzle system, only 90 percent of the available impulse is available for lateral control, but there is no noncontrol amplifier flow waste. The maximum theoretical operating efficiency η_{TH} of the four-output fluid amplifier system is therefore 0.9. The isentropic efficiency of the four-output valve is approximately 0.65. The actual operating efficiency η_{ACT} of the valve is now

$$\eta_{ACT} = (0.9)(0.65)(0.85) = 0.497 \qquad (3)$$

All of the above calculations were made for a preprogrammed flight. If an error signal is used to control the missile flight path, there will be an additional error on a spinning missile caused by the amplifier system. The correction for this additional error will slightly reduce the system operating efficiency.

2.3 System Selection

Comparison of the above systems shows that the single nozzle system is over 1.7 times as efficient as the double nozzle system. This primary consideration led to the selection of the four-output amplifier for use in the flight evaluation. The four-output amplifier also had the advantages of simplicity of design and ease of packaging.

2.4 System Hardware

Figure 3 shows the four-output fluid amplifier valve, the solenoid actuators, and the gas generator housing. The power jet nozzle and amplifier housing were fabricated from 304 stainless steel. The output ducts were formed from 1-1/4-in. 304 stainless steel tubing with a wall thickness of 0.063 in; 1/4-in. 304 stainless steel tubing with 0.035-in. wall was used to interconnect the actuator components. The nozzle was secured to the gas generator with eight 1/4-20 stainless steel cap screws and sealed with a 1/8-in. copper gasket. The power nozzle and the amplifier housing were held together with screws and sealed with vacuum grease. Gaskets were not required since an excellent seal was obtained without them.

A heavy-duty reuseable generator housing for system checkout tests was fabricated from existing parts, and a special housing (15-lb) was designed and built for the flight test. A lighter housing could have been built but because of the cost and development time required to reduce the weight by a few pounds, it was decided that the 15-lb model would be acceptable. An existing ignitor was found to be compatible with this system.

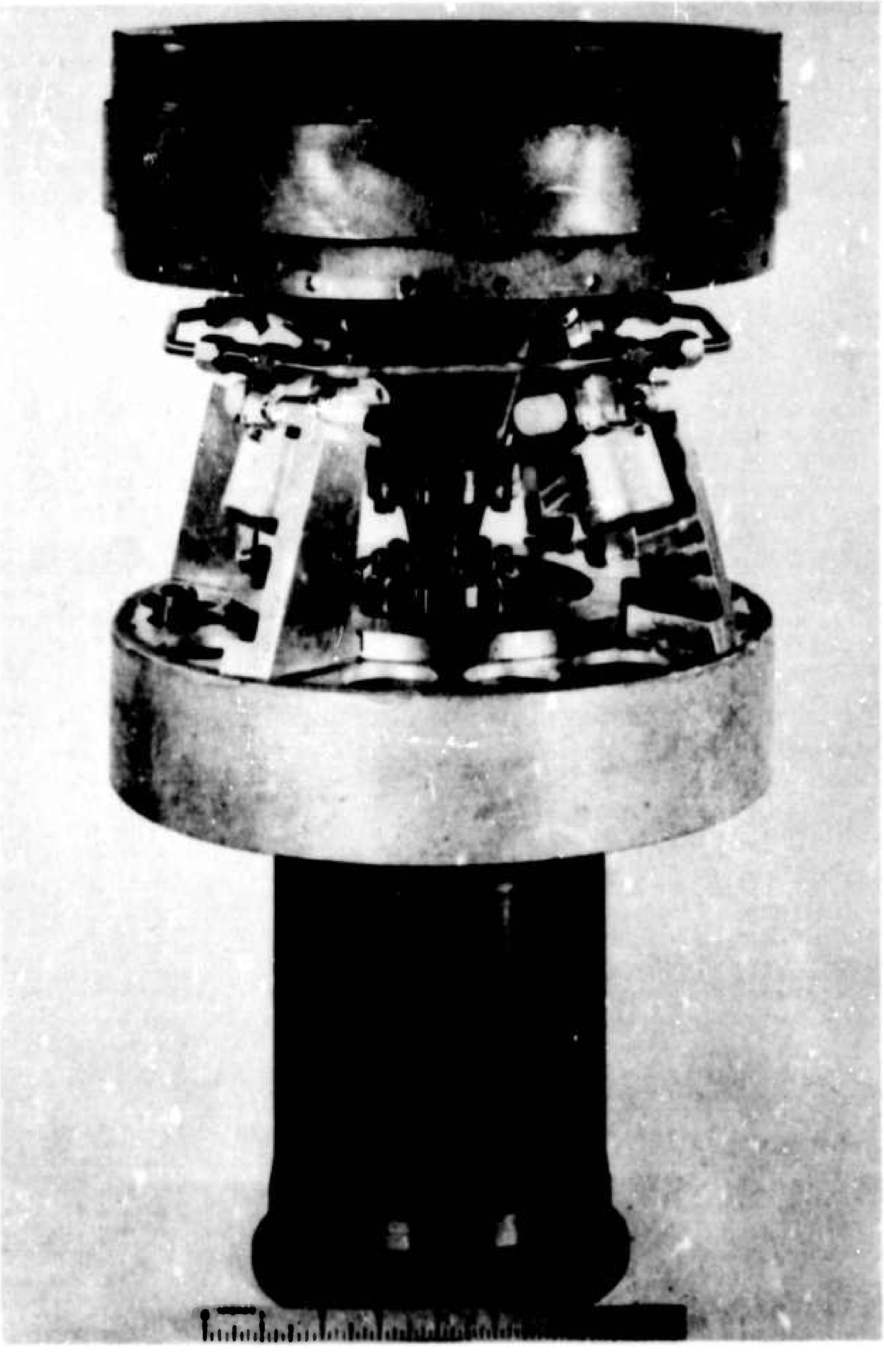

Figure 3. Four-output fluid amplifier valve.

The control jet actuators are four two-way normally closed solenoid valves, equipped with heavy-duty fast-action coils and a balanced poppet orifice design. The four-output amplifier can be switched on atmospheric pressure if the control ports are made large enough to pass the required flow. However, no solenoid valves could be found with the required 1/2-in. straight through port that would cycle at 30 cps. Using much smaller solenoid valves to achieve the required cycling rate means that a high pressure must be provided upstream of the solenoid valve to enable it to pass the required flow. It was found that a 3/32-in. orifice diameter was the minimum size that could be used with the actuator supply system.

The actuator supply system (fig. 4,5) was designed to deliver a constant flow and pressure through the regulator to the actuator valves and, upon command, to the fluid amplifier. In this system, high pressure air or nitrogen is stored in a 300-in.^{3} receiver. The volume of the receiver was determined by the space allotted to it in the TIM and the type of receiver that was commercially available.

The pressure-reducing dome regulator is designed to maintain a constant reduced pressure to the actuator valves regardless of the pressure drop in the receiver. The dome regulator is loaded directly from the inlet supply line through an internal loading tube. The output pressure is controlled by the adjustment of the loading and venting needle valves in the regulator. This system was designed to provide a constant flow of 60 scfm for a maximum operating time of 10 sec.

3. SYSTEM SPECIFICATIONS

The following list of specifications details each component in the system.

3.1 Air Receiver

Capacity	300 in.^{3}
Diameter	9 in.(OD)
Working pressure	3000 psi
Proof pressure	5000 psi
Brush pressure	6600 psi
Ambient temperature range	-65° to + 275°F
Gas	Air or N_2

3.2 Dome Regulator

Inlet pressure	1250 to 3200 psi
Outlet pressure	1150 ± 25 psi
Outlet flow	60 scfm

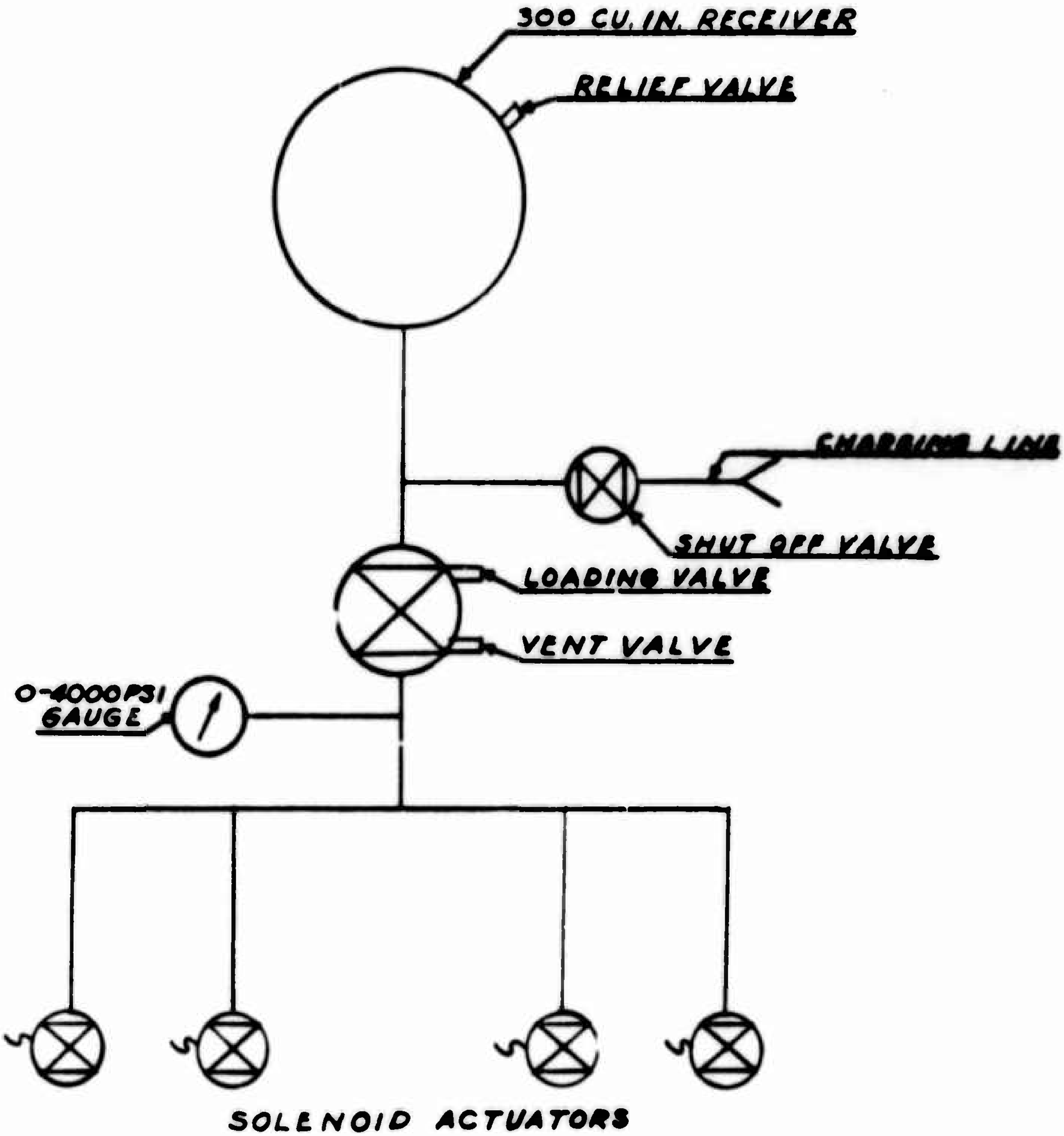

FIGURE 4. ACTUATOR SUPPLY CIRCUIT SCHEMATIC

FIGURE 5. ACTUATOR SUPPLY CIRCUIT

3.3 Solenoid Actuators

Pressure rating	3000 psi
Operating voltage	28 v dc
Coil current	2.8 amp
Cycle rate	30 cps
Orifice diameter	3/32 in

3.4 Gas Generator

Solid propellant	SMU 101
Operating pressure	800 ± 50 psi
Theoretical chamber temp	2505°F
Propellant weight	7.8 lb
Ignitor weight	8 GRAINS
Ignitor voltage	28 v dc
Field test housing weight	20 lb
Flight test housing weight	15 lb

3.5 Fluid Amplifier

Operating pressure	600 to 900 psi
Operating temp	2500°F, maximum
Operating time	10 sec, maximum
Output thrust	45 lb, nominal
Weight	8.0 lb

4. AIR TESTS

The basic aerodynamic design parameters for the hot gas fluid amplifier valve were derived from a brief series of high-pressure air tests. These tests were conducted to:

(1) Prove the feasibility of the four-output fluid amplifier valve concept.
(2) Define the operating pressure range.
(3) Verify the output thrust levels.
(4) Verify the operation of the complete system.

Both systems were tested using compressed air and solid propellant gases. Since the single nozzle system was adopted early in the test program, extensive testing of the double nozzle system was omitted.

The first model of the four-output valved exhibited operating characteristics compatible with the proposed system. Measurements were made of operating pressure, output thrust, and control flow. Upon completion of the preliminary air tests, a set of system specifications was drawn up, for design and fabrication, and submitted to the Solid Rocket Propulsion Laboratory at Picatinny Arsenal. The actuator supply system was designed to deliver a constant flow and pressure through the actuator

valves for 10 sec. This flow rate is determined by the regulated supply pressure and the actuator port design. The actuators were selected for orifice size and response time. It was found that orifice size is directly proportional to response time and response time is inversely proportional to solenoid coil current.

The actuator circuit was then assembled and checked out on a full-scale system air flow test (fig. 6). The test procedure consisted in:

(1) Pressurization of the air receiver to 3100 psi,
(2) Presetting the dome regulator output pressure to 1150 psi,
(3) Setting the fluid amplifier input pressure from 700 to 850 psi,
(4) Recording the resultant thrust of each amplifier output,
(5) Recording the regulated control pressure, and
(6) Plotting the output thrust and control pressure as a function of operating time.

The results of these tests are summarized in table I.

5. HOT-GAS GENERATOR PROGRAM

The Solid Rocket Propulsion Laboratory at Picatinny Arsenal completed work requested by the Harry Diamond Laboratories in support of this project. The purpose of this program was to:

(1) Design and build hot gas generators for both static and flight tests.
(2) Conduct four fully instrumented firings on two fluid amplifier designs.
(3) Fabricate one flight-weight gas generator housing.
(4) Fabricate one heavy-duty gas generator housing.
(5) Provide 13 propellant grains and 30 igniter squibs.

Work was initiated at Picatinny Arsenal on 6 May 1964. The gas generator requirements as specified by HDL are summarized in table II. SMU-101 propellant, a low flame temperature (2500°F) double-base propellant with mesa burning rate characteristics and unusually clean exhaust products, was selected for the fluid amplifier tests. An igniter previously designed for use with a similar grain design was selected to initiate the system. Heavy-duty hardware for static tests was designed using existing parts compatible with the program requirements.

A multicomponent thrust stand at Picatinny Arsenal was adapted for measuring the output thrust developed by the fluid amplifier control system. Due to a relatively low resonant frequency of the test stand, the cycle rate was below 1 cps for all tests. High-pressure nitrogen was used as the control gas (fig. 7).

Four preliminary static firings with heavy-duty hardware and blast-tube nozzle design were conducted to verify the gas generator performance and to check out test procedure and measurement techniques. These tests were followed by four additional tests with heavy-duty hardware using nozzle assemblies fitted with fluid amplifiers. Motion pictures of the four valve tests indicated clearly the high temperature zones in the amplifier output ducts.

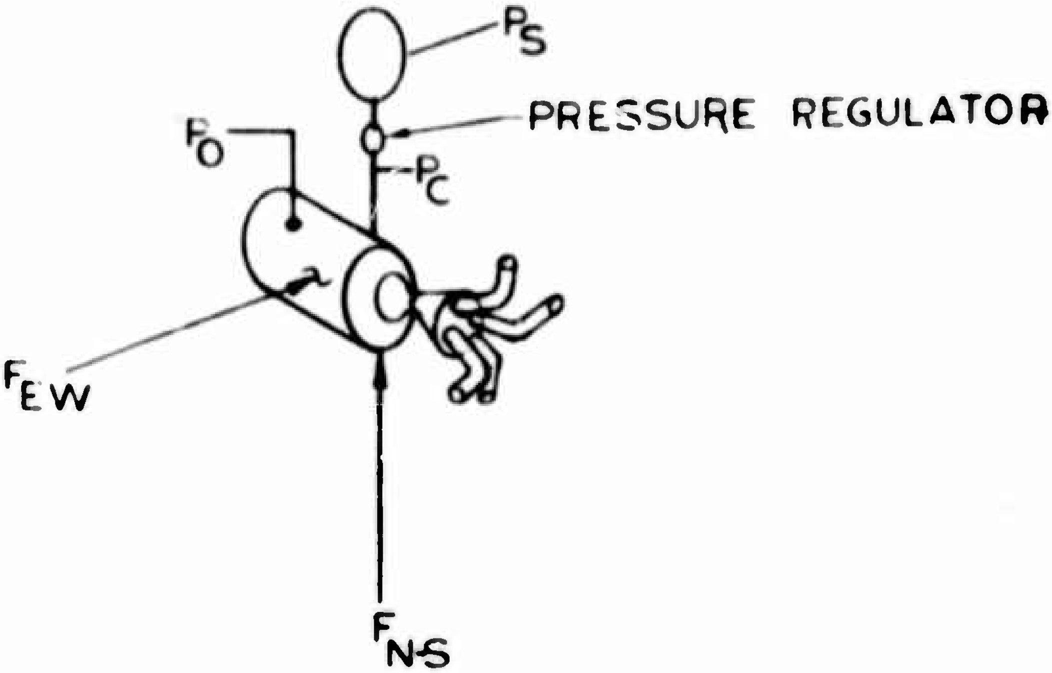

P_C = CONTROL STATIC PRESSURE PSIG
P_O = AMPLIFIER SUPPLY PRESSURE PSIG
P_S = CONTROL SPHERE STATIC PRESSURE PSIG

F_N, F_S, F_E, F_W = AMPLIFIER DIRECTED THRUST LB

FIGURE 6. TEST SYMBOLS AND NOTATION

P_O	F_N LB	F_S LB	F_E LB	F_W LB	P_C PSIG	P_S PSIG
700	50	47	45	46	1100	3000
750	51	46	47	49	1100	3000
800	46	44	44	48	1100	3000
850	48	46	47	49	1100	3000

TABLE-1 TEST RESULTS AIR FLOW EVALUATION

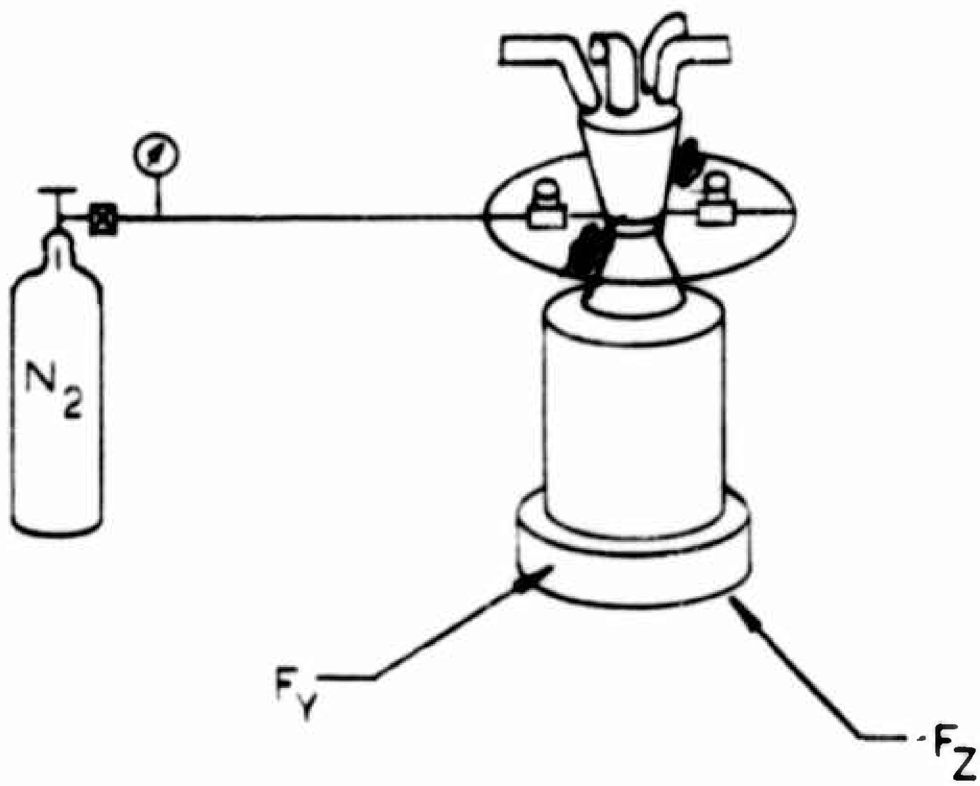

FIGURE 7 HOT-GAS FLUID AMPLIFIER TEST SET UP

TABLE II

HOT GAS GENERATOR REQUIREMENTS

	Requirements
Thrust	133 lb*
Pressure	700 Psig
Nozzle Throat Diameter	0.282 in.**
Propellant Flame Temperature	2500°F
Maximum Diameter	8 in.
Maximum Length	12 in.
Maximum Weight	20 lb***

*Based on a requirement of 40 lb from each of two fluid amplifier units with a 60-percent thrust efficiency.

**Based on a requirement of 0.125 in.^{2} for combined throat area.

***For flight-weight assemblies.

A lighter version of the heavy-duty hardware was designed for flight test purposes. The metal parts weight of the flight motor is approximately 15 lb. The propellant grain weight is approximately 7.8 lb. Therefore, the flight motor assembly, including igniters, is approximately 23 lb. This motor does not represent the optimum weight, but rather an inexpensive modification of the heavy-duty unit to approach to 20-lb weight limitation of a flight-weight unit. This procedure was considered acceptable at this stage of the program even though the weight limitation was exceeded. One motor was fabricated to this design.

Two successful complete system captive flight tests were conducted at the HDL Test Area on 29 and 30 April 1965. The system was returned to HDL for final inspection and was shipped to Redstone Arsenal for flight testing 11 May 1965. The system was successully flight tested on 11 June 1965. Preliminary data from the Test and Reliability Evaluation Laboratory at Redstone Arsenal indicated that the trajectory carried the missile near the programmed flight path. Telemetry reception was good and indicated that the missile was controlled as planned.

6. RECOMMENDATIONS

Upon evaluation of the telemetry and optical tracking data from the TIM flight at Redstone Arsenal, it is recommended that another flight be scheduled with the aim of replacing the mechanical control actuators with a pure fluid system. The pure fluid system would consist of an RC feedback-type fluid oscillator, a three-stage low-pressure fluid amplifier, and a high-pressure supersonic power amplifier. Such a system requires that a low-level pneumatic output signal from a sensor be modulated, amplified, and delivered as a variable reactive thrust output. The sensor required for this system could be of conventional form or the pure fluid rate sensor now being developed at HDL could be used.

REFERENCES

1. Holmes, Allen B. and Foxwell, John E., "Supersonic Fluid Amplification with Various Expansion Ratio Nozzles," Proceedings of the Fluid Amplification Symposium, Volume IV, pp. 123-146, May 1964.

2. Foxwell, John E. and Holmes, Allen B., "Proportional Fluid Amplification for Rocket Thrust Vector Control," Proceedings of the Fluid Amplification Symposium, Volume V, pp. 43-57, May 1964. Confidential.

HARRY DIAMOND LABORATORIES
WASHINGTON, D. C. 20438

APPLICATION OF FLUERICS TO MISSILE ATTITUDE CONTROL

by

CARL J. CAMPAGNUOLO
JOHN E. FOXWELL
ALLEN B. HOLMES
LEONARD M. SIERACKI

ARMY MATERIEL COMMAND   DEPARTMENT OF THE ARMY

ABSTRACT

This report describes the design, development, and evaluation of a control and thrust generating system consisting of an RC oscillator, a three-stage amplifier, and a supersonic single-stage power amplifier. These amplifiers were combined into a single four-stage fluid amplifier. The three-stage subsystem provides a modulated oscillatory control signal that enables the digital supersonic amplifier to deliver a proportional thrust output. The overall system has a power gain of 1×10^6 and a flow gain of 1.3×10^4 and delivers a maximum thrust of 70 pounds.

INTRODUCTION

The application of fluid interaction devices for reaction-jet control and chamber bleed thrust vector control has been demonstrated at HDL using compressed air and both solid and liquid propellants (ref 1-3). Subsequent work at HDL in the field of fluid sensors, logic circuits, and amplifiers has led to the development of a pure fluid missile control system.

The inherent advantage of such a control system is that it contains no mechanical moving parts or electronic components and is believed to be impervious to radiatic and vibration that impose limitations on conventional missile-control systems. Since it is necessary that a small signal from the fluid sensor be amplified and modulated to provide a usable thrust output, it is important to formulate realistic design criteria by investigating scaled laboratory models.

Experiments were conducted on a laboratory model of a control and thrust-generating system consisting of an RC oscillator, a three-stage digital amplifier, and a supersonic power amplifier. A complete analysis of the RC oscillator and low pressure modulating system is discussed in reference 4, and basic design criteria for the power amplifier are discussed in reference 2.

For a missile control system, it is usually desirable that the corrective force be proportional to the error signal emitted from a sensor. The RC oscillator enables the four-stage digital amplifier

to have a proportional thrust output. When no error signal is present, flow remains in each reaction-jet duct for the same amount of time, and the net thrust of the system is zero. Introduction of an error signal causes a proportional change in the time that the flow remains in each output duct. It is this change that produces an output thrust proportional to the error signal.

2. SUBSYSTEM DESCRIPTION

The RC oscillator and the first three digital units of the four-stage amplifier are referred to as the subsystem, which amplifies small sensor signals and provides enough flow and pressure to control the supersonic power amplifier.

The RC oscillator consists of a high gain digital amplifier supplied with a resistance-capacitance feedback loop (fig. 1). By means of a set of movable screws in the output ducts of the RC oscillator, it is possible to balance the flow output of the entire system. There are two methods of changing the base frequency of the subsystem. Small changes (10-20 cps) are obtained by adjusting the bias screws; large changes (60-300 cps) are obtained by varying the size of the RC network. The base frequency of the system is approximately 80 cps.

The first stage of the subsystem is provided with a dual set of controls (fig. 1). The controls nearest the power jet are fed from the oscillator, while the other set is fed by a proportional signal emitted from a pneumatic sensor. To maintain high gain, both sets of controls are located within the entrainment bubble of the power jet.

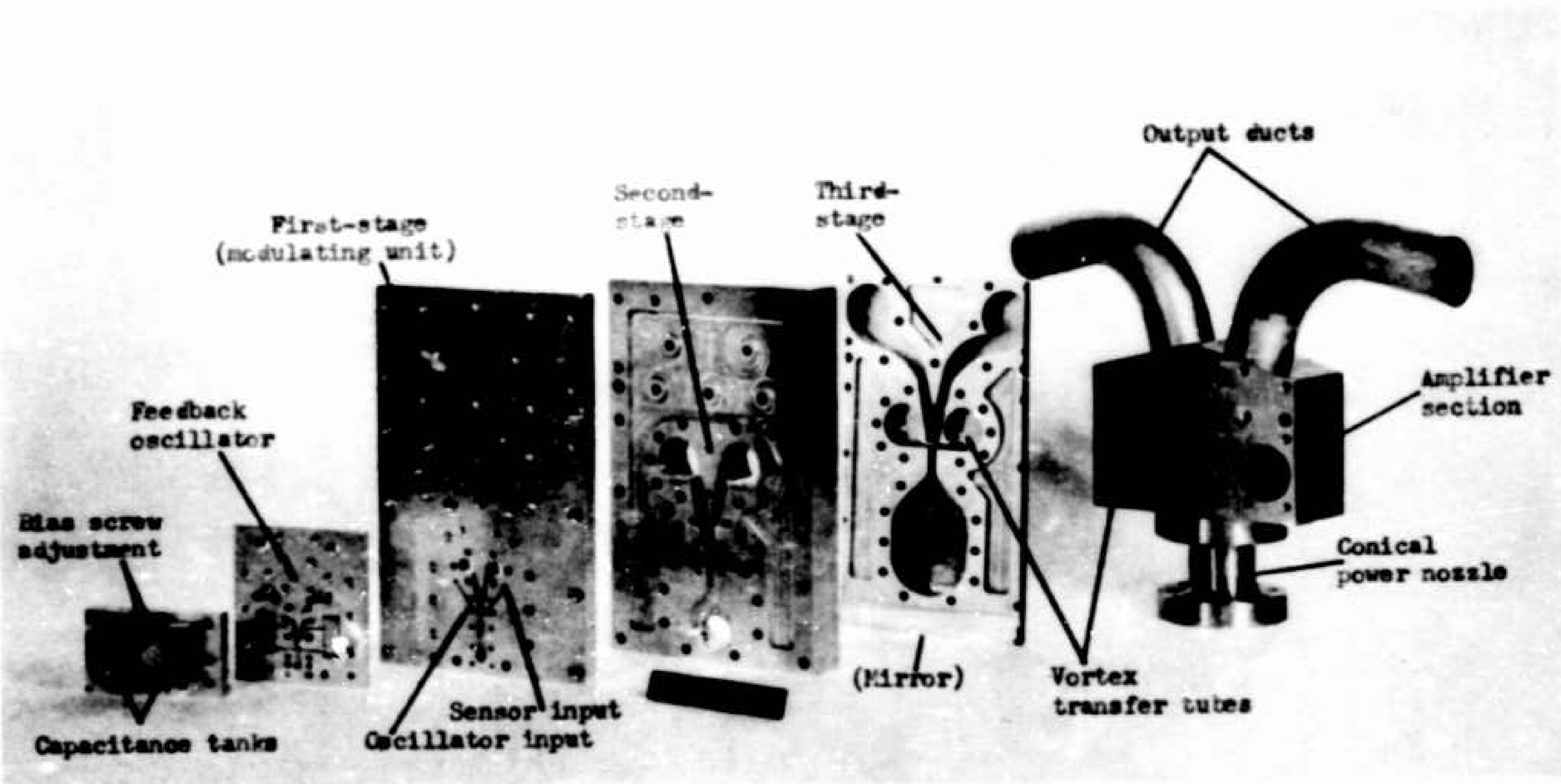

Figure 1. Four-stage fluid amplifier assembly

The three digital elements of the subsystem have a common power jet pressure and are cascaded in ascending order. High power and flow gains are achieved since each nozzle area is 10 times the nozzle area of the preceding stage. The first two stages of the subsystem are memory units and tend to stabilize the entire system; they have their splitters 18 w (nozzle widths) downstream of the power jet, catcher openings of 4 w, and a two-dimensional nozzle aspect ratio of 4 to 1.

The third stage of the subsystem is a nonmemory unit with its splitter placed in the core region (6 w) of the power jet and has catcher openings of 1.4 w. In this combination, the nonmemory unit enables the entire subsystem to have a high pressure recovery, while the memory units make the system fairly insensitive to the extreme low pressure (1-3 psia) existing at the control ports of the power amplifier. Each stage is matched into the succeeding stages by using vortex transfer techniques.

3. POWER AMPLIFIER DESCRIPTION

The power section of the four-stage amplifier is a high pressure digital supersonic unit designed to operate from a typical solid-propellant hot gas generator. This single axis power amplifier was designed to operate with the solid propellant grain SMU-101 to provide a reactive thrust output which is proportioned by means of the subsystem. Cold gas tests show that a thrust of 70 lb is attained at a power jet pressure of 700 psig.

The power amplifier has a conical stainless steel nozzle, a control or amplifier section, and a pair of 1-1/4-in diameter output ducts (fig. 1). The subsystem is matched to the control section of the power amplifier by means of the vortex tubes.

The high pressure input flow overexpands and separates from the walls of the interaction region. When both control pressures are low, the output flow distributes itself equally about the splitter. Switching is accomplished by raising the pressure in one of the vortex tubes to cause further separation of the power jet from one wall and attachment to the opposite wall.

4. TEST INSTRUMENTATION AND CONTROL DEVICES

All tests on the high pressure power amplifier and the complete system were made on a three-component thrust stand, comprising a framework in which load cells are located in the flexures to determine the impressed loads. The flexures behave effectively as pinned joints but provide high compliance in all lateral directions. They have sufficient tensile and compressive strength and column stiffness to withstand 500 lb of axial loading and 200 lb of lateral loading. The flexures were designed so that the spring constraints they impose do not contribute measurably to the forces being measured (fig. 2).

A single load cell was mounted in the horizontal plane to measure the net thrust output of the unit. The load cell was a 350-ohm resistive bridge type, with four active elements. Calibration was achieved by applying known loads W_1 and W_2 statically along

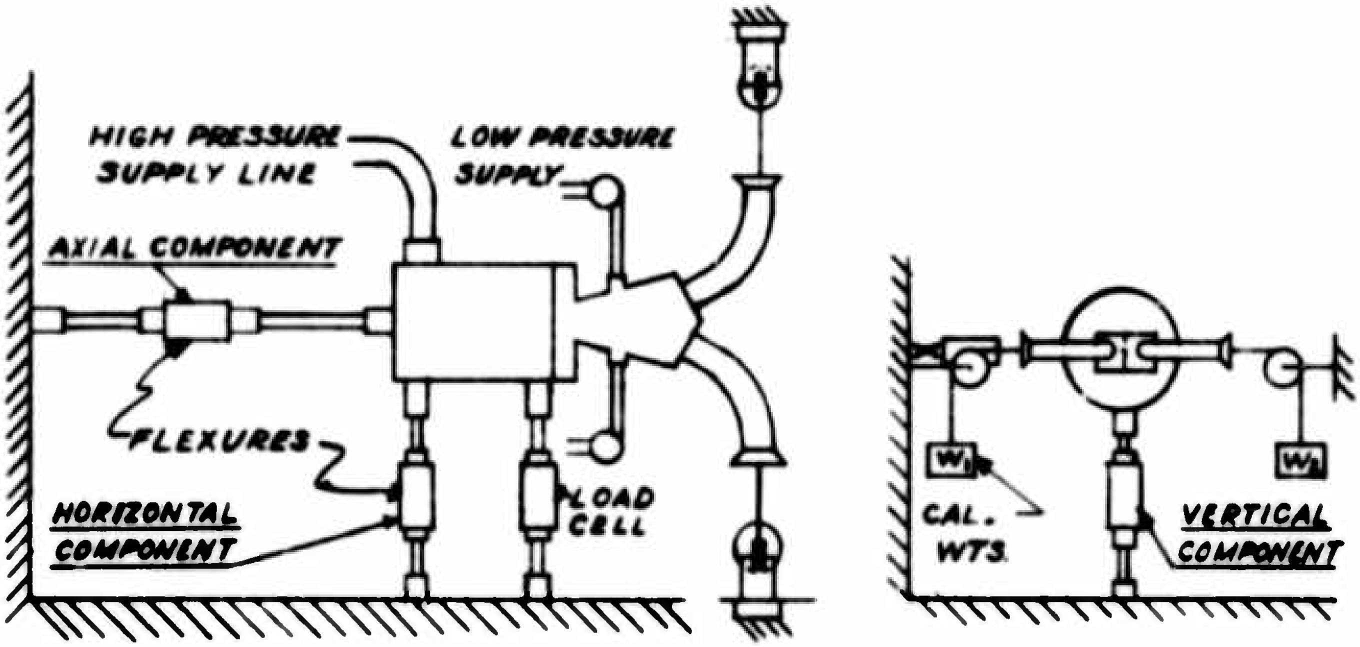

FIGURE 2 THE POWER AMPLIFIER SHOWN INSTALLED ON A THREE-COMPONENT THRUST STAND

the thrust axis of the amplifier. A resistor that simulated the combined resistance changes of the active bridge elements for the applied calibration load was keyed across one element of the transducer bridge. All measurements were made relative to the reference signal.

The power-nozzle and control-jet compressed air flows and pressures were metered through the use of dome regulators. The flow rates were measured periodically during each test run (fig. 3). When the three-stage fluid amplifier was adapted to the high pressure amplifier and mounted on the test stand, the feed pressure to the three-stage device was regulated through an additional dome regulator. Two types of input control actuators were used to meter the control flow into the oscillator controls. The first provided a digital differential input signal to the oscillator, and the second produced a time variant pressure signal. The response of the system to a modulated input control flow was determined by applying a time variant pressure signal to the oscillator controls and measuring the net output thrust as a function of the differential input control pressure. The control flow through the actuators was entrained directly from the atmosphere during all tests.

5. TESTS

The compressed air tests were conducted to determine the predominant operating characteristics of both the power amplifier stage and the complete four-stage system. The power amplifier test series

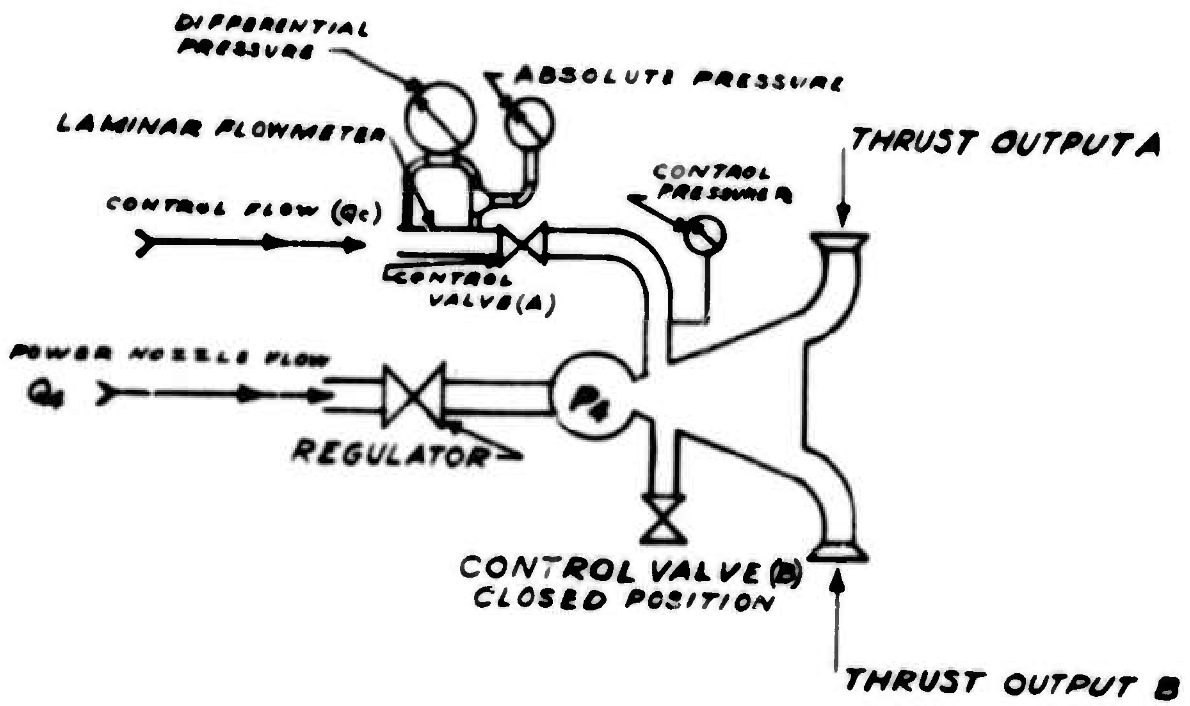

FIGURE 3 FLOW SCHEMATIC FOR POWER AMPLIFIER TESTS

was designed to evaluate the amplifier under two separate operating conditions: In the first, the opposing or nonactuated control port was sealed during switching; in the second, the nonactuated control port was open during switching, allowing a static pressure of 14.7 psia in that region. The second operating condition was designed to simulate system conditions where constant pressure and flow oppose the applied control signal. The procedures used for these tests were as follows.

Test I (fig. 3)

(1) Power nozzle pressure was preset at P_4.

(2) Control valve B was closed.

(3) Control pressure P_c was applied through valve A.

(4) Pressure P_c was recorded.

(5) Flow rate Q_c was recorded.

(6) Steps 1, 3, 4, and 5 were repeated with control valve B full open to allow a static pressure of 14.7 psia to exist in that region.

The curves in figures 4, 5, and 6 correspond to the unit being fully switched into output B, producing a maximum thrust F.

TEST I RESULTS

The first part of test I illustrates the typical characteristic flow and pressure curves for a supersonic fluid amplifier under normal operating conditions (fig.4-5). An analysis of the flow phenomena involved in the generation of these curves is given in reference 2.

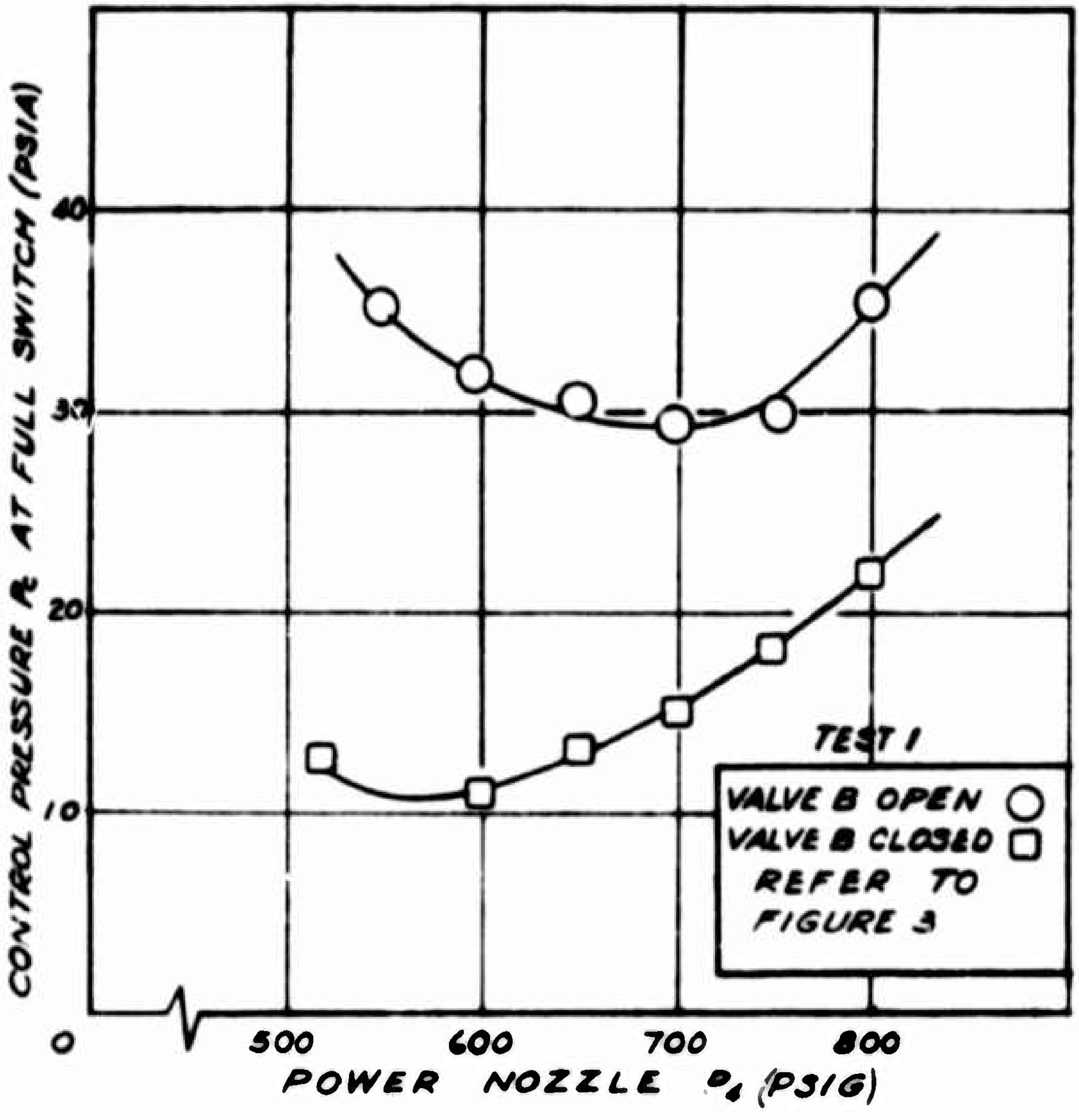

FIGURE 4 CONTROL PRESSURE AT FULL SWITCH AS A FUNCTION OF POWER NOZZLE PRESSURE

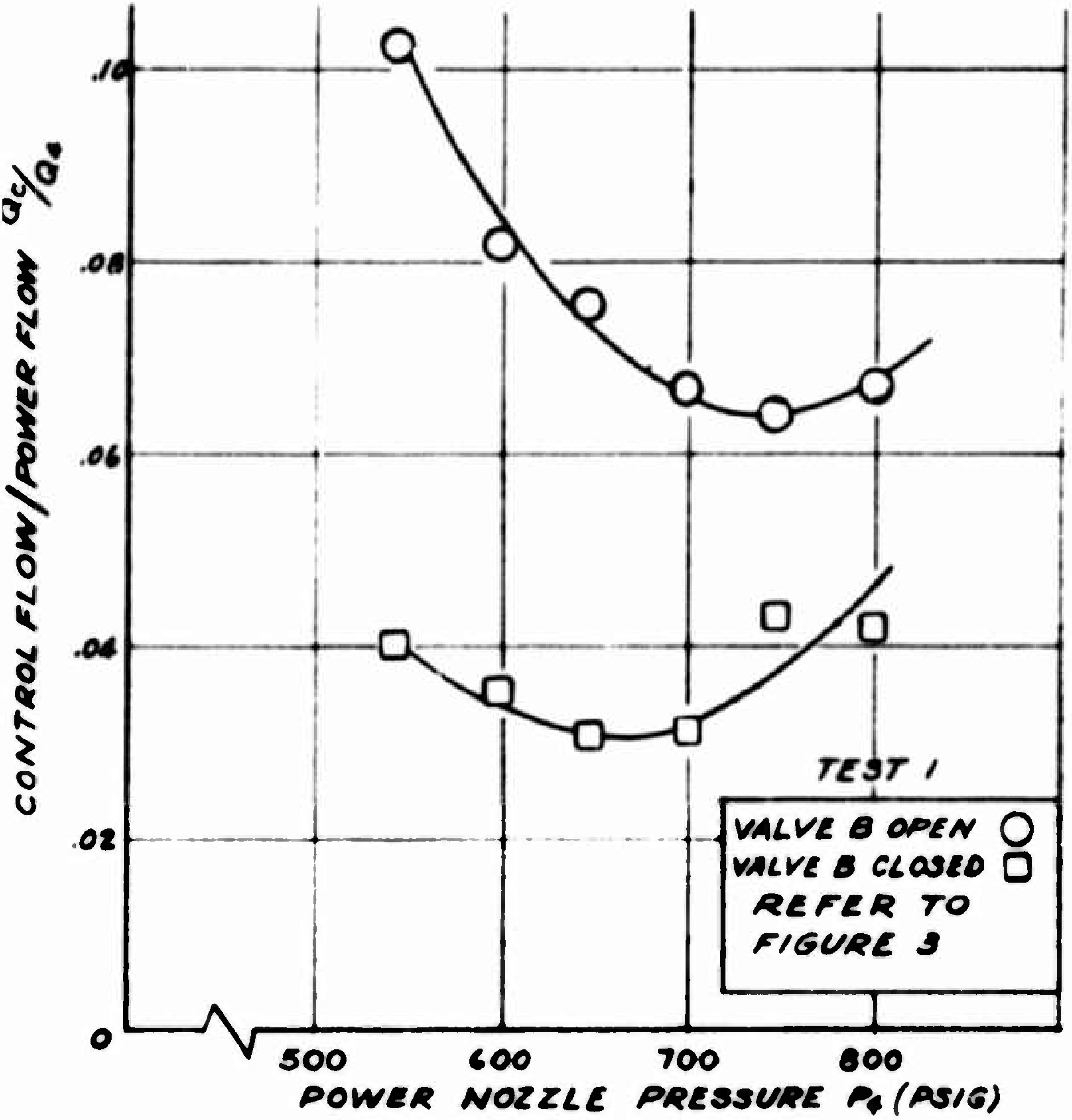

FIGURE 5 MEASURED CONTROL FLOW RATE AT FULL SWITCH COMPARED WITH CALCULATED ISENTROPIC POWER FLOW RATE AS A FUNCTION OF POWER NOZZLE PRESSURE.

The second part of test I illustrates that the flow gain (defined as the ratio of the power nozzle flow to the control flow) is reduced by a factor of approximately 2.5 under simulated system conditions. However, since the normal flow gain is relatively high (20-25), the reduction in gain does not significantly decrease the effectiveness of the power amplifier. This test was performed at a bias pressure of 14.7 psia, but a bias pressure of 20 to 25 psia could reduce the gain to a point where the power amplifier would cease to operate. The isentropic thrust efficiency of the power amplifier was altered only slightly when the non-actuated control port was open during switching (fig. 6).

There will always be a bias flow (corresponding to the non-actuated control port being open during switching) when the subsystem is connected to the power amplifier. This bias flow results from the extremely low static pressure in the interaction region of the power amplifier. However, the pressure associated with the bias flow can be reduced by the use of vortex transfer tubes. If the output flow and recovered pressure of the subsystem is excessively high, the gain of the power amplifier will be reduced. Thus, proper matching of the subsystem to the power amplifier is essential.

The purpose of the second and third test series was to verify the analytical analysis that preceded the design and assembly of the entire four-stage system. Tests were conducted to determine the variations between component performance and complete system perform-

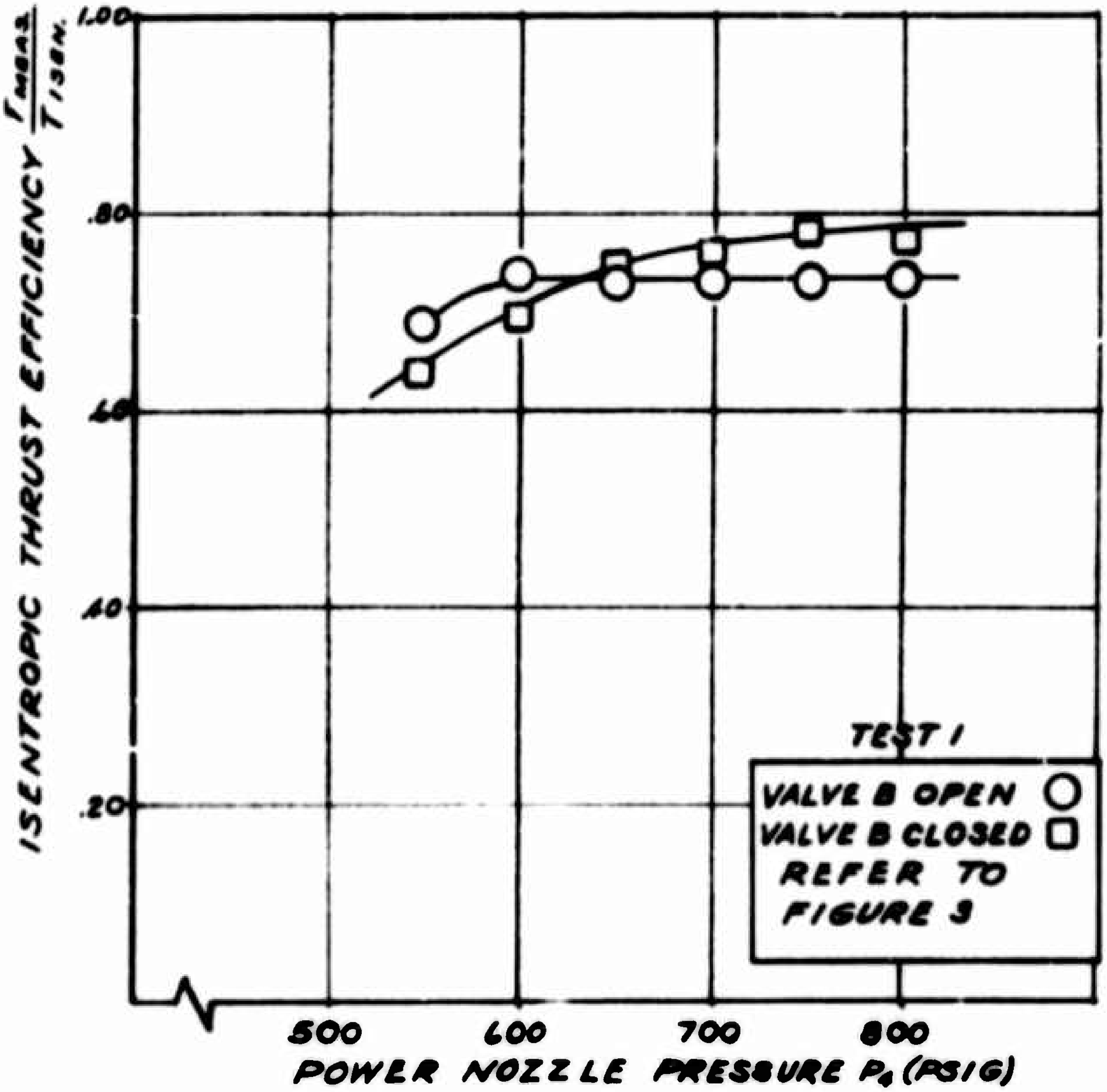

FIGURE 6 CALCULATED ISENTROPIC THRUST EFFICIENCY PLOTTED AS A FUNCTION OF POWER NOZZLE PRESSURE

ance. The parameters of main interest were power amplifier operating pressure and system output thrust recovery. The procedure used in the second test series was as follows.

TEST II (fig. 7, 8)

(1) Subsystem supply pressure was preset.

(2) Solenoid actuator valves R and L were alternately cycled at approximately 1 cps.

(3) Power amplifier supply pressure P_4 was applied at a rate of 25 psi/sec.

(4) Output thrust was recorded as a function of P_4.

(5) Maximum actuator control flow Q_C was measured.

TEST II RESULTS

Test II showed that the power amplifier operating pressure range was 200 to 800 psig. When the power amplifier was operating at a pressure of 700 psig, a system flow gain (defined as the ratio of the power amplifier flow rate to the oscillator control flow rate) of 13,000 was achieved.

TEST III (fig. 7, 9)

(1) The subsystem low pressure supply line was removed. Under this condition, the supply air flow to the subsystem was entrained directly from the atmosphere.

(2) Steps 2 through 5 i test II were repeated.

TEST III RESULTS

This experiment was performed to demonstrate the feasibility of operating the subsystem without an auxiliary power supply. The re-

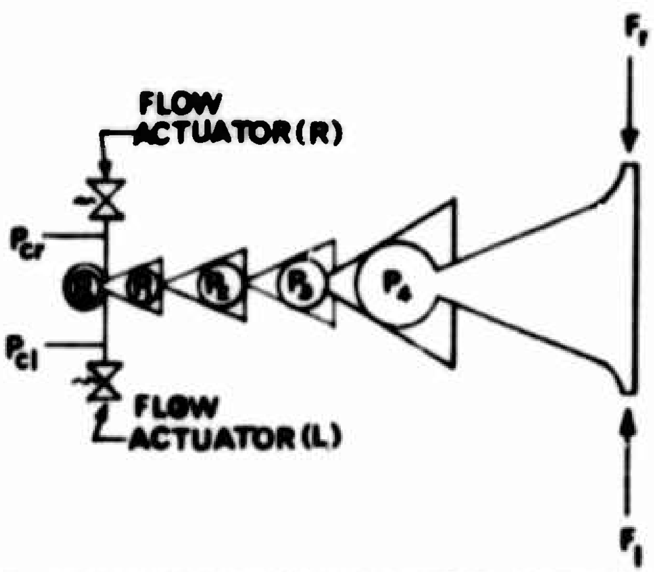

FIGURE 7 SCHEMATIC VIEW OF TEST SET UP FOR TESTS 2, 3 AND 4

TEST CONDITIONS AND DATA

TEST NO	P_0 PSIA	P_1 PSIA	P_2 PSIA	P_3 PSIA	P_4 PSIG	P_{cl} PSIA	P_{cr} PSIA	F_R LBF	F_L LBF	ACTUATOR
2	14.7	14.7	14.7	14.7	0-700	14.7	14.7	40-80	40-80	SOL. VALVE
3	54.7	54.7	54.7	54.7	0-800	14.7	14.7	0-80	0-80	SOL. VALVE
4	54.7	54.7	54.7	54.7	660	14.7	14.7	0-60	0-60	NEEDLE VAL

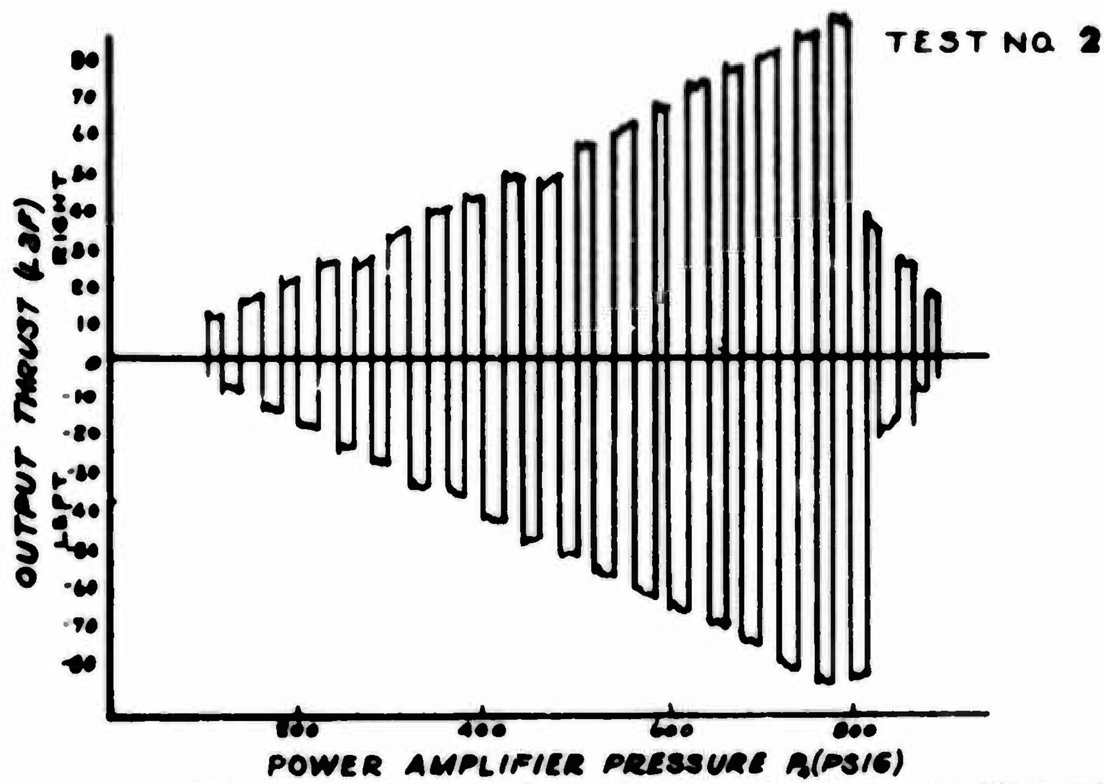

FIGURE 8 THRUST OUTPUT VERSUS POWER AMPLIFIER PRESSURE AT A SUBSYSTEM FEED PRESSURE EQUAL TO 40 PSIG.

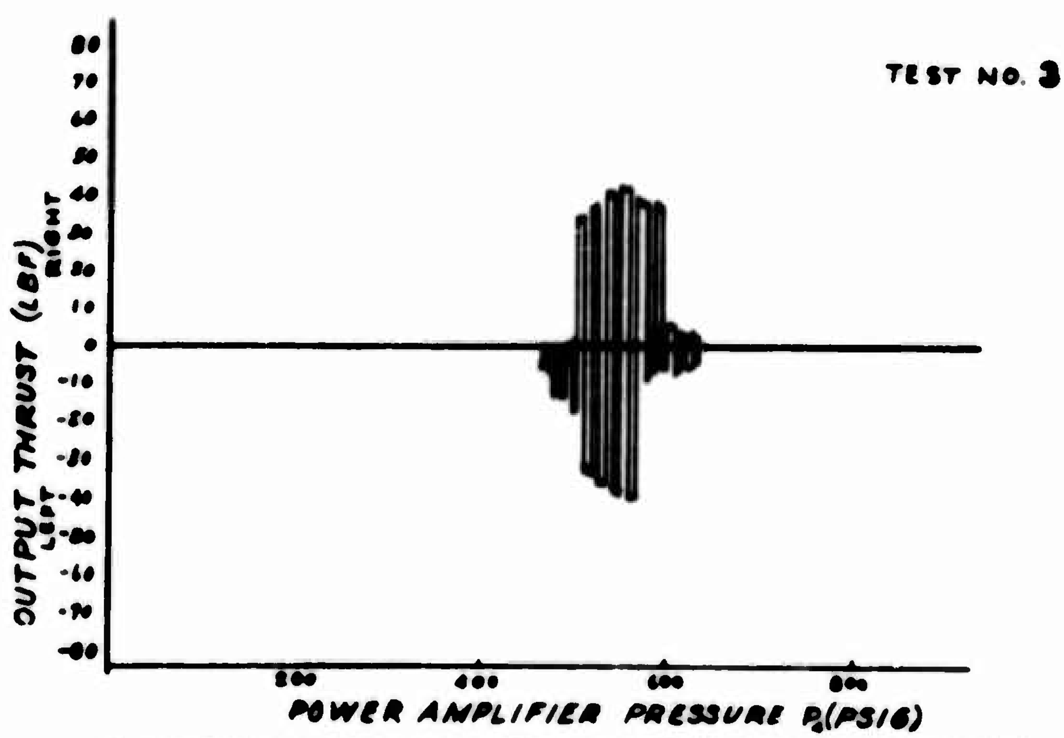

FIGURE 9 THRUST OUTPUT VERSUS POWER AMPLIFIER PRESSURE AT A SUBSYSTEM FEED PRESSURE EQUAL TO 14.7 PSIA.

sults indicated that this mode of operation is feasible, but the limited amount of entrained air and the associated pressure drops through the subsystem reduced the power amplifier operating pressure range to 500 to 600 psig. With larger passages in the subsystem, it appears that this range could be extended.

TEST IV (fig. 7, 10)

(1) Subsystem low pressure supply was preset.

(2) Power amplifier pressure was preset.

(3) Control pressure to the oscillator was varied by means of needle valves.

(4) The differential pressure existing in the oscillator controls was measured.

(5) The oscillator control flow was measured at system maximum thrust output.

(6) Net output thrust was measured.

TEST IV RESULTS

This test series was conducted to determine the linear operating regimes of the four-stage amplifier. Since these regimes are dependent upon various combinations of subsystem and power amplifier pressures, only a typical curve of differential control pressure versus net output thrust is presented in figure 10. This curve was generated using a subsystem power jet pressure of 40 psig and a power amplifier pressure of 650 psig. The results of this test indicated

TEST NO 4

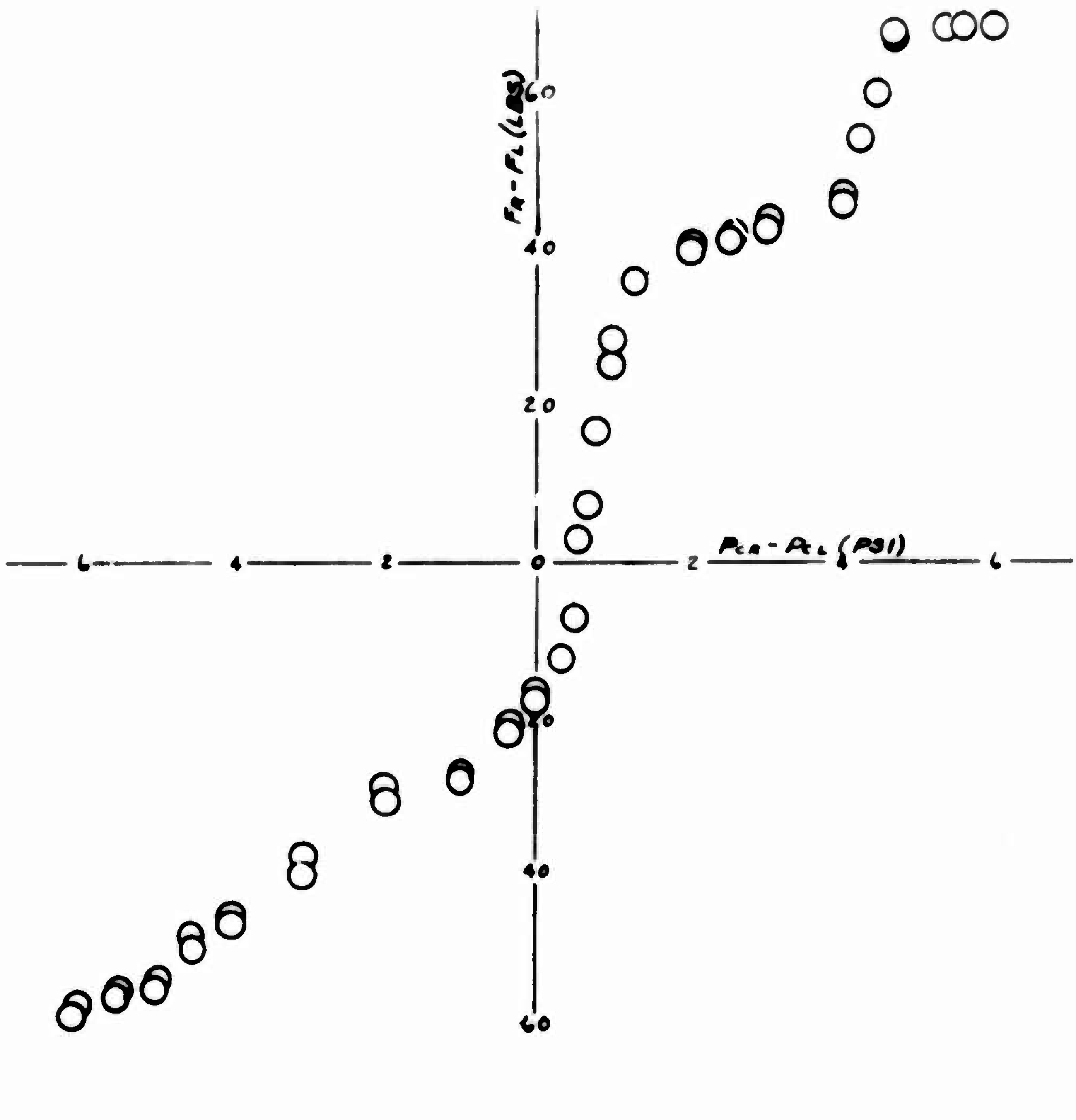

FIGURE 10 NET THRUST OUTPUT VERSUS DIFFERENTIAL OSCILLATOR CONTROL PRESSURE

that the entire unit was not balanced and did not perform in a linear manner. By correctly balancing the amplifier or forcing the curve through zero, it is possible to increase the gain and the linear operating range of the ystem (ref. 4). Further tests are necessary to determine whether the large step in the curve is an inherent characteristic of the amplifier or was caused by power jet misalignment, dirt in the subsystem, a machining error, or some other combination of asymmetries. The curve also indicates that it is possible to obtain a thrust output that is proportional to the input signal.

6. CONCLUSION

The results of this testing demonstrate that low pressure and supersonic elements may be cascaded to obtain high flow and power gains. Although the subsystem and power amplifier operated over a wide range of power jet pressures, 40 psig for the subsystem and 650 psig for the power amplifier seemed to provide the most desirable results. The subsystem tended to reduce the gain of the power amplifier but did not appreciably change its overall operating characteristics.

Three important conclusions may be drawn from these tests:

(1) Digital operation was achieved over a wide operating range of the power amplifier (200-800 psig).

(2) An output thrust was obtained that was proportional to the input control signal.

(3) It was possible to operate the entire system using atmospheric pressure to supply the subsystem.

These results are not considered optimum but are intended to illustrate the feasibility and adaptability of the four-stage amplifier. Further work is needed to improve the linearity and gain of the system.

REFERENCES

1. Foxwell, John E. and Holmes, Allen B. "Proportional Fluid Amplification for Rocket Thrust Vector Control," HDL Proceedings of the Fluid Amplification Symposium, Vol V, pp. 43-57, May 1964, Confidential.

2. Holmes, Allen B. and Foxwell, John E., "Supersonic Fluid Amplification with Various Expansion Ratio Nozzles," HDL Proceedings of the Fluid Amplification Symposium, Vol IV, pp. 123-146, May 1964.

3. Lehman, W. F. and Crommie, F. T., "Feasibility Study of Fluid Amplification Control for Exhaust Jet Deflection," Sixth Liquid Propulsion Symposium, sponsored by the Inter-Agency Chemical Rocket Propulsion Group, 23-25 Sept 1964.

4. Campagnuolo, C. J. and Sieracki, L. M., "A Digital-Proportional Fluid Amplifier for a Missile Control System," HDL Proceedings of the Fluid Amplification Symposium, Oct 1965.

A SECOND GENERATION OF FLUID SYSTEM APPLICATIONS

by

Dr. R. E. Bowles & E. M. Dexter
Bowles Engineering Corporation

R-7-23-65

A SECOND GENERATION OF FLUID SYSTEM APPLICATIONS

During the past three years, Pure Fluid Systems have progressed to the fabrication of integrated controls and some operational experience has been accumulated. These controls are more than breadboard samples; they have been built for specific applications. The manner of their execution is the result of an evolution. The first step in this evolution was to select applications which, on the surface at least, were compatible with Fluid Systems. Secondly, we would like to believe that the evolution represents a collective best judgment at each step. Each development approach is the result of a consideration of the best way.

The objective of this paper is to review some applications which represent the average or mean rather than the extremes (what is being done rather than what might be done) in an attempt to divine the future complexion of Fluid Systems. We have selected five of these middle-of-the-road applications. We think they cover a fair sampling of present day work and, therefore, are suitable to deduce some general characteristics of the applications of Fluid Systems. These five selections are: 1) a boiler control system; 2) a speed control; 3) a pressure discriminator for process control; 4) a course control for a torpedo; and 5) an automatic sequencing control system. For each of these we will describe the basic function of the control and point out some of the salient features of the end item hardware.

BOILER CONTROL

The application of Pure Fluid Systems to boiler control seems natural because of the compatability of the input and output signals with fluid computation. Boilers are currently operated by pneumatic systems, the air is available, the sensors and various parts of the loop are pneumatic, and the output actuators are pneumatically driven.

The boiler control regulates the air, fuel, and water to the boiler to maintain steam pressure (which is the reference signal) and boiler drum water level. Measurements of the airflow, water flow, water level, steam flow and fuel flow are feedback signals. This system is shown in block paragraph form in Figure 1. There are four major blocks. The first function of the control system is to sum the feedback signals and provide the desired attenuation and gain. The second major blocks are the airflow controller, the minimum signal selector for the fuel signal, the fuel controller and the water flow

---

The information contained in this paper is derived in part from the following contracts: Boiler Control, BuShips, Contract No. Nobs 88625; Speed Control, ONR, Nonr 4033(00); Torpedo Control, BuWeps, Now 65-0252f; V/STOL Study, U. S. Army Aviation Materiel Labs., DA 44-177-AMC-202 (T).

controller. With the exception of the minimum signal selector, the control subcircuits are relatively straightforward. Due to the slow response of the airflow loop during transients, the fuel flow must be limited to prevent the occurrence of a fuel-rich mixture. The minimum signal selector causes fuel flow to follow the demand established by steam flow and steam pressure error or the airflow feedback signal, whichever is the smaller. The four major circuits are shown in Figure 2.

Without considering any of the major subcircuits in any detail, it is interesting to note that the number of elements and the size of the circuit plates are very similar. The units have seven or eight elements and each is constructed with elements of .040-inch depth. The circuit plates are approximately 5 inches by 9 inches. In each case the circuit has with it an associated manifold and adjustable biasing restrictions. The circuits shown are of cast epoxy. Development work was performed using Optiform. The cast epoxy circuits provide long-term stability.

It is important to note that each of these modules provides a function. The breakdown is not dictated by the size of the plates, manufacturing restrictions, or a desire to implement a circuit from standard strips of amplifiers. Each of these are put together to fulfill a function.

Figure 3 is a schematic and silhouette of the minimum signal selector. The operation of this circuit is as follows: The two primary input signals are from the airflow feedback signal and the demand signal circuits. The function of the selector is to determine which is the minimum signal. Each input is divided, one being transmitted to the power input of an OR gate and the other to the input of a two-stage analog amplifier. The input signal to the amplifier shown in the lower portion of the figure is the difference between these two signals. The output drives a flip flop. The maximum signal determines which side the output of the flip flop is on and drives the switch with the maximum signal to the off position. The maximum signal selector, therefore, sees only the minimum input signal. This signal is transmitted to the output two-stage amplifier to bring the circuit to the desired gain; in this case, one. In addition to demonstrating the interplay of both analog and digital elements the circuit displays the use of a completely non-standard element, the maximum signal selector. Fluid circuits offer a great opportunity for special purpose elements for functions that would normally, in electronic equipment, be made up of an assembly of standard elements. This is a growing trend.

SPEED CONTROL

Another application worthy of note is the speed control which was demonstrated in breadboard form some time ago but which promises to find an application in the near future. This control is shown in schematic form together with the fluid circuit silhouettes in Figure 4. This governor functions by measuring the difference in frequency between a tuning fork reference, which is set at approximately 840 cycles per second, and a shaft speed frequency measurement made by interrupting a jet stream. The shaft speed signal is normally 800 cycles per second. This difference frequency is subsequently demodulated and passes through a stabilizing lead-lag network to drive the output actuator. In the figure the size of the elements is about half of the actual size in the demonstration model. There are two basic circuit elements, a frequency subtractor, which is a two-element circuit, and the discriminator and stabilizing network, which was made in a 9 x 12 circuit plate comprising 11 elements.

Note that the division of these circuit plates is on a functional basis. The frequency subtractor, located near the speed measurement, provides the function summation and the larger plate provides the demodulation and stabilization network. The circuit plate has an associated manifold, tanks and lines to provide necessary time constants. In many of the analog circuits, the required tank volumes are not compatible with the size of the circuit plate and are, therefore, executed externally.

PRESSURE DISCRIMINATOR

A good example of an application for fluid systems in process control is the amplifying and discriminator circuitry shown in Figure 5. The function of this Pressure Band Gate is to amplify an air gage, or other process measurement, to the normal 3 to 15 psi band used in current recorders, and in addition to provide a signal when the process is beyond tolerance. In this case the tolerance band can be adjusted to ± .2 psi, referred to the 3 to 15 psi range, or up to 6 psi band width. In most cases the output of this will be used in the controller or the band signal will be used to stop a process or give a warning signal that the system is not functioning properly. Note that the input signal is the fluid being used in the computer, which is air, and that the output is a pneumatic signal driving a pneumatic controller of a pneumatic actuator.

The circuit elements, both digital and analog, are .015 inches deep. The circuit plate was about 2 x 4 inches and contains 10 elements, 5 of which are digital and 5 analog. The circuit is injection molded. Most of the difficulties and cost of this device are associated

with the manifold. This observation dictates a trend to incorporate more of the manifold functions, such as fixed restrictions, in the circuit plate.

TORPEDO COURSE CONTROL

The fourth application is a torpedo course control system based on the vortex rate sensor. The rate sensor provides two pressure outputs which are both above ambient pressure level and which vary in opposite direction as a function of rate of turn. The integration of this signal is provided by converting these pressures to comparable frequencies and then maintaining a continuous totaling of the number of cycles from each output during the run. The difference in total count is a function of the course error.

The basic circuitry, Figure 6 , shows the rate sensor, the two pressure controlled oscillators, which convert the signals to frequencies, and the two counter strings with conversion networks. These counter strings are shown schematically in Figure 7 . The integration function is provided in two steps. The first circuit provides an analog signal proportional to the deviation in the total number of counts in the first four stages. The final three stages are handled by a more coarse technique by simply recognizing which counter string is ahead of the other and providing a saturating signal when this occurs. Therefore, if the count is less than 16, the circuit gives a proportional control signal and if the counter error exceeds 16, a saturating signal will maintain a constant output until this error is reduced. Notice that the torpedo control system desires to run at a zero count error so that normally only a minor count difference will exist. Also the process of changing course is provided by inducing error count into one of the counter strips.

The course control system is shown in Figure 8 on the rate table with an oscilloscope display of the PCO outputs. The course system includes: a fan and plenum to supply pressure to the rate sensor and circuitry; the rate sensor; pressure-controlled oscillators; oscillation output amplifiers; and three circuit assemblies. The circuit assemblies are: (1) the four-bit network with analog output; (2) the two-bit count circuit to distinguish if the count error exceeds 32; and (3) a reset circuit.

The first two circuits, Figure 9 , are composed of four circuit plates mounted back to back on two manifolds. This back-to-back arrangement is appropriate because the subtraction function requires a stage by stage comparison. An example is the four-stage count circuit shown in Figure 10 . The circuit plates are mirror images with interconnections through the manifold as indicated in the figure by common letters.

Each circuit of this pair is approximately 4 by 7 inches, and has a complement of seven .040-inch elements and the passive adder circuit. The material is a metal-filled epoxy. The second circuit is a pair of plates of about the same size assembled in the same manner. These two circuits are not symmetrical pairs. One has nine elements and the other eight. The third circuit, the reset function, has a single circuit plate and manifold. The circuit is 4 inches by 6 inches and has 7 elements.

These circuits are divided by function. For example, the first module and the third module can be used together to provide a useful combination.

It is notable that the circuit, exclusive of the reset function, could be combined on a single manifold using two circuit boards. The circuit, however, was divided to isolate the development problem and test procedures.

AUTOMATIC SEQUENCING SYSTEM

The function of this control system is to provide the logic for proper manipulation of a storage process. This system is not characterized by functional blocks. It is a long train of interconnecting logic sequences to prevent improper manipulations. More than 100 logic functions are involved in this control. The subdivisions were defined by categorizing modules that appeared repetitively and which have outputs in useful positions so that stacks of modules can be interconnected easily. The assembly is shown in Figure 11 .

The six basic modules defined in this sequencing system are shown in Figure 12 . These modules are 6 x 9 inches and have circuit elements of .040 inch. A module and an assembly with manifold are shown in Figure 13. In the upper left the module is shown from the manifold side, and at the right from the circuit side. Having the inputs and outputs as shown allows simple interconnecting with the modules staggered as shown in Figure 11

The circuit modules in this example were dictated by a desire to standardize rather than incorporate all the logic for a particular function. Some of the modules appear to have general application.

THE OPPORTUNITY FOR FLUID SYSTEMS

Intuitively it appears that Fluid Systems offer potential improvements in size, weight, reliability and cost. Generally we see improvements in all these areas, although it depends on the specific application particularly when considering a one-for-one substitution for conventional pneumatic controllers or conventional transistorized electronic equipment. The most prominent potential improvements are in reliability and in cost reduction of systems where it is advantageous to compute in the working fluid.

An example which we have studied quite exhaustively was that of a control system for a helicopter or short take-off and landing aircraft. This control system, shown in block diagram form in Figure 14 is made up of a short period stabilization system, which we expect will be hydraulic, and a long period attitude control, which will probably be pneumatic. The study indicates a comparison in weight, power and reliability shown in Figure 15. The values are given for a hypothetical Pure Fluid System and an operational electronic system. It should be recognized, of course, that these figures for the Fluid System represent today's state of the art. First we note that the numbers are very similar in weight and power. However, reliability appears to be much better for the Pure Fluid System. The table of Figure 16 shows that the apparent reliability of Fluid Systems may be limited by the reliability of the actuator itself.

At the present time there is really not enough evidence to completely define the reliability of Fluid Systems. At Bowles Engineering we have accumulated approximately 30,000 hours of recorded test time after burn-in. What we have noticed in our computations is that the reliability of Fluid Systems will be significantly affected by the connections much more so than by the fluid circuit. This prompts us to consider the reliability on the basis of the connections rather than on the basis of the fluid elements themselves. For example, the potential reliability from Fluid Systems has been related to that of a gasketed assembly which has been shown to have failure rates on the order of .03 per million hours of operation. This reflects a failure mode due to leakage which we believe will be the primary type of failure. On the other hand data collected for hydraulic lines indicates, in the most optimistic cases, .59 failures per million hours for the hose alone. Failure rates for fittings have comparable values. This results in a possible failure rate of 1.5 per million hours in aircraft use. Although these figures may not be strictly applicable, it is apparent that integrated circuitry will be the trend in improving reliability.

What of failure induced by wear-out or performance degradation? We don't know of any wear-outs except under high stress conditions.

What of cost reduction? It is too early to be specific. At the present time there are many conflicting examples. A one-for-one substitution for pneumatic controllers does not show a major reduction in price. The cost, however, is not in the fluid circuit; it is in the manifold and adjustments. For cost reduction we look to applications that eliminate the need to translate fluid information to electrical signals and vice versa.

CONCLUSIONS

We believe that integrated circuits, grouped on a functional basis will be the trend in Pure Fluid Systems. It appears that many functions are performed with approximately 10 elements. If we assume that gas circuits will use elements of .015-inch depths and an aspect ratio of 2, which seems to be the most desirable size, the circuit plates will be about 3 inches by 4 1/2 inches.

Reliability considerations will induce the designer to incorporate the maximum number of interconnections in the module. Cost considerations will tend to increase the functions provided by the circuit plate.

Overall, the major contributions of fluid circuits will be in applications which eliminate the need to translate information from one medium to another.

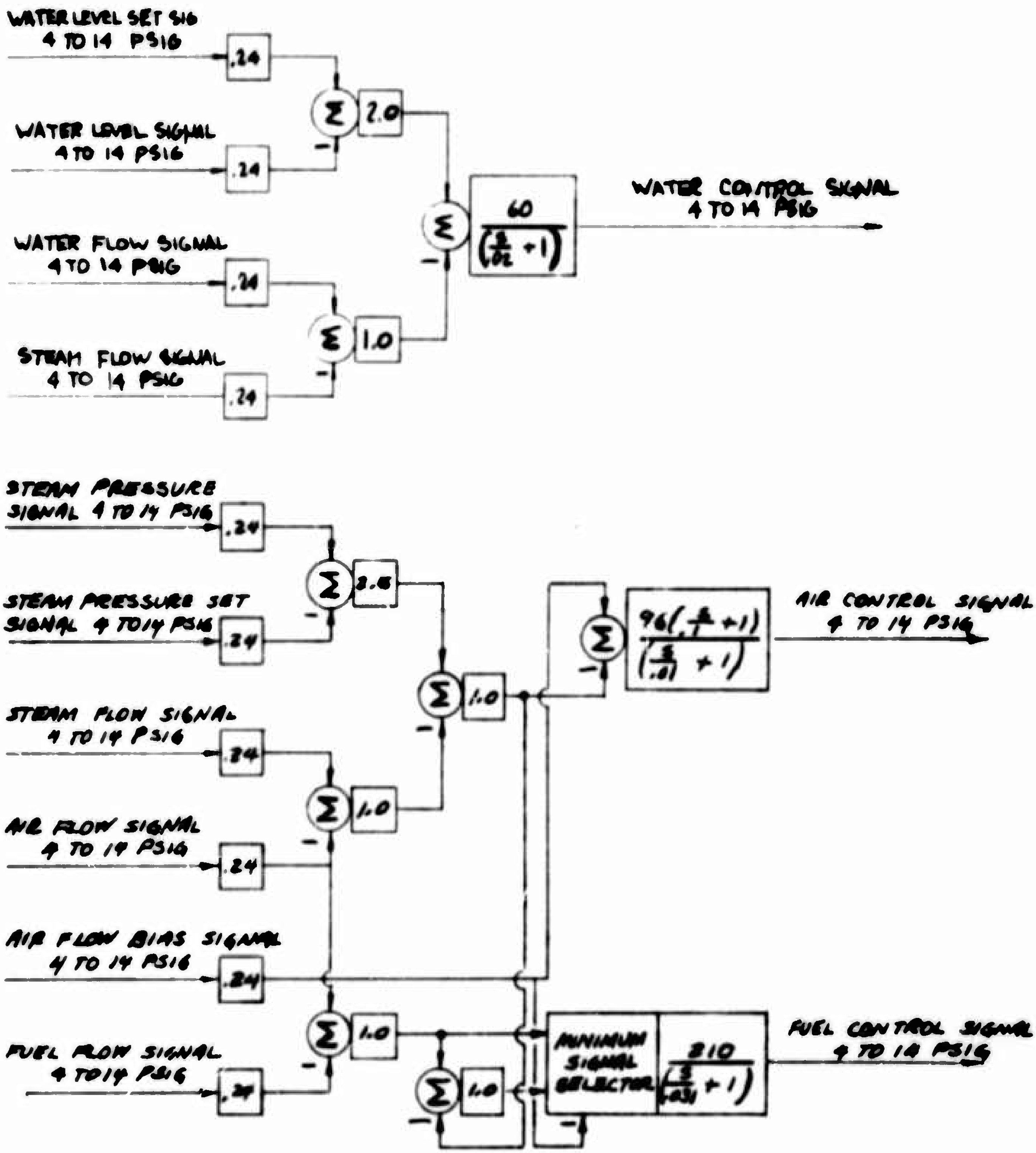

Fig. 1. Boiler control, control block diagram

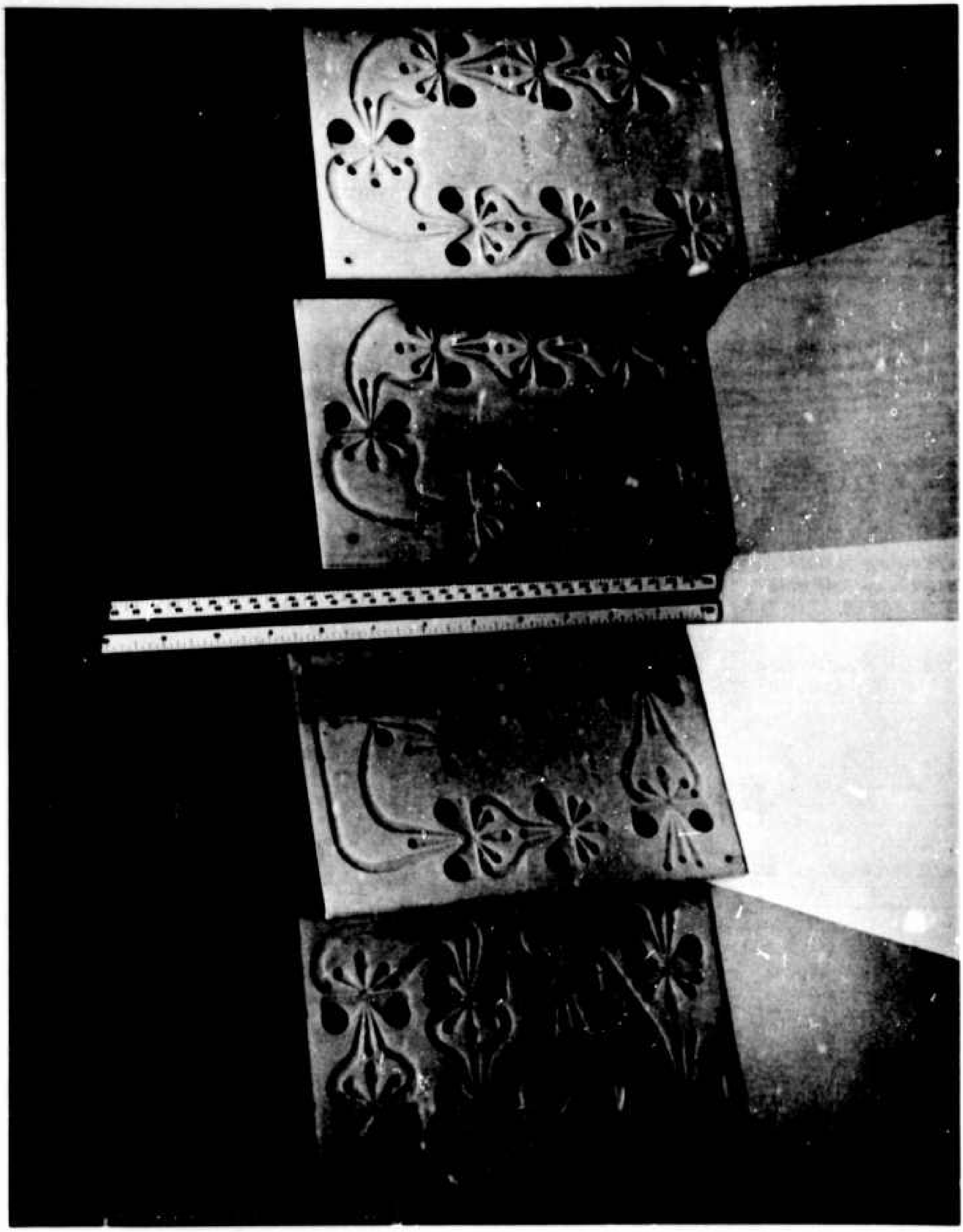

Fig.2. Boiler control, four major circuit assemblies

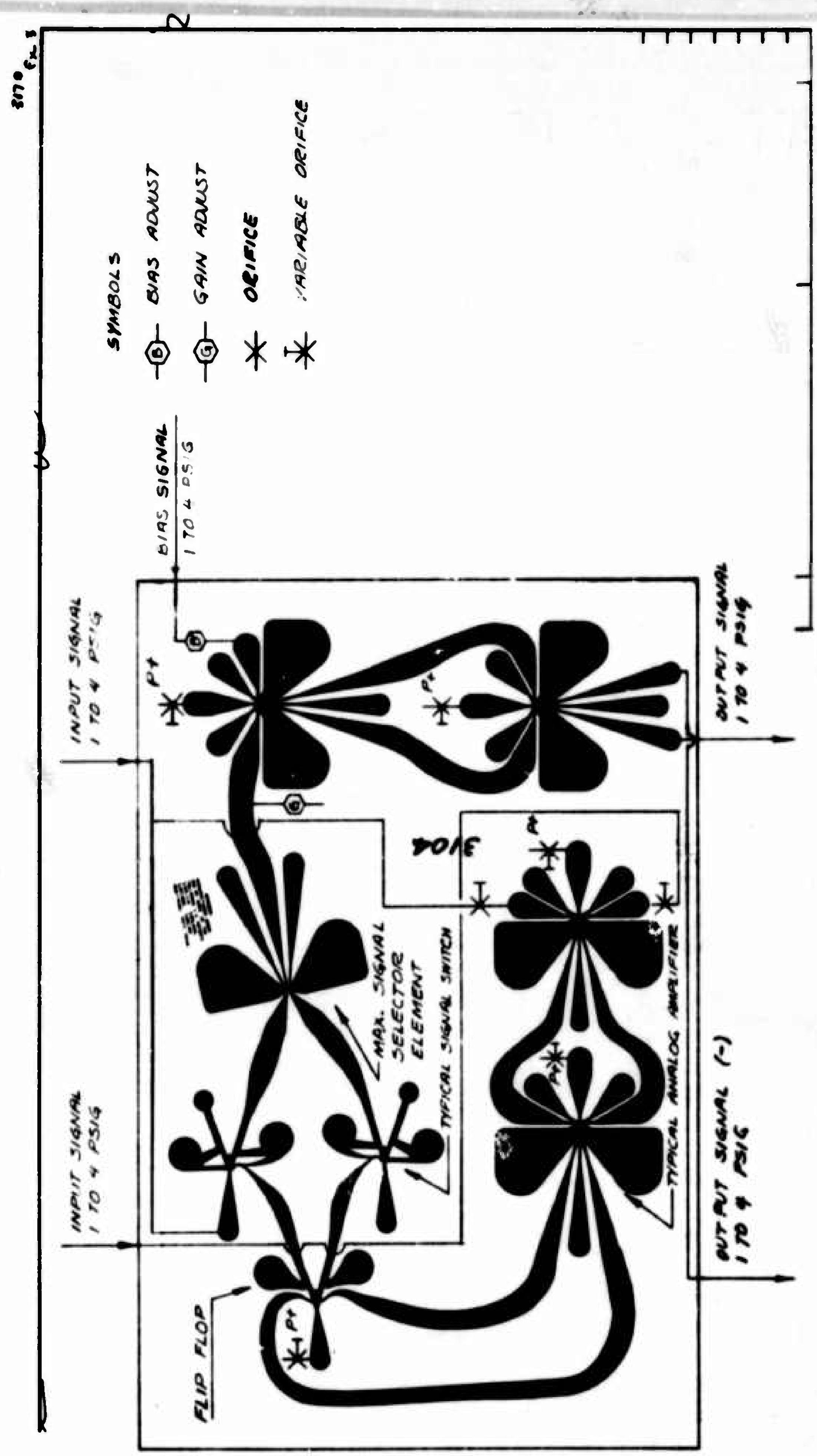

Fig. 3. Boiler control, minimum signal selector silhouette and schematic diagram

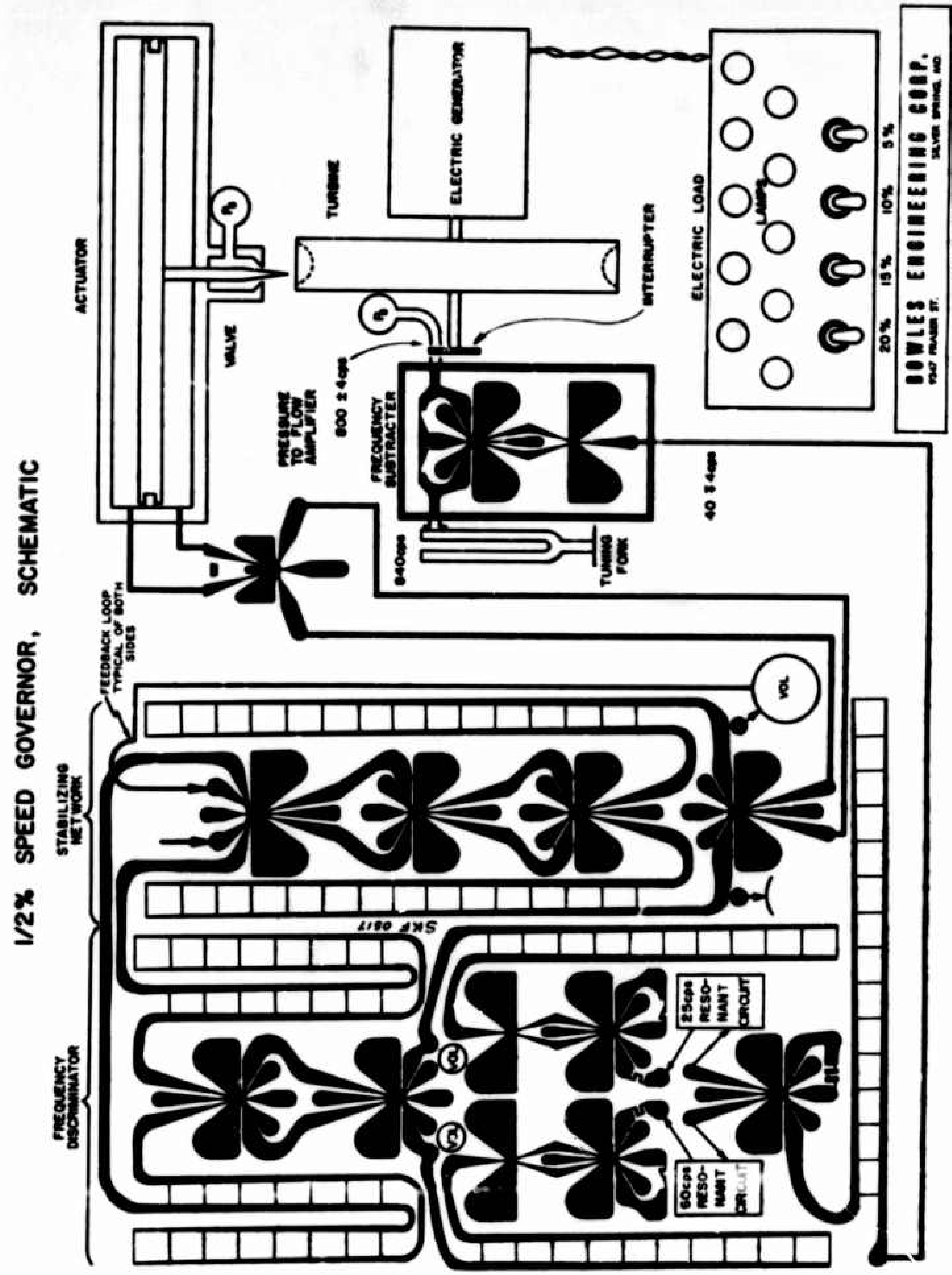

Fig.4 . Speed control, circuit silhouette and schematic diagram

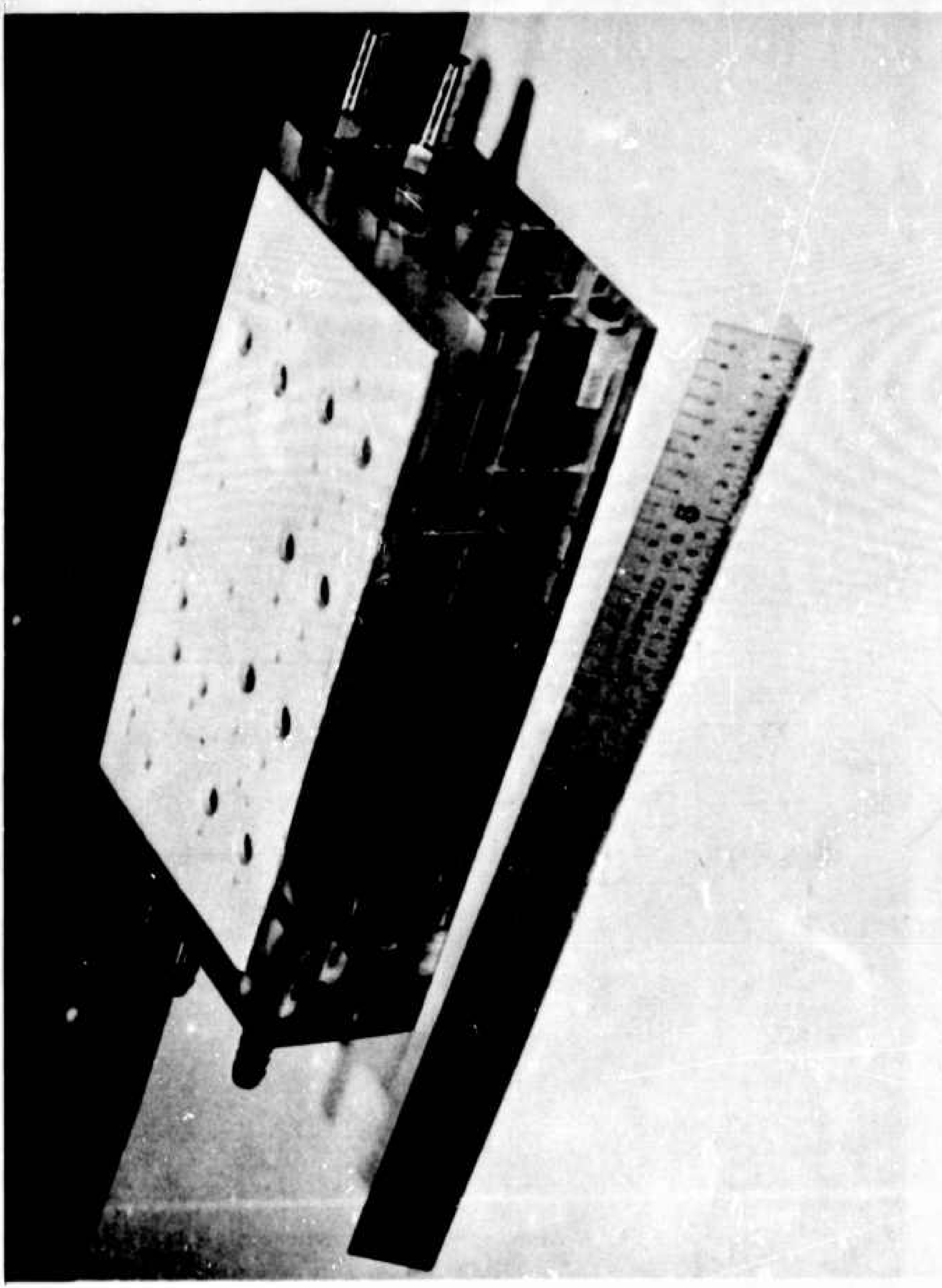

Fig.5. Amplifier and pressure level discriminator, circuit plate and manifold assembly

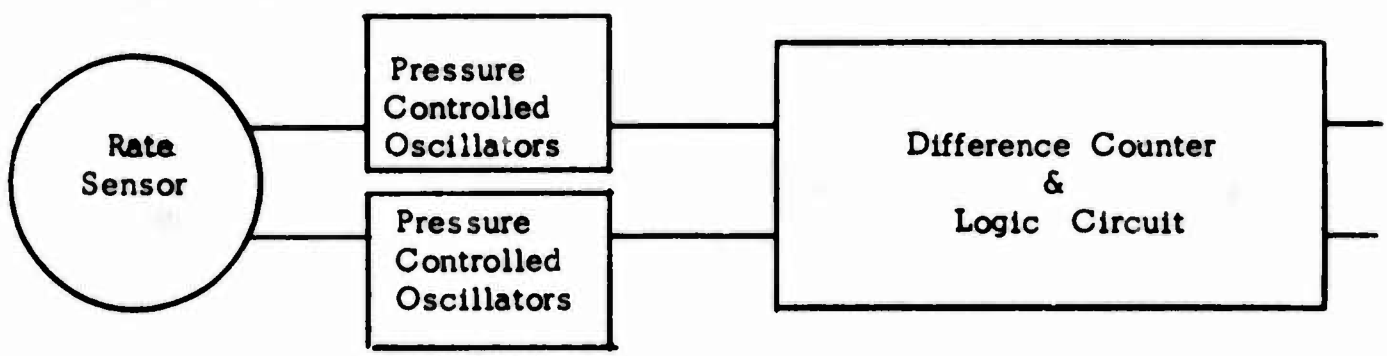

Fig. 6. Course control schematic diagram

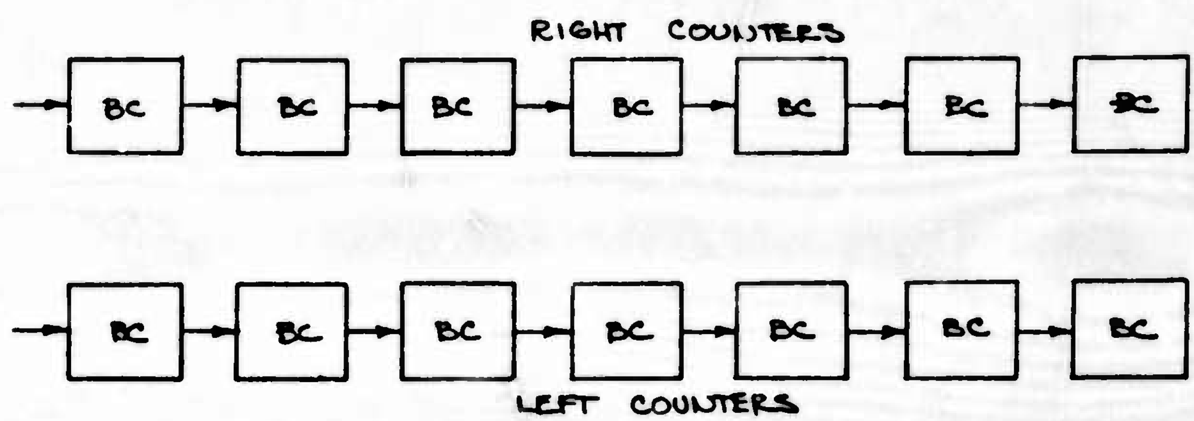

FIG. A

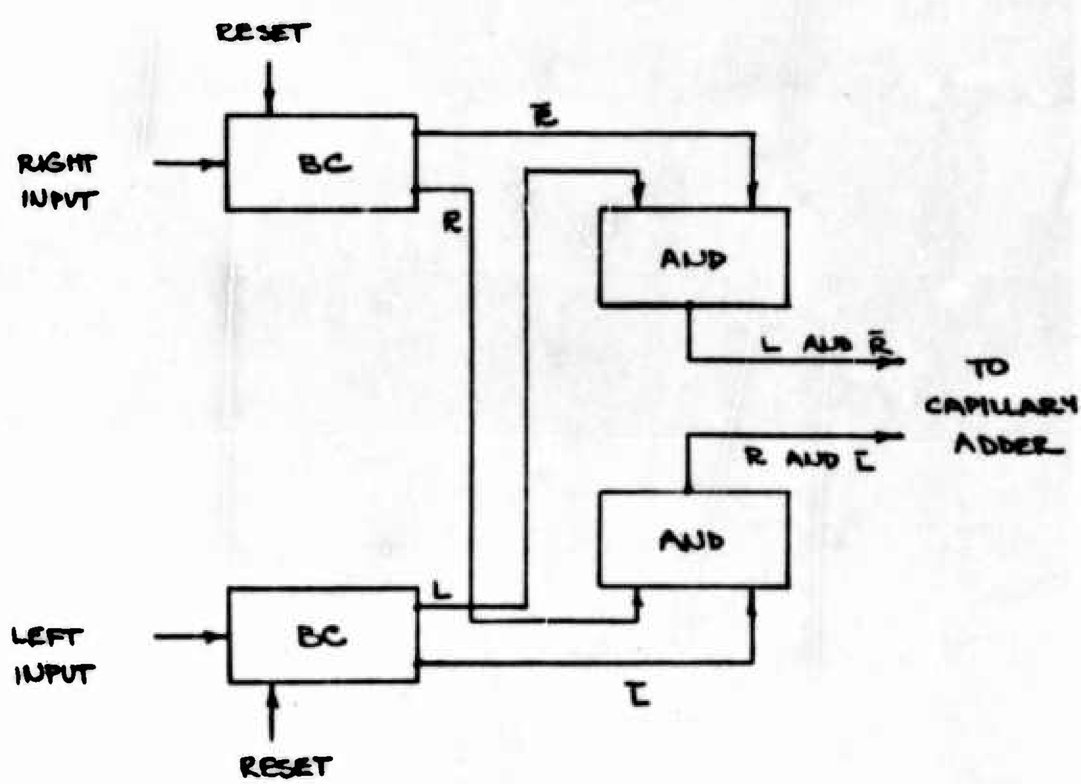

FIG. B

Fig.7. Course control, counter circuit schematic diagram

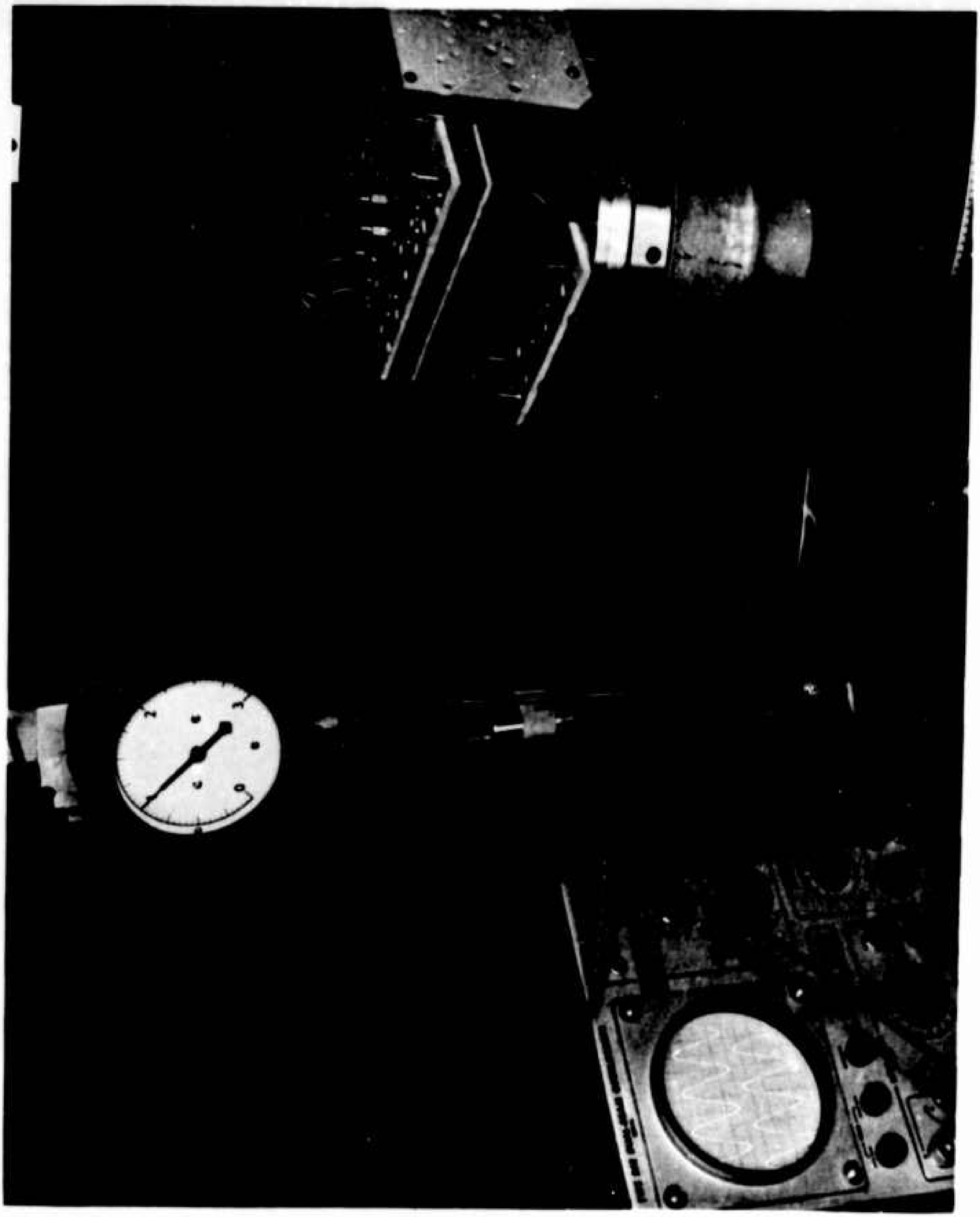

Fig.8. Course control system; fan, rate sensor and circuitry. Oscilloscope trace shows outputs of pressure controlled oscillators

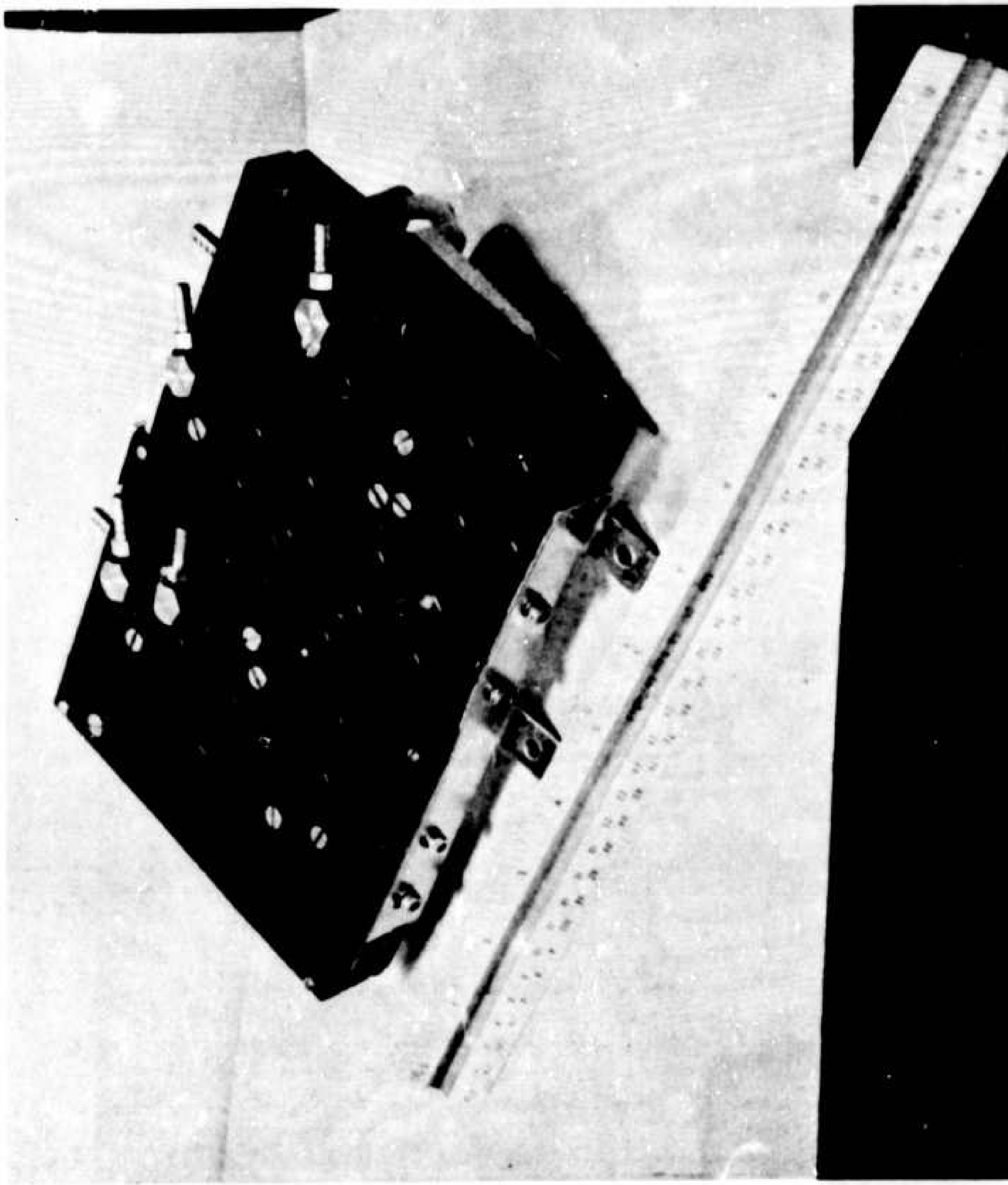

Fig. 9. Course control system; circuit assembly

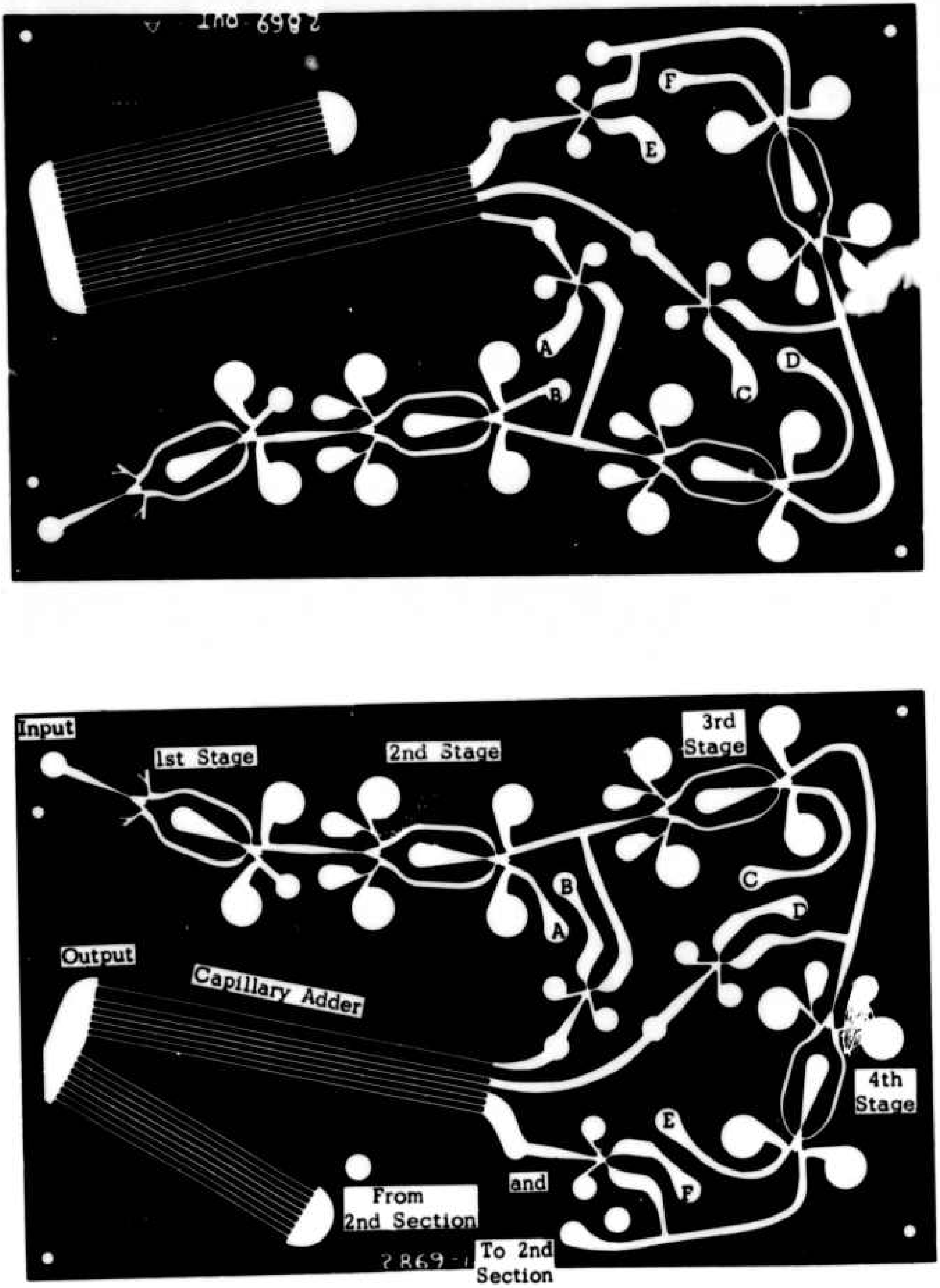

Fig. 10. Course control, counter circuit silhouette

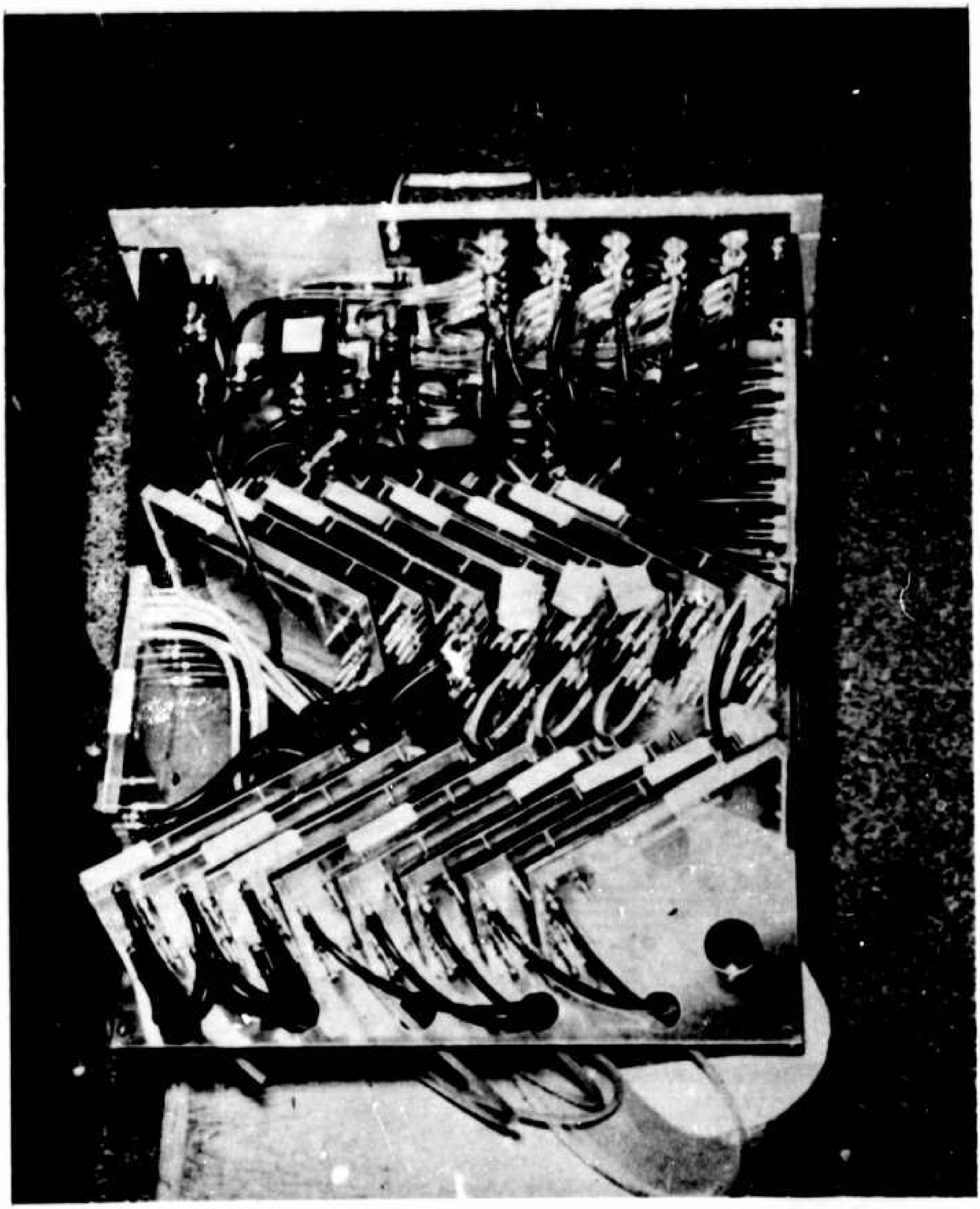

Fig.11. Sequence control assembly

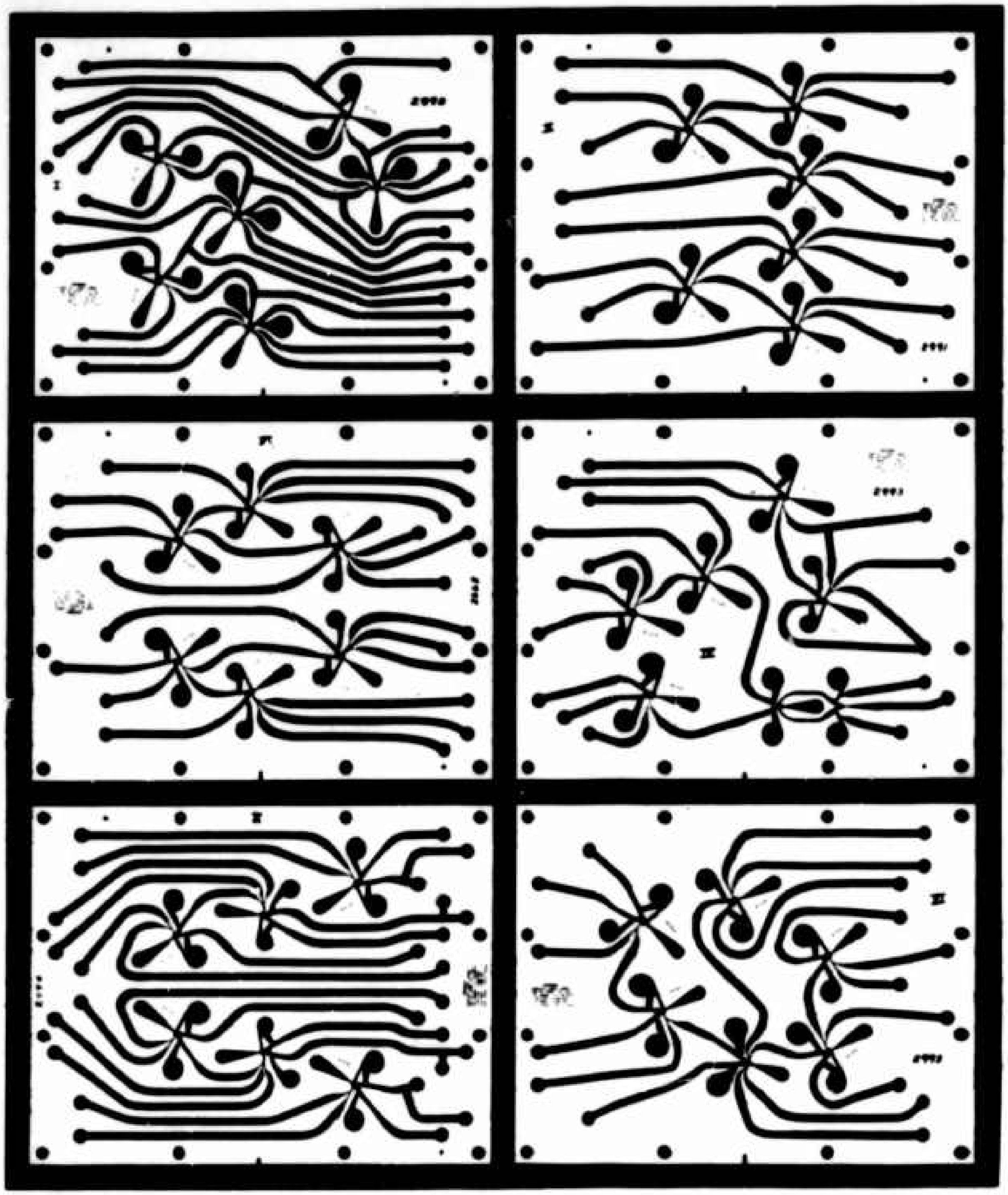

Fig. 12. Sequence control, silhouettes of circuit modules

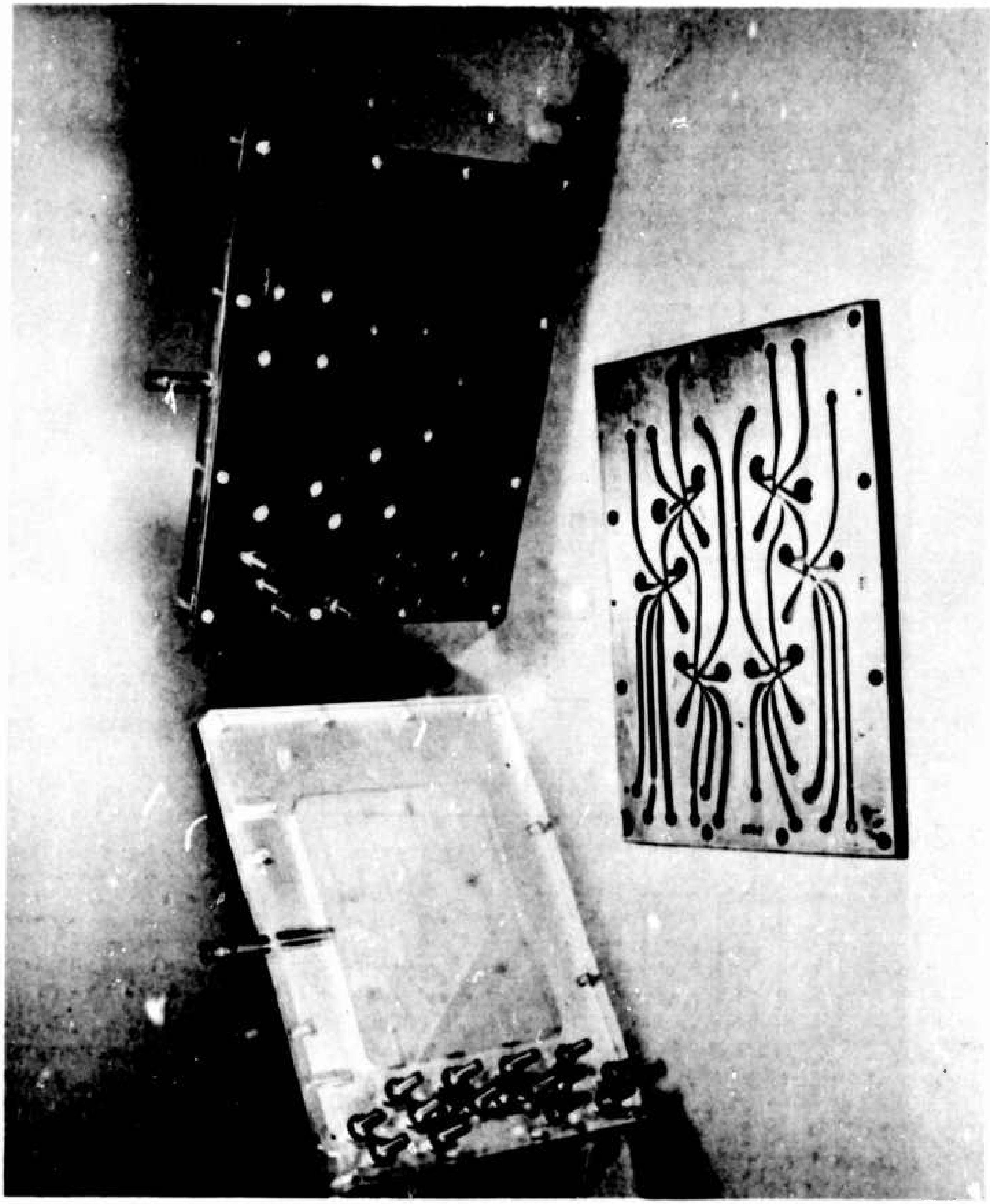

Fig. 13. Sequence control module assembly showing front view, rear view and a representative circuit board

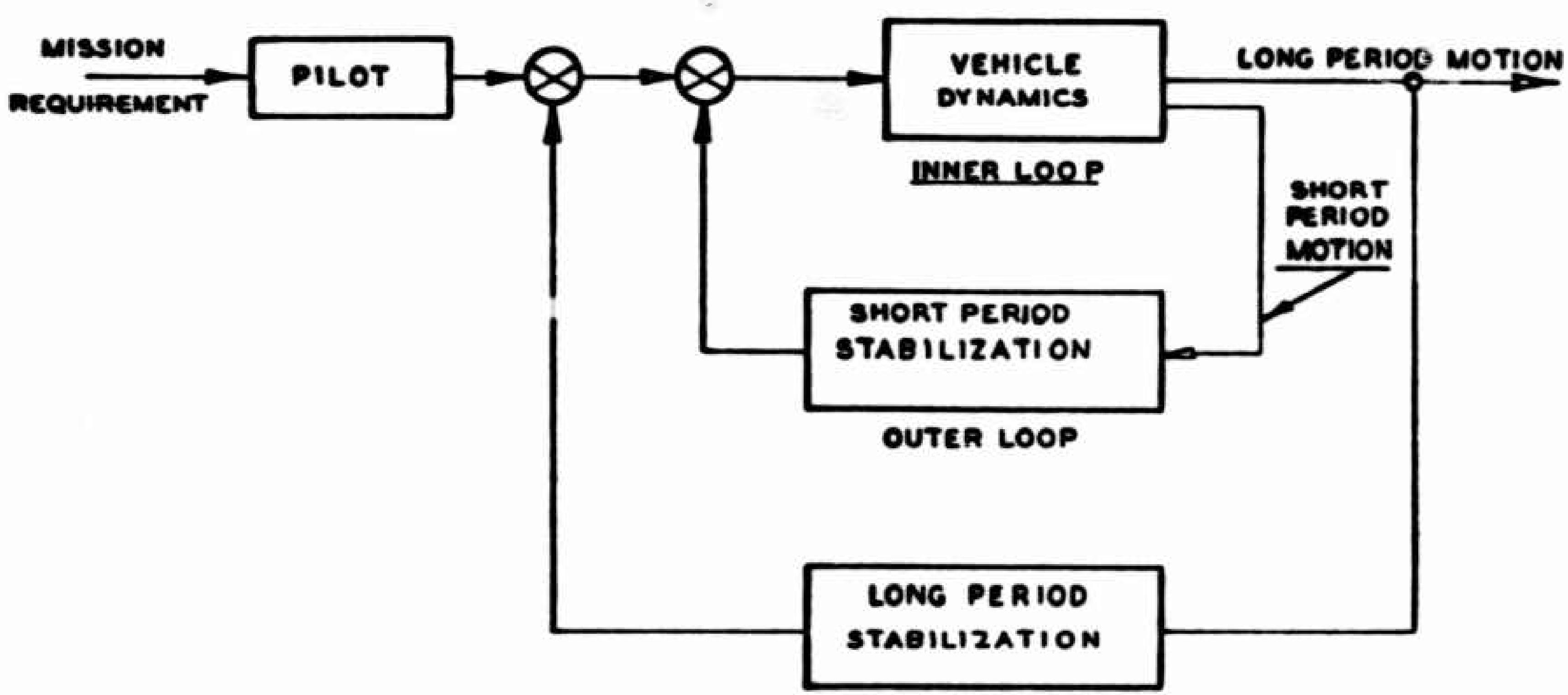

Fig. 14. Aircraft control system, schematic diagram

PURE FLUID VERSUS ELECTRONIC SYSTEMS
NON REDUNDANT SINGLE AXIS

	Pure Fluid System*	Electronic System	Ratio of Pure Fluid to Electronic System
Weight (pounds)			
Inner Loop	(10.1)	8.6	1.18
Outer Loop	(17.25)	13.3	1.30
Total	(27.35)	21.9	1.25
Power (watts)			
Inner Loop	(690)	470	1.47
Outer Loop	100	(185)	0.54
Total	(790)	655	1.20
Reliability			
Inner Loop	.9999	(.9956)	
Outer Loop	.9990	(.9890)	
Maintainability (hours/ hour of operation)			
Total	Less Than 0.1	Greater Than (0.1 to 0.2)	

Fig. 15 . Aircraft control system, comparison of a pure fluid control and an electronic system

STABILITY AUGMENTATION SYSTEM FAILURE RATE COMPARISON

	Electronic System	Pure Fluid System
Computing/Sensing	(2161)	25
Actuation	39	39
TOTAL	(2200)	64

Fig. 16. Aircraft control system, reliability comparison of a pure fluid system and electronic system

ASTROMECHANICS RESEARCH DIVISION
Giannini Controls Corporation
Malvern, Pennsylvania

A FLUID STATE ABSOLUTE PRESSURE RATIO COMPUTER

by

Charles A. Belsterling

A Paper Prepared For
The Third Fluid Amplification Symposium,
Harry Diamond Laboratories, Washington, D.C.
October 1965

ABSTRACT

This paper describes a pneumatic Absolute Pressure Ratio Computer with no moving parts (fluid state). It covers the concept and design of the components and circuits and includes an evaluation of the resulting demonstration system. The performance of the breadboard Fluid State Ratio Computer firmly establishes the feasibility of the concept. It demonstrates that sophisticated analog computing components can be developed to operate on fluid-state variables. It also illustrates that complex fluid state components can be interconnected into a useful system by means of straight-forward analytical techniques.

1. INTRODUCTION

1.1 Background

The purpose of this paper is to describe a pneumatic computer with no moving parts developed by the Astromechanics Research Division of Giannini Controls Corporation for the computation of the ratio of two absolute pressures (or flows). An operating demonstration Computer has been assembled successfully and recently delivered to the Air Force.

Several attempts had previously been made elsewhere to detect or compute the ratio of two absolute pressures with fluid state devices. without success. A more promising approach was made possible by the development by Giannini of new analog computing components, that is, the computation of ratios by straight-forward mathematical processes. Recognizing the potential for such a system in the computation of air data and the feedback control of jet engines, the Air Force Flight Dynamics Laboratory provided support for initial development of a demonstration computer, under Contract AF 33(615)-1534. Mr. Harry Snowball was the Air Force Project Officer.

1.2 Objectives

The functional requirements of the Fluid State Ratio Computer were 1) it should accept two variable absolute pressures, 2) compute the ratio of the absolute pressures, and 3) deliver an output proportional to the ratio at a power level adequate to drive instrumentation and be amplified with fluid state devices to any higher level.

2. SYSTEM DESIGN GOALS

2.1 Mach Sensor Requirements

The application which was selected to demonstrate the feasibility of a Fluid State Ratio Computer was Mach number sensing in a supersonic transport aircraft. The system was designed to accept static pressure and total pressure from conventional probes and compute the ratio of absolute pressures. As shown in Figure 1 this ratio can be converted to a signal directly proportional to Mach number through a

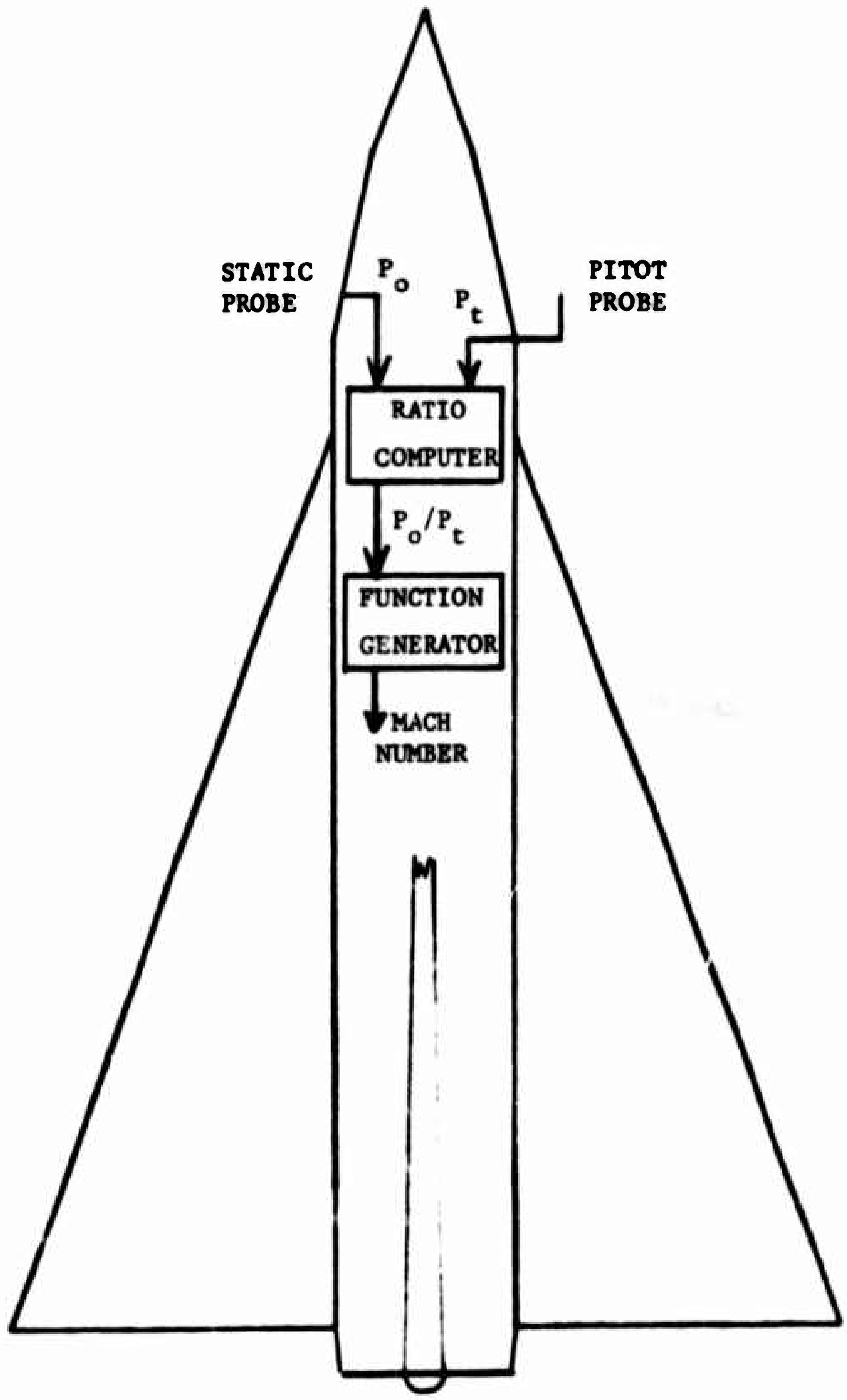

FIGURE 1 - DEMONSTRATION APPLICATION OF FLUID STATE RATIO COMPUTER

fluid state function generator, if so desired. The output can be used in pilot displays, air data computers, and engine controls.

2.2 Operating Envelope

The application selected defines an operating envelope for the Fluid State Ratio Computer as shown by the crosshatched outline in Figure 2. It is bounded by altitudes of 5000 and 57,000 feet, pitot pressures of 25 and 50 inches of mercury and Mach numbers of 1.0 and 3.0. The dotted envelope is typical for cruise operation of a supersonic transport. This illustrates that the choice of operating envelope is a realistic and representative one.

2.3 Dynamic Range of Variables

With reference to the operating envelope shown in Figure 2, the dynamic range of the variables (ratio of maximum to minimum) accommodated in the demonstration Fluid State Ratio Computer are defined as follows:

Variable	Absolute Range	Dynamic Range
Static Pressure P_o	2.4 to 24 in Hg	1 to 10
Total Pressure P_t	25 to 50 in Hg	1 to 2
Pressure Ratio P_o/P_t	0.083 to 0.53	1 to 6.4

2.4 Performance Goals

Although no requirements for performance were specified for the demonstration system, goals were defined at an early stage of development to serve as design guides. For the demonstration system these goals were 1) static accuracy better than 5% and 2) transient response less than 1 second.

3. RATIO COMPUTER DEVELOPMENT

3.1 System Design

A block diagram of the Fluid State Ratio Computer is shown in Figure 3. Note that the computation is simple and straight-forward, employing two key fluid state components: a function generator and a multiplier.

Total pressure P_t from the pitot probe enters the Computer through a passive network which conditions the signal for the next stage. The resulting signal representing P_t is fed to a fluid state function generator, programmed to compute the function $y = 1/x$. A signal containing $1/P_t$ appears at the output of the function generator and is applied to one input of a fluid state multiplier. Static pressure P_o from a static probe enters the Computer through a passive network which conditions the signal for further computation. The resulting signal

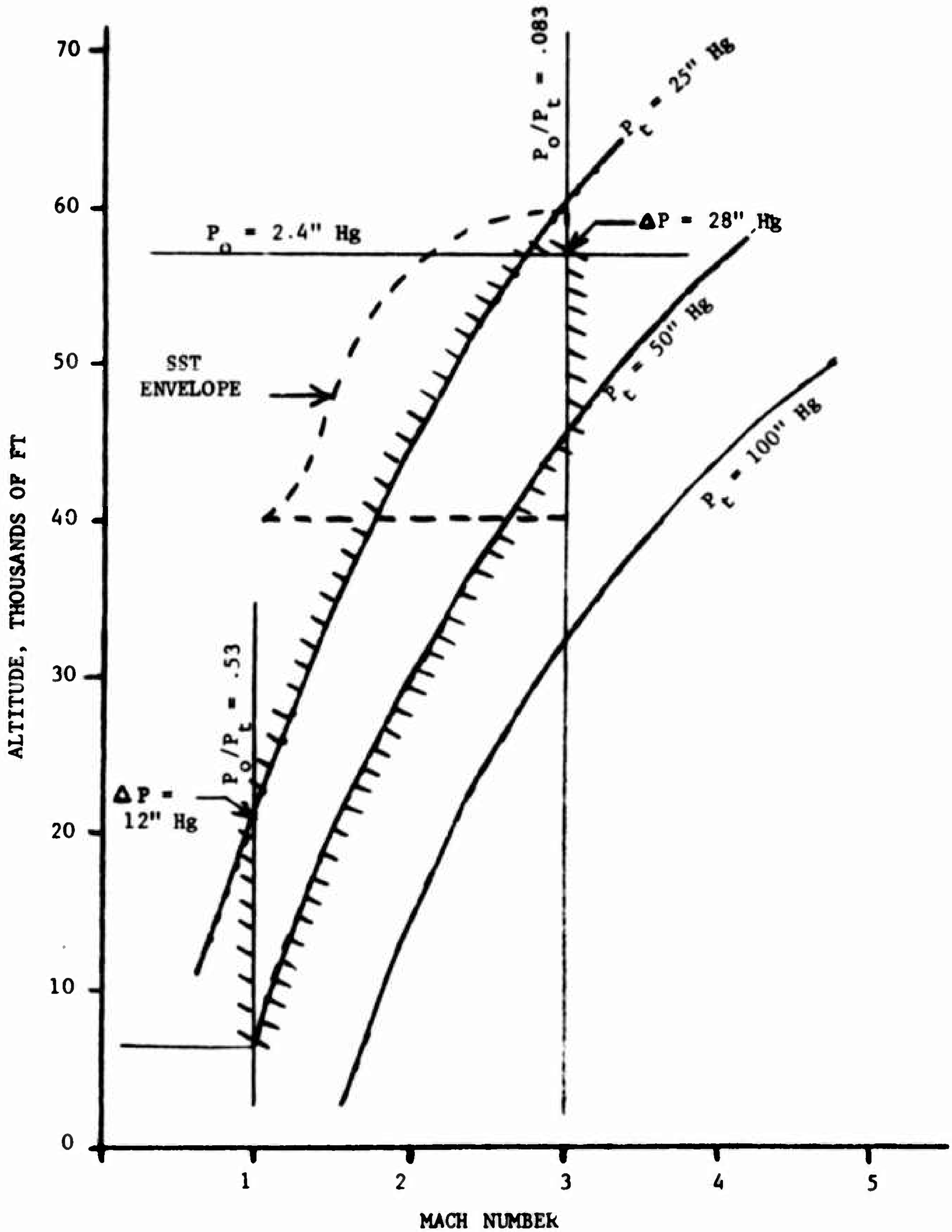

FIGURE 2 - RATIO COMPUTER OPERATING ENVELOPE

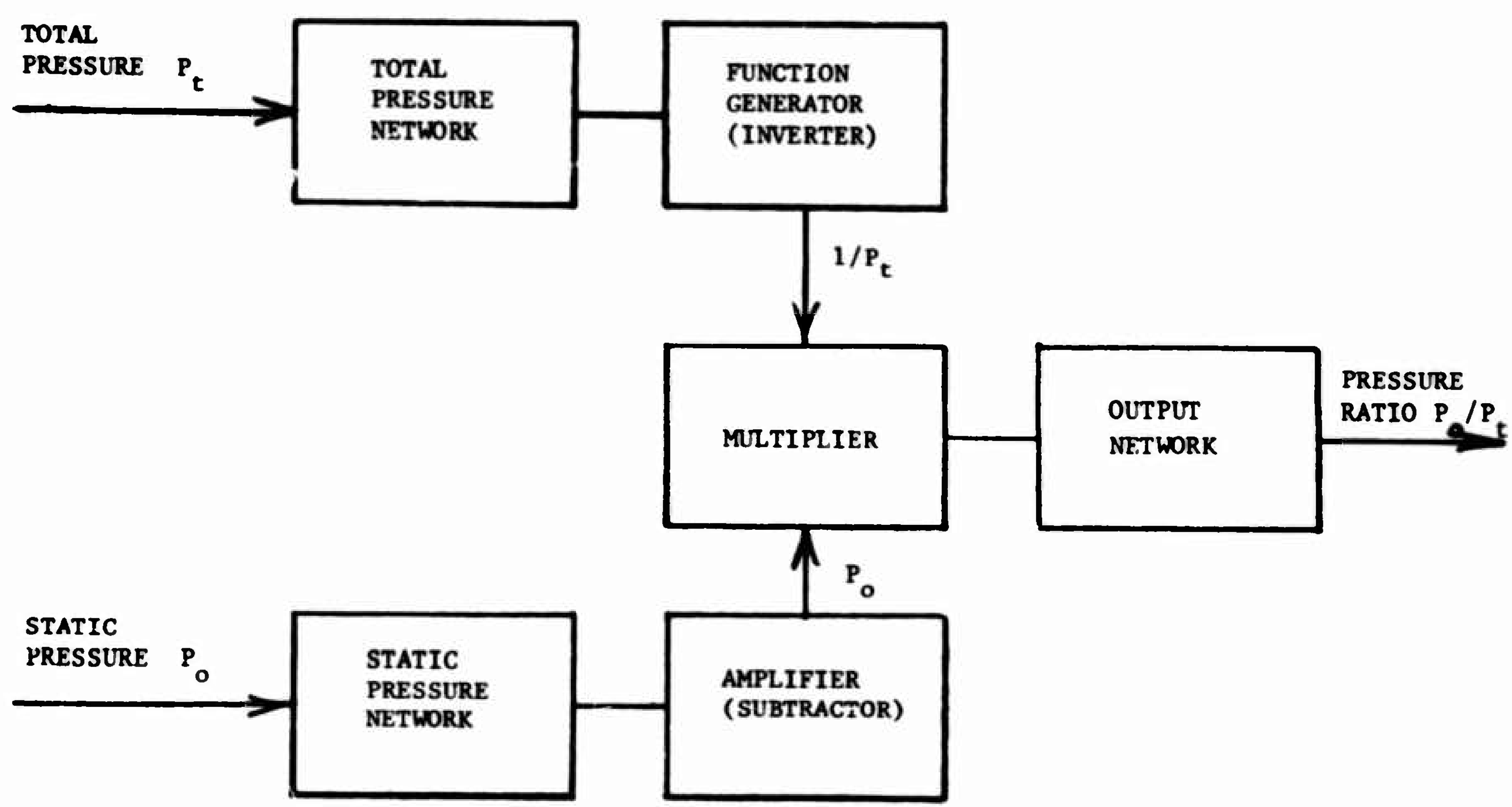

FIGURE 3 - BLOCK DIAGRAM OF FLUID STATE RATIO COMPUTER

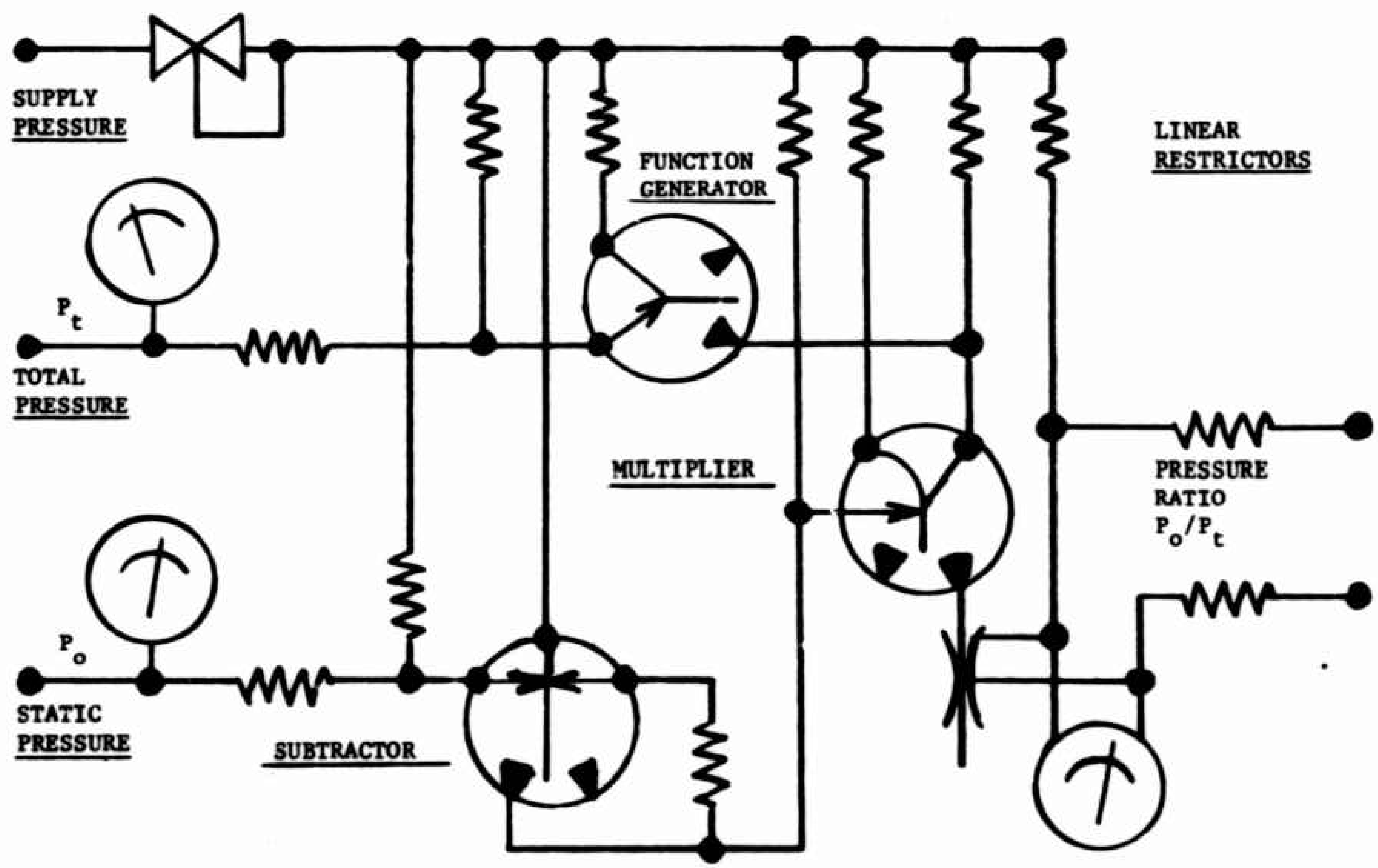

FIGURE 4 - CIRCUIT DIAGRAM - FLUID STATE RATIO COMPUTER

is fed to a linear amplifier. The output is an amplified signal proportional to the ratio of the absolute pressures P_o/P_t.

The circuit diagram of the Fluid State Ratio Computer is shown in Figure 4. The circuit is laid out to correspond to the block diagram of Figure 3. The entire network is powered by air supplied at approximately 22 psia. The return is common to all units in the computer and is to be regulated at (or slightly above) sea level atmospheric pressure, 14.7 psia.

Total pressure P_t detected with a pitot tube enters the Computer diagram at the upper left side. It is biased to the proper level by a network of linear restrictors and the resulting signal sent to a fluid state Function Generator (Inverter). The Inverter computes the function $y = k/x$ and so the output is a pneumatic signal proportional to $1/P_t$. This signal is properly biased by the addition of a fixed flow from the supply and applied to one input of a two-variable fluid state Multiplier.

Static pressure P_o enters at the lower left of the circuit diagram of Figure 4. It is properly biased in a specially designed non-choking network of passive restrictors and the resulting signal fed to a fluid state Subtractor. In the Subtractor, the signal representing P_o is subtracted from a constant, so the output varies in proportion to $-P_o$ (note that the sign change is only necessary to satisfy the input requirements of the Multiplier). The Subtractor output is then biased and fed to the second input of the Multiplier. The Multiplier continuously computes the product of the absolute value of the two inputs, $1/P_t$ and P_o, to deliver an output pressure which contains a signal proportional to the product, P_o/P_t.

3.2 Component Development

To implement the Ratio Computer network shown in Figure 4, it was necessary to accomplish three significant advances in the state of the art, the development of 1) a non-choking restrictor network, 2) a fluid state function generator and 3) a fluid state multiplier of two variables.

3.2.1. Non-Choking Restrictor Network

The input network for static pressure P_o must raise the signal to a level compatible with the Subtractor. This is a difficult problem considering the fact that the Subtractor operates above 15 psia and the static pressure can go as low as 1.2 psia. Because of the high ratio of absolute pressures, choking is certain to occur in any of the passages between the two. Choking is a phenomenon wherein, if the downstream absolute pressure is less than half the upstream pressure, and if the downstream pressure is reduced, the flow will not increase. If this condition were to occur in the static pressure input lines, it would be impossible to detect a change in P_o. The problem

was solved in an extremely straight-forward manner, simply by breaking up the restrictors in the static pressure network so that the absolute pressure ratio across any one section never reaches the critical number for choked flow.

3.2.2 Fluid State Function Generator (Inverter)

A fluid state component is required to compute the reciprocal of the variable pressure P_t; that is, generate the analog function $y = K/x$. In the course of the project a number of experimental devices were developed to do this successfully. The design selected for the demonstration Ratio Computer is the ultimate in simplicity. It employs two impinging jets which, in combination with proper wall shaping and receiver placement, is capable of generating the hyperbolic function $(y = K/x)$ (shown in figure 5) over a wide dynamic range.

3.2.3 Fluid State Multiplier of Two Variables

The Ratio Computer also requires a component for multiplying two variables in the fluid state. Note that an ordinary amplifier multiplies one variable times a constant; that is $P_o = K_1 P_{in}$ as shown in Figure 6(a). The constant is the amplifier gain. If the gain can be changed by means of a second variable then $P_o = K_2 P_2 P_{in}$. Thus a multiplier is simply a controlled gain amplifier with a family of characteristics shown in Figure 6(b). The multiplier developed for this project is basically a Double Leg Elbow Amplifier modified for controlled gain and closed-vent operation. Late in the development program, a second multiplier was developed of radically simplified configuration but it was too late for application in the demonstration system. However, the work resulted in a simplified, smaller and more powerful unit.

3.2.4 Linear Restrictors

In addition to these more interesting accomplishments we were also faced with the mundane problem of building linear restrictors. Linear restrictors are required at many places in the Ratio Computer network (see Figure 4) to convert pressures to flows (and vice-versa) without changing scale factors. Because of the wide and unusual range of sizes required, it was necessary to develop our own techniques for fabricating linear restrictors to satisfy the immediate requirements of the Ratio Computer program. As a result the linear restrictors in the breadboard Computer are constructed as follows.

Basic stock is a quantity of 4-inch lengths of 10-mil ID stainless steel hypodermic tubing. This length is sufficient to drop nearly 10 psi with laminar flow (that is, the resistance is constant up to nearly 10 psi). The proper number of 4-inch tubes is selected to give the necessary resistance, they are bundled together and spirally wrapped with black vinyl electrical tape. The end connect

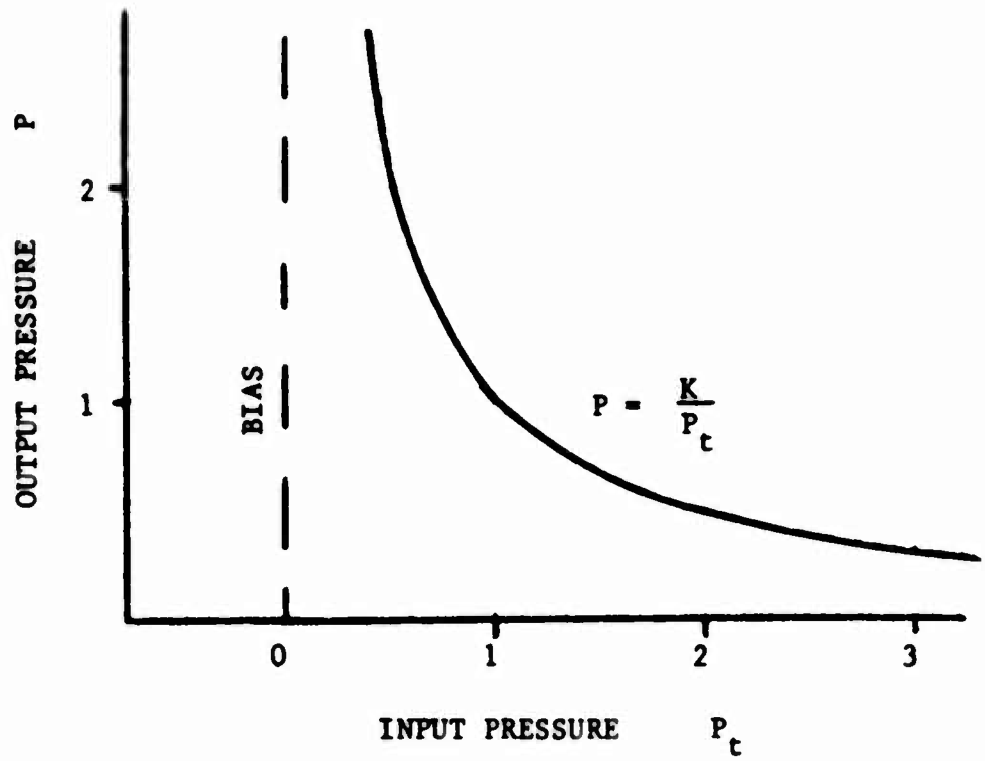

FIGURE 5 - PERFORMANCE OF FLUID STATE FUNCTION GENERATOR

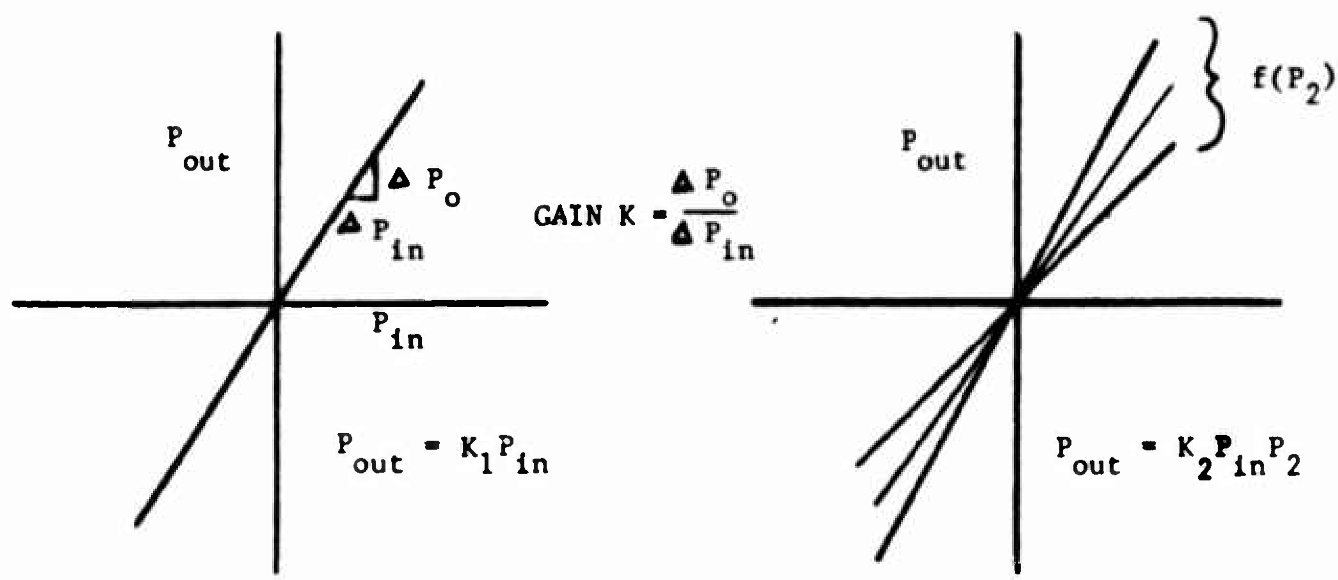

a) TRANSFER CURVE OF TYPICAL AMPLIFIER

b) TRANSFER CURVE OF TYPICAL MULTIPLIER

FIGURE 6 - GENERAL CHARACTERISTICS OF MULTIPLIER

sections are formed by choosing vinyl plastic tubing with an ID which requires some stretching to slip it onto the end of the tube bundle and over the tape.

Linear restrictors used in the Ratio Computer circuit range from 0.175 psi per millipound per second (psi/mlb/sec) requiring 613 tubes to 45 psi/mlb/sec requiring only 9 tubes.

3.3 System Integration

In system integration, the fullest advantage was taken of the most advanced analytical and graphical matching techniques. For example, input characteristics, transfer characteristics, and output characteristics were recorded for each circuit. In this way each one could be designed for proper matching with those connected to it. As a result of this approach it was possible to avoid the cut and try approach and achieve ratio computation the first time the system was connected together.

The demonstration Fluid State Ratio Computer is shown in Figure 7. The system is laid out exactly as the circuit diagram of Figure 4 for ease in tracing the flow of information and in identifying components. It is enclosed in a suitcase-sized Plexiglass case for ease in handling. It should be obvious that there was no attempt to minimize the size.

The Computer is fitted with its own input and output meters so it is a completely self-contained demonstrator. After this photo was made, the meter scales were altered to read inputs in <u>absolute</u> pressure units and outputs in pressure ratio as well as Mach number.

4. RATIO COMPUTER PERFORMANCE

4.1 Ideal Performance Curves

Prior to evaluating the performance of the breadboard Fluid State Ratio Computer, it is first necessary to generate a set of ideal performance characteristics.

Ideally, the Ratio Computer is an analog divider of two variables, P_t and P_o. It is dividing static pressure P_o by total pressure P_t. Thus, the output pressure is to be proportional to P_o/P_t and its performance can be described by a set of curves as shown, Figure 8. In this case we have chosen to plot the output as a function of P_t with P_o as the parameter. Then for a given value of P_o the output is K_1P_o/P_t; that is, the curve is a hyperbola. Note that when P_t is doubled, the output must decrease to half its initial value. If P_t is fixed and P_o varied, the output is K_2P_o; that is, the output increases linearly with P_o. Note that when P_o is doubled the output increases to twice the initial value. Thus we may generate the characteristics of an ideal Ratio Computer as a family of hyperbolae,

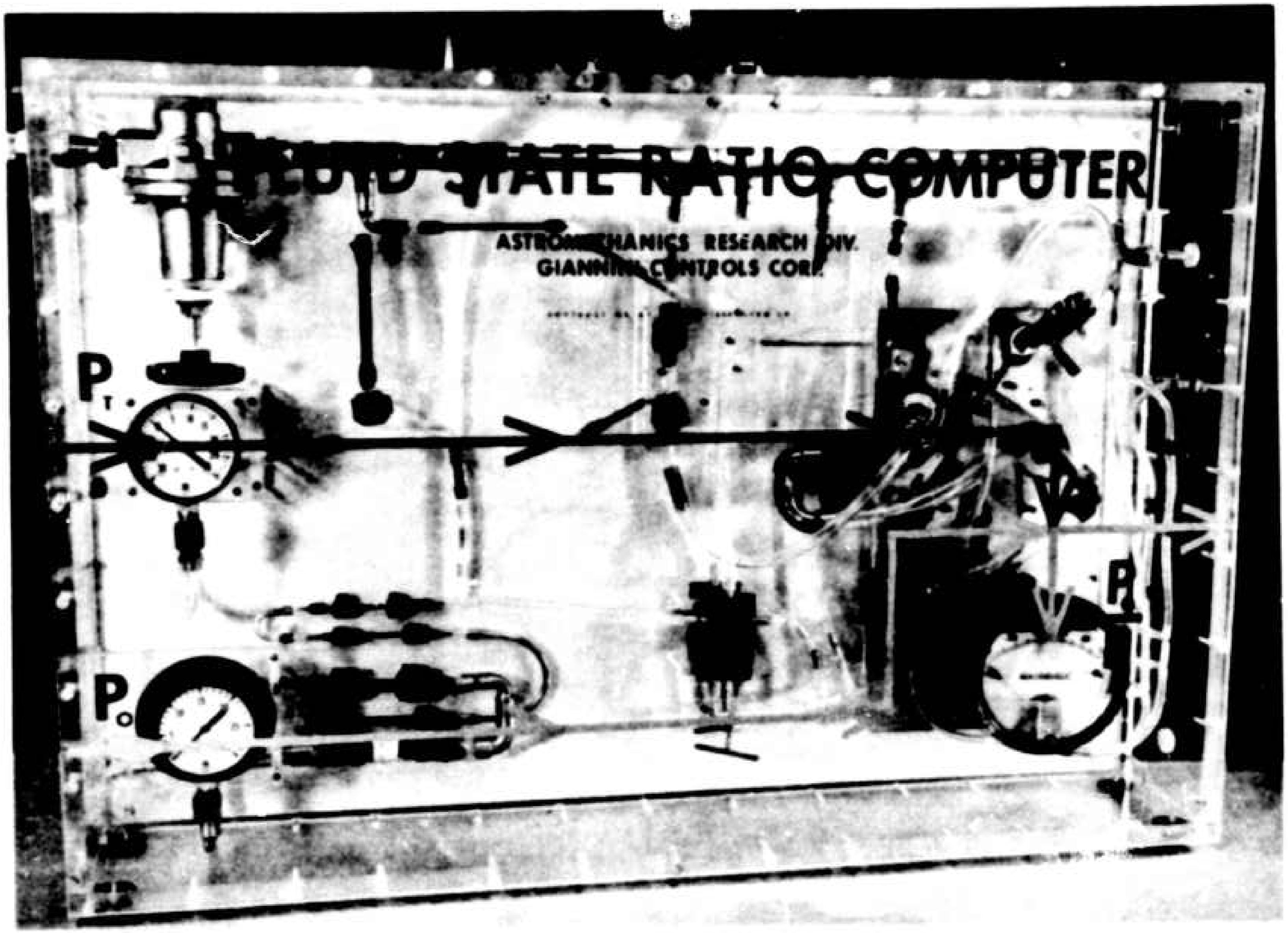

FIGURE 7 - DEMONSTRATION BREADBOARD RATIO COMPUTER

each curve separated by a distance proportional to its value (equally spaced) as shown in Figure 8.

The breadboard Fluid State Ratio Computer is designed to operate within the envelope illustrated in Figure 2. The resulting limits imposed on the variables are superimposed on the ideal characteristic in Figure 8.

4.2 Actual Performance Curves

The performance of the breadboard Fluid State Ratio Computer illustrated in Figure 7 is shown in Figure 9 for direct comparison with the ideal curves in Figure 8. Note that over the major portion of the operating envelope the Fluid State Ratio Computer is calculating the ratio of two absolute pressures within a few percent. However as either input pressure approaches the lower end of its range, the accuracy of the computation decreases. As described later these errors are primarily due to nonlinearities in the input networks because of the wide variation in air density. In future designs, suitable compensation will be included to eliminate these errors.

4.3 Transient Response and Noise

The delivered breadboard Fluid State Ratio Computer contains a "MAGNEHELIC" differential pressure indicator to provide a visual display of the computed ratio. With this meter in the system the dynamic response is inferior to that of the basic system alone as shown in the table below.

TRANSIENT RESPONSE

(Seconds to reach 63% of final value)

Variable	Without Meter	With Meter
P_o	-----	1.6
P_t	0.2	1.0

The basic system without the visual output indicator has a high (100:1 or better) signal to noise ratio over most of its operating envelope. However, there are a few regions near the extremes where the ratio decreases to about 10:1.

5. PERFORMANCE EVALUATION

5.1 Static Accuracy

In Figure 10, we illustrate the static accuracy of the breadboard Fluid State Ratio Computer by two contours superimposed on the ideal characteristics. Note that the accuracy is within the 5% design goal over the major portion of the operating envelope. At the lower extremes of total pressure and static pressure the errors are somewhat

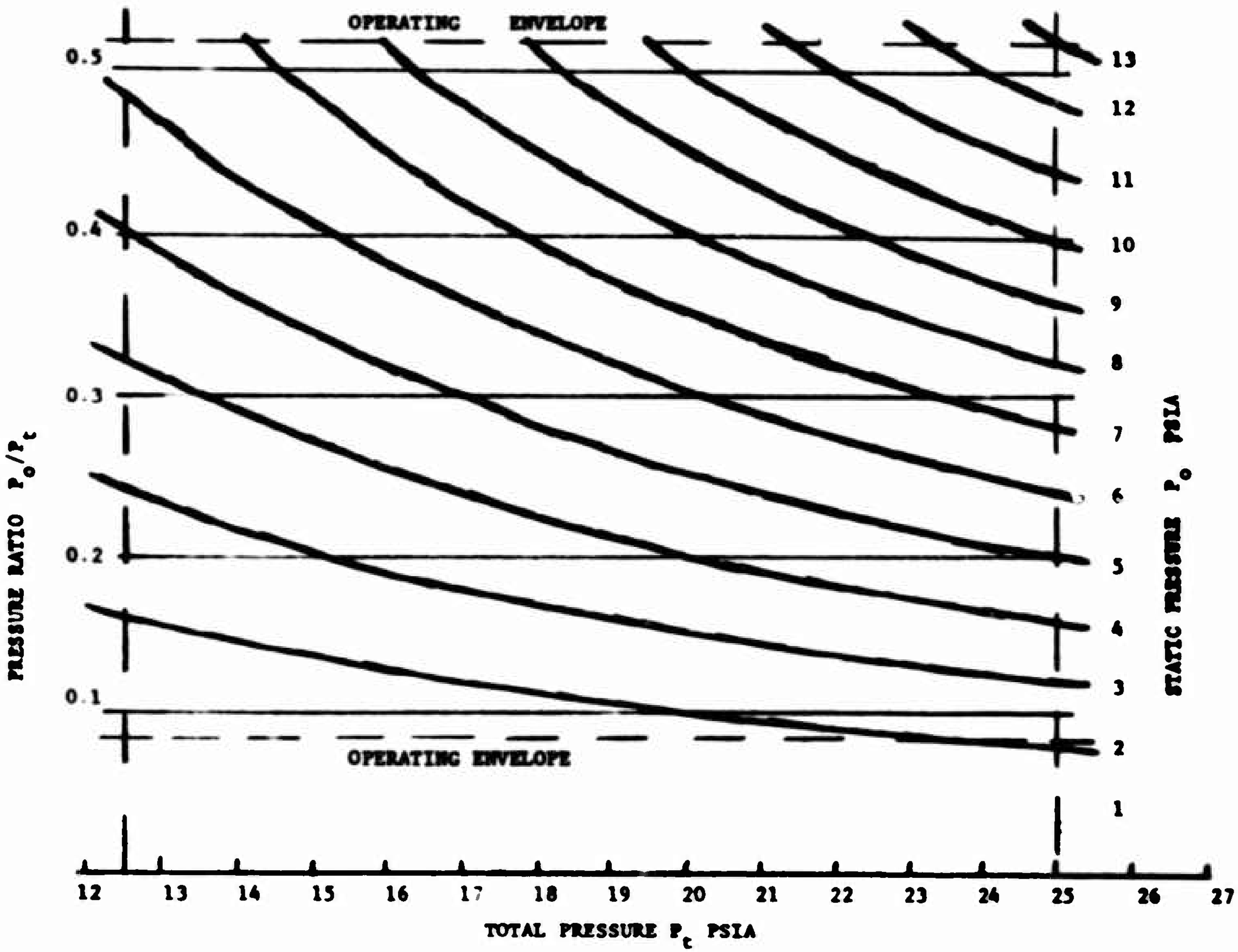

FIGURE 8 - IDEAL PERFORMANCE OF RATIO COMPUTER

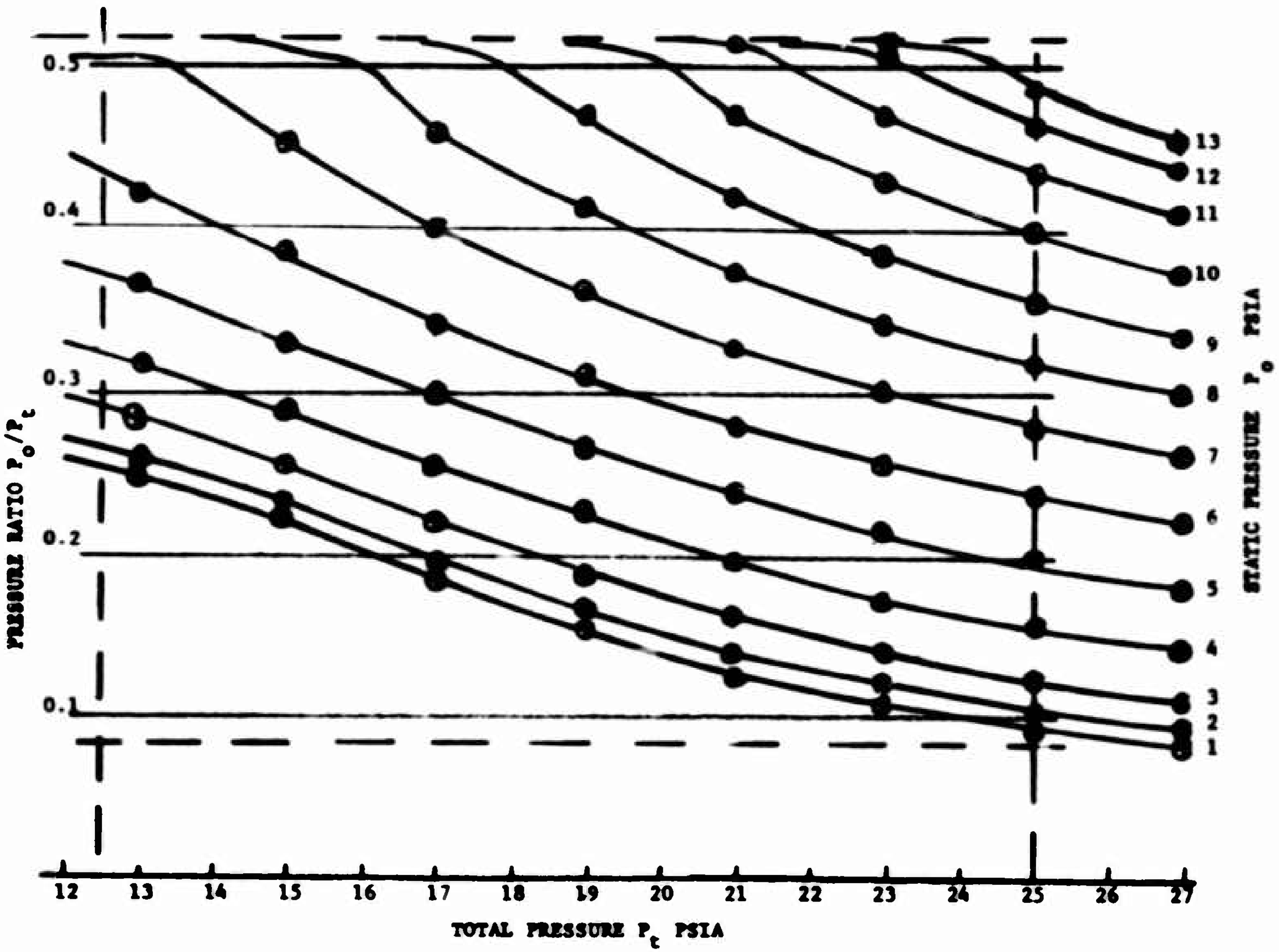

FIGURE 9 - PERFORMANCE OF FLUID STATE RATIO COMPUTER

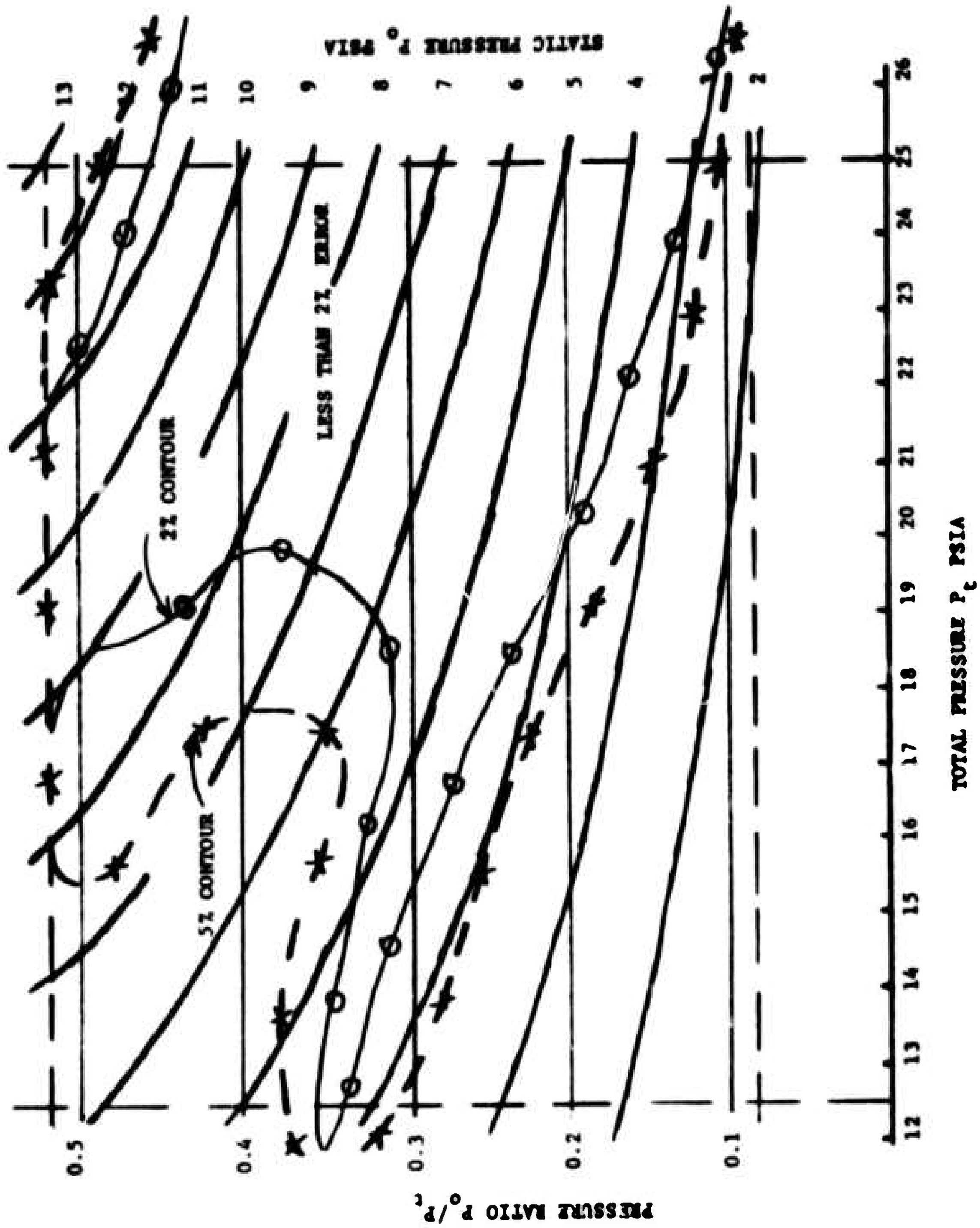

FIGURE 10 - ERROR CONTOURS FOR BREADBOARD RATIO COMPUTER

greater. In a region near the center of Figure 10 the errors are never higher than 2%.

The errors are primarily due to nonlinearities in the passive input networks. Because the impedance of the restrictors is inversely proportional to the average pressure, it increases rapidly as the static pressure input signal approaches 1 psi absolute. Since these are predictable errors which can be compensated for, we estimate that the optimized design will have no more than 1% static error over the entire operating envelope.

5.2 Transient Response and Noise

The transient response of the Fluid State Ratio Computer without the output meter is 0.2 seconds. This is far better than the original design goal of 1.0 seconds.

The major time delays in the 0.2-second response appear to be in the total pressure and static pressure input networks. They are the result of the combination of very high network impedances (to minimize input signal flow requirements) and volumes associated with the Function Generator and Subtractor. These time delays can easily be reduced by designing for low volume between the input networks and the Subtractor and Function Generator. Therefore we predict a response time of less than 0.01 second in the optimized design.

The most significant source of noise in the output signal is the Multiplier. Because of the low velocity of the air stream, the output contains some very low frequency components and therefore requires high-time-constant filtering. In future designs using simplified configurations and high velocity jets, the low frequency fluctuations can be eliminated. On this basis we predict that the optimized design will have a signal-to-noise ratio better than 100 to 1 over the entire operating envelope.

6. CONCLUSIONS

In summary, demonstration of the feasibility of the Fluid State Ratio Computer has been accomplished. The performance of the breadboard Computer has met or exceeded most of its design goals. Moreover, the demonstration system has pointed out areas where additional effort should be devoted to optimize the performance of future Fluid State Ratio Computers. Therefore, it is a significant advance in the state of the technology of fluid state analog computation.

HARRY DIAMOND LABORATORIES
WASHINGTON, D. C. 20438

A TEMPERATURE CONTROL SYSTEM USING PLUERIC COMPONENTS

by

RICHARD N. GOTTRON
WILMER GAYLORD

ARMY MATERIEL COMMAND DEPARTMENT OF THE ARMY

ABSTRACT

An all pneumatic system developed recently at the Harry Diamond Laboratories exhibits a pressure or flow output that is a function of the temperature of the gas in the sensing system.

Laboratory tests from 21° to 120°C showed the d-c output level to be proportional to frequency over this range. The frequency, in turn, is proportional to the gas temperature. The differential output pressure change was about 150 millibars.

1. INTRODUCTION

The temperature-sensing pneumatic oscillator (ref 1 and 2) has been utilized to generate a system having a pressure or flow output that is a function of temperature.

The frequency output of the system as a function of temperature is based on a difference in frequency of two pneumatic oscillators. The two oscillators are supplied air at the same temperature. The oscillators are similar in all respects except for temperature sensitivity; thus a difference frequency as a function of temperature is generated as temperature varies. The signals from the oscillators are mixed to yield sum and difference frequencies. The derivation of the difference frequency is necessary to lower the frequency to the response capability of the digital logic components. The range is approximately 100 cps for the unit described.

The sum and difference frequencies from the mixer are applied to an acoustic-to-pneumatic converter. A pneumatic signal for the purposes of this report is a signal that is not acoustic. The converter output is a pneumatic pulse, which has a repetition frequency identical with the applied oscillator difference frequency. The pulses from the converter are operated on by the digital logic circuit to yield a pulse of constant amplitude and duration, regardless of frequency.

These pulses are integrated to obtain a "d-c level" of flow or pressure that is a function of frequency and, hence, temperature.

This d-c level is amplified by staging of proportional amplifiers. The amplified (d-c) output, of course, may be applied to a servovalve (or equivalent device) to regulate fuel flow to an engine or to regulate exhaust area, etc.

2. DISCUSSION

The components of the system may be classified functionally as: sensing, coupling, mixing, acoustic-to-pneumatic conversion, digital logic function, and amplifying network. A diagram of the control system is shown in figure 1. Addition of the components shown in phantom (broken lines) would complete the control loop.

2.1 Temperature Sensing

Temperature is sensed as a frequency by two temperature-sensitive pneumatic oscillators (ref 1, 2). The frequency of the oscillators is necessarily above the response capability of the digital logic devices; a single oscillator cannot be used, since an oscillator of low enough frequency would be extremely large.

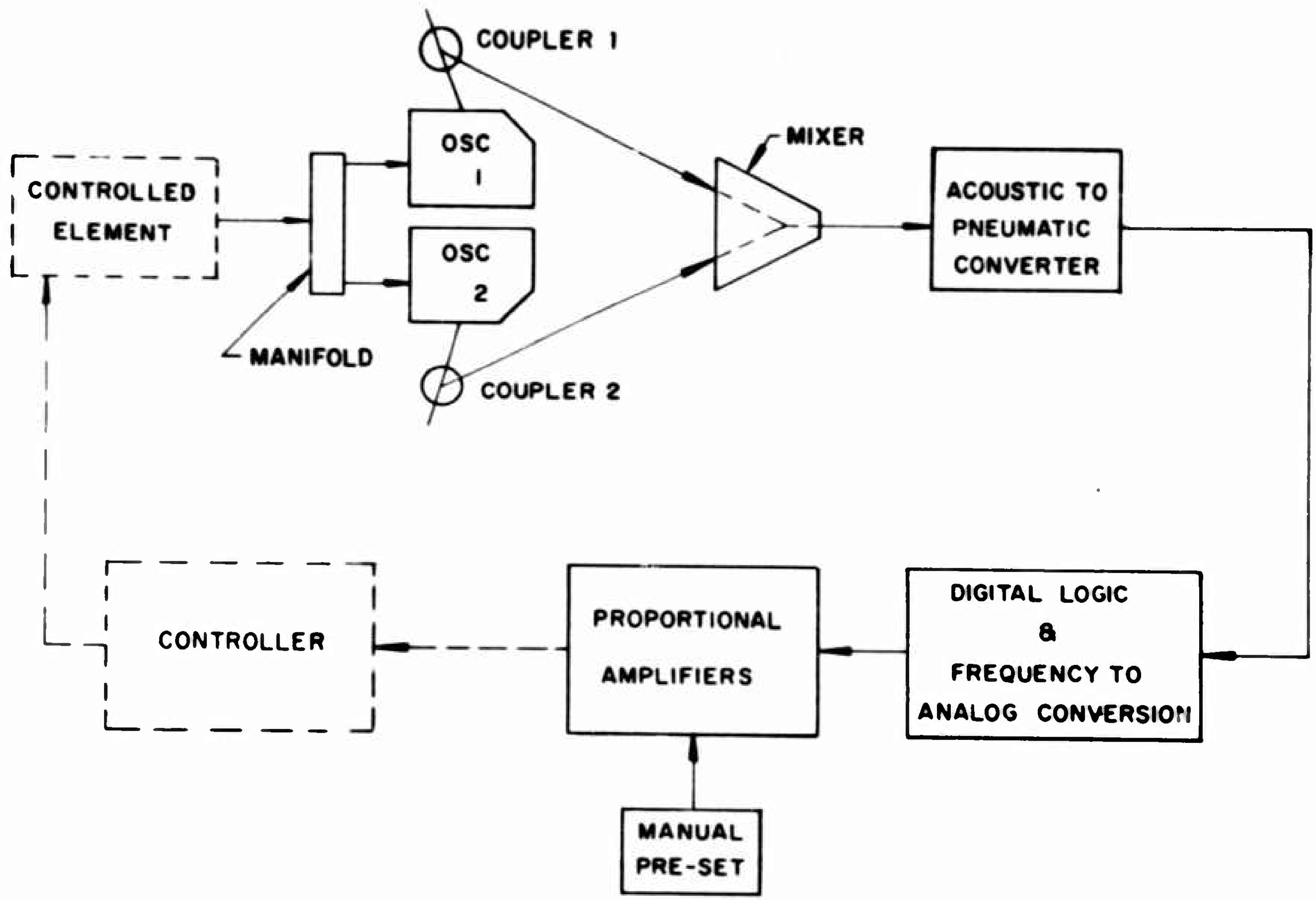

PROPORTIONAL TEMPERATURE CONTROL SYSTEM
FIGURE 1

The temperature then is sensed as a difference in frequency of the two oscillators. The difference in frequency of the oscillators as a function of temperature results from a difference in sensitivity. From reference 1, the change in frequency with temperature over a temperature range $\frac{\Delta f}{\Delta T}$ is given for a particular oscillator by

$$\frac{\Delta f}{\Delta T} = \frac{f_o}{T - T_o}\left[\left(\frac{T}{T_o}\right)^{1/2} - 1\right] \qquad (1)$$

It can be seen from this expression that the sensitivity over a range ΔT is a function of the frequency f_o at reference temperature T_o. To achieve a difference in sensitivity, the oscillators were designed to oscillate at a difference of 35 cps at 21°C. The cavity length required for each oscillator to produce its assigned frequency was determined from

$$f = \frac{(\gamma RT)^{1/2}}{4\ell} \quad \text{(ref 1)} \qquad (2)$$

where

R = gas constant for gas of interest
γ = ratio of specific heats
ℓ = cavity length

The difference in frequency as a function of temperature is determined by

$$f_1 - f_2 = \frac{KT^{1/2}(\ell_2 - \ell_1)}{\ell_1 \ell_2} \qquad (3)$$

where

f_1 = frequency of oscillator 1
f_2 = frequency of oscillator 2
$K = \frac{\sqrt{\gamma R}}{4}$

and ℓ_1 and ℓ_2 are the lengths of the cavities of the oscillators. A general relationship between the frequencies of the oscillators and temperature is shown in figure 2.

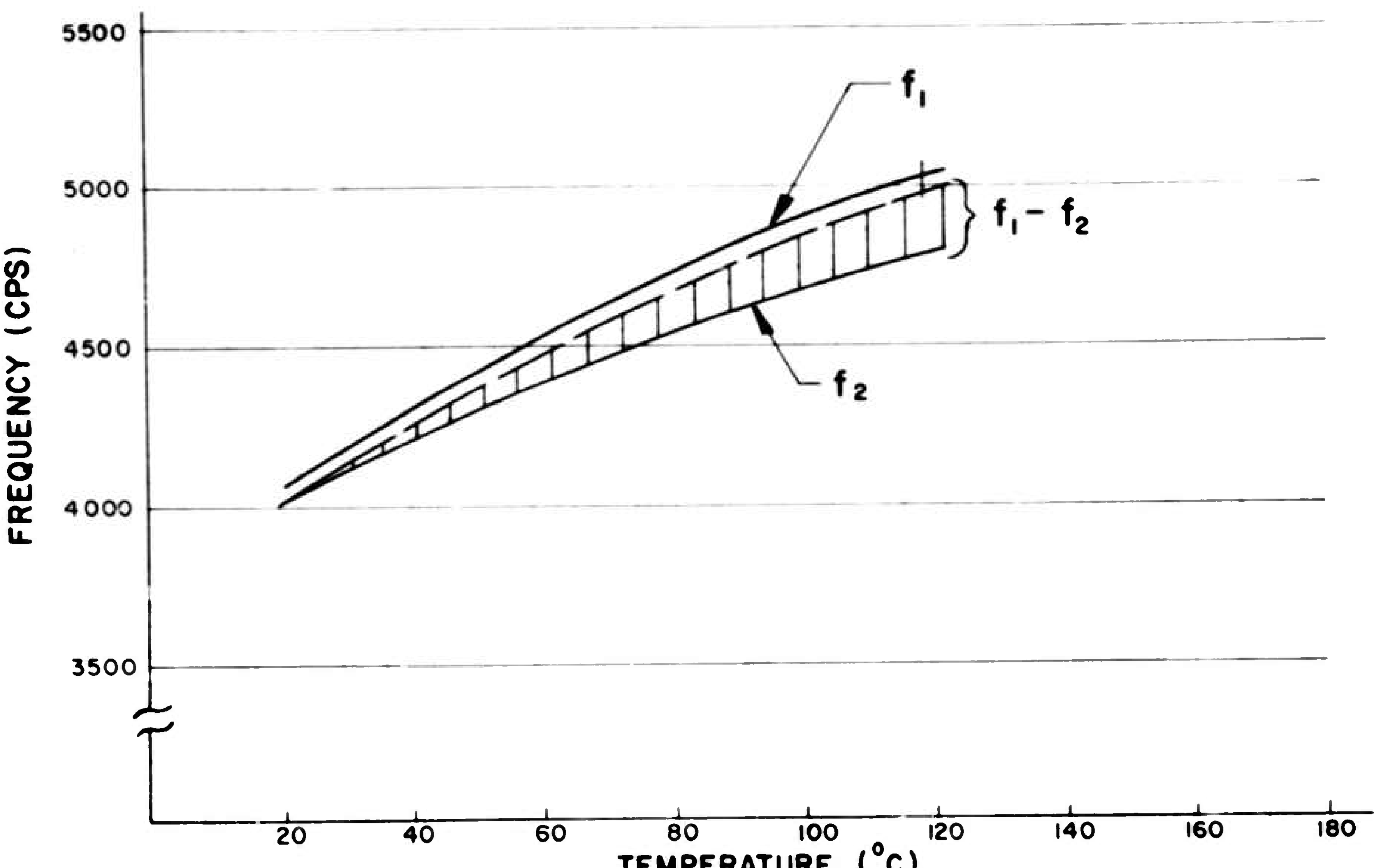

FREQUENCY DIFFERENCE AS A FUNCTION OF TEMPERATURE

FIGURE 2

2.2 Coupler

The coupler is shown in figure 3. This device "extracts" the oscillator signal (ac) from the combined signal (ac + dc) out of the oscillator. It is desirable to admit no d-c flow from the oscillator to the acoustic-to-pneumatic converter. This d-c flow, of course, would bias the converter and affect its output. The d-c flow extracted with the a-c signal was hardly measurable. The amplitude of the extracted a-c signal was a function of the supply pressure to the converter. For our case it was in the range of 10 to 30 percent of the amplitude of the signal from the oscillator.

2.3 Mixer

The mixer is shown in figure 4. Its purpose is to provide a region for mixing or adding the acoustic signals from the oscillators, to produce the difference frequency (fig. 2) on which the system functions.

2.4 Converter

The converter (fig. 5) converts the beat frequency from the mixer to a pneumatic signal of equivalent frequency. This means that the converter generates pneumatic pulses at a frequency that is a function of temperature as given in equation (3).

2.5 Frequency-to-Analog Conversion

The frequency-to-analog conversion system (fig. 6) comprises two distinct parts: (1) the digital logic setup (two digital amplifiers and a NOR unit), which puts out a pulse of constant duration and fixed amplitude for each input to the logic system, regardless of the frequency of the input pulses; (2) a tank to level out the pulses to a constant (d-c) flow and several stages of proportional amplification to increase the power of the d-c flow to a useable magnitude.

The input, (1) in figure 6, consists of the oscillatory pneumatic signal from the converter. The output of the first amplifier is a square wave with frequency equal to that of signal 1. Signal 2 is divided, with one signal (3) being utilized as the input of a passive NOR element. The other part of signal 2 (shown in figure 6 as signal 4).is used to control the second amplifier, which is used to provide a delay. The output of the second amplifier (signal 5) is utilized as the control of the passive NOR element. Since this control should be of small amplitude, signal 4 is made small by utilizing a large

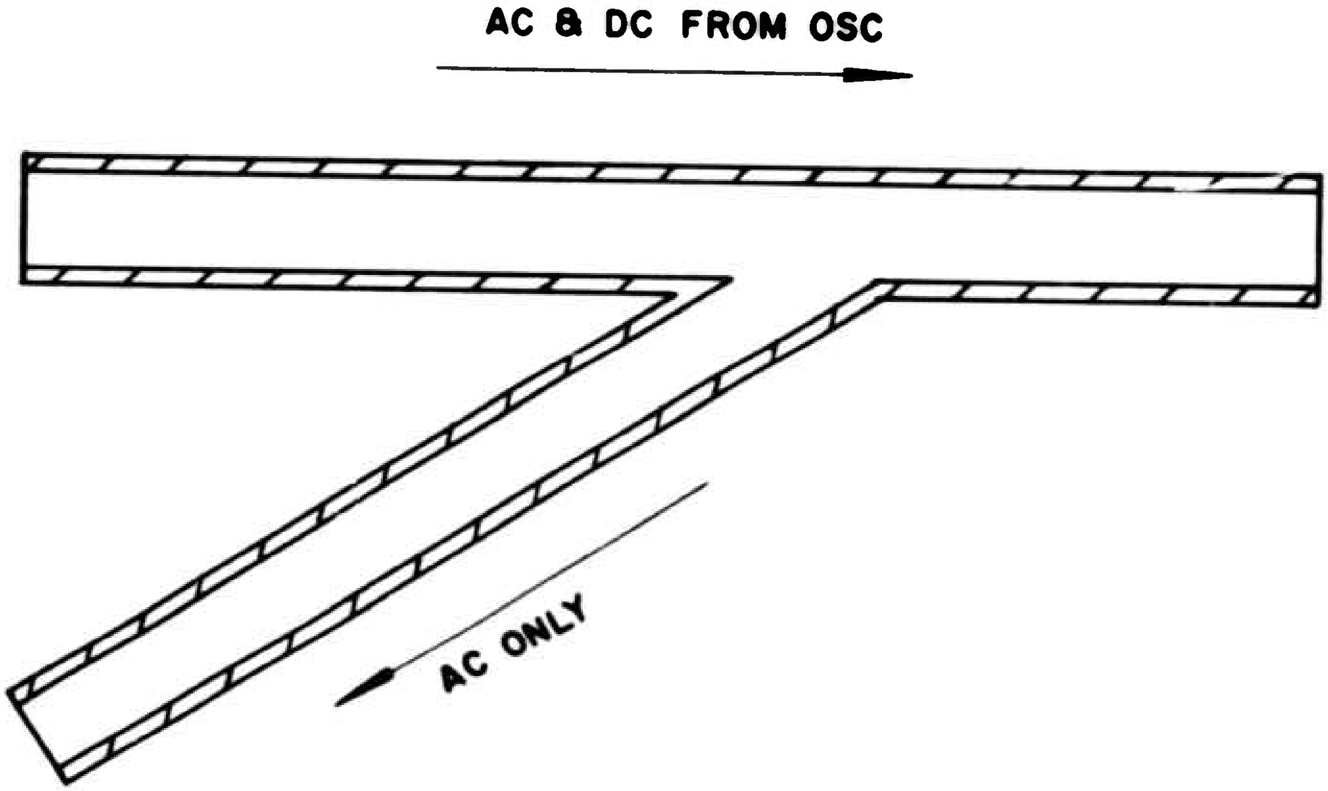

COUPLER
FIGURE 3

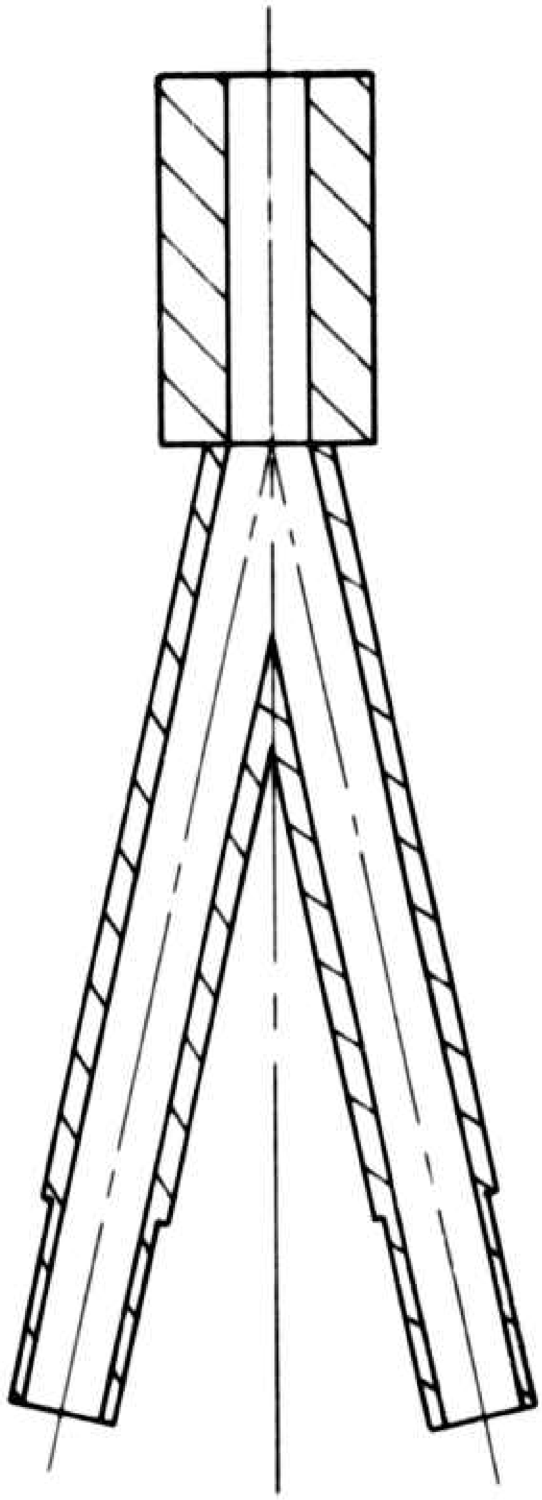

MIXER
FIGURE 4

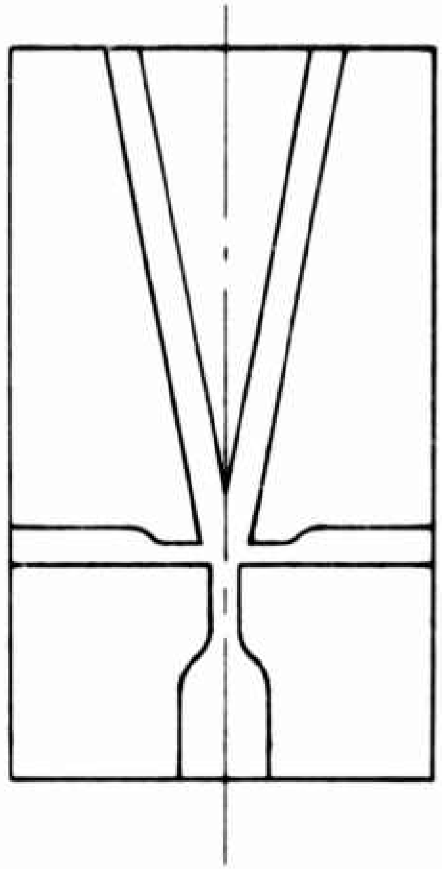

ACOUSTIC-TO-PNEUMATIC CONVERTER
FIGURE 5

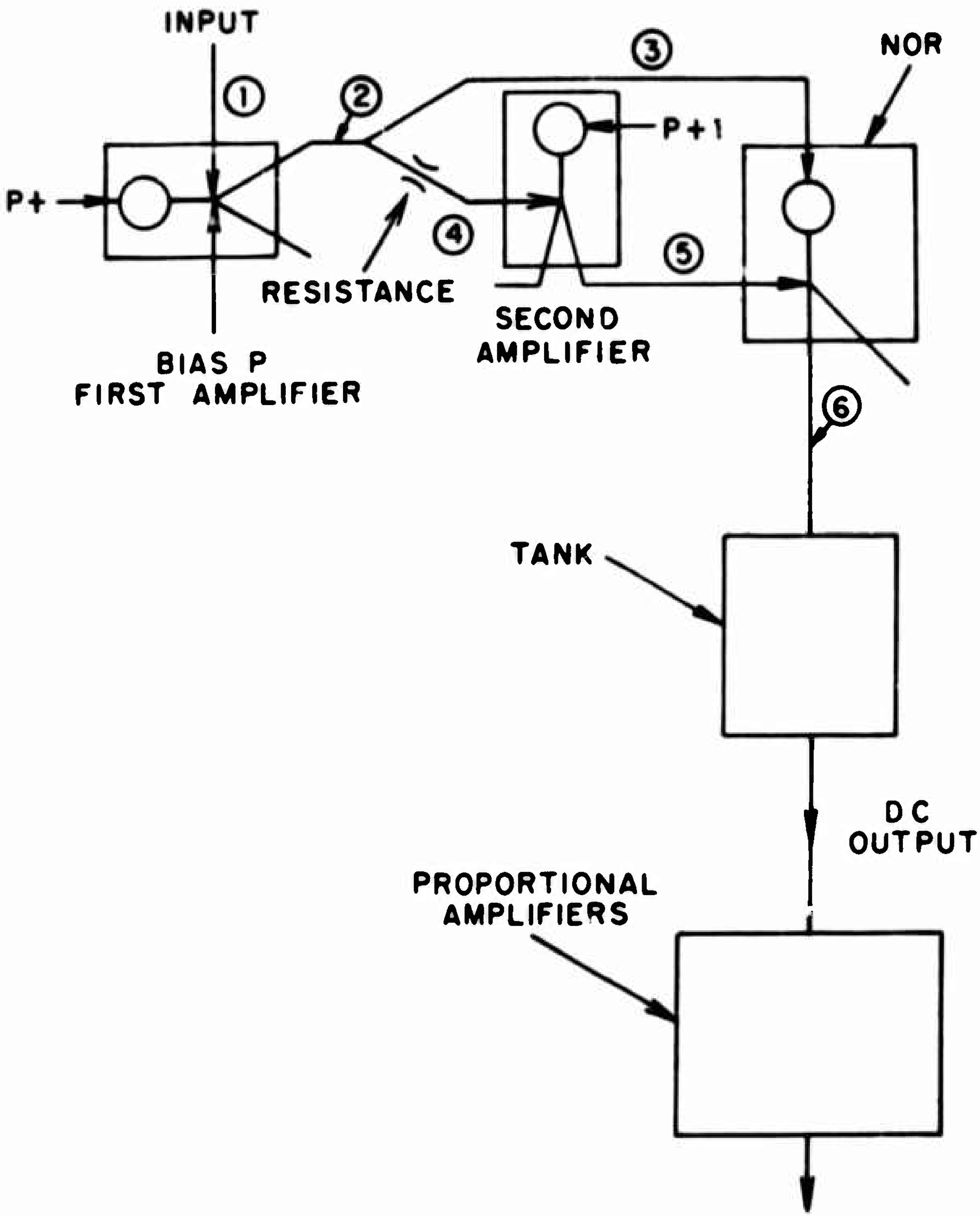

Figure 6. Frequency-to-analog conversion system.

resistance as shown in figure 6. The tank smooths out the output of the passive NOR, resulting in a d-c signal whose amplitude depends on the frequency of signal 1.

The time difference between signal 3 and 5, τ, is constant, since it depends entirely on the time response of the second amplifier. The amplitude of signal 3 (designated A) is constant since it is a function of P+ (input pressure to the first amplifier) and the resistance as previously described. Thus if f is the frequency of signal 1, the d-c level from the tank will be ideally $fA\tau$. Attenuation and losses due to the passive NOR unit will result in a somewhat smaller signal, which is proportional to $fA\tau$.

If τ is small, the magnitude of the d-c signal from the tank is small. Since a passive NOR unit is used, losses in pressure make A small also. Thus this d-c pressure is small. Therefore to utilize the the signal in an application where power is essential, stages of proportional amplification are required.

2.6 Amplifying Network

As shown in figure 1, the preset point is located in the amplifying network. This preset point is the bias control of the first stage of proportional amplification. By adjusting this bias, control begins at a predetermined temperature, without affecting the difference frequency of the two oscillators.

3. DESIGN CONSIDERATIONS

The proportional temperature control system was developed from components that were available at HDL and did not necessarily yield the optimum overall system performance. Observation of the system performance indicated, however, which design considerations are more important in general.

In a practical application of the system, the most important characteristics are: system sensitivity, frequency response, control range and system output.

These are dependent on the individual components. Sensitivity and control range are directly related; and both are governed by the maximum frequency response of the system. The effect of these characteristics on the system will become apparent from a separate discussion of each.

3.1 System Sensitivity

The system sensitivity is designated as the change in difference frequency, $f_1 - f_2$, with respect to change in temperature. An indication of the effect of design variable manipulation on sensitivity

can be seen from the relationship of design and operational parameters in equation (4).

$$f = \frac{KT^{1/2}}{\ell} \tag{4}$$

The sensitivity of a single oscillator at any temperature is

$$\frac{df}{dT} = \frac{K}{2\ell T^{1/2}} \tag{5}$$

The system sensitivity is then the difference in the sensitivities of the two oscillators.

$$\frac{df_1}{dT} - \frac{df_2}{dT} = \frac{K(\ell_2 - \ell_1)}{2\ell_1 \ell_2 T^{1/2}} \tag{6}$$

It can be seen from equation (6) that the system sensitivity may be varied by manipulating ℓ_1 and ℓ_2. It can be seen also that the sensitivity is inversely proportional to the one-half power of temperature, so the temperature range over which the system operates affects the sensitivity.

The maximum sensitivity the system can utilize depends on the temperature range and the frequency response of the system. Since the frequency difference increases with temperature, the sensitivity should be adjusted to accommodate the maximum temperature the system will experience.

3.2 Frequency Response

The frequency response of the system is governed by the response of the digital logic system. The devices in this portion of the system are available with 300-to-400 cps response capability.

3.3 Control Range

Given two oscillators of cavity length ℓ_1 and ℓ_2, the control range can easily be determined from the equation

$$T^{1/2} - T_o^{1/2} = \frac{\ell_1 \ell_2}{K(\ell_2 - \ell_1)} \left[(f_1 - f_2)_T - (f_1 - f_2)_{T_o} \right] \qquad (7)$$

where T is the maximum temperature to be controlled, T_o is the initial control temperature, $(f_1 - f_2)_T$ is the difference frequency at T, and $(f_1 - f_2)_{T_o}$ is the difference frequency at T_o. These difference frequencies must be made compatible with system sensitivity and response requirements.

The controlled range can be made extremely broad by an appropriate choice of ℓ_1 and ℓ_2. Control of temperatures to well over 1000°C is feasible as can easily be shown by the use of equation (7).

The preset point can be utilized to reduce the maximum range of control as was previously discussed. The lower temperature limit T_o can be adjusted by adjusting this preset point.

3.4 System Output

The system output (pressure or flow) is determined by three major factors: (1) the output of the acoustic-to-pneumatic converter; (2) the characteristics of the digital logic system; and (3) the gain of the stages of the proportional amplifying network.

The output of the acoustic-to-pneumatic converter can be regulated by varying setback and splitter distance. These can be adjusted to yield a maximum output for a given applied acoustic signal. Obviously, the separate units of the digital logic system and the amplifying network should also be adjusted for maximum gain, to increase system gain.

4. TEST RESULTS

Laboratory tests were conducted to determine the practicability of a fluidic temperature control system and to compare experimental results with theoretical considerations. The tests were conducted to 120°C using the system just described.

Figure 7 shows the frequency variation with temperature from 21° to 120°C; $f_1 - f_2$ is the difference frequency of the two oscillators over the same temperature range. This difference frequency was also monitored by observing the pulse frequency out of the digital logic system.

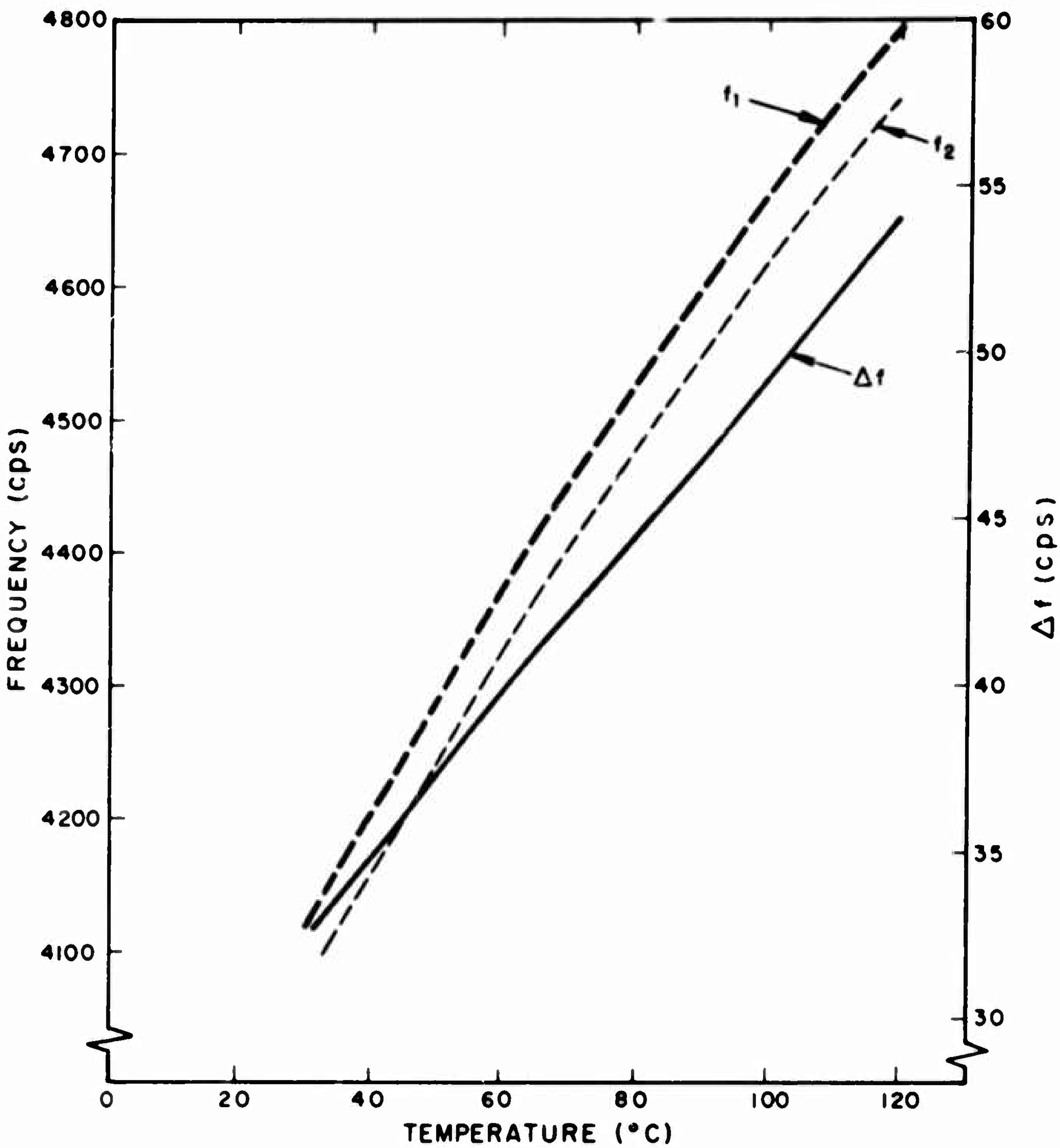

Figure 7. Oscillator frequencies and difference frequency as a function of temperature.

Theoretically, the frequency of each oscillator can be determined using equation (2). However, experimentally, the frequency did not vary as the 0.5 power of temperature. Results show that the exponents were 0.553 and 0.537 for the higher frequency and lower frequency oscillators, respectively. Theoretically, $f_1 - f_2$ at 120°C should be 38 cps, but because the oscillator with the higher exponent had the higher sensitivity, $f_1 - f_2$ increased from 32 to 56 cps over the total range of temperatures tested. Exponents greater than 0.5 are attributed to the circulatory flow in the oscillators, which results in a pulse speed greater than that given by equation (2).

Figure 8 is a plot of the differential pressure (blocked output) at the output of the last proportional amplifier as a function of the temperature. This difference pressure was nearly directly proportional to the difference frequency.

Additional tests were conducted to determine the range of operation of the converter. The results quoted are representative of one system tested. The results varied with changes in impedance and input pressures. The resistance shown in figure 6 was adjusted to obtain the maximum analog output. Any variation in this resistance will reduce the output flow and pressure.

Figure 9 shows oscilloscope traces of the acoustic beat input and the digital system output. Reflections occur in the digital pulses as shown in the figure.

Figure 10 is a plot of the differential pressure output of the last stage of the four-stage proportional amplifier as a function of the difference frequency. The output was linear from 30 to approximately 95 cps. For beat frequencies above 95 cps, the digital logic system skipped pulses, since the response of the digital units used was approximately 95 cps. Thus the output leveled off and then dropped as the input frequency was increased further.

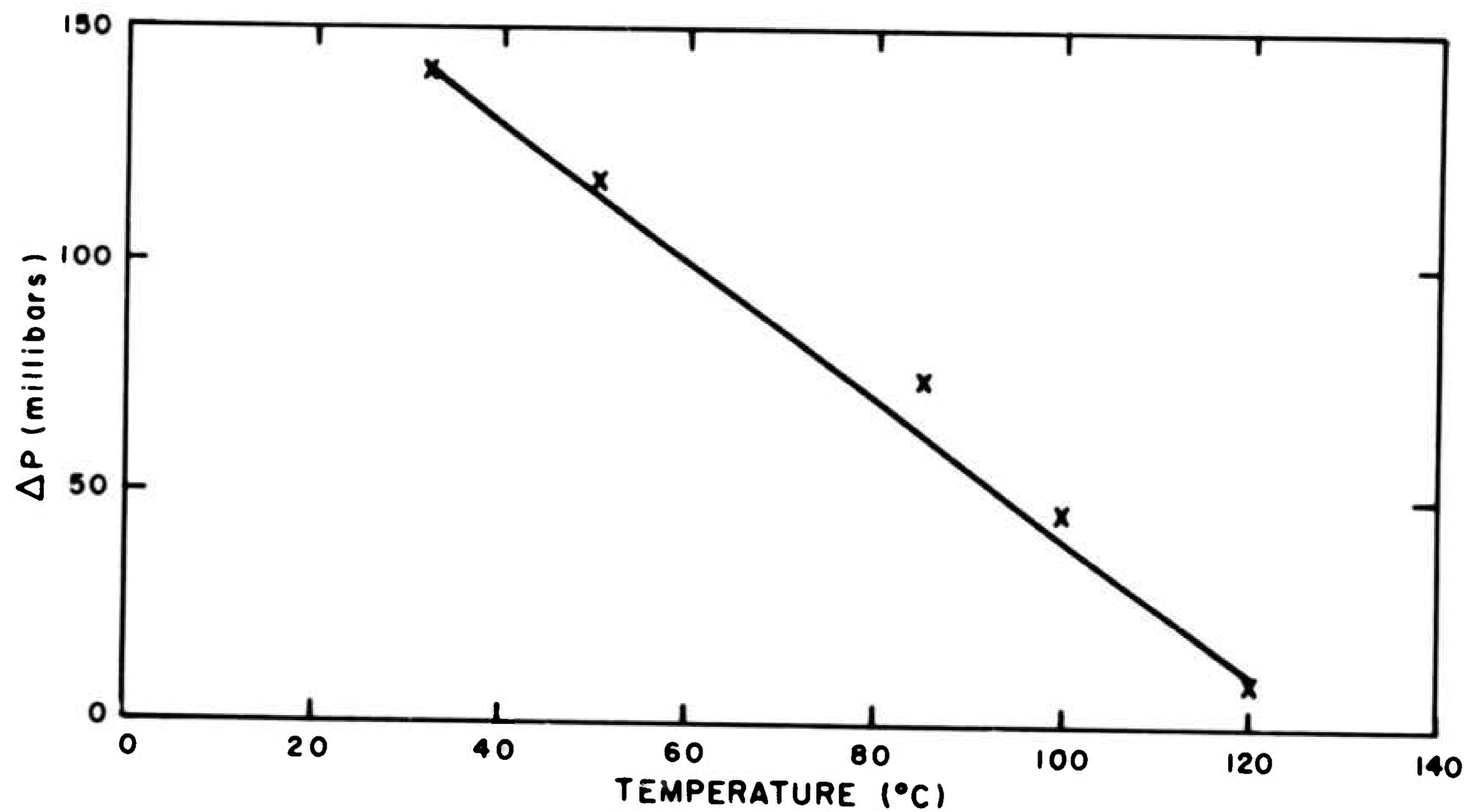

Figure 8. Difference pressure output as a function of temperature.

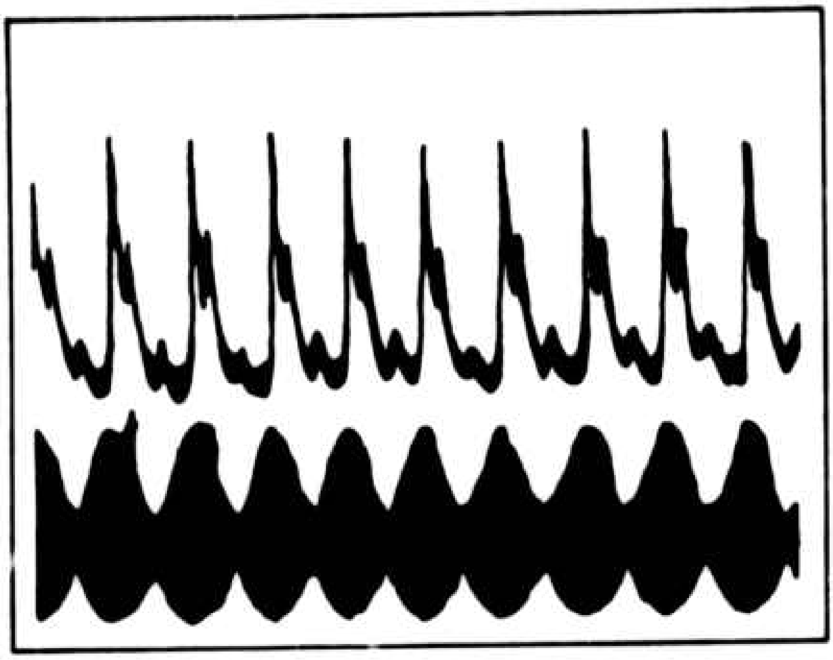

Figure 9. Oscilloscope Traces.

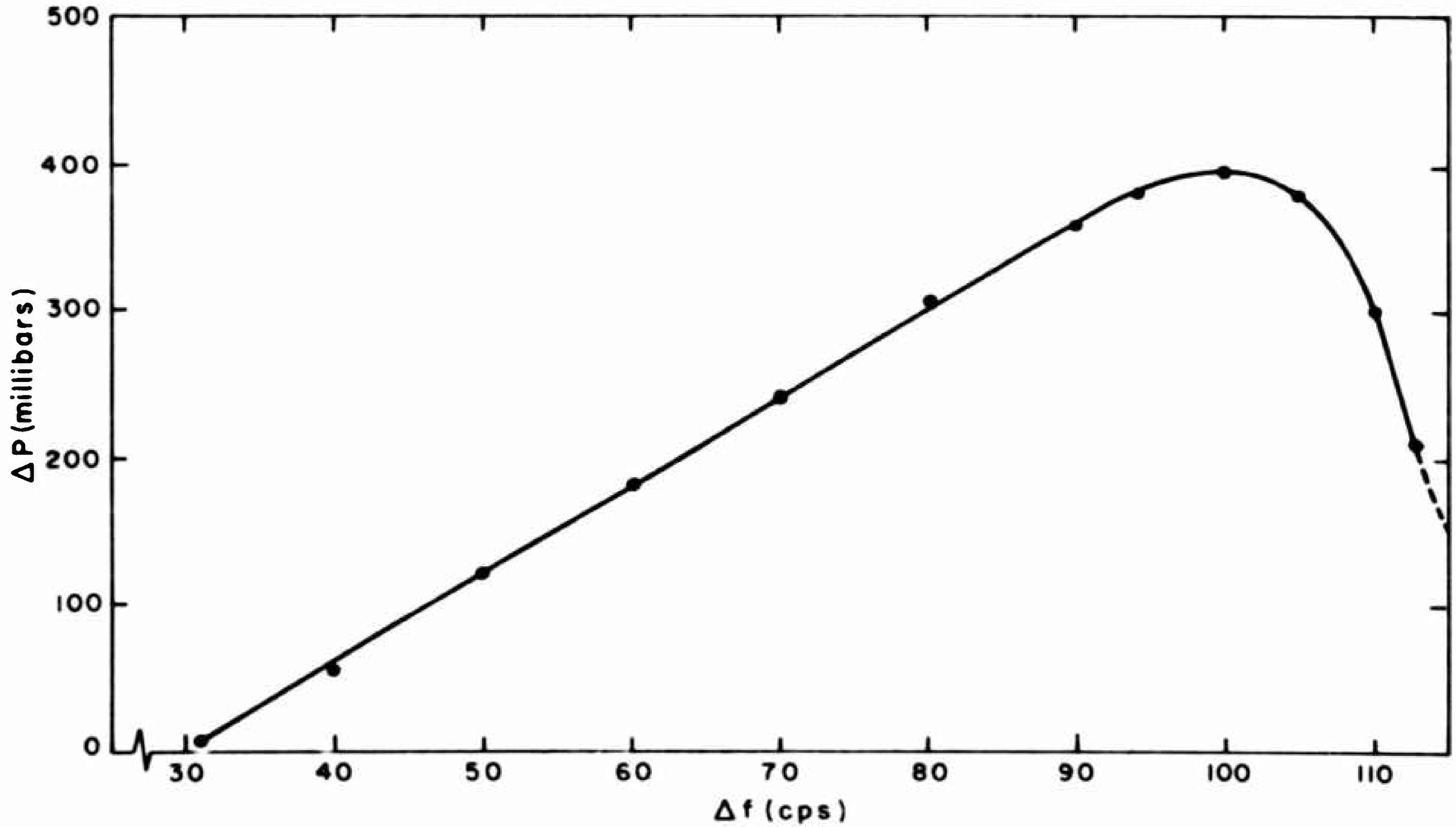

Figure 10. Frequency-to-analog conversion differential pressure output as a function of the difference frequency.

5. CONCLUSIONS

A proportional temperature control system has been assembled at HDL using fluidic logic elements and proportional amplifiers. The output of the system is a differential pressure that is a function of the temperature of the input gas to the oscillators. This no moving-mechanical-parts system is rugged and simple. To maintain generality, no emphasis has been placed on the controlled mechanism. The output could be utilized to perform a number of functions, such as controlling a hydraulic valve, a fuel valve, or reactor arm.

The system tested was limited to a low (100-cps) frequency response. Since existing hardware was utilized to build this system, no emphasis was placed on optimizing the individual units. This limitation would not exist if digital elements with high frequency response were utilized.

As shown in equation (6), the system sensitivity decreases with increasing temperature. This sensitivity can be increased significantly for a given control range by increasing $f_1 - f_2$. Another interesting phenomenon that increases the system sensitivity became apparent during the tests. The temperature exponents given as 0.5 in equation (6) were in fact not 0.5 but of slightly higher value and were different for each oscillator. As reported in section 4, one exponent was 0.553 and the other was 0.537. If the higher exponent oscillator is used as f_1 (the higher frequency), the sensitivity is increased since the difference frequency is greater than the theoretically calculated value. Thus, as shown in figure 8, Δp as a function of temperature is nearly linear.

The system should be tested to higher temperatures before the exponents can be determined accurately. Tests should also be conducted to determine the method by which these exponents can be manipulated.

Another method that will enhance the sensitivity is the use of a constant frequency oscillator that may or may not be pneumatic. After having assumed a desired temperature range, $(f_1 - f_2)_{T_O}$ is chosen so that the maximum $(f_1 - f_2)_T - (f_1 - f_2)_{T_O}$ can be obtained. Thus the sensitivity of the system will be the same as that of the temperature controlled oscillator. This, however, will limit the range of control, since, as stated previously, $(f_1 - f_2)$ cannot exceed 400 cps.

REFERENCES

1. Gottron, R., and Gaylord, W., "A Temperature Sensing Pneumatic Oscillator," TR-1224, Harry Diamond Laboratories, 4 May 1964 (Confidential).

2. Gaylord, W., and Gottron, R., "Design Considerations of the HDL Pneumatic Temperature Sensor," TR-1273, Harry Diamond Laboratories, 10 Feb 1965 (Confidential).

FLUID TIMER DEVELOPMENT

S. B. Martin - Sandia Corporation

E. R. Phillips - Univac, Division of Sperry Rand Corporation

INTRODUCTION

A fluid timer has been developed by UNIVAC, Division of Sperry Rand Corporation to the specifications of Sandia Corporation. A preliminary report of this development was presented at the 1964 Fluid Amplification Symposium.[1] Development has resulted in an integrated modular design which utilizes no tubing interconnections. Major functional modules are assembled to a combination manifold and base plate which contains all channels necessary to interconnect the modules. This feature makes possible a compact unit with efficient space utilization which is environmentally rugged. This timer was designed to operate from -65°to +165°F and to meet typical shock and vibration requirements.

A photograph of the timer is shown in Figure 1.* A fluid-mechanical oscillator provides the time base. All counting and logic functions are performed by pure fluid digital circuits. A total of 35 active elements and 85 passive elements are used. The timer has two variable-time channels which may be preset with a selector switch from 10 to 59 seconds in 1-second increments. Four fixed-time outputs of 0.20, 0.82, 1.00, and 1.37 seconds are also provided. Output of the timer is the closure of normally open electrical contacts.

At the time of submittal of this paper, three units are in various stages of assembly. Compatibility of major subassemblies has been established, but final testing of the complete components remains to be done.

---

1 "Development of Two Pure Fluid Timers," by G. V. Lemmon and E. R. Phillips, Proceedings of the Fluid Amplification Symposium, May 1964, Vol. II, P.481, ff.

*Figures appear on pages 279 through 287.

II. LOGIC

A digital interval timer requires a time base or frequency source, a counter, a mechanism to select the desired time, a method of starting the timing function, a decoder to determine when the desired time has elapsed, and an output device.

The logic of the present fluid timer is based upon flip-flops, amplifier-inverters, passive AND gates, and passive OR gates. A block diagram of the logic circuit is shown in Figure 2. III

The clock to provide the necessary stable time base is a fluid oscillator synchronized by a torsional spring-mass system. The 32-cps output of the clock drives a 12-stage binary counter. Each stage of the binary counter is designed to give an initial "zero" output when power is applied. Timing begins when power is supplied to the unit. Thus, Binary Counter (BC 1) will initially turn to the "one" state at 1/32 second, BC 2 at 1/16 second, BC 3 at 1/8 second, etc. This system is followed through BC 9, which turns to the "one" state at 8 seconds. However, BC 10 is initially turned to "one" at 10 seconds to allow use of a setting switch with a units and a tens selector. A decade converter is used to convert the pure binary number to a binary-coded decimal number. Basically, the decade converter drives BC 7 at the normal 1/2-cps rate of BC 6 until 8 seconds have elapsed. Between 8 and 10 seconds, the decade converter drives BC 8 at 2 cps. Thus, the first nine counter stages are recycled every 10 seconds to provide the units signal. The last three stages, which initially give outputs at 10, 20 and 40 seconds, respectively, provide the tens signal.

Decoding is a multiple AND logic function. The outputs of the proper binary counters are ANDed together to give the desired outputs to set memory flip-flops. The memory flip-flops convert the pulsed outputs of the decoder into steady-state outputs. These steady-state outputs actuate pressure switches to close electrical contacts. It is a simple matter in the case of the four fixed-time channels to permanently interconnect the proper counter outputs. However, in the case of the two variable-time channels, the interconnection problem is more complex. The outputs of BC 6 through BC 12 are individually ORed with an output from the selector switch for each channel. The selector switch is essentially a group of valves which control flow from the

supply manifold. Flow is supplied from the selector switch to each OR gate whose corresponding binary-counter input is not included in the desired time setting. The seven ORed signals are then ANDed to give an output when the desired combination of binary counters is in the 1 or ON state. The output from the series of AND gates is amplified to actuate the output memory. The two variable-time output memories are interlocked using an OR and an AND gate so that Channel A always actuates before Channel B.

III. OSCILLATOR

The Sandia Timer developed by the UNIVAC Division of Sperry Rand Corporation is used to indicate the passage of a predetermined time interval by means of counting the pulses from a fluid oscillator. Since the accuracy of the time interval depends on the constancy of the pulse rate, a device (see Figure 3) for controlling the frequency of the pulses was added to the basic fluid circuitry.

This device, which is essentially an oscillating mass-spring system whose period of oscillation is dependent on the value of the mass and spring rate, nullifies the effects of varying pressures and temperatures on the simple pure fluid oscillator. By use of the proper materials, the mechanical properties of the system remain approximately constant with varying temperature and pressure. The mass oscillating at the system's natural frequency interrupts a fluid jet and produces in turn fluid pulses occurring at precise intervals. In this case a torsional mass-spring system (Figure 4) was chosen because of its relative immunity to vibration.

This simple oscillator could have been employed directly to drive the counter assembly but because of the possibility of vibration and shock affecting the mechanical system, it was decided to use the output pulse as a synchronizing signal for the pure fluid oscillator. So long as the mechanical system is oscillating, the pure fluid oscillator will oscillate at the same frequency as the mechanical system. However, should the mechanical system fail, the pure fluid oscillator will continue to operate and drive the counter assembly. When operating without synchronizing pulses, the pure fluid oscillator operates at a pulse rate determined by the gas temperature and pressure. It is the fluid oscillator output, not the fluid

output of the mechanical system, that drives the counter assembly and produces the power to operate the mechanical oscillating system. (Refer again to Figure 3.)

The signal from the clock, or oscillator, assembly is a two-phase pulse operating at 32 pulses per second. The pure fluid oscillator operating at this frequency requires 0.6 cubic inch of space. The synched oscillator allows the Timer to perform within the time accuracy specified with inlet pressures ranging from 2.0 to 6.0 psi.

Testing on a breadboard assembly of the fluid oscillator synched with a torsional oscillating mass indicated only a 0.3-percent drift in frequency over a temperature range of 155°F.

IV. BASIC FLUID ELEMENT

A fluid bistable element or flip-flop was chosen as the fundamental fluid element because of its many advantages where a counting function is to be performed. Since a bistable device possesses memory, fewer elements are required for performing the counting function, and this conserves power and package space. This basic element was utilized exclusively in the fabrication of the counter assemblies and decoding logic circuits.

The power nozzle of the flip-flop is 0.014 inch wide by 0.022 inch deep and operates with supply pressures ranging from 1 to 5 psi. The basic device was developed with a two-input AND gate driving signal inputs on each side of the power jet. The AND gates are designed to incorporate isolation, and the presence of only one signal at either input to the AND gate has no effect on the power jet of the flip-flop and will not load the "OFF" AND gate input, a characteristic which allows for simple, trouble-free interconnection. The AND gate nozzles are 0.008 inch wide by 0.022 inch deep and are the smallest nozzles found in the Timer. A sketch of the flip-flop with AND gate inputs is shown in Figure 5.

The device has a maximum "fan-out" of eight devices from either output channel which results in a pressure gain at this loading condition of more than 2. Pressure gain is defined as the output pressure divided by that pressure at the inputs of the AND gate

necessary to cause the flip-flop to change state. Thus the gain figure quoted includes the loss incurred in the passive AND gate. If the passive gate and accompanying venting are eliminated, the pressure gain can approach 20 with a fan-out of 5. The high fan-out capabilities and resulting gain margin make the device extremely attractive where space utilization and minimum power are paramount.

One important result of the flip-flop program to date has been the excellent manufacturing yield. Circuit plates with several dozen elements will not be possible unless the basic element can be reproduced with high yield. It is obvious that circuit plates cannot be reproduced economically if the basic device itself has, say, only an 80 per cent yield. To date, UNIVAC has used production equipment, operated by production personnel, to mold over 1000 flip-flops from the same die without a single defective flip-flop. These results indicate that if consideration of the manufacturing process is factored into the design of the digital element, excellent reproducibility can result. While the data are not conclusive, the indications are that complicated circuit planes, employing high performance fluid elements, can be molded on standard production presses and that extremely low cost fluid circuits can be manufactured.

V. THE BINARY COUNTER CIRCUIT

The binary counter circuit makes use of two flip-flops each employing two input AND gates. (See Figure 6.) The circuit design is such that no delays are required and, consequently, pulses of any duration can be accepted. The performance of the circuit with regard to fan-out and gain makes intermediate amplifiers between stages unnecessary.

Basically, the purpose of each of the two flip-flops in a counter stage is to serve as a memory device for the other. While one flip-flop is switching, the other flip-flop provides the memory necessary for eliminating the customary timing problem. The size of a binary counter stage is 1.7 inches by 3.0 inches by 0.060 inch. It is probable that a 50-per cent reduction in counter volume can be achieved by improved space utilization.

A typical six-stage counter was tested to determine the maximum oscillator frequency for use in the Timer application.

Figure 7 shows an oscilloscope photograph of a six-stage binary counter stack responding to an input frequency of 500 pulses per second. The sweep is actually the electrical summation of the outputs of both the second and sixth stages. The sine wave is a 60-cps reference signal. The maximum frequency has yet to be determined, but it is assumed that the maximum frequency will be less than 1000 pps.

VI. VARIABLE TIME SELECTION CIRCUIT

Of the 6 time channels within the timer, 2 channels may be preset to any time from 10 to 59 seconds. Figure 8 shows schematically how this is accomplished. The decoding occurs in what is called the Variable Decode plate, which is a series of AND-OR devices in cascade. For an output to exist, a signal must be present at either of the inputs to each of the seven OR gates. Thus, at least seven inputs are needed to produce an output. The inputs to the OR gate can come from either the binary counter assembly or the Selector Switch. Each of the seven OR gates is associated with one binary increment, that is, 1 sec., 2 sec., 4 sec., 8 sec., 10 sec., 20 sec., or 40 sec. If the number 10 is to be decoded, the fluid inputs to the Variable Decode for the numbers 1, 2, 4, 8, 20, and 40 will originate at the manual Selector Switch and are present from time zero. The number 10 (10 sec.) signal will be generated by the Binary Counter Assembly. When the Binary Counter Assembly produces the number 10, all seven inputs will be present (six from the Selector Switch and one from the Binary Counter), and an output will be produced. Similarly, the number 59 would require inputs originating in the Binary Counter Assembly for the numbers 40, 10, 8, and 1, which total 59. The remaining three signals, 2, 4, and 20, would be produced by the Selector Switch. The Selector Switch inputs are manually preset by adjusting the switch thumb wheels prior to starting the Timer.

The Selector Switch also performs a decade-to-binary conversion; the wheel readout is represented in typical decade fashion, but the fluid signal from the switch is applied to the Variable Decode plate as a binary signal.

Since the mechanical equipment within any fluid circuit presents the greatest reliability problem, an effort was made to obtain the best fluid valving scheme for the Selection Switch. A

moving disc or card which relies on the sealing of a passage or hole appeared least desirable since sliding would be necessary and contamination could occur. Sealing between the sliding part and the hole could also represent a problem in miniature circuits where near zero leakage would be required. Therefore, a non-contacting jet interrupter scheme was finally chosen; this scheme involves merely opening or closing a jet traveling between a nozzle and a recovery hole. The interrupter operates freely without contacting either the nozzle or the recovery hole.

Two identical circuits within the Timer provide two separate variable time channels. Both channels are driven by the same binary counter output, and either channel may be set to any number from 10 to 59 seconds. Figure 9 shows a photograph of two Selector Switches (one for each channel) fabricated within the same housing. It is necessary to include one Variable Decode plate for each time channel.

VII. FIXED TIME DECODING

Of the six time channels, four of these, labeled the Fixed Decode Channels, are not adjustable; the decoding logic is permanently interconnected. These four fixed times (in seconds) are 0.2, 0.82, 1.0, and 1.37. Figure 10 shows the logic necessary for decoding the four channels. Maximum use was made of the standard AND-drive flip-flop with the exception of one three-input AND flip-flop. Each of these flip-flop elements also served as a memory for each of the time channels, and once the logic is complete, each flip-flop switches and remains switched. When switched, each of the four flip-flops in the Fixed Decode energizes a pressure switch; this action is the ultimate function of all the fluid time channels.

VIII. START-UP AND CLEAR

Since the Timer must begin at time zero with a count of zero, each element in every counter stage must turn on to the zero state. This may be accomplished by introducing a separate clear signal which "forces" the elements to start-up in the proper state. This approach would require considerable circuitry and power to "clear" the 12 binary counter stages, which total 24 elements.

This Timer was developed by use of a clear technique which requires no separate clear signals. While the flip-flops are geometrically symmetrical and do not prefer one side or the other, it was found that control of the downstream geometry, mainly the resistance and capacitance as seen by each flip-flop output leg, can cause the device to switch to the state desired when power is applied (see Figure 6). The Timer, as designed, reliably clears to the zero state during start-up, and no auxiliary circuits or elements are required.

The start-up and resulting "clear" do not require any special type of turn-on procedure, and all bistable elements in the Timer clear automatically when power is applied.

The present design of the binary counter stages prevented 100-percent incorporation of this approach in the current Timer hardware. The stages now provide this method of clearing for only the first flip-flop in each counter plate, i.e., only half of all the active elements. However, clearing this flip-flop does produce a clear condition on the second flip-flop due to the manner in which the interconnection is made. At the time of this writing on production-type counters with 16 elements, testing has yielded three to five errors per thousand starts. With the incorporation of the concept to all circuit components the turn-on reliability should be several orders of magnitude higher. Even with the clear applied to only the first flip of each stage, some counter circuits with 16 flip-flops have cleared without error for 2000 starts.

IX. BINARY TO DECADE CONVERSION

To simplify the construction of the manual Selector Switch, a conversion from a binary to a binary coded decimal count for counters BC 6 through BC 9 became advisable; as a result, the counter was separated into two sections, one section counting the units and the other producing the tens. For counters arranged in this manner the count could be decoded by observing simultaneously the unit counters (0 through 9) and the tens counters (10, 20 and 40) and then by adding the units to the tens.

A normal binary counter will count from 0 to 15 and will require four counter stages. To convert a binary four-stack

to a decade four-stack, it is merely necessary to force all four stages to the 1 or ON state just prior to the count of 10. After counting to 10 (actually, the decade counter in the Timer has counted to 320 oscillator pulses prior to recycling), the units counters revert to the zero or clear state.

Figure 11 shows the necessary logic to accomplish the conversion. Essentially, counters BC 7 and BC 8, representing the counts of 2 and 4, respectively, are cycled at four times the normal rate between the 8 count and the 10 count to allow all the counters to be in the 1 or ON state just prior to a normal count of 10. To do this, either of two gate circuits can drive counters BC 7 and BC 8. One circuit represented by AND-AMP device No. 1 is driven by the 1 counter (BC 6) between the 0 and 8 counts. The gate in this instance is the zero side of the counter BC 9, which represents the 8 count. At the count of 8 the gate changes from AND-AMP device 1 to AND-AMP device 2 by gating with the 1 side of counter BC 9; thus, the gating merely depends on whether the count is above or below the count of 8 seconds, which is represented by the state of counter BC 9. Many schemes for binary to decade conversion exist; however, this scheme appears to be the most reliable from a timing consideration.

X. PRESSURE-ACTUATED ELECTRICAL SWITCH

The ultimate function of each time channel is the closing of a pair of electrical contacts. Considering the extremely low pressure signals available at the minimum Timer supply pressure, as well as shock, vibration, and temperature extremes, the design requirements for such a pressure switch became quite severe.

The hardware which resulted from the final design operated considerably beyond the requirements of the specifications and has become an extremely important research instrument as a digital indicator. The only moving element, a very thin, stretched membrane, 0.75 in.^{2}, contains the electrical contact. The other contact is adjustable with respect to the stretched membrane for setting the closing pressure. The switch is shown in Figure 12.

After assembly and test, the switches are encapsulated in epoxy, and no further adjustment is possible or required.

Switches have operated for billions of cycles with less than a 15-percent change in the pressure necessary to effect closing. One package of six switches was subjected to the complete specification test procedure, including temperature, shock, and vibration with a change in pressure of less than 0.5 inch of water required for closing the switch.

With regard to frequency response, the switches have been operated at a rate of 3000 pulses per second. The switches operate without detectable bounce. Operation with an electronic counter, where bounce causes considerable error, is an accurate readout technique.

XI. MANUFACTURING TECHNIQUES

All bistable elements were transfer-molded by use of production presses and were made from Diallyl Phthalate, a thermosetting plastic. The dies were made by standard milling techniques, and one die produced over 1000 elements without detectable change in the performance for the total number molded. The flip-flop was designed to allow maximum manufacturing tolerances and it was possible to build circuits and indiscriminately mix the flip-flops molded from three dies with excellent results. The minimum radius of all corners and dividers within the flip-flop geometry was 0.007 inch. The absence of sharp edges appears to allow digital circuits an ease of manufacturability not normally found in proportional-type systems. All circuit plates were fabricated by pantomilling on the molded flip-flop blanks the interconnections required. Templates were made for all pantomilling to reduce machining time.

The circuit plates were sealed by bonding the bottom of one plate to the top of another. As many as 12 plates were bonded in this manner in one assembly; usually all bonding for a 12-plate stack was accomplished at the same time. A typical stack is shown in Figure 13. Pressure and temperature were required for curing the adhesive, a thermosetting plastic. The adhesive was applied to the 12 plates making up the assembly and bond-cured simultaneously on all plates in a heated platen press. Results from the process were excellent with increasingly higher yields as the technique became perfected. Bonding of the 0.008-inch-wide nozzles represented no problem, and it was believed that 0.002 or 0.003-inch-wide nozzles could be bonded with similar results.

While the techniques which had to be developed proved quite satisfactory, areas for improvement exist with regard to better space utilization, more efficient power distribution, and more complete interstage isolation. With regard to packaging density, it appears certain that a 50-per cent reduction in space can be realized with more effective circuit design without reducing the size of the basic flip-flop element. However, because of the ease with which the flip-flops were manufactured, a reduction in the size of the flip-flop element also appears possible; this would ultimately lead to a considerable reduction in the package size.

XII. INTERCONNECTIONS BETWEEN MAJOR ASSEMBLIES

Each of the subassemblies, such as the fluid oscillator and fixed decode, was assembled into one of three stacks of circuit plates. One stack included the fluid oscillator, fixed decode, and binary counters 1 through 6. Once the stacks were assembled, it was necessary to channel signals from one assembly to other major assemblies and to supply all the stacks with fluid power. This was accomplished by the master manifold which is an assembly of four plates with all the necessary channeling and holes for interconnection and power distribution. Two plates of the manifold are shown in Figure 14; this manifold assembly also served as a mounting plate for the stacks and as the means for mounting the Timer. All assemblies, including the mechanical oscillator, the Selector Switch, pressure switch, and all logic stacks, were physically mounted to the master manifold.

XIII. CONCLUSIONS

Substantial advances have been demonstrated in the use of fluids to perform timing functions since the first breadboard timer was constructed.

1. The volume has been reduced by a factor of 60.

2. The number of active elements has been reduced from 100 to 35.

3. Power requirements have been reduced by a factor of 4.

4. Over one thousand flip-flops have been manufactured.

5. The present unit was designed to be environmentally rugged.

However, there are still several areas where additional work will be required before fluids are utilized for ordnance timers.

1. A satisfactory power supply has yet to be demonstrated.

2. Packaging must be improved further.

3. Element size must be reduced.

4. Additional environmental test and reliability data must be obtained.

This development effort has, in a relatively short time, advanced fluid timers to the point where they can begin to compete with conventional ordnance timers. With further development it is anticipated that fluid timers will be used in ordnance applications.

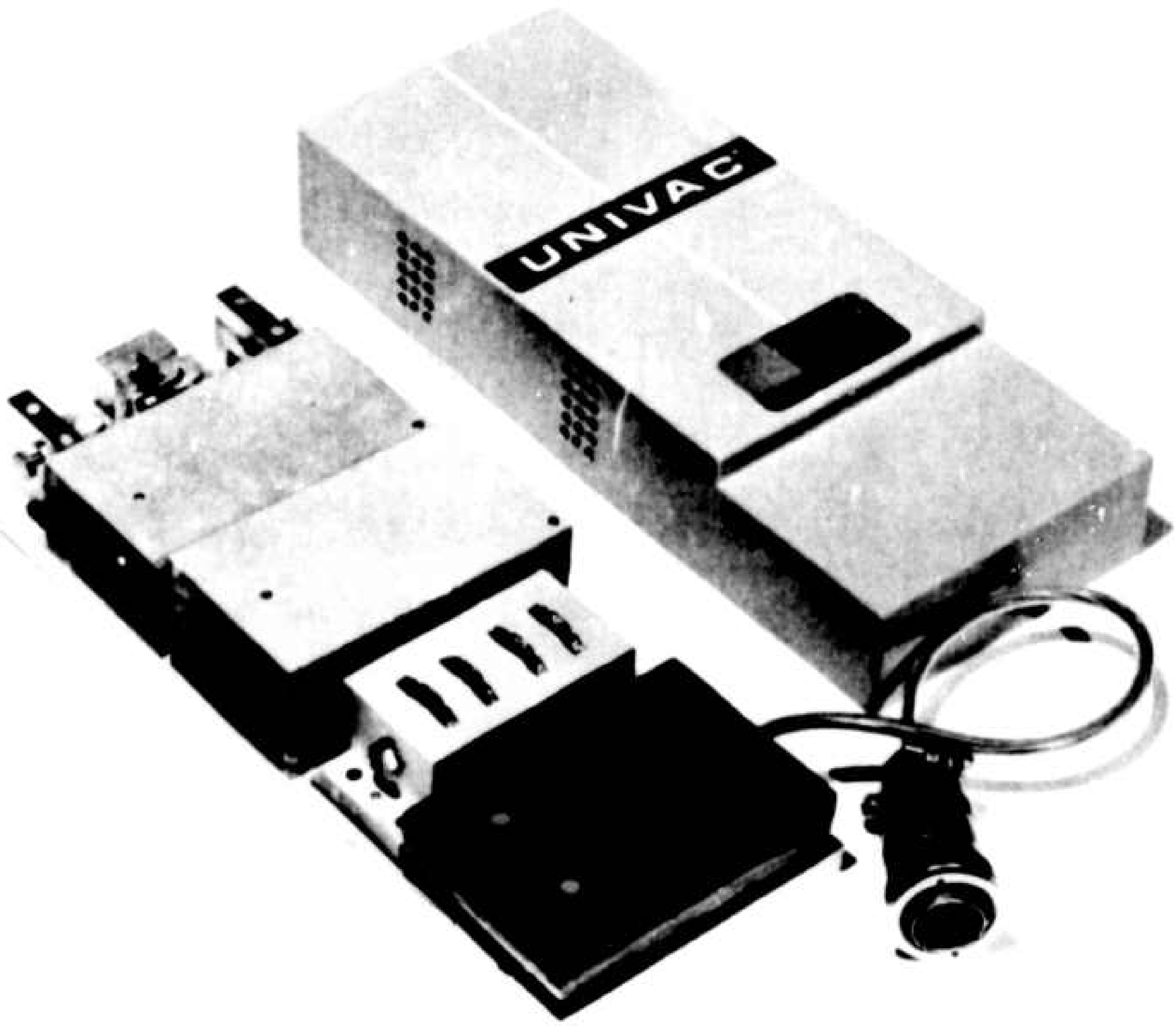

333-11

Figure 1. Sandia Fluid Timer

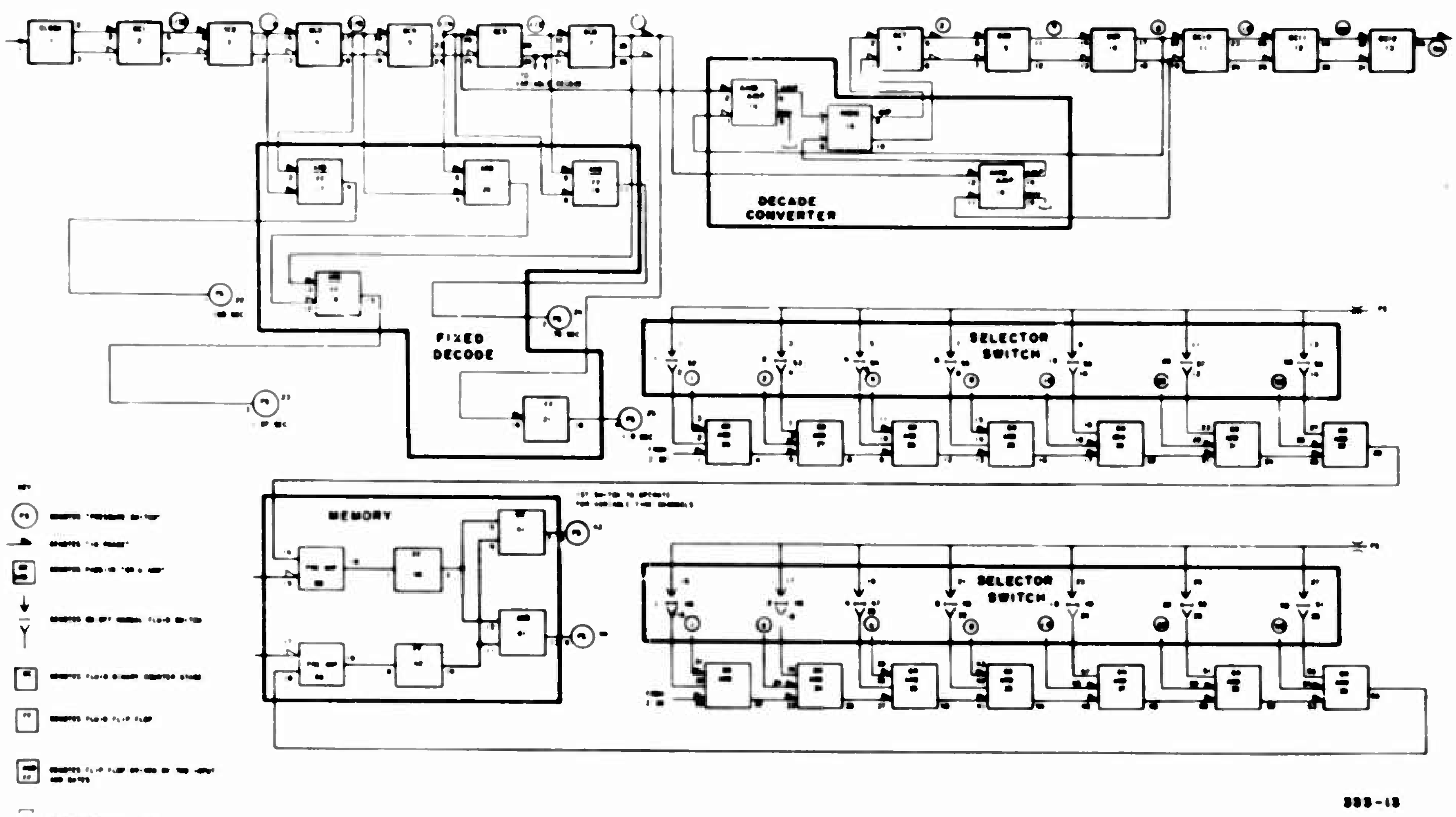

Figure 2. Sandia Timer, Block Diagram

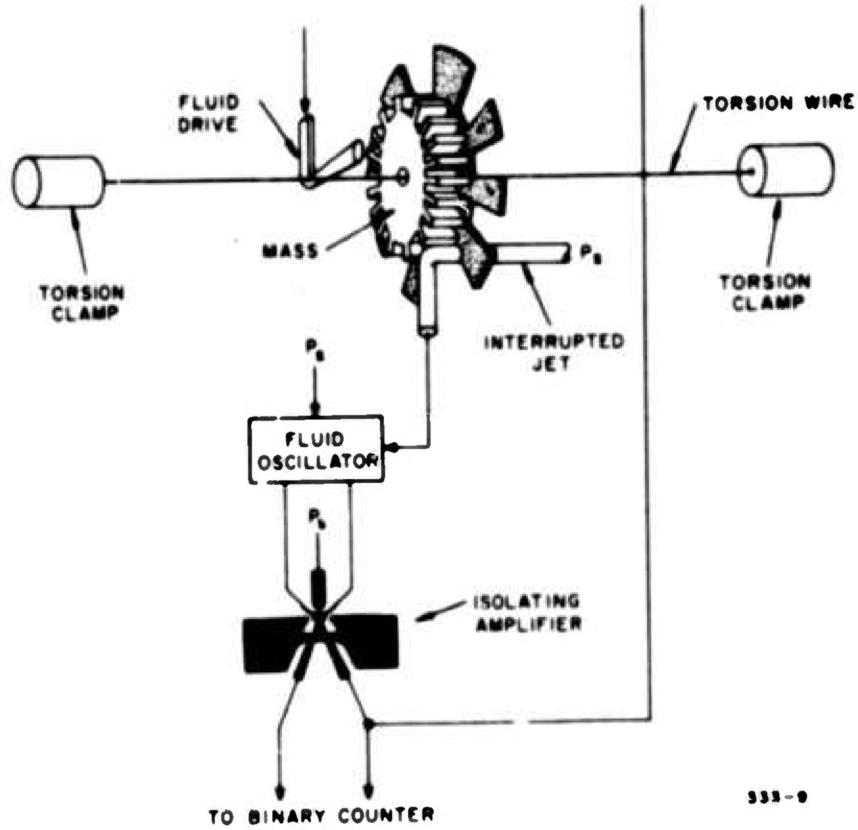

Figure 3. Oscillator, Schematic Diagram

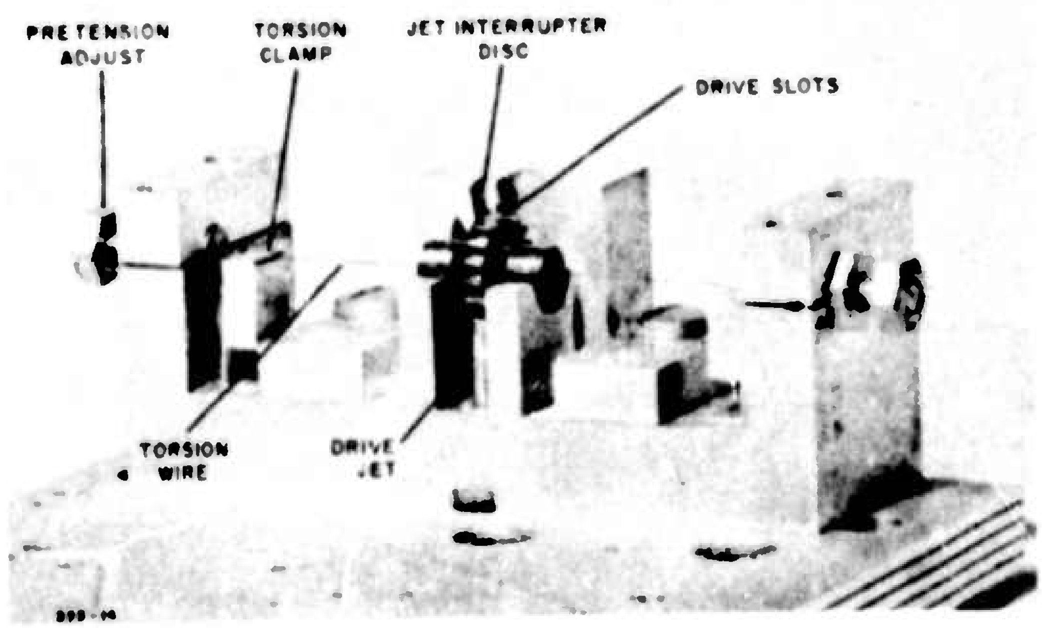

Figure 4. Mechanical Oscillator

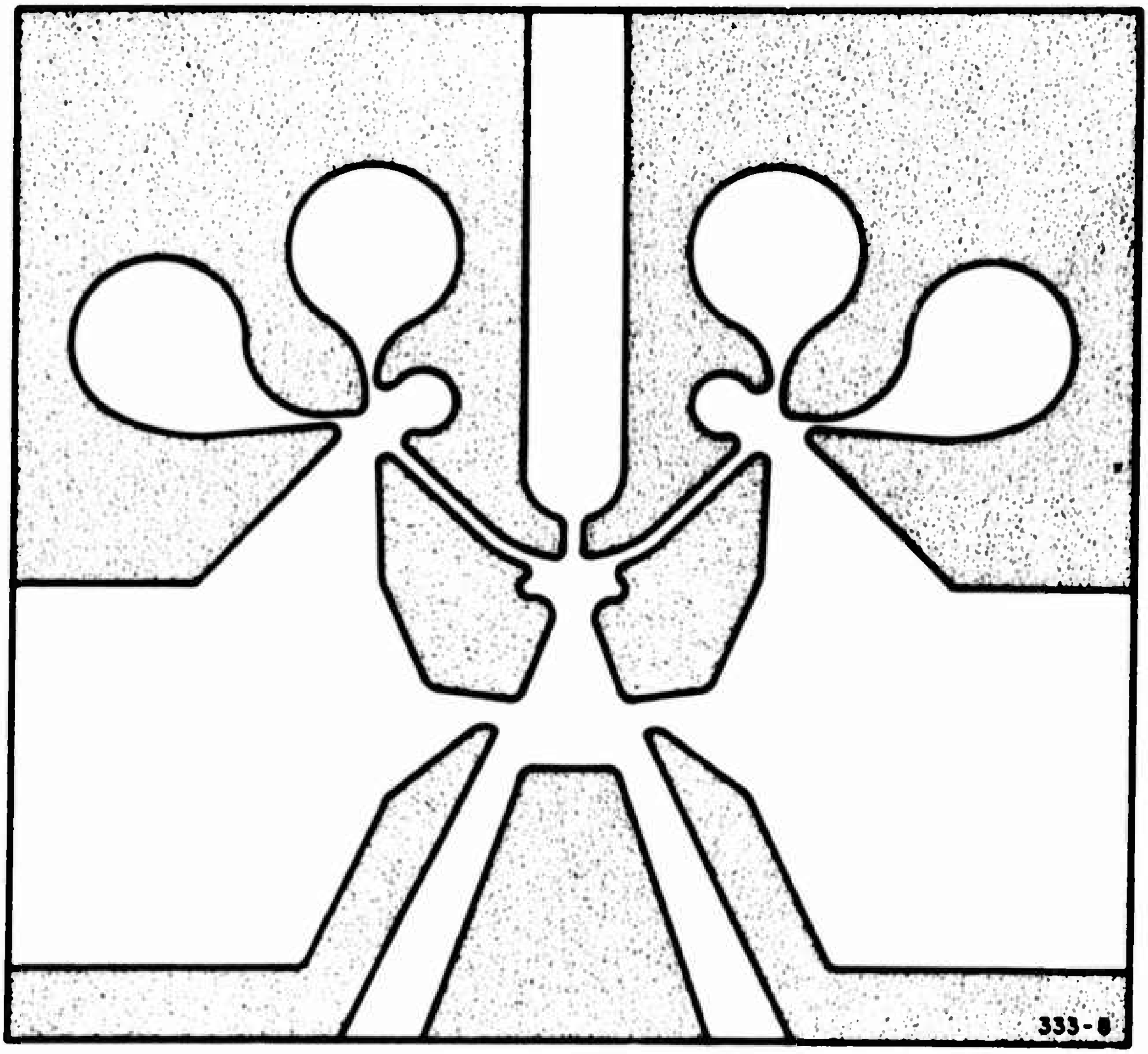

Figure 5. Fluid Flip-Flop Element

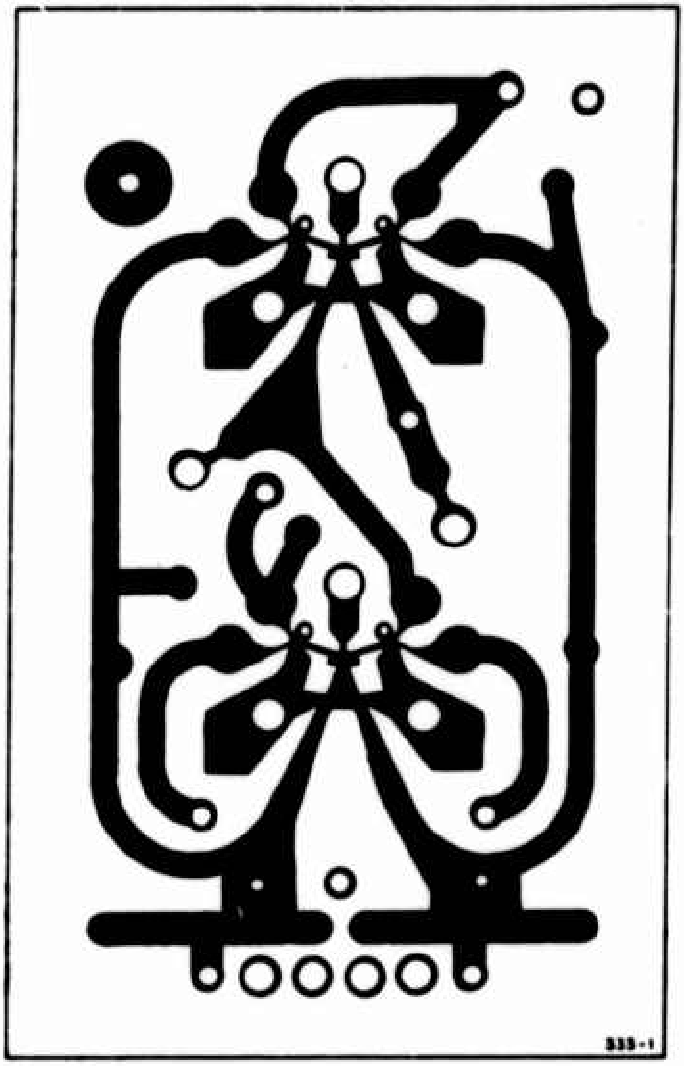

Figure 6. Binary Counter Fluid Circuit

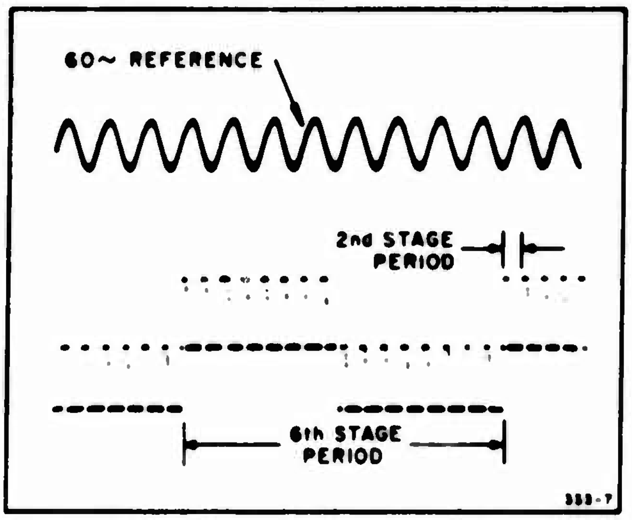

Figure 7. Six-Stage Binary Counter
(500 pps Input Frequency)

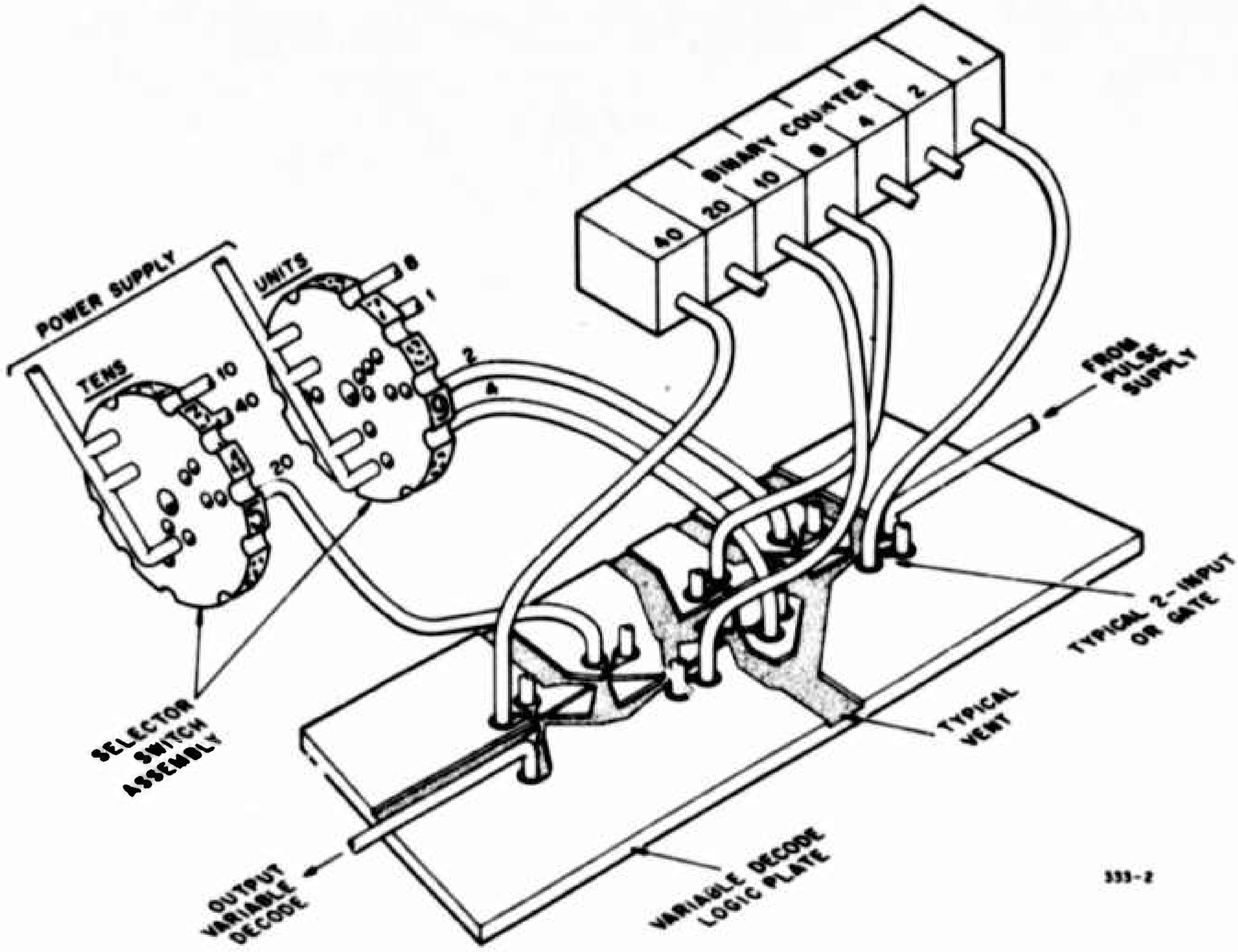

Figure 8. Variable Decode Time Channel, Schematic Diagram

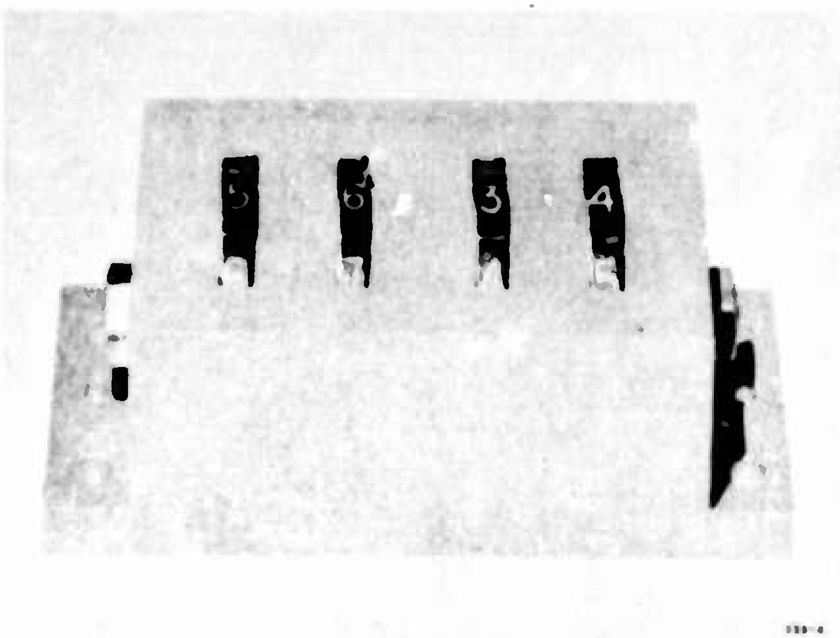

Figure 9. Selector Switches

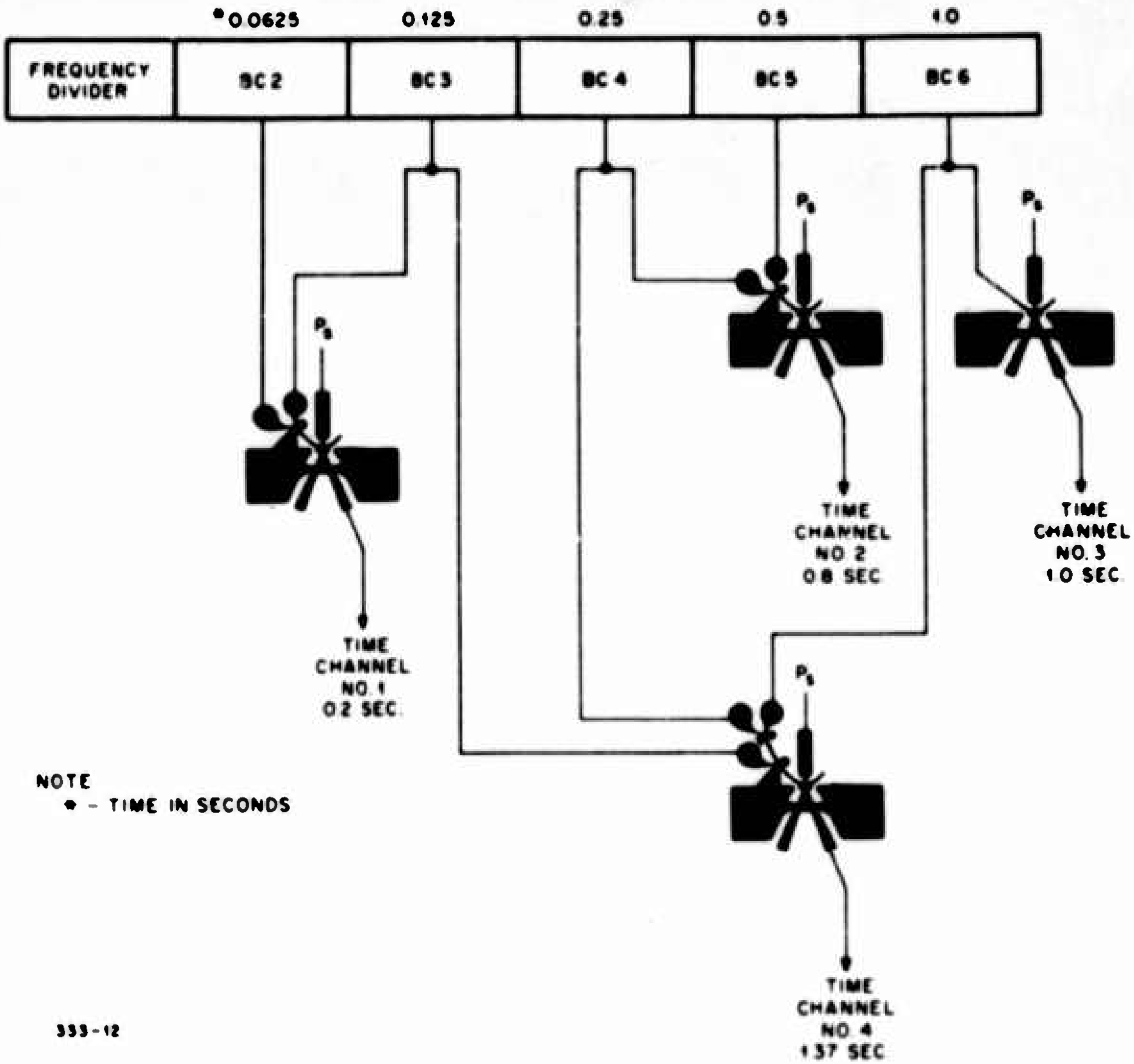

Figure 10. Fixed Decode, Block Diagram

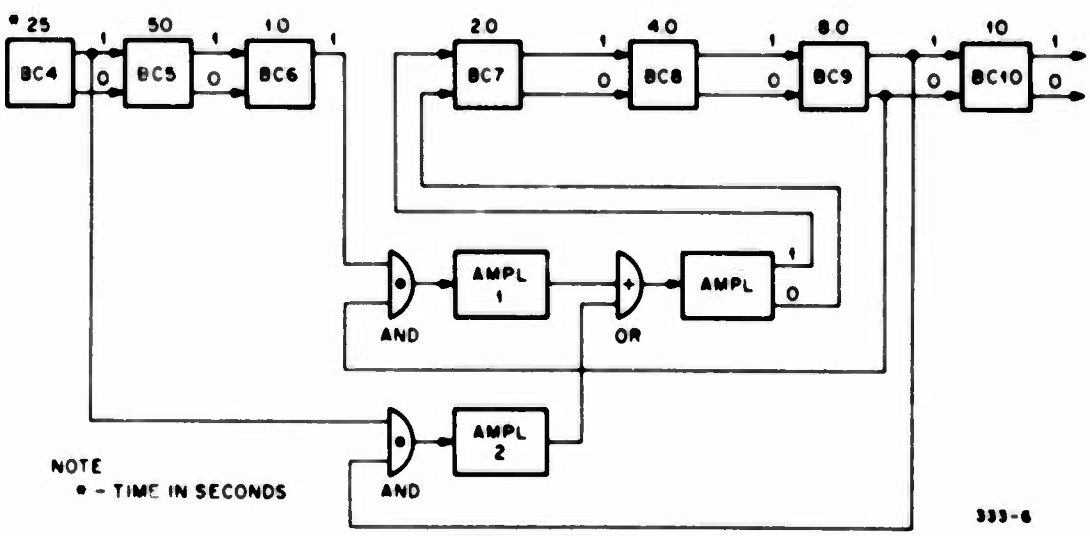

Figure 11. Binary-to-Decade Converter, Block Diagram

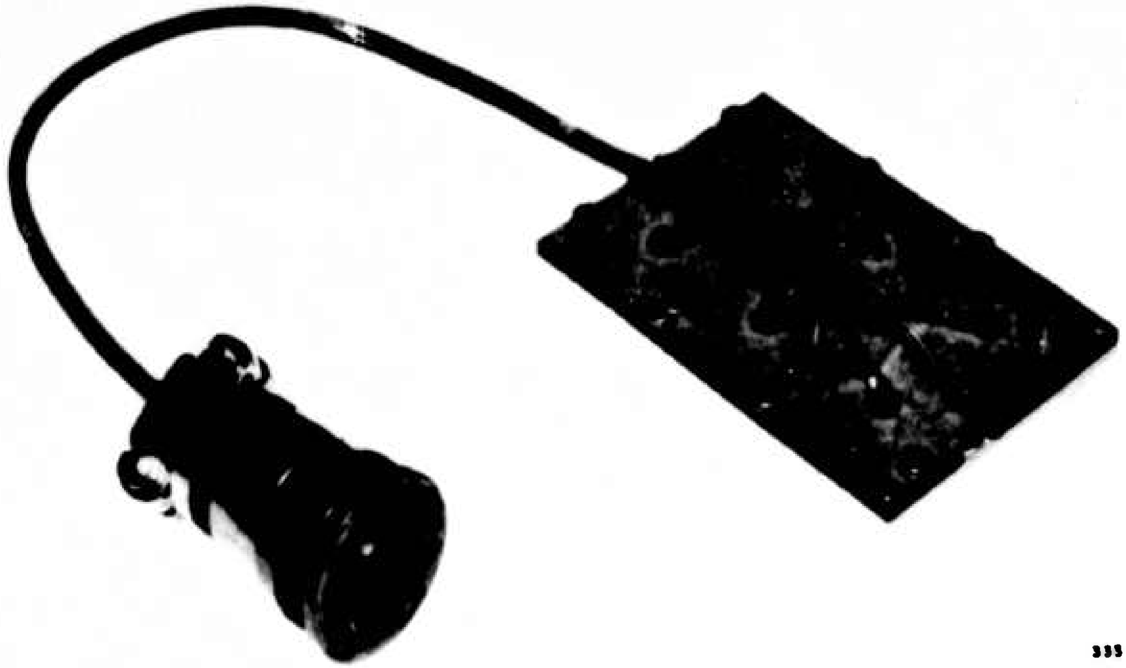

Figure 12. Pressure Switch

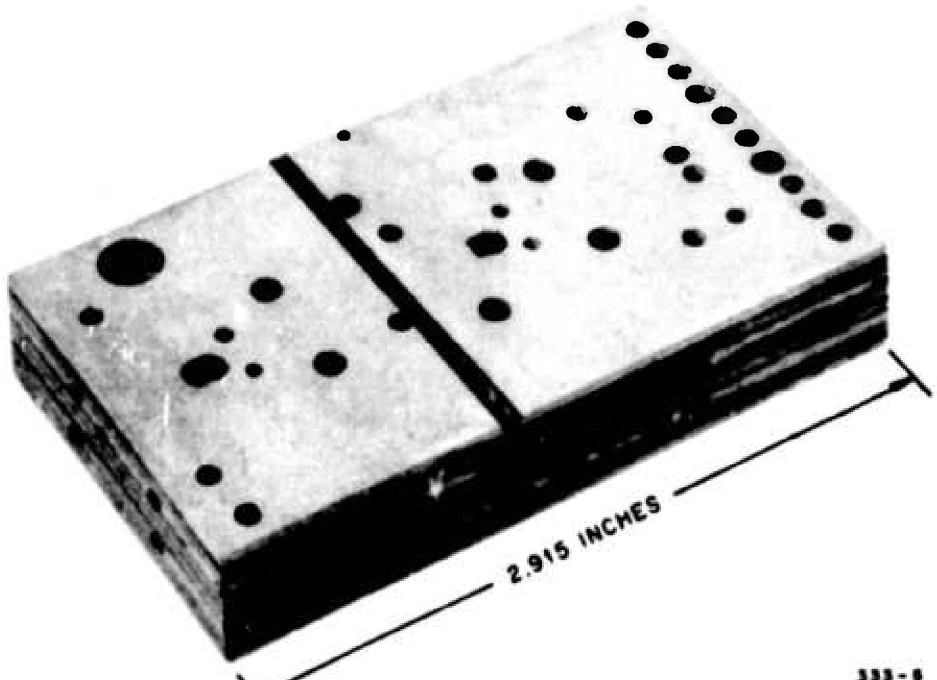

Figure 13. Binary Counter Stack

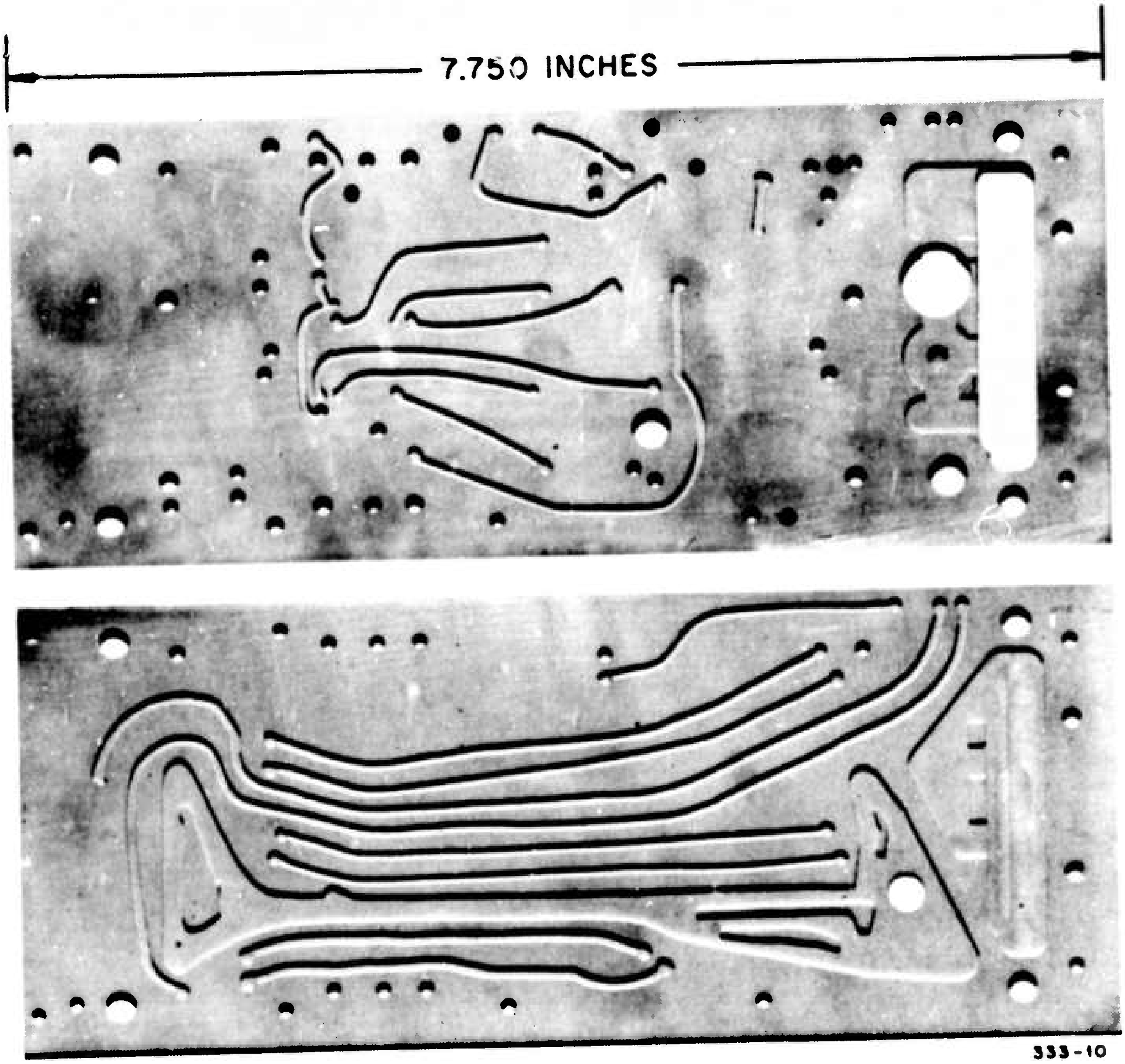

Figure 14. Master Manifold Plates

THE USE OF A FLUID AMPLIFIER IN AN INTERMITTENT STREAM RELEASE VALVE FOR HIGH ALTITUDE RESEARCH

by
Tom Morton
Research Engineer - Fluid State Technology
Aviation Electric Limited, Montreal, Quebec, Canada.

1. INTRODUCTION

For the past two years, McGill University (Montreal, Canada) has been firing upper atmosphere probes[1] from a modified 16-inch naval gun installed on the island of Barbados in the British West Indies. As a part of this High Altitude Research Program (HARP), the air currents at altitudes of up to 400,000 feet are studied by releasing a stream of reactive liquid and observing the distortion of the resultant trail over a period of 15-30 minutes. Both continuous and interrupted trails are used - the interrupted trail having the advantages of vertical as well as horizontal wind shear determination plus an extension of the altitude range over which the observations can be made with any one shot.

The very high accelerations experienced during gun launch, and the reactive characteristics of the liquid used to produce the high altitude trail create special problems for the valve designer and offer special opportunities for the application of fluid state devices. This paper describes the design and performance of an intermittent stream release valve using tri-methyl aluminum (TMA) as its working fluid and operating over a pressure range of 200 - 50 psig to deliver 35 puffs per minute at approximately 100 cc per puff.

A sketch of the vehicle used to display the TMA trail is shown in Figure 1.* This vehicle, which has been designated by McGill University as the MARTLET II, carries a 10-lb charge of reactive liquid.

Tracking is facilitated if it is possible to focus on a single puff rather than one part of a continuous trail and also allows the detection and measurement of vertical air currents in addition to the

---

*Figures appear on pages 299 through 307.

1. (continued)

horizontal variety. Finally, since the vehicle payload is limited, interrupting the trail would have the effect of lengthening it (i. e. the same as an increase in payload). This cannot be accomplished by decreasing the rate of continuous flow since there is a rate below which the trail is no longer visible.

The ruggedness and simplicity of fluid amplifiers made them particularly attractive for use in this stream release valve. The fact that the vehicle was to be fired from a gun at an initial acceleration of 10,000g made the design of an electromechanical interrupter somewhat difficult, especially since the vehicle was very simple and carried no on-board power source.

2. DESIGN DESCRIPTION

The final valve design incorporates a bistable fluid amplifier which uses the TMA as both a power and a control source. The fluid element alternately switches the TMA flow into a storage volume and then to atmosphere, while the fluid in the storage volume is being dumped overboard. The valve is completely self-contained, requiring no power supply, exterior control, or even a start signal. It is screwed into the rear of the vehicle and automatically begins releasing an intermittent stream when the high pressure TMA is admitted. A spool valve controlled by a pure fluid element operates to ensure complete cut-off of the TMA flow and also serves to keep the flame from the burning TMA from working back into the valve components during the cut-off portion of the cycle. Because of the requirement for complete cut-off, use of a vented fluid element was not practical.

The complete valve (shown in Figure 2) is of cylindrical shape, 4 inches in diameter by 3 inches long and weighs 3 lb. The outside diameter is threaded to facilitate fitting into the rear of the vehicle. The disassembled unit is illustrated in Figure 3, the main components being the valve block, fluid element plate, the end plate, the piston, the valve spool and the spring. All fluid passages are inside the valve body. The valve parts are made of aluminum with the body being anodized to prevent sticking of the piston and spool. The "O" ring seals are made of a special material "Viton A" which does not react with the TMA liquid. The piston has a di-

2. (continued)

ameter of 2.5 inches and a stroke of 0.84 inches, giving a displacement of 4.1 cubic inches. The force necessary to compress the spring is 65 lb, requiring a pressure of 15.5 psi below the piston.

The fluid element is milled into the element plate, the power and control nozzles being 0.030 in. wide by 0.080 in. deep. Output and control passages are 0.187 in. wide and lead through the connecting passages to different units in the valve block. The fluid element has an offset of 0.015 in. and a boundary wall angle of 12°.

3. VALVE OPERATION

A schematic diagram of the fluid circuit is shown in Figure 4. The main components are a fluid element, a storage volume, and a spool valve. Some 50 seconds after launch, an interval which is determined by an explosive time delay valve, the high pressure TMA is allowed to flow into the power jet of the fluid element. If flow initially starts in leg A, pressure is applied to close the spool valve, and the flow is fed into the storage volume. The output leg recovery pressure lifts the piston against the force of the spring above it and when the piston reaches the top of its travel, a small port is uncovered allowing the liquid to flow along Channel C to the left-hand control jet of the fluid element. The element then switches to output B and pressure in this leg opens the spool valve, allowing the spring to force the fluid in the storage volume out through the outlet vent. The volume at the top of the piston is also filled, but as it is relatively small, the total flow from the power jet cannot be accommodated. The stability of the fluid element is, however, sufficient to keep the main flow attached to outlet B, while the extra flow is spilled at low pressure into output A, where it passes into the storage volume and out into the outlet vent with the rest of the fluid.

When the spring has forced the piston to the bottom of its travel, a port is opened in the small volume above the piston. This allows the liquid to flow along passage D to the fluid element which is switched back to output A. This causes the pressure in output leg A to rise which, along with a drop in the pressure in leg B, moves the spool valve to the closed position, stopping the output. This

3 (continued)

completes the cycle and the storage volume commences to fill again.

4. DEVELOPMENT HISTORY

Development testing of the element was conducted on a high pressure fuel test stand (see Figure 5) using JP-4 test fluid, the density and viscosity of which approximate those of TMA.

The valve input supply pressure variation was theoretically determined on the basis of both adiabatic and isothermal expansion of the pressurizing nitrogen gas in accordance with the equations:

Isothermal expansion

$$PV = P_i V_i \text{ — — — — — — — } (1)$$

Adiabatic expansion

$$PV^{\gamma} = P_i V_i^{\gamma} \text{ — — — — — — } (2)$$

where P = nitrogen pressure

V = total nitrogen volume

P_i = initial nitrogen pressure (200 psia)

V_i = initial nitrogen volume (144 in^3)

γ = ratio of specific heats.

The resulting nitrogen pressure variation as a function of percentage of TMA expelled is illustrated in Figure 6.

Assuming that the isothermal expansion more closely approximates the actual nitrogen gas expansion process, the relationship between the TMA volume expelled and time may be determined as follows:

Equation for isothermal expansion of the nitrogen

$$P(V_i + V) = P_i V_i \qquad (3)$$

Velocity of TMA expelled through the valve orifice (0.030" × 0.080" fluid amplifier power jet nozzle) assuming a discharge coefficient of 1.0 and zero ambient pressure at the altitude of TMA release:

$$Vel_1 = \sqrt{\frac{2gP}{\rho}} \qquad (4)$$

where Vel = TMA velocity

g = acceleration due to gravity

ρ = TMA density

but $dV = VA\,dt$ (5)

where A = orifice area

Substituting equations (3) and (4) into equation (5)

$$dV = \sqrt{\frac{2g}{\rho} \frac{P_i V_i}{(V_i + V)}} \quad A\,dt$$

Therefore

$$\sqrt{V_i + V}\, dV = \sqrt{\frac{2g}{\rho} P_i V} \quad A\,dt \qquad (6)$$

Integrating equation (6) results in

$$\frac{2}{3}\left(V_i + V\right)^{\frac{3}{2}} = \sqrt{\frac{2g}{\rho} P_i V_i} \quad At + C$$

where C = constant of integration

When t = o; V = o

Therefore $$C = \frac{2}{3}(V_i)^{3/2}$$

Hence $$t = \frac{\frac{2}{3}(V_i + V)^{3/2} - \frac{2}{3}(V_i)^{3/2}}{A\sqrt{\frac{2g\, P_i V_i}{\rho}}} \qquad (7)$$

The resultant variation of TMA released and nitrogen pressure as a function of time is illustrated in Figure 7.

Accordingly, experimental fluid amplifier elements were tested on an incompressible fluid test stand as shown schematically in Figure 5 with the power jet supply pressure variable from 200 psig to 35 psig.

Preliminary tests were conducted to determine the stability and output characteristics of a bistable fluid amplifier design when operating with the incompressible test fluid (JP-4 fuel) over the anticipated supply pressure range. The utilization of vents on the output legs of the amplifier in order to attain impedance matching through the accommodation of excess mass flow under high load conditions, is precluded on the basis of the requirement for complete cut-off of valve outlet fluid flow during the "OFF" portion of the cycle.

Early experimental fluid amplifier models which were milled from 0.080" thick plastic and clamped between heavy cover plates, used the conventional jet wall attachment method to attain stability coupled with a pointed splitter (uncusped). Experimental results as illustrated in Figure 8 indicated that the amplifier stability progressively decreases with increasing power jet pressure until unstable oscillatory operation resulted at supply pressures of approximately 220 psi. The data quoted was determined with low amplifier output impedance loads. Back pressure switching occurred at supply pressures as low as 100 psi as the amplifier output load was progressively increased towards infinite impedance.

It is likely that the power jet wall reattachment point moves progressively further downstream with increasing amplifier supply pressure (i.e. increasing power jet momentum), thereby

progressively reducing the amplifier stability margin.

Fluid amplifier water tunnel flow visualization studies, based on the reflection of monochromatic light from aluminum particles suspended in the water, demonstrated that the amplifier stability could be maintained over a wide range of operating pressure through the inducing of a vortex at the jet interaction cavity. The introduction of a vortex-generating cusp on the splitter resulted in a much higher stability level over the full operating range but a higher switching pressure was required as indicated in Figure 10. Progressive modification to the cusp configuration resulted in an amplifier design which demonstrates stability over the full range of supply pressures with the active outlet completely blocked and both control jets closed.

The infinite impedance load pressure recovery was higher than 50% over the full operating range.

Tests indicated that increasing the load on the active outlet leg only had a second-order effect on the flow rate through the amplifier power nozzle. As the active leg was loaded, the back pressure built up, spilling the excess mass flow out through the unloaded inactive leg, while maintaining the power jet attached to the active outlet side. The simultaneous loading of both outlet legs resulted in a substantial increase in the amplifier interaction region static pressure and a corresponding decrease in the amplifier power jet flow rate.

The valve circuit is designed so that the amplifier active leg impedance is high (i.e. when the power jet is attached to leg B) only when the inactive leg impedance is low. The variation of valve flow as dependent upon the amplifier load conditions is thereby avoided.

The performance characteristics of the resultant bistable amplifier design were determined using the test circuit, as illustrated in Figure 9. The performance characteristics over the full operating range are given in Figure 10, the results being determined with both control jet valves closed and anticipated valve circuit loading conditions simulated.

As evident from the graph, the necessary condition of the ampli-

fier switching pressure being between the active and inactive leg pressure has been attained. Additionally, the close correlation between the inactive leg pressure and the inactive side control jet pressure indicates the absence of any entrainment bubble on this side of the amplifier.

The complete experimental valves were tested extensively on the incompressible fluid test stand facility (Figure 5). The valves operated satisfactorily and without adjustment from 35 to 250 psi input pressure, typical valve characteristic test results being given below:

Supply Pressure + psig	Cycles per Minute	Cycle 'On' Duration seconds	Volume per puff cu. in.	Flow Rate cu. in/sec.
200	48	1.25	6.92	5.54
175	45	1.33	6.92	5.19
150	42	1.43	6.92	4.85
125	39	1.54	6.92	4.50
100	36	1.67	6.65	3.92
75	34	1.76	6.42	3.37
50	27	2.22	6.08	2.74

The TMA volume ejected per cycle and the 'ON' cycle duration remains relatively constant as may be expected considering that the valve circuit is based on a constant volume accumulator. The variation of cycle frequency and the corresponding average flow rate result directly from the decrease in valve supply pressure during the vehicle flight.

4. CONCLUSIONS

An intermittent stream valve incorporating a bistable fluid amplifier has been designed for modulating a stream of liquid ejected from a gun-launched high-altitude vehicle. The adaptation of fluid amplifier techniques results in an intermittent valve which is lightweight, simple and extremely rugged. The valve is completely self-contained in that only the supply of the pressurized stream fluid is required to operate the valve. The valve operates over a wide range of input pressures and has a wide environmental tolerance band.

(4) (continued)

The principle of the valve circuit appears adaptable to other applications where the modulation of an incompressible fluid stream is required and where the inherent size, cost and environmental tolerance features of fluid devices may be of advantage.

REFERENCES

(1) Development of Gun-Launched Vertical Probes for Upper Atmosphere Studies - Dr. G.V. Bull - CASI Journal - October 1964.

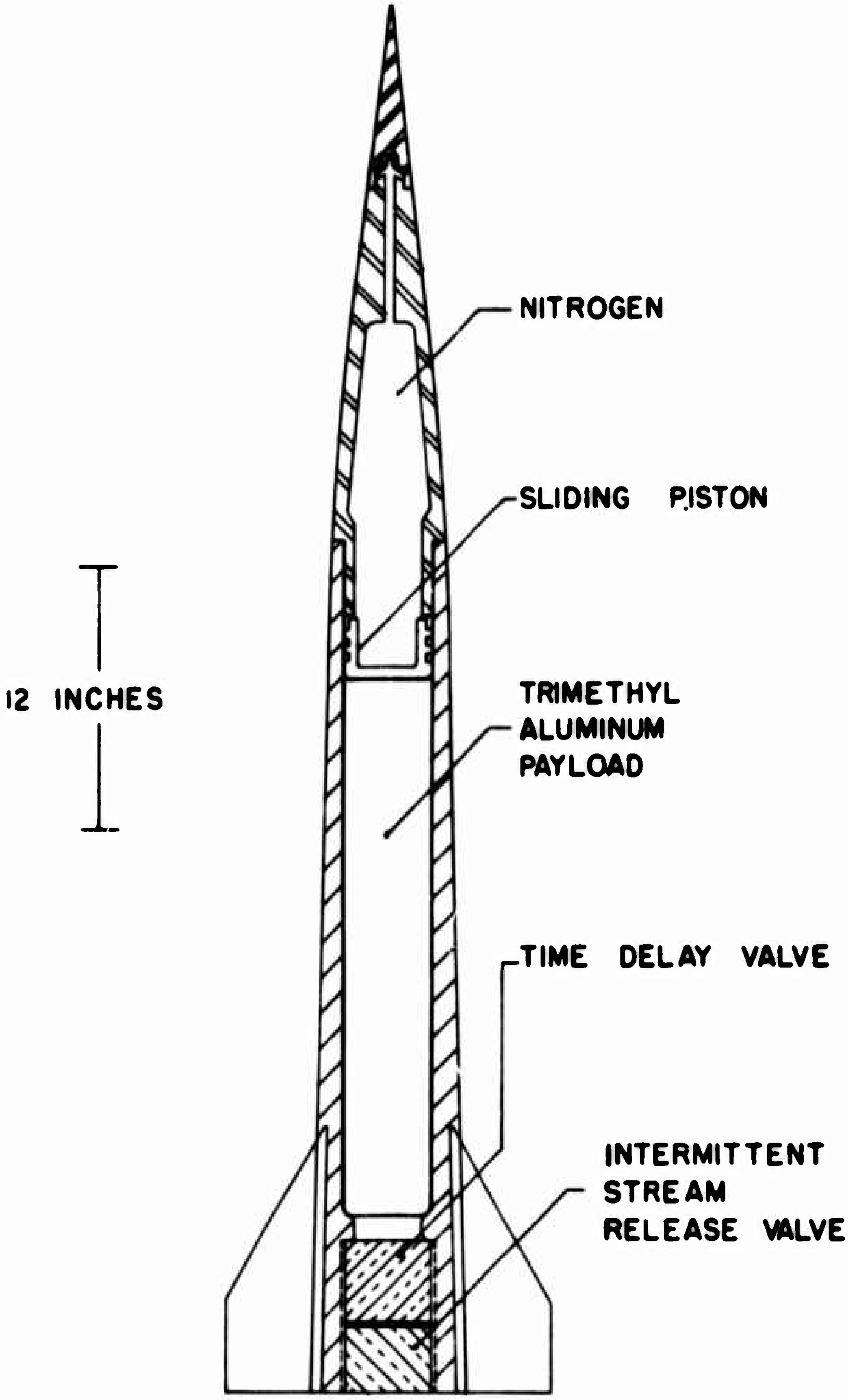

FIGURE 1

GUN-LAUNCHED HIGH-ALTITUDE BALLISTIC VEHICLE

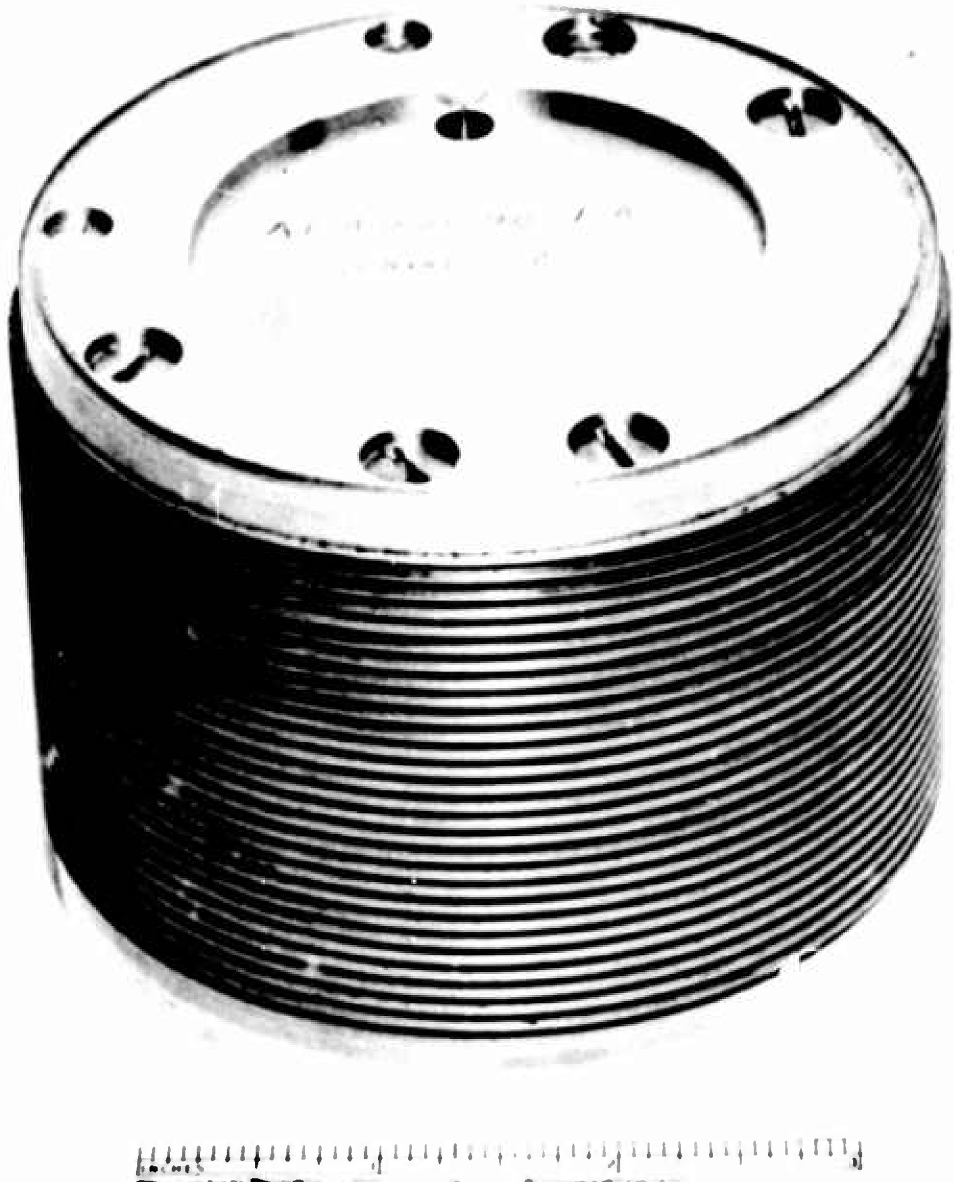

FIGURE 2

INTERMITTENT STREAM VALVE

EXTERNAL CONFIGURATION

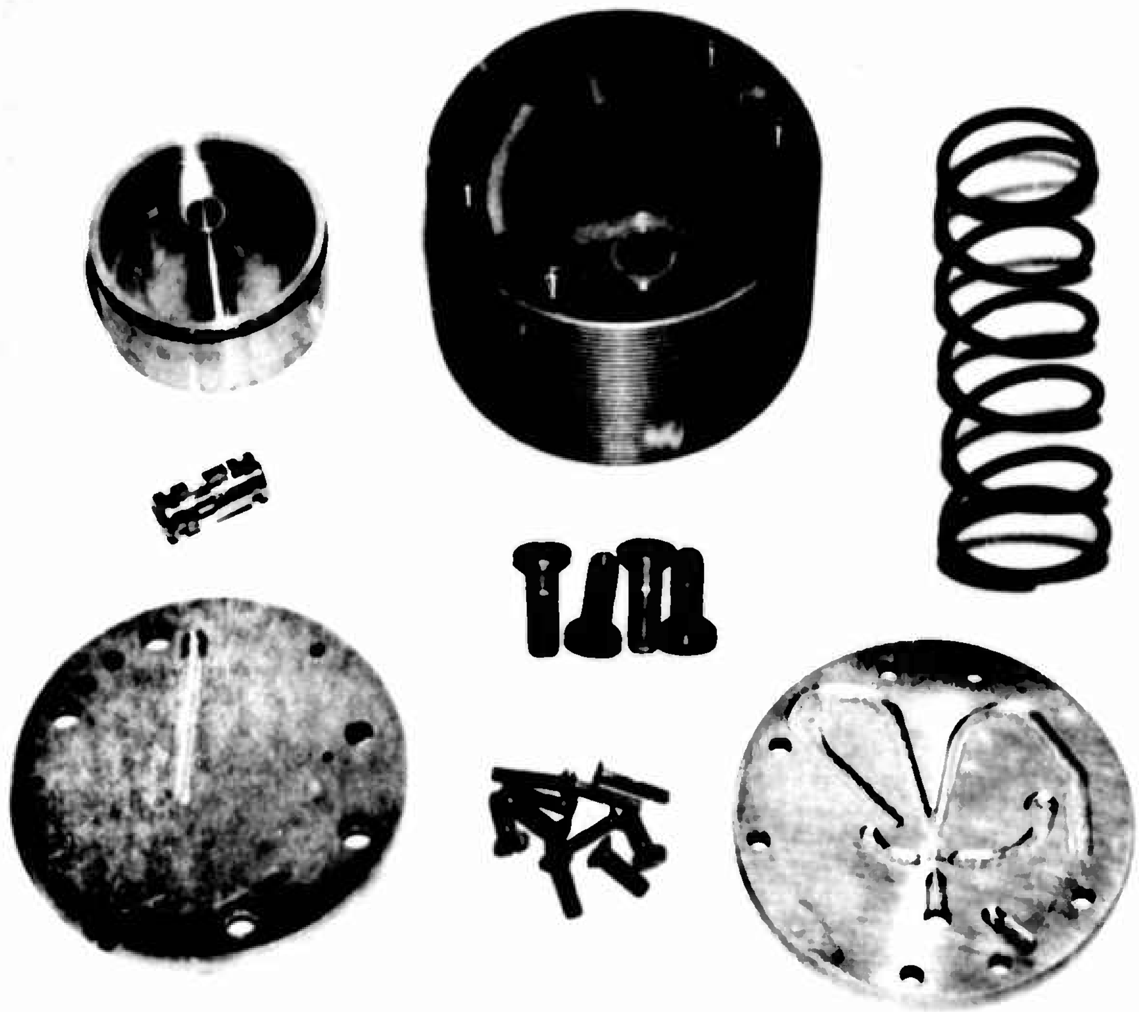

FIGURE 3

DISASSEMBLED VIEW OF INTERMITTENT

STREAM VALVE SHOWING FLUID AMPLIFIER ELEMENT

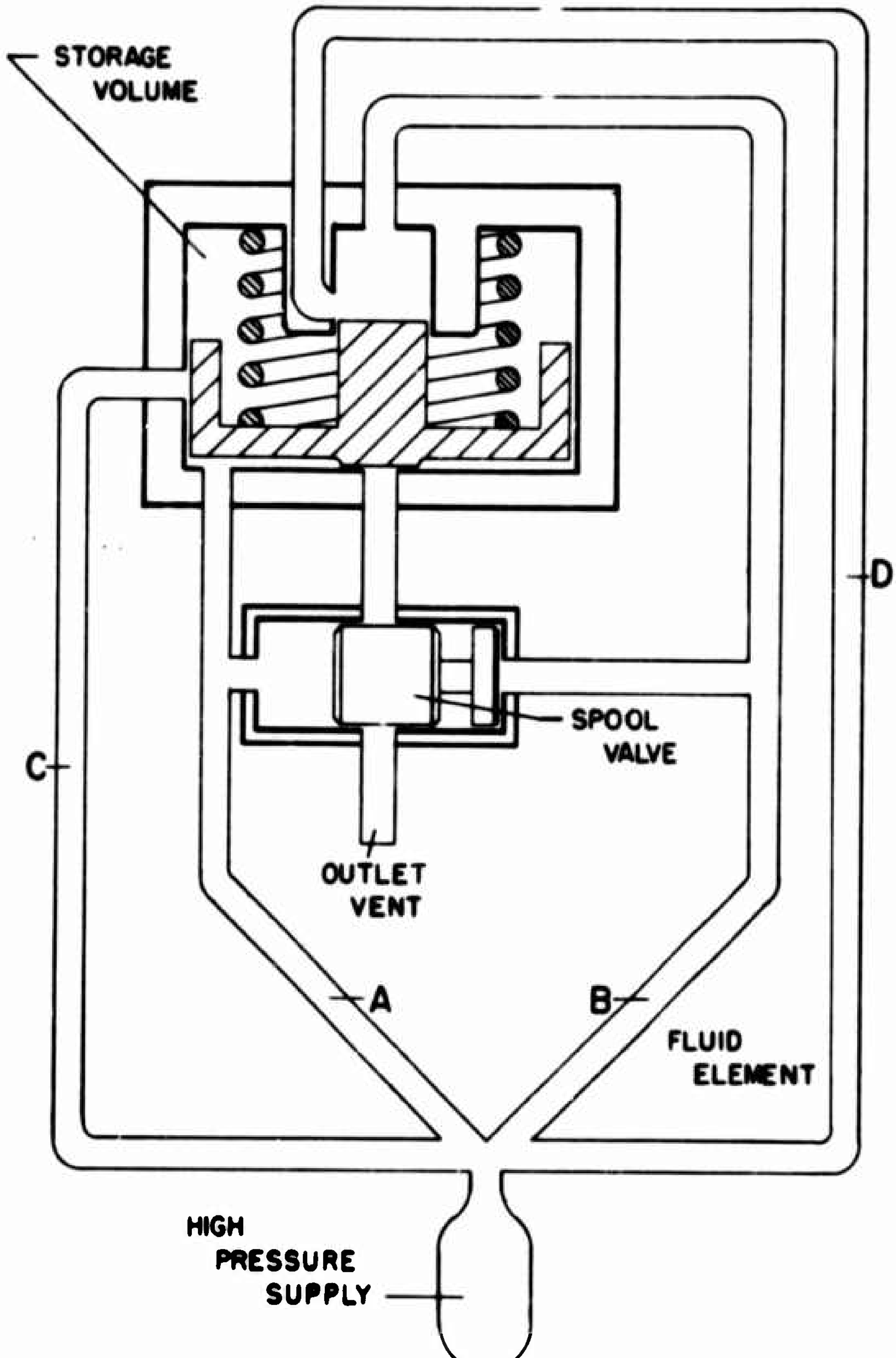

FIGURE 4

SCHEMATIC DIAGRAM INTERMITTENT
STREAM RELEASE VALVE FLUID CIRCUIT

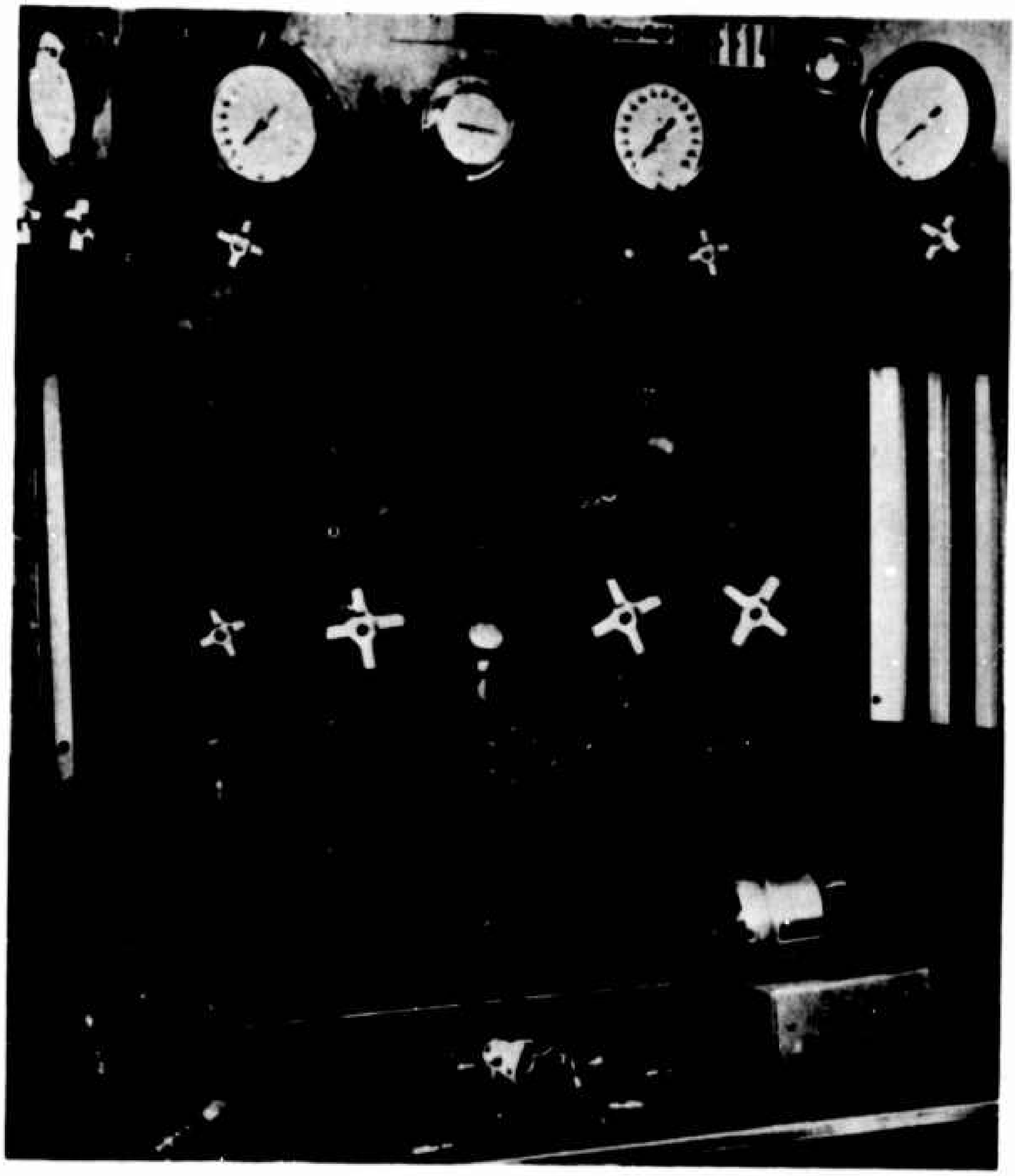

FIGURE 5

INTERMITTENT VALVE INCOMPRESSIBLE

FLUID TEST STAND FACILITY

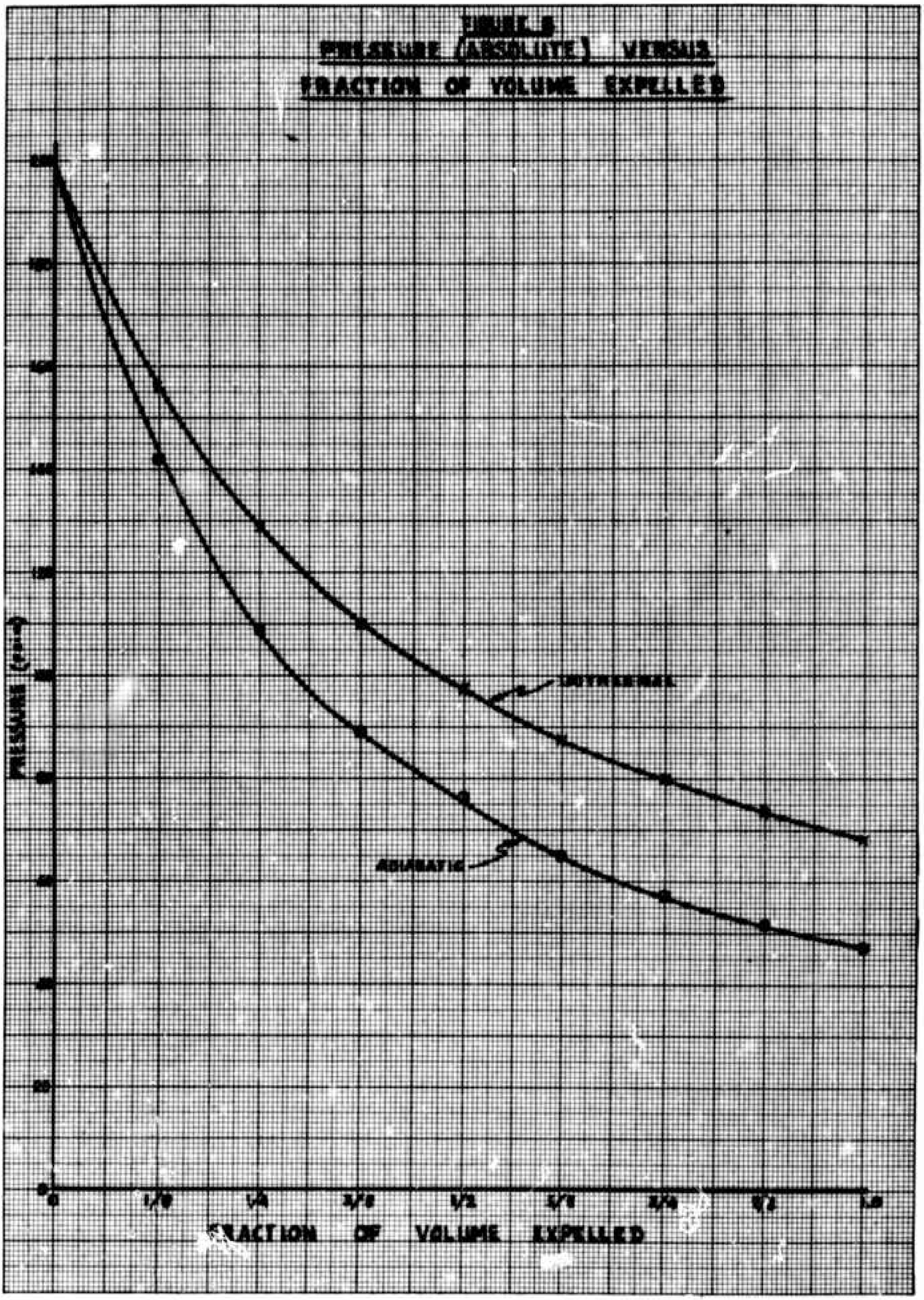
PRESSURE (ABSOLUTE) VERSUS
FRACTION OF VOLUME EXPELLED
PRESSURE
ISOTHERMAL
ADIABATIC
0
1/8
1/4
3/8
1/2
5/8
3/4
7/8
1.0
FRACTION OF VOLUME EXPELLED

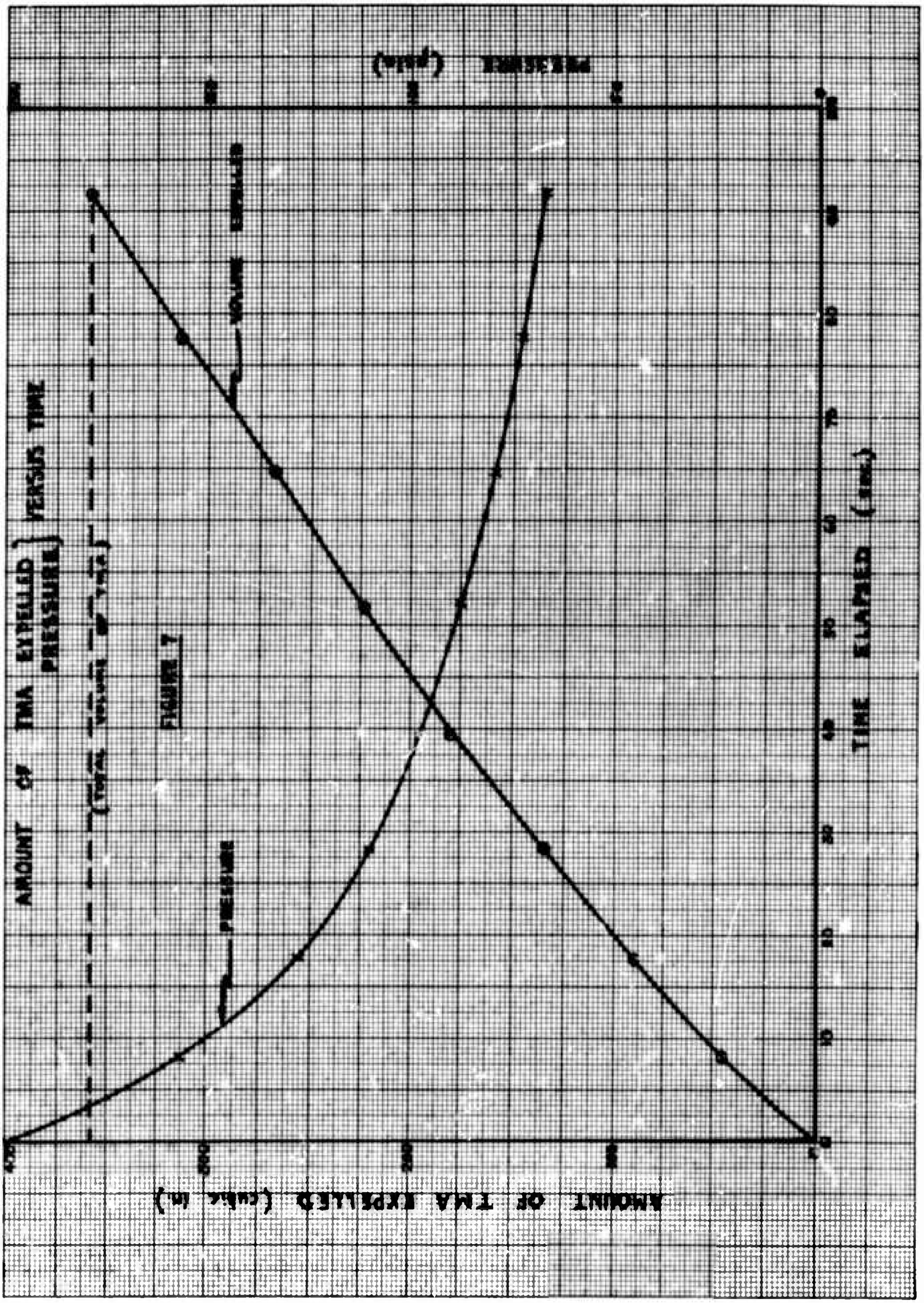
AMOUNT OF TMA EXPELLED VERSUS TIME
PRESSURE
(TOTAL VOLUME OF TMA)
FIGURE 7
VOLUME EXPELLED
PRESSURE
TIME ELAPSED (sec.)
AMOUNT OF TMA EXPELLED (cubic in.)
PRESSURE (psia)

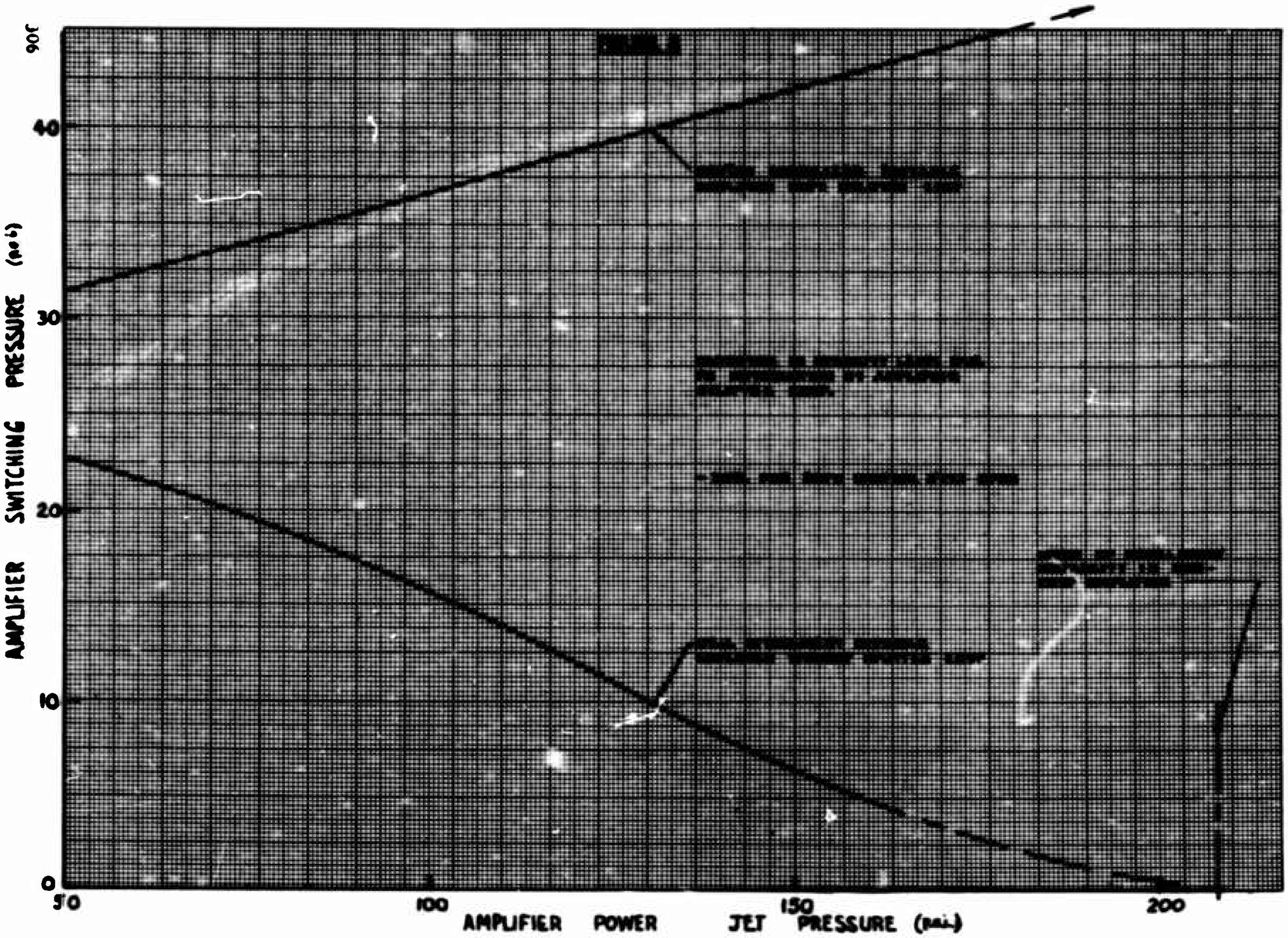
AMPLIFIER SWITCHING PRESSURE (psi)
0
10
20
30
40
50
100
150
200
AMPLIFIER POWER JET PRESSURE (psi)

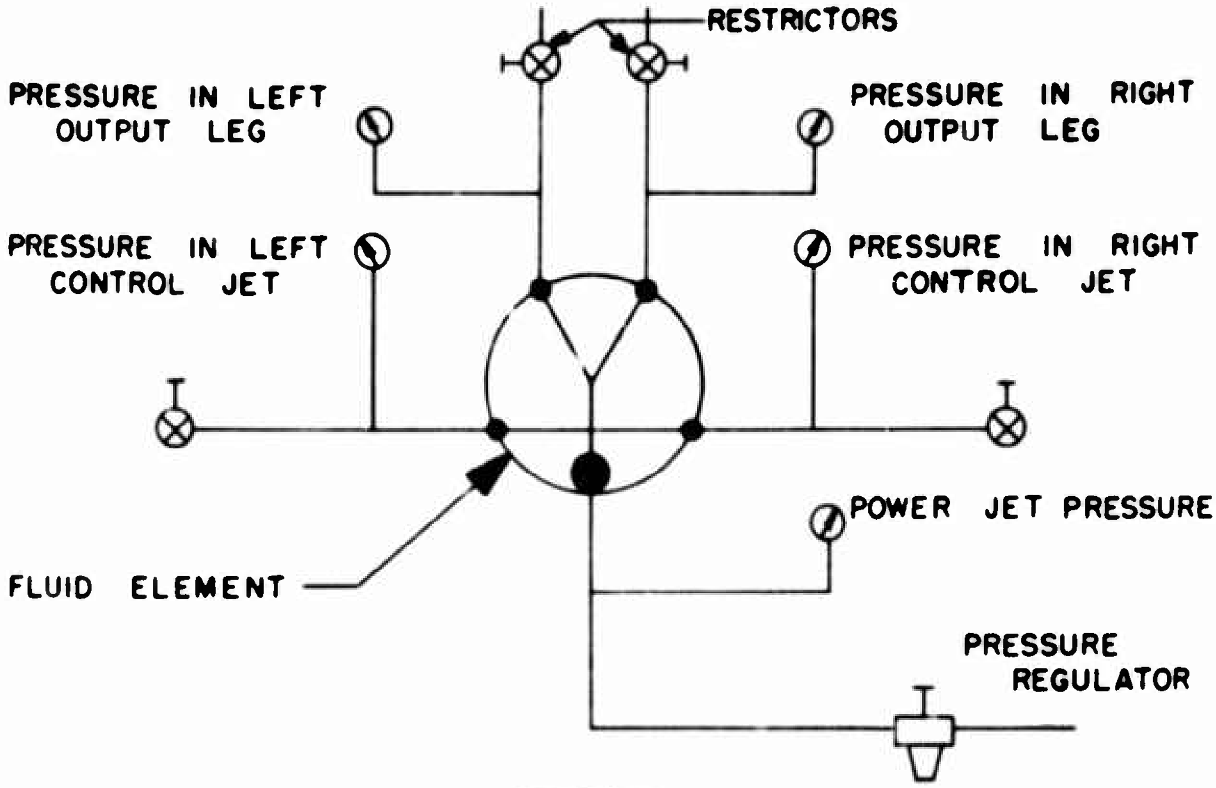

FIGURE 9

BISTABLE FLUID AMPLIFIER TEST CIRCUIT

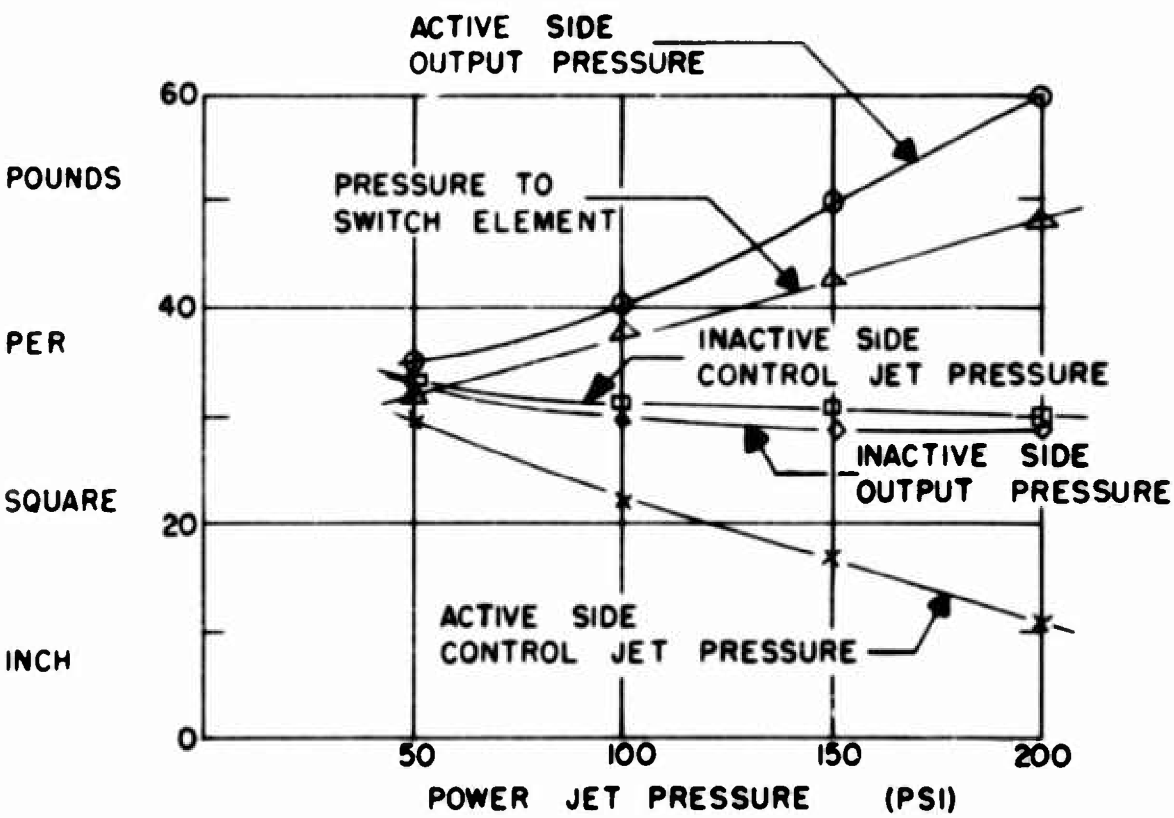

FIGURE 10

PERFORMANCE CHARACTERISTICS

OF VALVE FLUID AMPLIFIER

An Evaluation of a Fluid Amplifier, Face Mask Respirator

Henrik H. Straub*, M.S.E. and James Meyer**, M.D.

1. INTRODUCTION

At the second fluid amplifier symposium last year, a paper (ref 1) was presented by the Harry Diamond Laboratories describing four fluid-amplifier-controlled medical devices. One of these was a respirator (fig. 1)† having no moving parts and slightly smaller than a cigarette pack. In spite of its lack of moving parts, it is able to perform complex respiratory functions. It can function, for example, as an assistor for those patients needing support or as a controller in the absence of spontaneous respiration.

Breathing gases are supplied to the respirator through the power nozzle, forming a turbulent jet. Uneven gas entrainment from the two control nozzles, one connected to the face mask and the other open to atmosphere, causes the power jet to attach to one of the walls. When the jet is exhausting to the left receiver, the breathing gas is forced into the face mask and lungs of the patient. The face mask pressure increases, causing flow through the feedback line to the left control nozzle. At a predetermined mask pressure, the jet entrainment on the left side of the power jet is satisfied, and the jet is switched to the right wall. The power jet then exhausts to the atmosphere through the right receiver, allowing the patient to exhale. The pressure in the feedback line now decreases below atmosphere due to entrainment of gas from the face mask until the control pressures are sufficiently unbalanced to switch the jet from the right to left receiver. This switching occurs in the absence of an inspiratory attempt by the patient.

The respirator operates to assist respiration since the inspiratory effort of the patient reduces the pressure in the left receiver and feedback line below atmosphere, switching the power jet into the left receiver and thereby initiating inspiration. Consequently the operation of the respirator is synchronized with the breathing of the patient.

2. ENGINEERING TESTS

On a lumped parameter system basis, the human breathing circuit can be represented as a series combination of resistance and capacitance. Tanks and airway resistances of various values have been used in the engineering laboratory to simulate the range of breathing impedances. Flow rates, cycling pressures, and frequencies are controlled in the respirator by adjusting setscrews in the passages to the control orifices and the input pressures to the power nozzle.

Figure 2 shows the flow requirements in liters per minute for various power nozzle pressures.

*Harry Diamond Laboratories, Washington, D. C.
**Walter Reed Army Institute of Research, Washington, D. C.

† Figures appear on pages 312 through 315.

Figure 3 is a graph of the face mask cycling pressure for various input pressures for one position of adjustment of the controls. Respirator input pressures above 2.5 psig would normally not be used on patients.

Figure 4 summarizes the performance of the respirator when cycling into tanks of various compliances. The curves were unaltered when a 20-cm H_2O/ℓ/sec airway resistance was inserted between tank and respirator.

3. MEDICAL TESTS

The respirator was tested on dogs weighing about 35 lb. All animals were anesthetized, intubated, and ventilated with oxygen from 1 to 5-1/2 hr. The respirator performed well both as a controller and assistor, the mode of operation depending on the condition of the animal. Average arterial blood gas samples registered pO_2 of 392 mm Hg and pCO_2 of 30 mm Hg, indicating good pulmonary ventilation.

The respirator was also used for periods up to 15 min on various human patients. In all cases it performed well both as an assistor and controller.

4. DISCUSSION

Several of these respirators have been distributed to hospitals interested in participating in the evaluation of this new resuscitative tool. Most of the evaluators reported that cycling functions were generally adequate; however, high expiratory resistance impeded the quick and comfortable expiration of the breathing gases. This resistance creates a high mean pressure in the lungs and impedes the flow of blood returning to the heart.

To decrease the expiratory resistance and still retain all the other desirable functions of the fluid amplifier respirator, a special breathing valve was constructed, which consists of two moving parts and fits directly between respirator and face mask. During inspiration the valve is closed to atmosphere, and all breathing gases flow into the lungs of the patient. At the beginning of expiration, the valve opens and the patient quickly exhales until the pressure in the face mask becomes atmospheric. At that instant the valve closes due to the entrainment characteristic of the left receiver of the fluid amplifier. The pressure in the face mask decreases due to entrainment to some preset negative cycling pressure, and the fluid amplifier then cycles back into the load. A set screw in the right receiver of the fluid amplifier acts as an adjustable exhaust load, decreasing the entrainment in the left receiver during expiration and providing a sufficient expiratory pause. Comparative pressure traces of the respirator cycling into a 76-liter tank without and with a breathing valve are shown on figures 5 and 6, respectively.

5. CONCLUSION

A small fluid amplifier respirator has been evaluated. Results indicate that the respirator performs well on both animals and humans. High expiratory resistance, a characteristic of the device, is overcome with the addition of a specially designed breathing valve that can be eliminated, if necessary, for certain types of patients with respiration difficulties requiring higher-than-normal mean lung pressures. The elimination of moving parts in the respirator itself makes this device extremely reliable, easy to operate, and inexpensive to manufacture.

REFERENCE

1. Woodward, K.; Mon, G.; Joyce, J.; Straub, H.; and Barila, T., "Four Fluid Amplifier Controlled Medical Devices," Proceedings of the Fluid Amplification Symposium, May 1964, Volume IV.

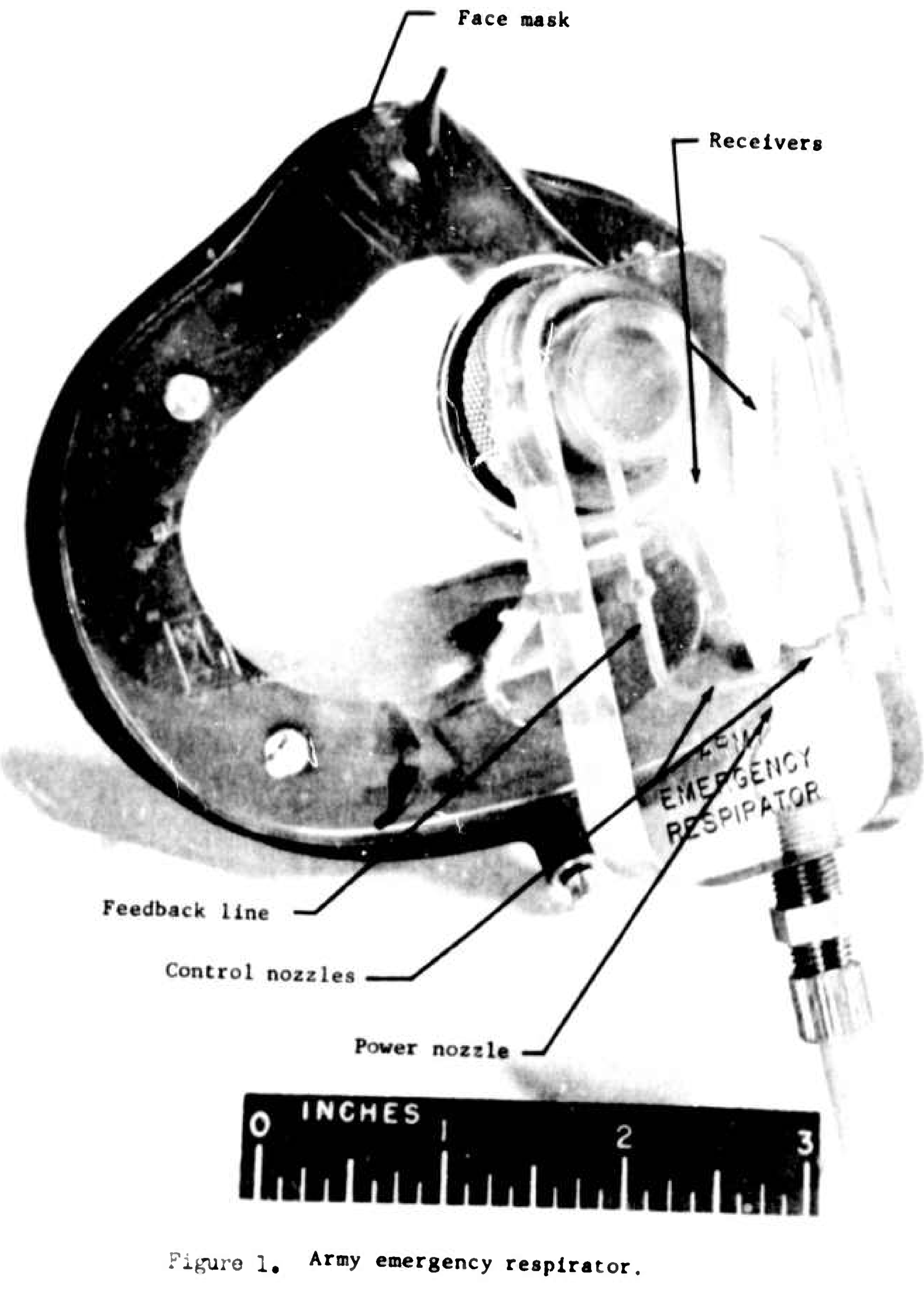

Figure 1. Army emergency respirator.

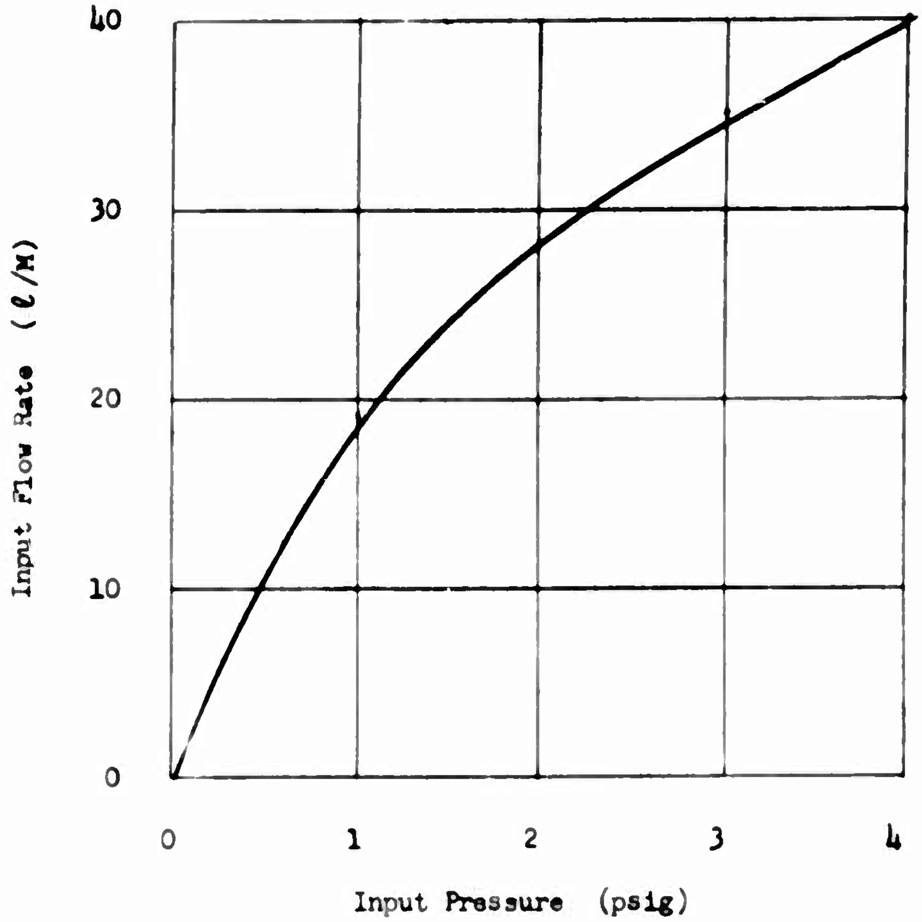

Figure 2. Gas flow requirement

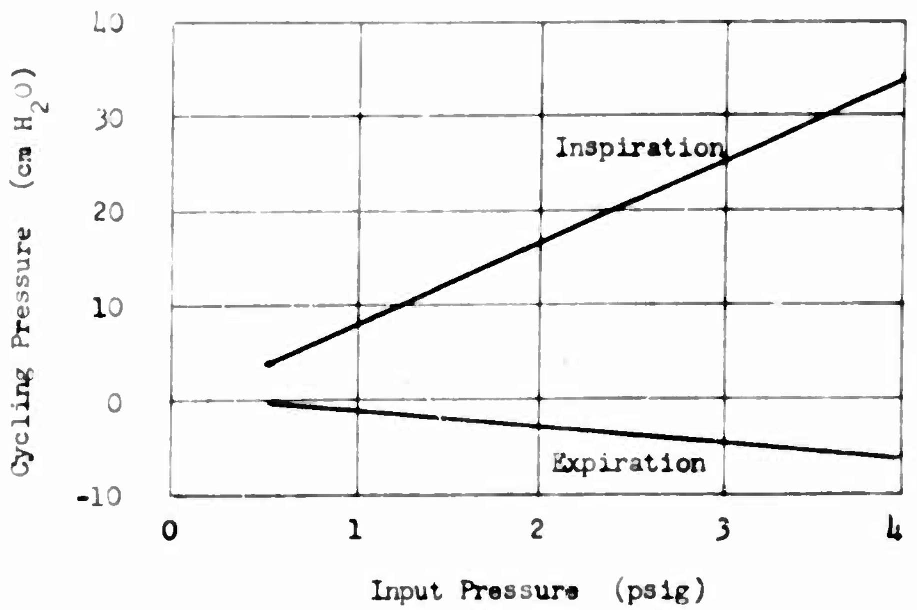

Figure 3. Respirator cycling pressures

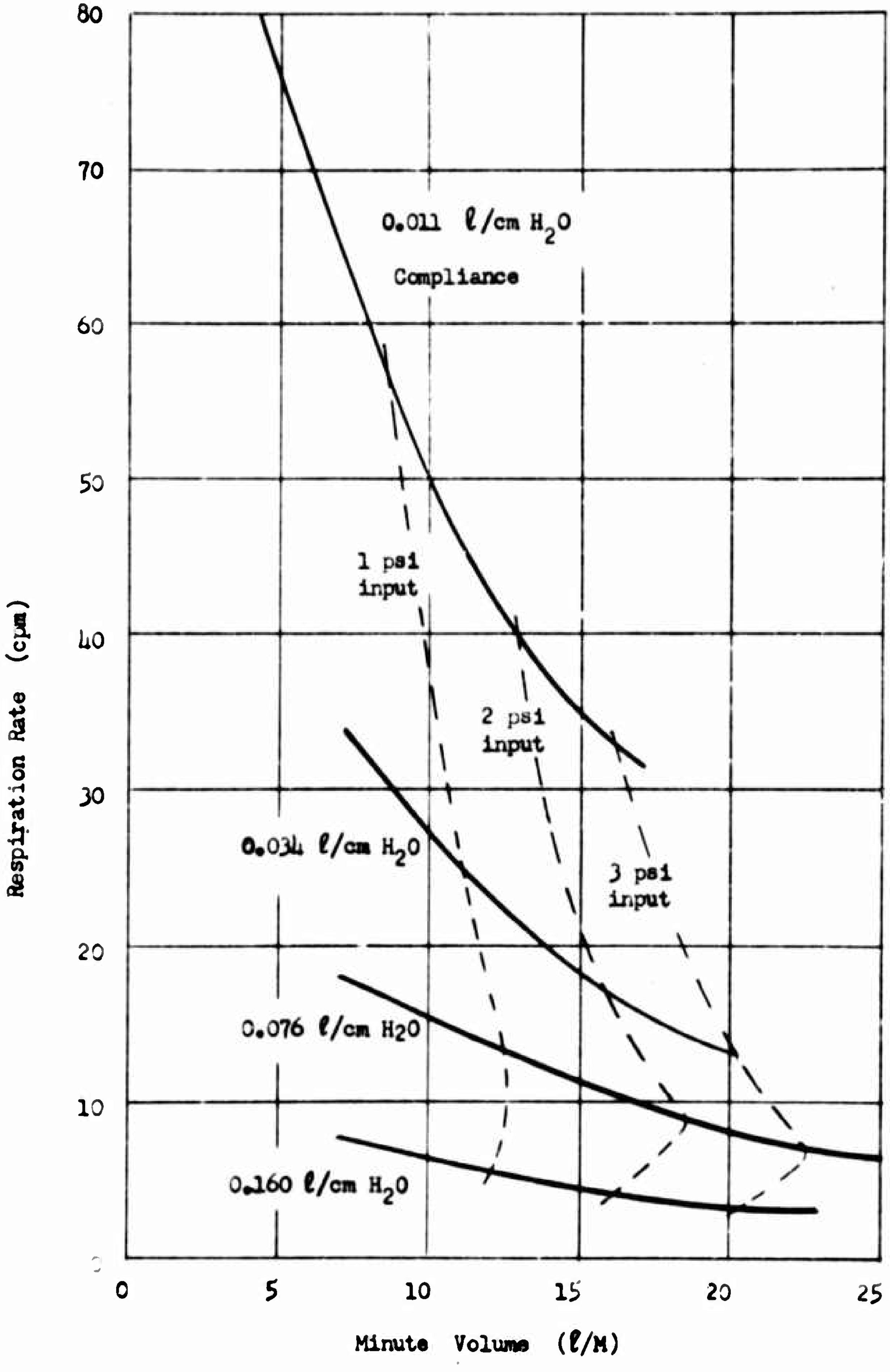

Figure 4. Respirator performance characteristics

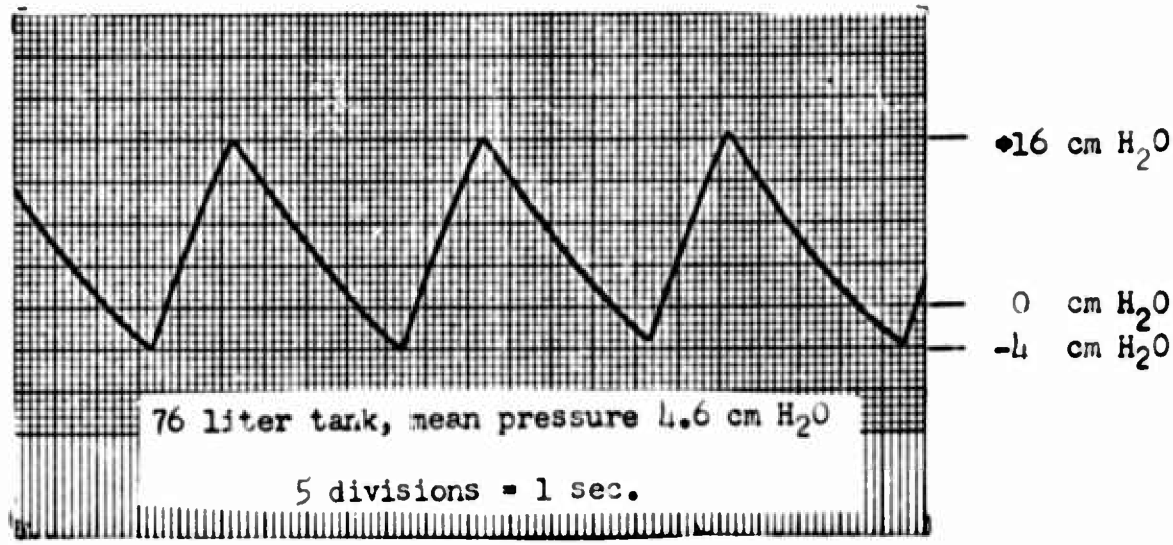

Figure 5. Pressure trace - without breathing valve

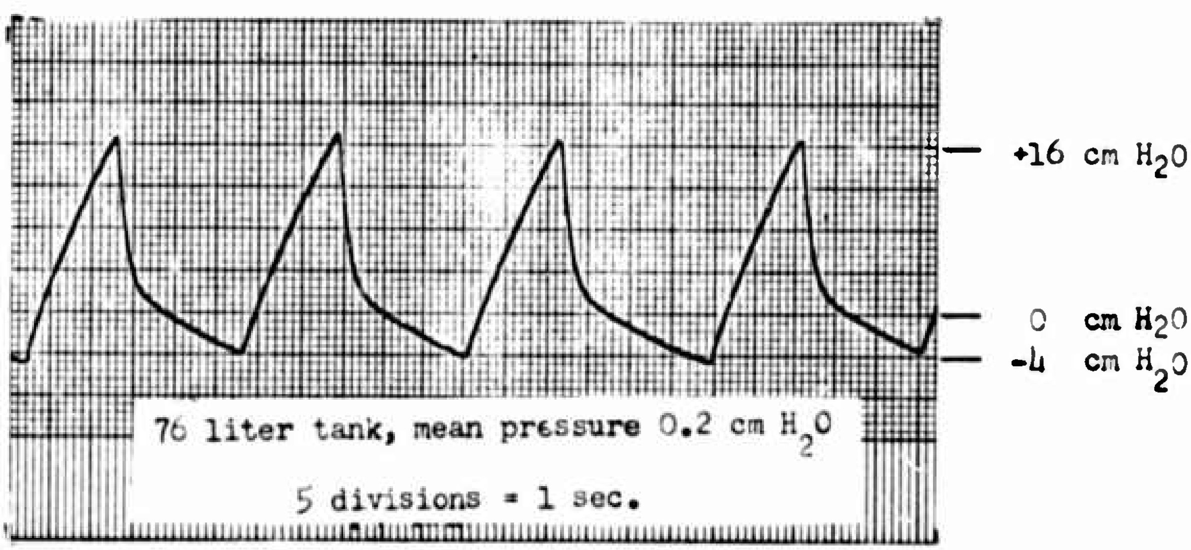

Figure 6. Pressure trace - with breathing valve

A FLUID OPERATED DIESEL LOCOMOTIVE TRANSITION CONTROL UNIT

by

Charles H. Meyer - New York Central System

Richard S. Gluskin - Sperry Rand Corp. Univac Division

The modern diesel railroad locomotive is essentially a mobile electric generating plant utilizing diesel fuel to produce direct-current power, which in turn energizes traction motors to turn the drive axles. Control of direction, speed and torque accomplished by opening and closing electric relays and power contactors to apply current of the proper direction and magnitude to the traction motors. One of the most prevalent causes of delays, loss of power and reduced utilization of locomotives is control-circuit failures ranging from dirty or burned contacts to shock and vibration damage.

In the interest of improved efficiency through higher utilization time of equipment, and therefore improved customer service as well as increased operating profit, the New York Central System has initiated a number of development programs leading toward both modification of present equipment and inclusion of these modifications in specifications for future purchases. Among these programs, the most radical departure from convention is the application of fluid logic to the traction motor control circuits in locomotives. The first phase of this program was initiated late in 1964. In March of 1965, a contract was awarded to Sperry Rand's Univac Division, and by May 15, 1965 the first fluid logic equipped locomotive was operating in normal road-freight service. The objective of this paper is to briefly describe normal electrical control of this locomotive and to review the development steps leading to a successful installation of fluid logic control.

The locomotive selected for this program was an Electro-Motive Diesel Type GP-9, rated at 1750 horsepower, weighing approximately 245,000 lbs., and equipped for freight service up to speeds of 65 MPH. This type of unit was chosen because the Central has a great number of GP-9 locomotives which are not yet approaching retirement, and thus will be considered for similar modification.

The electrical system consists essentially of a 600-volt D.C. generator coupled directly to the V-16 diesel engine to provide current to four axle-mounted traction motors. The motors are series wound with contactors in the field circuit to either reverse the direction of current flow or weaken the field by shunting part of the current around the field coils, or both. Further control is accomplished by selectively connecting two motors in either series or parallel across the generator voltage. The normal sequence of motor connections, known as "Transition", consists of four steps: Series-Parallel, Series-Parallel Shunt, Parallel, and Parallel Shunt. These terms indicate that in the first step, which is the starting connection, two motors are series connected to operate in parallel with two other series-connected motors. In the second step a shunt is placed across the field of each motor to reduce the field strength. In the third step the shunts are removed and all four motors are connected in parallel. Finally, in the fourth step with the locomotive up to speed and power requirement reduced, the shunts are again placed across the motor fields. These steps are shown schematically in Figure 1*. The closing of either "P" or "S" contacts connects the motors for parallel or series operation, while closure of FS contacts shunts part of the motor current around the series field. Proper sequencing of these contactors is the function of the transition control.

Transition is accomplished automatically by means of voltage and current sensing relays which operate at pre-set values. These relays activate solenoid valves which admit high pressure air to power cylinders to drive power contactors. Forward transition, already described, takes place during acceleration from start to high speed, while backward transition takes place automatically in the event of speed reduction due either to lower throttle setting or to increased load such as is encountered on an uphill grade.

---

*Figures appear on pages 327 through 333.

Speed adjustment is accomplished by a governor which sets diesel engine speed in eight steps from 275 rpm to 835 rpm in increments of 80 rpm, the governor being controlled by a manually operated drum switch. The drum switch signals activate electric solenoids located in the governor where their positions are converted to the desired speed setting.

The greatest single problem in railroading is traction. When a drive wheel begins to slip on the rail, tractive effort is lost, fuel is wasted, the wheels are overheated, and the rail suffers burned spots. One solution to this problem is application of sand to the rails. However, it is also necessary to automatically recognize wheel slip immediately and reduce excitation until the slipping wheels have recovered their traction on the rail. This is accomplished by comparing the currents drawn by two motors and reducing excitation on the main generator when these currents suddenly become unequal.

While the foregoing is intended to be very brief, it would be incomplete without mention of the "Train Line", the 27-conductor circuit running from end to end of every locomotive. When two or more locomotive units are operated in "Consist", their control circuits are all connected together through 27 conductor jumper cables between units so that all are controlled by the operator from the lead unit. Thus, all diesel engines will respond to throttle position by operating at the same speed, but each unit will make transition and will control temperature and wheel slip independently. All locomotives owned by the railroad, regardless of age or manufacture , must operate in Consist with any other unit.

Past experience has shown that by far the greatest number of equipment failures resulting in either delays or loss of equipment utilization or both are electrical in origin. Typical problems begin with dirty or broken control circuit contacts, or other relay failures. If the failure occurs on the road and the crew attempts to make repairs, the problem may be made more serious. If road repairs are not attempted, a delay in service is the minimum penalty to the railroad.

In the event that the problem does not cause a road failure, but instead is discovered during periodic inspection, repairs may often be made without excessive cost or delay. In this case, however, trouble shooting and repairing one circuit may create a previously non-existent problem in another circuit through accidental damage in the shop. These secondary problems may not show

up until the locomotive is ready to leave the shop, in which case it must be re-scheduled for the additional tests and repairs.

Because of these problems, the New York Central System has actively sought a means of replacing present electrical equipment with a control system more suitable to locomotives. It was recognized that functions such as controlling direction of heavy current flow would still require contacts. However, the control of power contactors could be accomplished in several ways, the most promising of which appeared to be fluid logic.

The most appealing attribute of Fluidic control was the complete lack of moving parts, and thus freedom from the potential hazards of the shock and vibration on a locomotive. Thus, devices might be expected to better survive the environment. Another significant benefit would result from use of a circuit in which neither crew nor careless service personnel could cause abnormal operation (such as by closing relays with a flag stick) or induce new problems in the course of trouble shooting.

Expected low cost for Fluidic controls added the appeal that the above objectives could be accomplished at a cost saving and with the further advantage that complete replacement of controls would be economically justified if maintenance did become necessary.

The benefits of Fluidics in locomotive control were apparent almost from the start, but an early decision was needed on the scope of the first conversion which would provide adequate feasibility data in as short a time as possible. Obviously full fluid control would provide complete operating experience, but it also presented major interface problems such as a temperature to air flow transducer, wheel slip to generator excitation, etc. Therefore, in the interest of rapid accumulation of operating experience, it was decided to modify only the transition control as the first phase of the program. This permitted taking a number of relays out of service, using fluids for a large segment of control, and avoiding the interface problems which trainline circuits would introduce.

Figure 2 is a partial schematic diagram of NYC Locomotive #5950 showing all circuits involved in transition control, but without many of the other functions such as temperature, speed, battery charging, lighting and signalling. Figure 3 is a further simplification in that only the transition logic circuits are shown.

Step-by-step operation of the transition control circuit depends upon the main generator voltage and current which are sensed by three relays— FSR, FTR and BTR. These are the Field Shunting Relay, Forward Transition Relay, and Backward Transition Relay, respectively. FSR and FTR respond to generator voltage to control all steps of forward transition and backward transition from the shunting positions (i.e. 4 to 3 and 2 to 1). BTR responds to generator current to control backward transition from the parallel position. Normal operation starts only after the reversing control has been moved to either "Forward" or "Reverse". This energizes the transition control circuits shown in Figure 3, closes Series Contactors S_{13} and S_{24}, and allows the locomotive to start in its low speed/high torque connection. With the throttle in the highest position the locomotive will accelerate and the generator voltage will increase with the speed. At approximately 965 volts the FSR picks up and closes the field shunting contactor FS. This causes the traction motors to draw more current, reducing the generator voltage and continuing acceleration of the locomotive. Again the voltage increases, and at 965 volts the FTR picks up, this time dropping out the FS contactor and the Series Contactors, and connecting all four motors in parallel through contactors P_1, P_2, P_3, and P_4. The fourth step is also initiated by FSR, and the locomotive reaches top speed with the motors operating in parallel-shunt.

Backward transition takes place either under normal speed reduction or as a result of slowing due to hills, and is initiated by reduction of voltage on the coil of FSR. If load continues to increase, BTR will respond to the increasing current, and transition to the next step down takes place.

Standard controls include additional features such as time delays to prevent hunting, but these were not changed on #5950.

After reduction of the circuits under study to those of Figure 3, the logic equations of Figure 4 were derived as a starting point for the Fluidic circuit design.

In the interest of having at least two different fluid transition controls for performance analysis, it was decided that one system would be designed and fabricated by Central and another system would be designed and fabricated by UNIVAC. The two systems were to be completely interchangeable with regard to fluid inputs and fluid outputs. Thus, comparative tests would require merely removal of one control module and replacement by the other. The interface devices, consisting of solenoid valves, bellows-type pressure switches

and diaphragm-activated air valves, were to be installed in enclosures separate from the fluid logic systems, and thus would become a virtual part of the locomotive rather than a part of the fluid system under study.

A major factor in the decision to use standard industrial hardware as interface devices was the desire to begin acquiring operating data as soon as possible. An optimum design could have taken many months of development, where the above approach provided a working system within about ten weeks after purchase of the first part. It was recognized that these devices added potential trouble to the system, but this hazard was considered negligible when charged against the benefits of acquiring early information on actual operation of a fluid logic control system.

Another factor in the interface problem was the "Train Line" requirement that would permit #5950 to operate in "Consist" with any other locomotive on the system as either a lead unit or a trailing unit. As explained earlier, all communication between units is electrical and therefore the experimental unit had to operate with electrical input and electrical output information. Relaxation of this requirement will be discussed later.

From this point, UNIVAC and Central worked independently to produce systems meeting the performance requirements and operating as specified by the equations of Figure 4. The resulting designs are shown schematically in Figures 5 and 6. The transition control unit, built at the UNIVAC facility, uses NOR logic exclusively, and is made up of 24 NOR gates. These elements, developed by UNIVAC personnel, have been used extensively in many pure fluid applications, including the UNIVAC® Fluid Computer. The devices have a fan-in and fan-out of four. They are provided with four input terminals — a signal into any one of the four inputs will switch the device "OFF". The output is divided and channeled into four output terminals so that four identical NOR elements can be controlled by one. The logic for the UNIVAC control is shown in Figure 6. Both the UNIVAC transition unit and the NOR element are shown in Figure 7.

The two transistion controls mount interchangeably on a panel inside the existing control cabinet. Available space was in excess of one cubic foot, but both units were considerably smaller than this. The small size of the three major fluid assemblies — input interface, control, and output interface — permitted location of the complete transition control system including pressure

® Registered Trademark of the Sperry Rand Corporation.

regulators and air filter in the control cabinet in a manner that did not block access to other equipment, and left the outward appearance of the locomotive unchanged.

Installation required merely disconnecting electrical contacts and coils being taken out of service, taping unused wire terminations, and removal of interlock contacts and solenoid valves from power contactors to provide mounting space for diaphragm valves. Air interlocking was provided by miniature plunger valves to give pneumatic indications of contactor position, but this is being replaced by grooves in the piston rods to provide the same function with no additional moving parts. All connections were made with color-coded vinyl tubing. The two controls were provided with identical connections and mountings so that change-over would consume a minimum amount of time.

After the installation was completed and all circuits checked, the air was turned on and the locomotive was run through simulated transition by inserting appropriate signals into the control circuit. Satisfactory operation was confirmed, and #5950 was dispatched to yard service in Cleveland, Ohio.

After one week of local service by itself, the locomotive was put into "Consist" with two other units and released to normal road freight service. This duty continued for nearly a month without further attention until the next periodic inspection date arrived. As of this writing, there is no evidence of dirt build-up in the system and no indication that severe service will reveal new difficulties in the application.

The early performance of the Fluidic transition control was completely successful and proved that fluid logic was indeed well suited to the solution of circuit problems in the environment of a railroad locomotive. However, as indicated earlier, the system installed in locomotive #5950 utilized standard industrial valves and switches to solve interface problems as an expedient to gaining experience. The next major phase of the project was to devise a means of converting electrical information to fluid flow and back again. In addition, many control problems capable of Fluidic solution were still to be investigated.

Thus, it was decided that a second locomotive would be converted to Fluidic control. This unit is to be equipped with transition control identical with that on the first unit, but in addition is to serve as a working laboratory for the development of additional Fluidic systems. Still to be considered

are control of engine temperature, engine speed, and axle speed, as well as transition interface devices. This phase of the project is currently in progress, and will hopefully be ready for reporting in the near future.

Meanwhile, it may be of interest to mention other specific areas of railroad operation in which fluid devices may play an important part in the future.

The first item is another locomotive application. Upon completing the conversion of individual locomotives to fluid control, the next project will be to change the 27-conductor Train Line from electrical to fluid power. With fluidic components in each unit, it will be logical to also use fluids to interconnect multiple units. Previous attempts at pneumatic interconnection have failed. They were based on pressure level coding of information and suffered problems of variable restrictions and time lag. The speed and stability of fluid logic systems promise to provide the ideal medium for processing pulse-coded information between locomotive units and thus eliminate the troublesome jumper cables.

Another potential application of immediate interest, and one which actually can provide a much greater saving to railroads than can locomotive conversion, is the wayside interlocking plant. At every turnout or crossover involving the main line of the railroad, a complex electrical circuit is installed in a permanent building to perform such functions as: informing the Central Traffic Control operator of the location of trains, reporting on the setting of the track switch and signals, prevention of switch operation until all trains are clear, and checking routes to prevent trains from proceeding until safety from collision is assured. The basic component of this system is the railroad safety relay — a heavy-duty glass-enclosed assembly developed over the years to render the most reliable service possible in spite of severe ambient conditions ranging from heat and humidity to extreme cold, lightning, and dust storms. Safety relays cost from $75 to several hundred dollars each, and may be as large as a shoe box. They process information received from electric contact closures or resistance changes on the track, energize electric motors to move the track switches, light signal lamps, and transmit verification of these operations to Central Traffic Control.

In the interest of simplifying the design and construction of interlocking plants, New York Central prepared a complete specification for a typical

interlocking plant that would meet the requirements of better than 90% of existing and planned junctions. The input and output functions were specified along with logic to be performed, reliability criteria to be met, and environmental conditions to be considered as minimums. However, the medium of this system was not specified. Thus, both electro-mechanical relays and solid-state electronics have been considered for the system. Now it is possible that Fluidics can out-perform either relays or electronics in this application. The power supply could be a small air compressor instead of a battery charger; the power storage device, an air reservoir instead of a battery; the track switch operator, an air cylinder instead of an electric motor. Some electrical systems would remain, such as signal lamps and communication with Central Traffic Control. A fluid operated system would be capable of fulfilling the performance specifications, and perhaps at significantly less expense. Certainly the interlocking plant should be considered to be an excellent application to utilize the advantages of Fluidics.

Other potential railroad applications are less impressive but would perhaps be worthy of attention because they offer the opportunity of immediate field testing. These include:

Tank Car Filling
Fueling of Locomotives
Track Level Gauging
Freight Car Weighing
Track Occupancy Indication

In review, the decision to investigate fluid logic controls for locomotives was based upon the following potential advantages:

1. Insensitivity to environmental conditions of shock, vibration, dirt, and electrical transients.
2. Anticipated reduced maintenance time via complete replacement due to low cost.
3. Small space requirements.
4. Promise of greater reliability.

All of these lead ultimately to both higher utilization time and lower investment. Thus, with assistance from the Sperry Rand Corporation's UNIVAC Division, the New York Central System has accepted initial successes in fluid controls as a challenge to carry this development further with the expectation that the ultimate objective—increased profitability—will be realized.

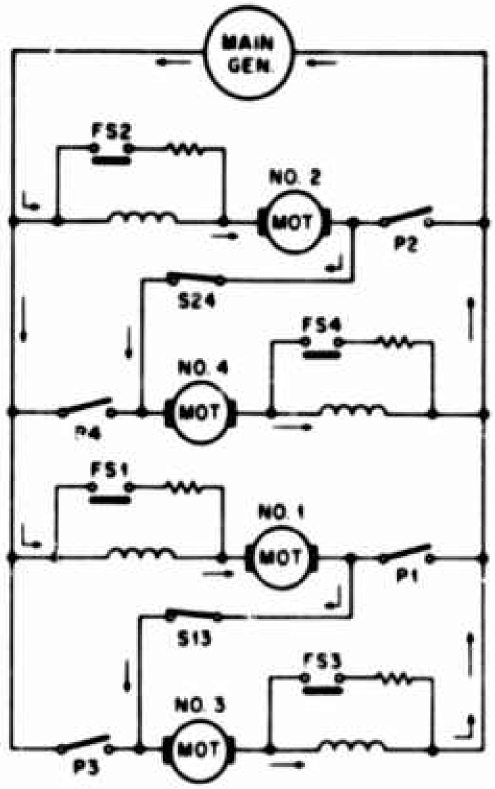

a. Series-Parallel

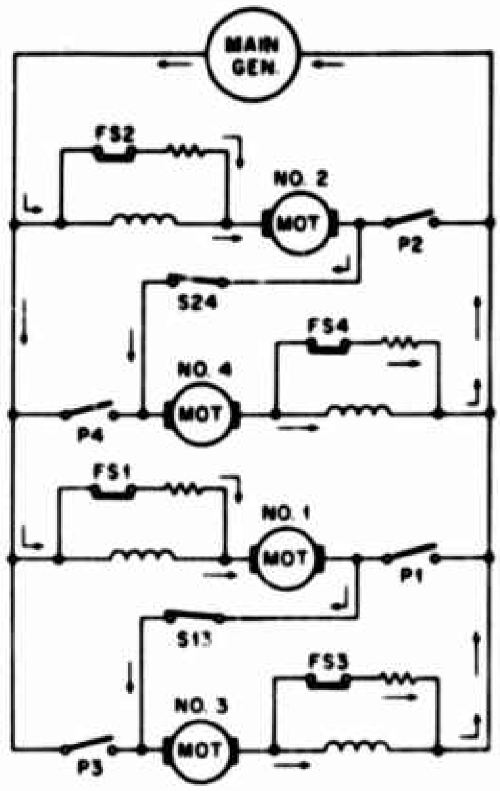

b. Series-Parallel Shunt

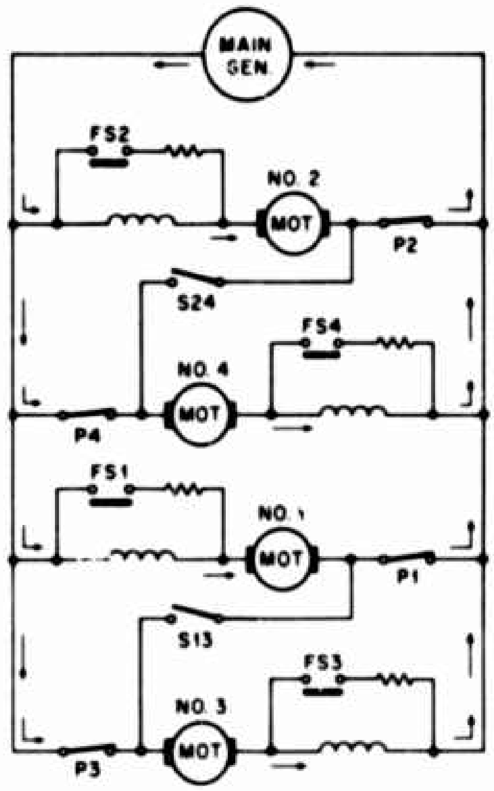

c. Parallel

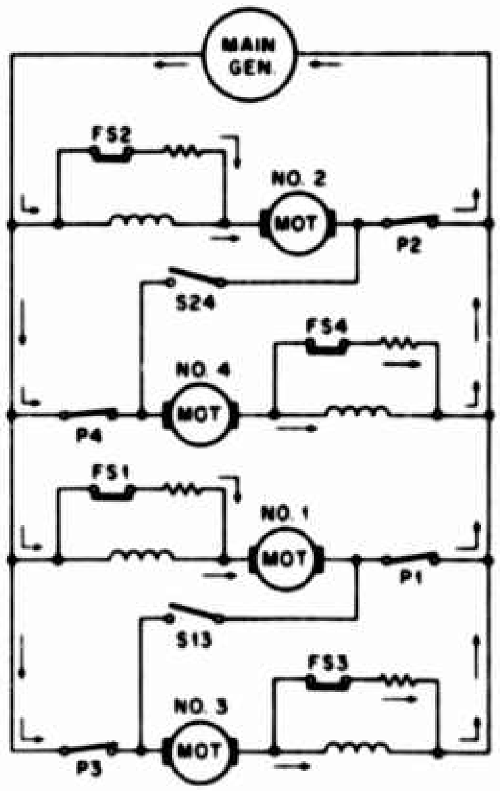

d. Parallel Shunt

Figure 1. Simplified Main Power Circuit Showing Motors, Fields, and Power Contactors

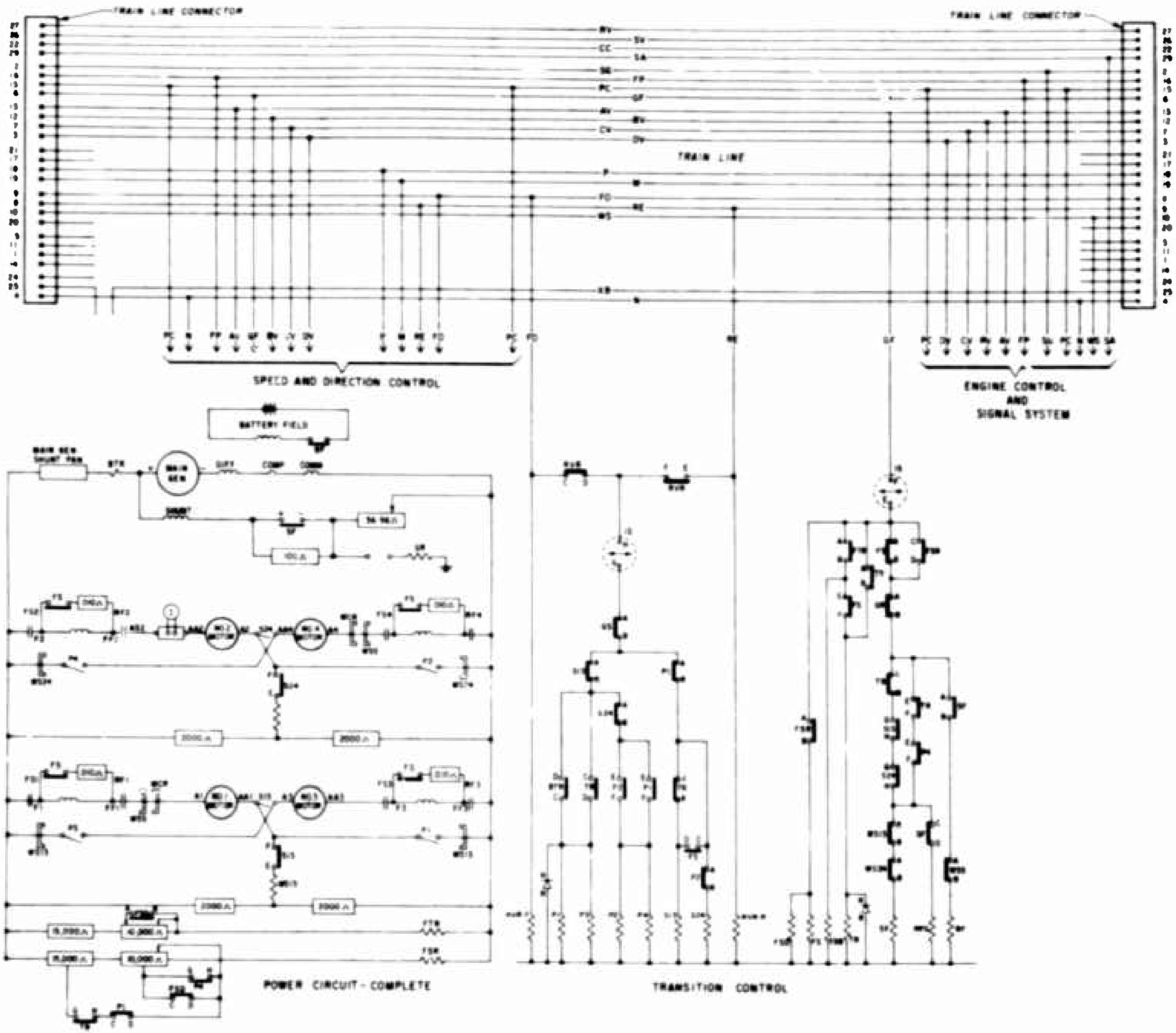

Figure 2. GP-9 Locomotive-Transition Control, Train Line, Power Circuit

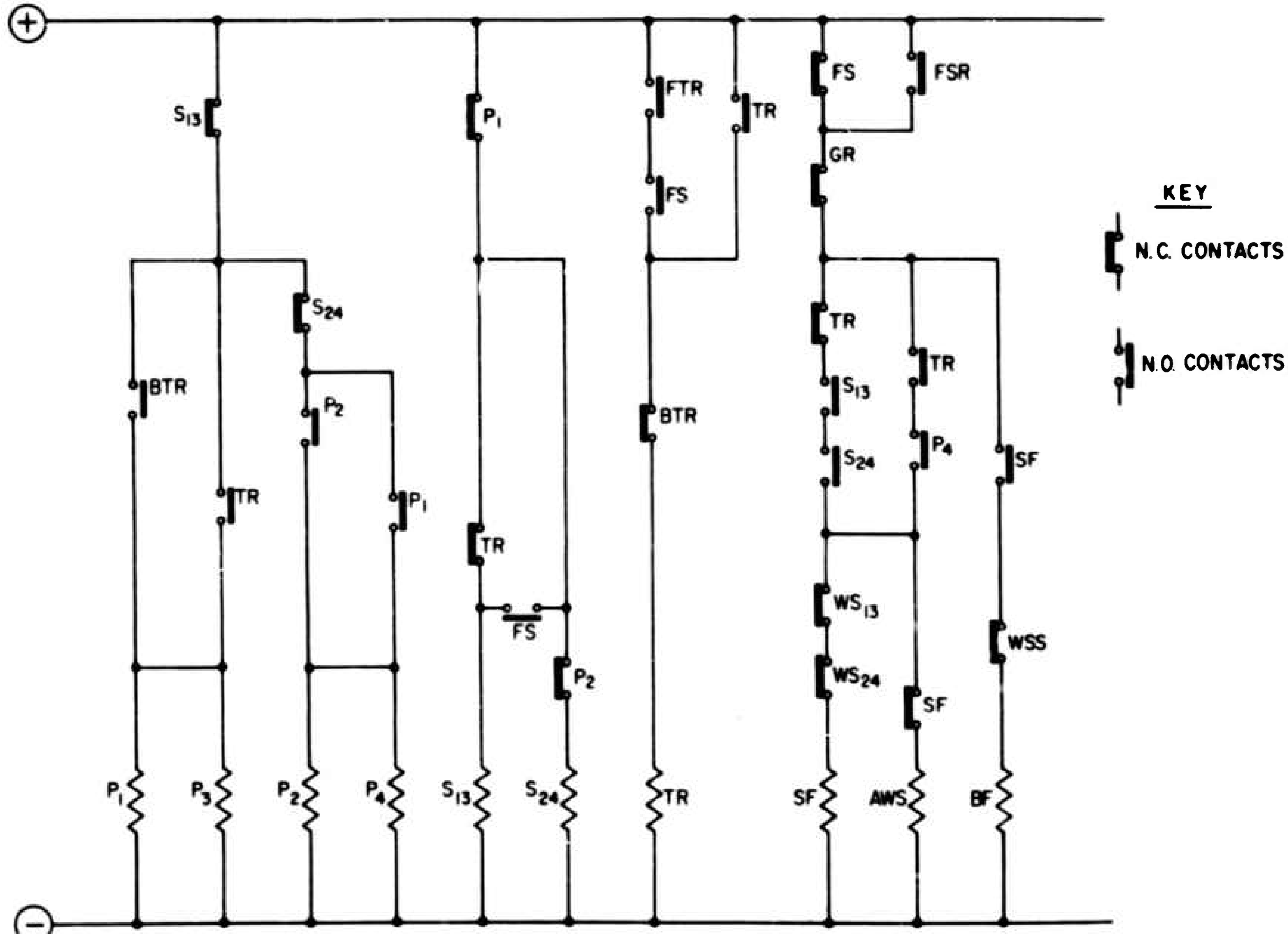

Figure 3. Transition Control Circuits NYC No. 5950 Prior to Modification

$$P_1 = \overline{S_{13}} \cdot (TR + BTR)$$

$$P_3 = \overline{S_{13}} \cdot (TR + BTR)$$

$$P_2 = \overline{S_{13}} \cdot \overline{S_{24}} \cdot (P_1 + P_2)$$

$$P_4 = \overline{S_{13}} \cdot \overline{S_{24}} \cdot (P_1 + P_2)$$

$$S_{13} = \overline{P_1} \cdot (FS + \overline{TR})$$

$$S_{24} = \overline{P_1} \cdot \overline{P_2}$$

$$TR = \overline{BTR} \cdot \left[(FS \cdot FTR) + TR \right]$$

$$SF = \overline{WS_{24}} \cdot \overline{WS_{13}} \cdot \left[(S_{24} \cdot S_{13} \cdot \overline{TR}) + (P_4 \cdot TR) \right] \cdot \overline{GR} \cdot (\overline{FS} + FSR)$$

$$AWS = \overline{SF} \left[(S_{24} \cdot S_{13} \cdot \overline{TR}) + (P_4 \cdot TR) \right] \cdot \overline{GR} \cdot (\overline{FS} + FSR)$$

$$BF = \overline{WSS} \cdot SF$$

Figure 4. Transition Logic Equations for GP-9 Locomotive Based on Circuits of Figure 3

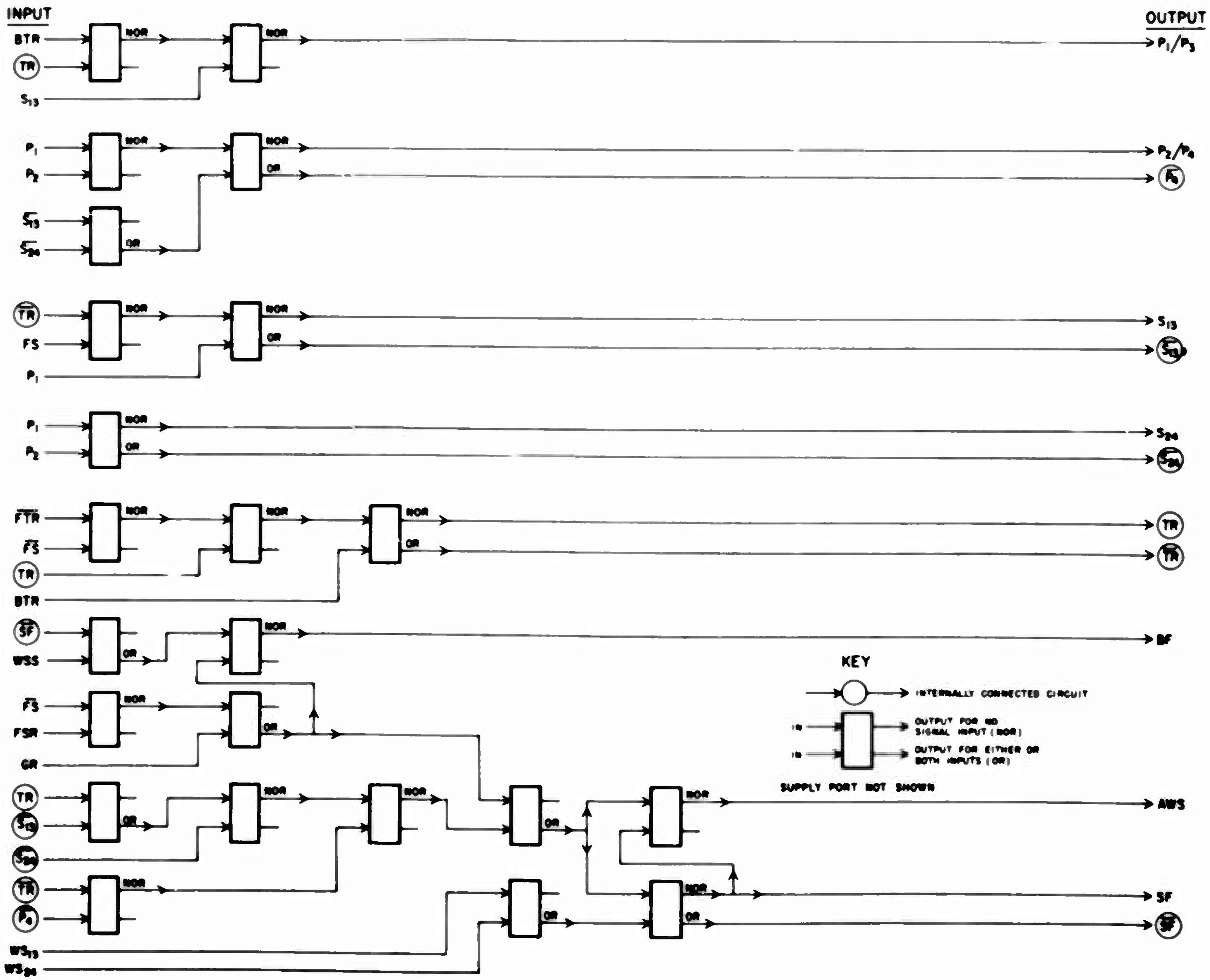

Figure 5. "OR/NOR" Fluid Schematic

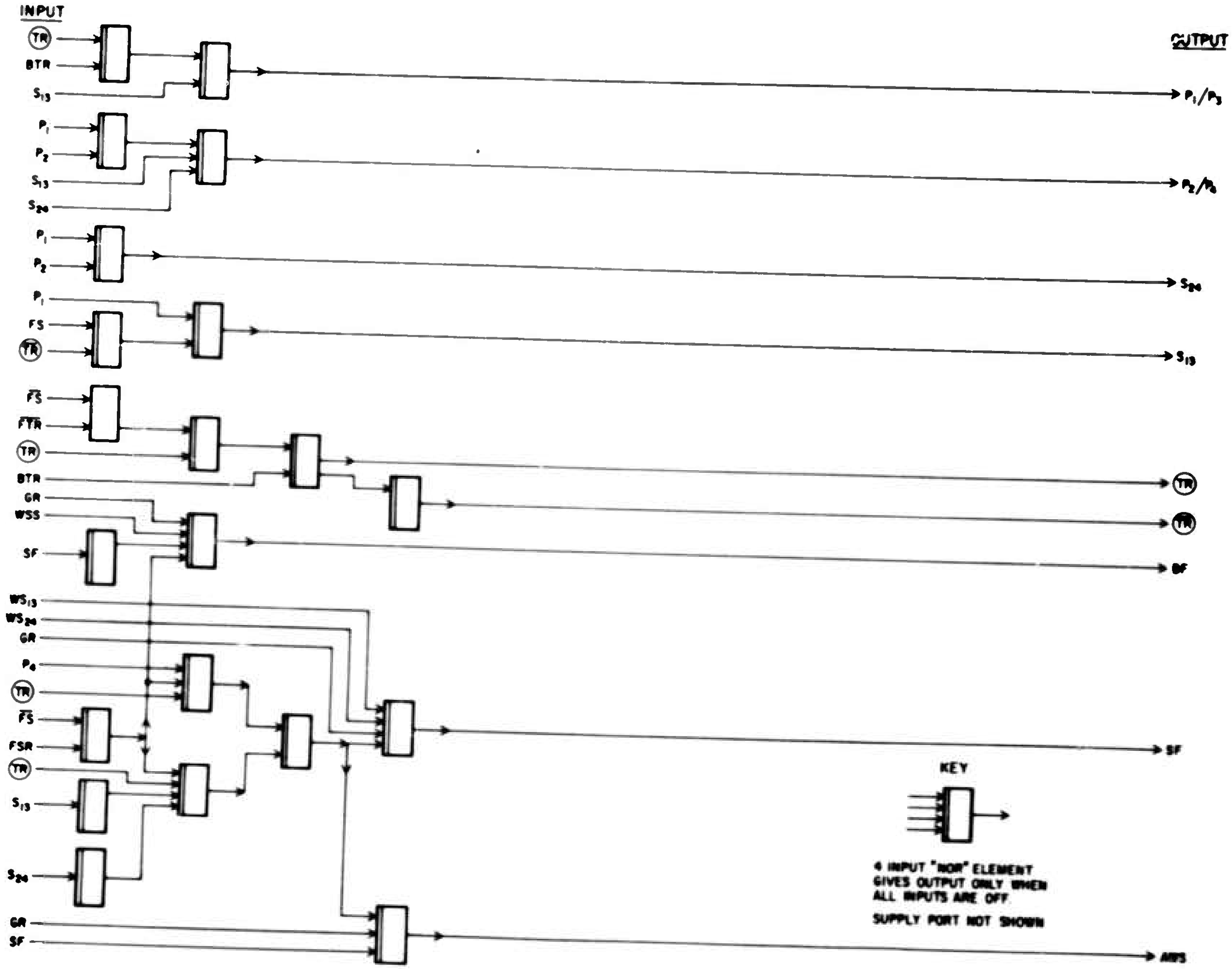

Figure 6. UNIVAC Fluid "NOR" Gate Schematic

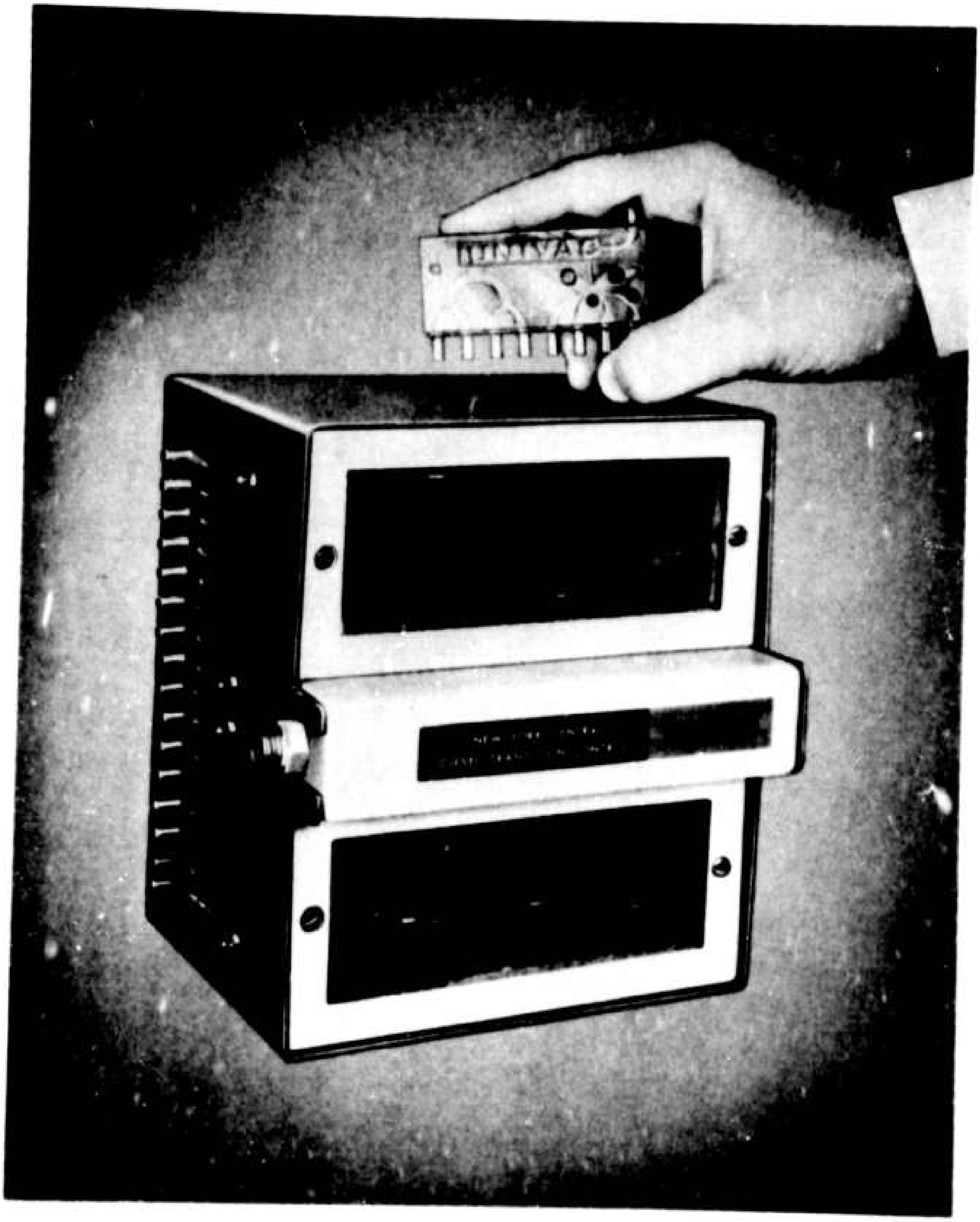

Figure 7. Transition Control Unit and UNIVAC "NOR" Gate

AREA EXPERIENCE IN MODERATE

VOLUME FABRICATION OF PURE FLUID DEVICES

by

R. W. Van Tilburg

of

CORNING GLASS WORKS

ABSTRACT

A discussion of the background of Fluid Amplifier development leads into the decisions on production organization. Specifications in their most phenomenal sense are covered and the logic behind the specifications is explained briefly.

Production experience is summarized with facts on selections of specific devices produced to specific specifications. Conclusions indicate that Fluid Amplifiers have selection criteria similar to other control components. Other conclusions are drawn.

INTRODUCTION

During the period of time when the basic phenomena of pure fluid devices, as they are known today, were under investigation at the Diamond Ordnance Fuze Laboratories, there was considerable concern that the emergence of this new technology from a laboratory curiosity to an established product might be substantially delayed by the lack of effective manufacturing methods. Because this was truly a new technology, vastly different from any then in existence, there were no comparable products in volume production anywhere in the world, and as a result of this fact, there was no sound basis for predicting costs, selections, required capital equipment, or actually whether or not they could be made at all at high selection to reasonable specifications.

The potential value of these "no moving parts" control and sensing devices rapidly became apparent, to the degree that many organizations, both military and industrial, undertook the development of devices and circuits confident that fabrication techniques could be developed. In the relatively short period of three years, both of these objectives have been accomplished to the degree that functional pure fluid control circuits are being used effectively in a truly amazing variety of applications.

However, although many organizations do not publicize their work in this field, and their degree of accomplishment is not generally known, there are very few cases where either devices, or circuits, have been reproduced in quantity, and no information has been made public regarding the fabrication of a relatively large number of devices of widely varying function and degree of

complexity.

Public acceptance of the concept of fluid logic has increased to the point that it is now not only possible, but necessary, to fabricate devices, and relatively simple circuits, in quantities of thousands or more. This is not significant in terms of numbers as such because these are still small numbers, but it is significant in terms of product when the quantities required become great enough to preclude the exclusive use of experienced engineering and technical personnel in the manufacturing area.

Although many different types of fluid amplifiers, and almost as many manufacturing techniques, have been developed in the last two years, some concern is still evident. It is generally accepted that these devices can be made functional, in limited quantities, but it has yet to be proven that an increase in demand can result in the improved performance and the decreased costs which must be achieved before pure fluid circuits can approach their full potential.

As a result of demand for breadboard components, and a decision by the Corning Glass Works to offer fluid devices as a standard product line, the step from laboratory curiosity to product has been taken and the responsibility for manufacturing has been transferred at Corning from the technical staff, which was organized around fluid amplifiers, to plant personnel, the majority of whom, as recently as three months ago, were aware of the existence of this product only because of a sign on the door of the development laboratory.

SIGNIFICANT DECISIONS

Of the multitude of basic decisions which were required before this step could be taken, there are several which are felt to be of more than passing significance to the ever increasing number of organizations exhibiting interest in this technology.

Primary, of course, is the decision to manufacture. Although progressive organizations routinely invest Research & Development funds in promising new products and processes, which either threaten to obsolete existing product lines or show sufficient potential as new items, the decision to divert profitable manufacturing effort and equipment to an, as yet, unproven market, is substantially more complex. Accepting the fact that the ability to fabricate the product to some high quality level has been established, the most important considerations are market size and unit cost. These two factors exhibit a complex interrelationship which could not adequately be developed within the scope of this discussion.

Further evidence of the growing industrial confidence in the future of fluid devices and circuits can be seen in the decision by the Imperial Eastman Corporation to market fluid products in their established distribution network. This decision was also based on careful market and product analysis, and lends further credence to the fact that there is a future for these devices in the military and industrial world.

In a more practical vein, accepting the decision to manufacture, it became necessary to choose the correct course of action relative to the establishment

of a non-technical, line-level operation. It was reasoned that the immediate establishment of a manufacturing group using only plant people would result in the best long-term efficiency, since development people are not usually production oriented, and to divert their efforts in that direction would result in a substantial decrease in the rate of product development and improvement Among other things, this forces the development of specification concepts and quality detail frequently overlooked by development operations. Although the latter course of action has resulted in many short-term problems, it is significant to the Fluid Amplifier Industry in that it has been proven that these devices and circuits can be made by non-technical people, who, being subjected to seniority regulations, change jobs with production level variations. Specifically, Fluid Amplifiers are out of the laboratory and into the factory, in the strictist sense of the word. They are in production at increasing rates and at high levels of quality.

PROCESS

The process used by Corning to fabricate these devices is that developed for the manufacture of Fotoform glass and Fotoceram glass ceramics. This process was discussed in detail in a paper delivered at the 1963 DOFL Symposium, and these details need not be repeated at this time. Fabrication steps consist of artwork preparation, optical exposure, thermal development, chemical machining, and thermal diffusion bonding. Each one of these operations is critical, to some degree, in some cases more so on one type of product than on another, and in almost every case, substantially more so as the size is decreased.

PRODUCTS

The primary reason that it was felt that this discussion might be of interest to the Fluid Amplifier industry as a whole lies in the fact that, although all of the designs are basically HDL configurations, a rather broad range of product function has been covered, and some data are available relating selections and performance to product type and size.

The product types to be discussed are as follows:

A) Digital

1) Bistable

a) Load sensitive (. 010 x . 040, and . 020 x . 080 power nozzle).

b) Load insensitive (. 010 x . 040, and . 020 x . 080 power nozzle).

2) Monostable

a) AND Gate (. 010 x . 040 power nozzle).

b) NOR Gate (. 010 x . 040, and . 020 x . 080 power nozzle).

3) Bistable & Monostable

a) Binary Counter (. 010 x . 040 power nozzle).

B) Proportional

1) Without Center Dump (. 010 x . 025, and . 020 x . 050 power nozzle).

2) With Center Dump (. 010 x . 023, and . 020 x . 050 power nozzle).

TEST PROCEDURES

In every case above, it was necessary to establish several basic performance criteria before manufacturing operations could be initiated. Specifically, it is a relatively simple matter to define each of these devices in general terms, for the sake of discussion. For example, a two-input NORgate could be defined as a device in which a relatively high energy fluid stream is diverted from one of two outputs to the other by the presence of either or both of two relatively low energy fluid streams, and remains in the diverted position as long as, and only as long as, either or both of the relatively low energy fluid streams are present.

However, definition of a two-input NORgate for quality control purposes becomes substantially more complicated, in that such terms as relatively and diverted must be expressed numerically, and an effective set of test conditions under which these numbers apply must be established. This situation is further complicated when a number of different kinds of devices are included in the product line, and each must be functionally compatible with the others. In addition, these performance criteria must be carefully established in a manner which will not preclude, or even complicate, the development of new products and their inclusion in the overall product line.

Taking the NORgate (.010" x .040" Power Jet) as an example, the following are some of the variables which must be defined:

A) Power Jet

1) Operating range - all devices must function in a satisfactory

manner at any power jet pressure between 1. 5 psig and 15. 0 psig.

2) Size - the size of the power nozzle shall be such that, when subjected to a 1. 5-psig pressure differential, it will pass between . 070 SCFM and . 072 SCFM. Since power nozzle width is fixed by the negative, this is a direct control over depth and etch ratio.

There is a basic significance to the choice of 1. 5-psig power jet pressure for the above test. Digital devices of this design, which are fabricated in the previously defined manner, continue to function as digital devices at power jet pressure levels substantially in excess of the 15. 0-psig maximum indicated. The 1. 5-psig minimum is, however, approaching a functional limit. In the early stages of manufacturing, it was deemed necessary to establish the performance of each device fabricated, on a 100% basis, using definitive, meaningful tests. It was decided that such tests for a digital device would establish the relationship between the controls and the outputs, at a given power jet pressure; 1. 5 psig was chosen because it had previously been proven that marginal devices were more apt to malfunction at the lower power jet pressures. Specifically, if a digital device of a given design will switch sharply and completely at a power jet pressure of 1. 5 psig, it will continue to do so at pressures up to, and substantially beyond, the 15. 0 psig specified as maximum.

B) Control Jets

1) Switching range - the switching range of all devices was again defined in terms of pressure, as follows:

a) Level - with one control open to ambient, the power jet fixed at 1.5 psig, and the outputs loaded in a manner to be defined in a later section, the other control must cause the device to switch, and permit it to return while the pressure level in that control is in the range of .010 to 0.05 psig.

b) Rate of change - since momentum is a factor in the performance of these devices, and since the effects of volume must be fixed so that a fixed pressure relationship exists between the nozzle under test and the point of read-out, the length and diameter of all interconnections are specified, and the maximum rate of change of control jet pressure has been established at 0.06 psig per second.

C) Outputs

1) Loading - in all devices, including those described as load insensitive, the output flow pressure relationship, and therefore the amount of pressure recovered in the output, is a function of the amount of resistance encountered by the stream. For this test the outputs are loaded with the equivalent of the sum of the areas of three of its control nozzles.

2) Recovery - when loaded as defined above, the outputs must recover a minimum of 0.25 psig when activated, and a maximum of $+.02$ psig and a minimum of $-.02$ psig when not activated.

3) Hysteresis - within the limits of switch pressure previously specified, the hysteresis band must be at least 0.0125 psig ΔP_C in the positive direction, and the maximum pressure change permitted in the output just prior to switching in either direction is 0.04 psig.

As indicated, these numbers and procedures apply specifically to the smaller of the two NORgates, but they are, in general, used for all digital devices, of both sizes. There are exceptions to this rule, of course, as with the ANDgate in which case the fixed control must be held at a pressure slightly in excess of the maximum acceptable switch pressure. Also, the binary counter operates at a 3-psig minimum power jet level and must receive a pulse input to function properly.

Proportional devices do not have a critical minimum power jet pressure, and 5 psig was arbitrarily chosen as the fixed value for that variable. Loading was fixed at an area equivalent to one control nozzle, and the test bias level was set at 10% of the power jet pressure. Limits were set on minimum pressure gain, linearity, stability, and zero balance.

PERFORMANCE

Although actual selection figures are generally proprietary, some extremely

interesting relationships were developed during the course of this manufacturing effort, and it is felt that a discussion using some actual numbers might be of more than passing interest to device designers.

Information presented here was obtained from routine test data taken on over 15,000 devices, made from six basic designs, five of which were fabricated in the two power nozzle widths listed previously.

The average of the selections of the eleven groups represented was 50%. Although this is not a number which is particularly impressive to manufacturing oriented people, it was felt to be reasonable for early stages of production. Of the total made, less than 10% did not function in the intended manner, and the majority of those were from one design. As an example, the .010" power nozzle load sensitive flip-flop selection was 50% for a first order quantity of 400. Of the 800 devices made to select the 400 required, only 2 (0.25%) did not switch as intended, the remaining 398 being rejected about evenly for low recovery (low fan-out), high switch point (low fan-in) and low switch point (too sensitive). All of these devices, except the two which were set, would function in a satisfactory manner in any multi-component circuit in which the fan-out was held to a maximum of two.

The case of the 0.010" power nozzle NORgate will help to emphasize what is felt to be an extremely important point. A low selection figure necessitated the fabrication of large numbers of devices to recover the required number

of acceptable units. At first glance it would seem that this design could never be used in a multi-component circuit and yet ten experimental binary to decimal converters were fabricated, and fusion sealed with 17 NORgates of this design in each unit, and all ten performed in a satisfactory manner. The reason for this can be seen in an analysis of the rejects which showed the average switch pressure of the upper control of this design to fall almost exactly on the upper limit. Because of this, half of the devices fabricated were rejected for high switch pressure (low fan-in). The majority of the remaining rejects exhibited a negative hysteresis (Oscillation at the switch point) or tended to proportion within the specified switching range. Again, less than 1% of these devices failed to perform the NOR function, and these were set to the OR side. With the exception of the set devices, the only rejects which would cause a multi-component circuit to malfunction were those which switched high, and then only if the device feeding that control were fanned out excessively.

The significance of this is that the circuit designer who knows the limitations of his components and designs away from these limitations can expect a reasonably complex (25 component) circuit to function in an acceptable manner.

The effect of size was quite noticeable also, in that designs fabricated with power nozzles .020" wide averaged high selections, while the same designs reduced to one-half that size averaged 50% lower selections. The fact that the larger devices performed more consistently is to be expected, since

some of the process variables are relatively independent of size, but the amount of the difference is somewhat surprising. This would seem to indicate that further reduction to .005" power nozzles would result in excessively low selections, and data available from small lot testing tend to verify this indication. There are, however, instances where designs have been reduced to .005" power nozzle size and have functioned well, so it would appear that miniaturization to that degree will prove difficult but not impossible.

In addition to the effect just discussed, size can have a profound effect on devices of marginal design, as attested by the fact that the highest selection rate was obtained with the .020" load insensitive flip-flop, whereas the lowest selection rate was obtained with the exact same device optically reduced to one-half that size. Although the large size device performed beyond expectations, the small devices did not perform the intended function at all. In every other case, all but about 1% of the devices were useable (some under restricted conditions), whereas, in this case, the rejects were either set to one side, or they were not bistable. This admittedly is only one case in five, but it does prove that a device which performs well at one size and set of conditions may actually be marginal to the degree that it cannot be directly miniaturized.

Both proportional designs proved to be substantially less sensitive to the effects of size reduction than any of the digital designs. The non-center dump design for example, selected at a rate of 45% for the .020" power

nozzle size, and 42% for the .010" power nozzle size. As in most of the other cases, the rejects were functional devices which performed the proportional function in an adequate manner, but which were not quite up to the capability of the design. Small lot experience indicated that a gain (pressure) of 7.0 was reasonable for this design, if a 30% selection level were acceptable. Under the assumption that performance would improve as people and procedures were developed, a pressure gain minimum limit was established at 7.0. Obviously, the difference between a device with a gain of 7.5 (acceptable) and one with a gain of 6.5 (rejectable) is simply one of degree, and in most cases the difference is negligible.

CONCLUSIONS

In general, the transition from small quantities fabricated by skilled technical people to relatively large quantities manufactured by production oriented people with no prior fluid amplifier experience was successful. The average selection for all designs of 50% in early stages of production is encouraging.

Selections of 50% or less do not preclude the use of designs in multi-component circuits, because, in almost every case, the percentage of devices that do not perform the intended function is less than 1%.

In every case, the variation in performance was greater in the smaller sizes, although must less so in proportional designs.

It is possible for a design to perform well at one size and not perform at all at one-half that size.

DOCUMENT CONTROL DATA - R&D

(Security classification of title, body of abstract and indexing annotation must be entered when the overall report is classified)

1. ORIGINATING ACTIVITY (Corporate author) Harry Diamond Laboratories, Washington, D. C. 20438	2a. REPORT SECURITY CLASSIFICATION UNCLASSIFIED
	2b. GROUP

3. REPORT TITLE

PROCEEDINGS OF THE FLUID AMPLIFICATION SYMPOSIUM--Volume III, October 1965

4. DESCRIPTIVE NOTES (Type of report and inclusive dates)

Compilation of 17 papers on flueric theory and devices.

5. AUTHOR(S) (Last name, first name, initial)

6. REPORT DATE October 1965	7a. TOTAL NO. OF PAGES	7b. NO. OF REFS

8a. CONTRACT OR GRANT NO.	9a. ORIGINATOR'S REPORT NUMBER(S)
b. PROJECT NO. DA-1P010501A001	
c. AMCMS Code 5011.11.71200	9b. OTHER REPORT NO(S) (Any other numbers that may be assigned this report)
d. HDL Proj No. 31100	

10. AVAILABILITY/LIMITATION NOTICES

Qualified requesters may obtain copies of this report from DDC. DDC release to Clearinghouse for Federal Scientific and Technical Information is authorized.

11. SUPPLEMENTARY NOTES	12. SPONSORING MILITARY ACTIVITY Hq. AMC

13. ABSTRACT

This document is the third of five volumes, covering the October 1965 symposium on fluid amplification at the Harry Diamond Laboratories. These volumes include 55 papers, prepared by personnel from various Government agencies, universities, and industrial firms.

DD FORM 1 JAN 64 1473